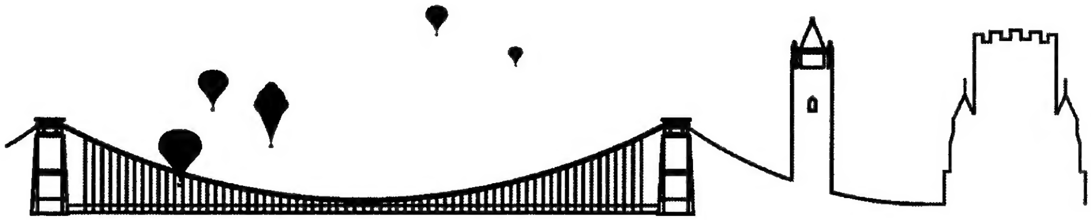

18th INTERNATIONAL SYMPOSIUM ON GAS KINETICS

BRISTOL

AUGUST 7 - 12 2004

BOOK OF ABSTRACTS

REPORT DOCUMENTATION PAGE

Form Approved OMB No. 0704-0188

1. REPORT DATE ***(DD-MM-YYYY)***	**2. REPORT TYPE**	**3. DATES COVERED** *(From – To)*
29-07-2004	Conference Proceedings	7 August 2004 - 12 August 2004

4. TITLE AND SUBTITLE
18th International Symposium on Gas Kinetics

5a. CONTRACT NUMBER
FA8655-04-1-5012

5b. GRANT NUMBER

5c. PROGRAM ELEMENT NUMBER

6. AUTHOR(S)
Conference Committee

5d. PROJECT NUMBER

5d. TASK NUMBER

5e. WORK UNIT NUMBER

7. PERFORMING ORGANIZATION NAME(S) AND ADDRESS(ES)
University of Bristol
Cantocks Close
Bristol BS8 1TS
United Kingdom

8. PERFORMING ORGANIZATION REPORT NUMBER
N/A

9. SPONSORING/MONITORING AGENCY NAME(S) AND ADDRESS(ES)
EOARD
PSC 802 BOX 14
FPO 09499-0014

10. SPONSOR/MONITOR'S ACRONYM(S)

11. SPONSOR/MONITOR'S REPORT NUMBER(S)
CSP 04-5012

12. DISTRIBUTION/AVAILABILITY STATEMENT

Approved for public release; distribution is unlimited. (approval given by local Public Affairs Office)

13. SUPPLEMENTARY NOTES

14. ABSTRACT

The Final Proceedings for 18th International Symposium on Gas Kinetics, 7 August 2004 - 12 August 2004

The biennial International Gas Kinetics Conference will bring together internationally recognized experts in experimental, theoretical and modelling studies of gas kinetics, combustion and plasma diagnostics, reaction dynamics and atmospheric chemistry. The meeting is being organized in conjunction with the Gas Kinetics Group of the Royal Society of Chemistry and will feature both invited and contributed oral contributions, and two major poster sessions. Plenary speakers include Nobel Laureate Professor Mario Molina (MIT) and Polanyi Medal winner, Professor David Clary (Oxford). The Symposium will have sessions on modern experimental and theoretical gas kinetics, including the following topics: Atmospheric Chemistry, Combustion and Plasma Chemistry, Reaction and Photodissociation Dynamics, Gas-Surface Interactions, Inelastic Scattering and Energy Transfer, Astrochemistry.

15. SUBJECT TERMS
EOARD, Kinetics

16. SECURITY CLASSIFICATION OF:			**17. LIMITATION OF ABSTRACT**	**18, NUMBER OF PAGES**	**19a. NAME OF RESPONSIBLE PERSON**
a. REPORT	**b. ABSTRACT**	**c. THIS PAGE**			
UNCLAS	UNCLAS	UNCLAS	UL	195	INGRID J. WYSONG
					19b. TELEPHONE NUMBER *(Include area code)* +44 (0)20 7514 4285

Sponsors

We wish to thank the following for their contributions to the success of this conference. More information about our sponsors can be found from the links on the Symposium website.

EPSRC
Engineering and Physical Sciences Research Council

European Office of Aerospace Research and Development, Air Force Office of Scientific Research, United States Air Force Research Laboratory.

NATURAL ENVIRONMENT RESEARCH COUNCIL

NERC Centres for Atmospheric Science
NATURAL ENVIRONMENT RESEARCH COUNCIL

Ocean Optics BV
First in Photonics™

PHOTONIC SOLUTIONS PLC

LEYBOLD

LASER COMPONENTS

ELLIOT LTD

COHERENT

Kurt J. Lesker Company

RS•C

Programme

Saturday 7 August

16:00	Registration at Wills Hall
19:00 – 20:30	Dinner
20:30	Reception in Wills Hall

Sunday 8th August

07:30 – 08:45	Breakfast
08:45 – 09:00	Introductory remarks
	Session 1: Atmospheric chemistry Chairman: M. Kawasaki
09:00 – 09:50	**Plenary Lecture** J.M.C. Plane (University of East Anglia) *The uptake of meteoric metal atoms on polar mesospheric clouds*
09:50 – 10:10	L. S. Alconcel, D. J. Robichaud, M. Okumura, S. P. Sander *Near-IR kinetic spectroscopy of peroxy radical reactions*
10:10 – 10:30	C. Percival, T. Raventos-Duran, A. Bacak, M. Bardwell *Experimental studies on the reactions of peroxy radicals with NO_2*
10:30 – 11:00	**Coffee break**
	Session 2: Atmospheric chemistry Chairman: W. Bloss
11:00 – 11:20	M.V. Ghosh, D.E. Shallcross, J.M. Dyke *Study of the atmospherically important reaction - Cl_2 with dimethylsulphide*
11:20 – 11:40	P.H. Wine, J.M. Nicovich, M.L. McKee, K.M. Kleissas, S. Parthasarathy, F.D. Pope, A.T. Pegus *Kinetics, spectroscopy, and thermochemistry of the Cl–DMSO adduct*
11:40 – 12:00	G. Boakes, D.M. Rowley *Kinetics of the ClO + ClO and the ClO + BrO reactions*
12:00 – 12:20	K. Takahashi, T. Nakayama, Y. Matsumi *Laser-induced fluorescence detection of $O(^1S)$ atom from O_3 photolysis and its application for kinetic study of the reaction of $O(^1S)$ with atmospheric molecules*
12:20 – 12:40	J.N. Harvey *Ab initio modelling of atmospheric oxidation reactions*
12:40 – 14:00	**Lunch**

Session 3: Energy transfer
Chairman: M.N.R. Ashfold

14:00 – 14:50	**Plenary Lecture** K.G. McKendrick (Heriot-Watt University) *Alternative spectroscopic probes of collisional energy transfer*
14:50 – 15:10	M.A. Blitz, N. Choi, T. Kovacs, M.J. Pilling, P.W. Seakins *Mechanisms for quenching $^1CH_2$ – reactive, nonreactive and combinations thereof*
15:10 – 15:30	T. Lenzer, H. Frerichs, M. Hollerbach, K. Luther *Investigations of collisional energy transfer of highly vibrationally excited trans-stilbene*
15:30 – 16:00	**Tea break**

Session 4: General gas kinetics
Chairman: R. Zellner

16:00 – 16:20	V. Bernshtein, I. Oref *Trajectory simulations of polyatomic-polyatomic collisions*
16:20 – 16:40	K. Sekiguchi, C. Lee, K. Oum, K. Luther, J. Troe *The role of van der Waals radical complexes in combination reactions of polyatomic radicals at high pressures*
16:40 – 17:00	M.J. Almond, N. Goldberg, R. Walsh, R. Becerra, J.P. Cannady, J. S. Ogden *Experimental and theoretical evidence for homogeneous catalysis in the gas-phase reaction of SiH_2 with H_2O (and D_2O). A combined kinetic and quantum chemical study*
17:00 – 17:20	Y. Gao, R.G. Macdonald *Time-resolved absorption studies of radical-radical reactions involving $NCO(X^2\Pi)$ and simple alkyl radicals: $H(^2S)$, $CH_3(X^2A_2'')$ and $C_2H_5(X^2A'')$*
18:00 – 19:00	**Poster session A**
19:00 – 20:30	**Dinner**
20:30 – 22:00	**Poster session A continued**

Monday 9th August

07:30 – 08:45	**Breakfast**

Session 5: Reaction dynamics
Chairman: S. Vázquez

09:00 – 09:50	**Plenary Lecture** G.C. Schatz (Northwestern University) *Reactions of hyperthermal atomic oxygen: surprising reaction mechanisms, intersystem crossing effects and collisional energy transfer processes*

09:50 – 10:10	J.-H. Choi *Exploring radical-radical reaction dynamics*
10:10 – 10:30	G. Capozza, E. Segoloni, G. G. Volpi, P. Casavecchia *Crossed molecular beam studies of the $O(^3P)$ + C_2H_4 reaction using "soft" electron impact ionization: Primary products, reaction dynamics and branching ratios*
10:30 – 11:00	**Coffee break**
	Session 6: Reaction and photodissociation dynamics Chairman: M.L. Costen
11:00 – 11:20	F. Ausfelder, A.E. Pomerantz, R.N. Zare, S.C. Althorpe, F.J. Aoiz, L. Banares, J.F. Castillo *The H + D_2 reaction: a challenge for experiment and theory*
11:20 – 11:40	M.P. de Miranda, R.A. Pettipher *Recent studies of the state-to-state stereodynamics of elementary reactions*
11:40 – 12:00	G. Hancock, S.J. Horrocks, P.J. Pearson, G.A.D. Ritchie, D.F. Tibbetts *From vibrationally cold to vibrationally mediated ozone photodissociation: Probing orientation and alignment of the singlet oxygen products*
12:00 – 12:20	M. Brouard, R. Cireasa, A.P. Clark, T.J. Preston, C. Vallance *Orbital polarization effects in molecular photodissociation*
12:20 – 12:40	M.P.J. van der Loo, G.C. Groenenboom, D.C. Radenović, A.J.A. van Roij, D.A. Chestakov, A.T.J.B. Eppink, J.J. ter Meulen, D.H. Parker, M.E. Greenslade, M.I. Lester *One and two-photon processes in the hydroxyl radical*
12:40 – 14:00	**Lunch**
	Session 7: Astrochemistry Chairman: J.P. Reid
14:00 – 14:50	**Plenary Lecture** I.R. Sims (Université de Rennes 1) *Gas-phase kinetics and dynamics at very low temperatures: Obtaining data for astrochemistry*
14:50 – 15:10	N. Choi, M. Blitz, M.J. Pilling, L. Wang, P.W. Seakins *H-atom branching ratios from CN + C_2H_2, C_2H_4 reactions as a function of temperature and pressure*
15:10 – 15:30	R. J. Cody, A. S. Pimentel, W. A. Payne, F. L. Nesbitt *Outer planets' atmospheric chemistry: Rate constant for the CH_3 + C_2H_5 reaction at low temperatures and pressures*
15:30 – 16:00	**Tea break**

Session 8: General gas kinetics
Chairman: J.C. Whitehead

16:00 – 16:20	W. D. Geppert, F. Hellberg, A. Ehlerding, F. Österdahl, R.Thomas, J. Semaniak, M. Kamińska, A. Al-Khalili, M. af Ugglas, N.Djurić, A. Paál, M. Larsson *Unexpected branching ratios in astrophysically important dissociative recombination reactions*
16:20 – 16:40	S.A. Carl, H M.T. Nguyen, R.M.I. Elsamra, R.M. Kulkarni, M.T. Nguyen, J. Peeters *An experimental and theoretical investigation of the $C_2H + NH_3$ reaction*
16:40 – 17:00	W. Roth, T. Schüssler, C. Alcaraz, I. Fischer *Dissociative photoionisation of hydrocarbon radicals*
17:00 – 17:20	G. Friedrichs, M. Fikri, Y. Q. Guo, J. Neumann, F. Temps *Time-resolved cavity ringdown measurements of fast reactions: retrieving rate constants from non-exponential ringdown signals*
17:20 – 17:40	R.S Mason, I.P. Mortimer, D.J. Mitchell, N.A. Dash *The glow discharge plasma is a Rydberg gas*
18:00 – 19:00	**Poster session B**
19:00 – 20:30	**Dinner**
20:30 – 22:00	**Poster session B continued**

Tuesday 10th August

07:30 – 08:45	**Breakfast**
	Session 9: Combustion and high temperature kinetics Chairman: H. Hippler
09:00 – 09:50	**Plenary Lecture** J. Warnatz (Universität Heidelberg) *The long way from reaction kinetics experiments to rate data usable in technological applications*
09:50 – 10:10	C.A. Taatjes, T. Kasper, A. McIlroy, T.A. Cool, K. Nakajima, J. Wang, M.E. Law, A. Morel, P.R. Westmoreland, L. Poisson, D.S. Peterka, M. Ahmed *Synchrotron photoionization molecular-beam mass spectrometric characterization of intermediates in rich flames*
10:10 – 10:30	D.M. Matheu, A.M. Dean, J.M. Grenda, W.H. Green Jr. *Systematic, automated model construction for high-conversion ethane pyrolysis*
10:30 – 11:00	**Coffee break**

Session 10: Combustion and high temperature kinetics
Chairman: J. Peeters

11:00 – 11:20	H. Hippler, N. Krasteva, F. Striebel *The thermal unimolecular decomposition of HCO*
11:20 – 11:40	A. Fontijn, S.M. Shamsuddin, P. Marshall, W.R. Anderson *The products of the NH + CO_2 and H_2O reactions. Practical and fundamental aspects*
11:40 – 12:00	J.T. Herbon, R.K. Hanson, C.T. Bowman, D.M. Golden *The reaction of CH_3 + O_2: Experimental determination of the rate coefficients for the product channels at high temperatures*
12:00 – 12:20	W. Hack, K. Hoyermann, J. Nothdurft, M. Olzmann, T. Zeuch *Formation and decomposition of chemically activated c-C_5H_9O radicals in the gas phase*
12:20 – 12:40	A. Goumri, J. Naidoo, E. Mitchell, Y. Gao, P. Marshall *Addition reactions of sulfur species: S + NO, O + SO_2, and S + N_2O*
12:40 – 19:00	**Excursion to Bath** Coaches leave Wills Hall at 1 pm.
19:00 – 20:30	**Dinner**
20:30 – 21:30	**Polanyi Medal Lecture.** Chairman: D.E. Heard D.C. Clary (University of Oxford) *Quantum reaction dynamics of polyatomic molecules.*

Wednesday 11th August

07:30 – 08:45	**Breakfast**
	Session 11: Surface chemistry Chairman: H.P. Loock
09:00 – 09:50	**Plenary Lecture** A.M. Wodtke (UC Santa Barbara) *Do we know how to think about surface chemistry? Electronically non-adiabatic interactions in molecule metal-surface scattering.*
09:50 – 10:10	S.P.K. Köhler, M. Allan, H. Kelso, D.A. Henderson, K.G. McKendrick *Gas-liquid interfacial reaction dynamics between $O(^3P)$ atoms and squalane*
10:10 – 10:30	M. Kawasaki, H. Tachikawa *Hydrogen atom production from the photolysis of water ice particles*
10:30 – 11:00	**Coffee break**

Session 12: Atmospheric chemistry
Chairman: P.H. Wine

11:00 – 11:20	P. Behr, A. Terziyski, U. Scharfenort, R. Zellner *Reversible gas adsorption in coated wall flow tube reactors. Model simulations and application to the uptake of acetone on ice around 200 K*
11:20 – 11:40	F. Louis, G. Leyssens, J.P. Sawerysyn, V. Feigenbrugel, S. Le Calve, P. Mirabel *Uptake measurements of phenolic compounds by water droplets and determination of their Henry's law constants over the temperature range 278-303 K: Implications for tropospheric multiphase chemistry*
11:40 – 12:00	J.P. Reid, R.M. Sayer, R. Symes, R. Gilham, R. Hopkins, A. Cotterill *Towards examining single aerosol particle dynamics*
12:00 – 12:20	T. J. Wallington, M. P. Hurley, M. P. Sulbaek Andersen, J. C. Ball, D. A. Ellis, J. W. Martin, S. A. Mabury *Atmospheric degradation of fluorotelomer alcohols: a significant global source of perfluorinated acids?*
12:20 – 12:40	L. Vereecken, J. Peeters *Tropospheric oxidation of terpenes and isoprene: Ring closure in unsaturated oxy- and peroxy radicals*
12:40 – 14:00	**Lunch**

Session 13: Combustion chemistry
Chairman: M.J. Pilling

14:00 – 14:50	**Plenary Lecture** K. Kohse-Höinghaus (Universität Bielefeld) *Investigations of high-temperature gas phase systems*
14:50 – 15:10	J. V. Michael, M.-C. Su, J. W. Sutherland, N. Srinivasan *High-T measurements in reflected shock waves of rate constants for $CH_3 + O_2$*
15:10 – 15:30	T. Bentz, R.X. Fernandes, B.R. Giri, H. Hippler, M. Olzmann *High-temperature kinetics of propyne and allene: decomposition vs. isomerization*
15:30 – 16:00	**Tea break**

Session 14: General gas kinetics
Chairman: R. Walsh

16:00 – 16:20	D. Johnson, P. Cassanelli, R.A. Cox *The isomerisation of simple alkoxyl radicals: new temperature-dependent rate data and structure activity relationship*
16:20 – 16:40	P. Cleary, K. McKee, M. Blitz, P. Seakins, L. Wang, M.J. Pilling *Reaction kinetics of $OH + C_2H_{2n}$ from 200 - 300K*
16:40 – 17:00	J. Troe *Breakdown of variational transition state theory in barrierless recombination reactions of large radicals*

17:00 – 17:20	S. J. Klippenstein, Y. Georgievskii, L. B. Harding *An efficient and accurate direct transition state theory approach for radical-radical associations*
17:20 – 17:40	D.C. McCabe, B. Rajakumar, I. W. M. Smith, A. R. Ravishankara *Temperature-dependent rate coefficients for removal of OH ($v = 1$) by several species*
18:30	**Bus departures for @Bristol**
19:00	**Reception at @Bristol**
20:00	**Conference Banquet**
23:30	**Bus departures for Wills Hall**

Thursday 12th August

07:30 – 08:45	**Breakfast**
	Session 15: Reaction and photodissociation dynamics Chairman: R.J. Donovan
09:00 – 09:50	**Plenary Lecture** S.R. Leone (UC Berkeley) *Femtosecond soft X-ray photoelectron molecular dynamics*
09:50 – 10:10	N. H. Nahler, O.P.J. Vieuxmaire, J.R. Jones, M.G.D. Nix, R.N. Dixon, M.N.R. Ashfold *Photodissociation studies of state-selected molecular ions by velocity map ion imaging*
10:10 – 10:30	Y. Ganot, A. Golan, X. Sheng, I. Bar, S. Rosenwaks *Adiabatic and non-adiabatic dissociation of rovibrationally excited acetylene and its homologues*
10:30 – 11:00	**Coffee break**
	Session 16: Atmospheric Chemistry Chairman: D.E. Shallcross
11:00 – 11:20	A.J. Hynes, L. D'Ottone, P. Campuzano-Jost, M. Fardy *Kinetic and mechanistic studies of product isomer branching in the recombination of OH with NO_2*
11:20 – 11:40	N.I. Butkovskaya, A. Kukui, N. Pouvesle, G. LeBras *Formation of nitric acid or its isomer, peroxynitrous acid, in the gas-phase HO_2 + NO reaction studied by high pressure turbulent flow reactor/ chemical ionization mass spectrometry*
11:40 – 12:00	J.R. Barker, Y. Liu, L.L. Lohr *Dynamics of the $OH + NO_2 \rightarrow HONO_2$ recombination reaction*

12:00 – 12:20	T. Gierczak, E. Jimenez, V. Riffault, J.B. Burkholder, A.R. Ravishankara *HO_2NO_2 thermal decomposition rate coefficient measurements and $\Delta_r H^0_{298K}$ determination*
12:20 – 12:40	T.J Dillon, D. Hoelscher, J.N. Crowley *Laboratory studies of iodine oxide chemistry*
12:40 – 14:00	**Lunch**
	Session 17: Atmospheric chemistry Chairman: R.A. Cox
14:00 – 14:50	**Plenary Lecture:** M. Molina (MIT) *Laboratory and field studies of the atmospheric oxidation of volatile organic compounds.*
14:50 – 15:10	C.S.E. Bale, C.E. Canosa-Mas, R.P. Wayne *A study into the kinetics of the reaction of IO with CH_3O_2*
15:10 – 15:30	S.B. Couling and A.B. Horn *Deposition of nitric acid on to molecularand ionic sulfuric acid hydrate thin films*
15:30 – 16:00	**Tea break**
16:00	**End of the Gas Kinetics Symposium**

Posters

Poster session A Sunday 8th August **Poster session B Monday 9th August**

A1 *Temperature dependence of the reactions between a series of acetates and Cl atoms*, A. Notario, C.A. Cuevas, E. Martínez and J. Albaladejo

B1 *Low pressure kinetic and mechanistic study of the reaction of Cl with acrolein*, A. Aranda, Y. Díaz de Mera, A. Rodríguez, D. Rodríguez, L. Morales, E. Martínez and E. Jiménez.

A2 *Experimental study of the interaction of HO_2 radicals with soot surface*, Y. Bedjanian, S. Lelievre and G. Le Bras.

B2 *Absorption cross sections for the second and third OH-stretch overtone of pernitric acid, nitric acid, and hydrogen peroxide*, H. Stark, M. Aldener, S. Brown, J.B. Burkholder, and A.R. Ravishankara.

A3 *Laboratory measurements of particle nucleation in monoterpene ozonolysis,* J.B. Burkholder, T. Baynard, E.R. Lovejoy, and A.R. Ravishankara.

B3 *Atmospheric chemistry of furans: kinetic and mechanism study of their reactions with NO_3 radicals and Cl-atoms*, B.Cabañas, M.T. Baeza, F. Villanueva, M.P. Martín, S. Salgado and E. Monedero.

A4 *Studying the fundamentals of the uptake of NH_3 onto micron sized acidified water droplets using a laser induced fluorescence technique*, A.J. Cotterill, J. Buajarern, R.M. Sayer and J.P. Reid.

B4 *Laser induced fluorescence studies of atmospheric mercury cycling: ultra-sensitive detection and laboratory kinetics*, D. Donohoue, A.J. Hynes and D. Bauer.

A5 *The contribution of sea salt to the marine submicron aerosol mode: size segregated and total sea salt aerosol distributions at a coastal marine site*, D. Donohoue, P. Campuzano-Jost , H. Maring and A.J. Hynes.

B5 *Kinetics of the reactions of CH_2Br and CH_2I radicals with O_2 at atmospheric temperatures*, A. Eskola, D. Wojcik, E. Ratajczak, and R. Timonen.

A6 *A pulsed Laval nozzle apparatus for the study of kinetics at very low temperatures*, A. Goddard, D.E. Heard and S.E. Taylor.

B6 *Studies of iodine monoxide by laser-induced fluorescence*, T. Gravestock, M.A. Blitz, W.J. Bloss and D.E. Heard.

A7 *Measurement of the chemical lifetime of OH in the atmosphere during TORCH*, W. J. Bloss, J. Davey, D. E. Heard, T. Ingham, G. P. Johnson, M. J. Pilling, D. E. Self, S. C. Smith and J. Stanton.

B7 *The North Atlantic Marine Boundary Layer Experiment (NAMBLEX),* D.E. Heard and the NAMBLEX consortium.

A8 *Reactions of partially oxidised hydrocarbons (POH) with OH*, D. Hölscher, T.J. Dillon and J.N. Crowley.

B8 *Using pulsed laser techniques to probe the mass transfer dynamics of multicomponent aerosol droplets*, R.J Hopkins, R.M. Sayer, J.P. Reid.

A9 *The influence of inorganic iodine compounds on the oxidative capacity of the marine boundary layer*, D.M. Joseph, S. H. Ashworth and J. M. C. Plane.

B9 *Reactions of halogen atoms and halogen monoxides with dimethyl sulfide*, S. Enami, Y. Nakano, S. Hashimoto, S. Aloisio, and M. Kawasaki.

A10 *Kinetic measurements of CH_3S addition to isoprene between 213 and 373 K*, L.C. Koch and A.R. Ravishankara.

B10 *Continuous wave diode laser cavity ring-down and cavity enhanced absorption spectroscopy for trace gas detection*, R.E Lindley, M.I. Mazurenka, A.M. Parkes, R. Wada, A. Shillings and A.J. Orr-Ewing.

A11 *Mechanism of the ozonolysis of unsaturated compounds leading to SOA formation*, Y. Ma and G. Marston.

B11 *Detection of the Criegee intermediate by fast flow coupled to FTIR*, S.A. Kennedy, R. Walsh, G. Marston, R.J. Knight, K.M. Smith and R.G. Williams.

A12 *Formation of $O(^3P)$ atoms in the photolysis of N_2O at 193 nm and $O(^3P)$ + N_2O product channel in the reaction of $O(^1D)$ + N_2O*, Y. Matsumi, S. Nishida, and K. Takahashi.

B12 *Accurate determination of the absolute quantum yield for $O(^1D)$ formation in the photolysis of ozone at 308 nm*, Y. Matsumi, K. Takahashi, S. Hayashi, and T. Suzuki.

A13 *Reaction of hydroxyl radical with oxygenated organic compounds. A variational transition-state theory approach*, M. Ochando-Pardo, I. Nebot-Gil, À. González-Lafont, J.M. Lluch.

B13 *Examination of the OH formation mechanism in the reactions CH_2CHO + O_2 and CH_3CHCHO + O_2*, T. Oguchi, Y. Sato, and H. Matsui.

A14 *Absolute rate determination and mechanistic analysis for the reaction of Cl atoms with CH_2I_2*, V.G. Stefanopoulos, V.C. Papadimitriou, Y.G. Lazarou, and P. Papagiannakopoulos.

B14 *Measurement of the rate constant for the reaction H + C_2H_5 at low pressure and low temperature*, A. S. Pimentel, W. A. Payne, F. L. Nesbitt, R. J. Cody, and L. J. Stief.

A15 *Theoretical study of the OH addition to the β-pinene*, V.M.R. Ramírez.

B15 *The master chemical mechanism – latest improvements (MCMv3.1)*, S.M. Saunders, M.E. Jenkin, C. Bloss, V. Wagner, A.R. Rickard, L. Whitehouse, S. Pascoe and M.J. Pilling.

A16 *The development of a novel sodium atom chemiluminescence technique for measuring the concentration of OH in the atmosphere*, D.E. Self, J.M.C. Plane, D.E. Heard and W.J. Bloss.

B16 *Kinetic studies of the reaction of R + O_2 (R = C_6H_5, C_2H_3)*, K. Tonokura, H. Chishima, and M. Koshi.

A17 *Gas-phase reactions of the OH radicals with catechol*, E. Turpin, A. Tomas, C. Fittschen, N. Locoge, P. Devolder.

B17 *Discharge-flow studies of the kinetics of the reactions of NO_3 with CH_3O_2, $C_2H_5O_2$ and CF_3O_2*, S. Vaughan, C.E. Canosa-Mas and R.P. Wayne.

A18 *Atmospheric chemistry of $CF_3CFHCF_2OCF_3$ and $CF_3CFHCF_2OCF_2H$: reaction with Cl atoms and OH radicals, degradation mechanism, and global warming potentials*, T. J. Wallington, M. P. Hurley, M. P. Sulbaek Andersen, and O.J. Nielsen.

B18 *Laser flash photolysis kinetics study of the NO + O_3 reaction*, E.G. Estupinan, J.M. Nicovich, and P.H. Wine.

A19 *Negative-ionization mass spectrometry studies on the reactions of alkyl peroxy radicals with NO*, J.-H. Xing, Y. Nagai, M. Kusuhara, and A. Miyoshi.

B19 *Gas-phase reaction of OH radical with a series of linear ketones: kinetics and temperature dependence between 228 and 405 K*, E. Jiménez, B. Ballesteros, E. Martínez and J. Albaladejo.

A20 *Kinetic studies on the reactions of hydroxyl radicals with a series of alkoxy esters*, S.M. O'Donnell, H.W. Sidebottom. J.C. Wenger, A. Mellouki and G. Le Bras.

B20 *Kinetics of the OH radical reaction with amides*, G. Solignac, A. Mellouki, G. Le Bras, I. Barnes.

A21 *Photochemistry of formaldehyde*, M.N.R. Ashfold, A.J. Orr-Ewing, F.D. Pope, D.E. Shallcross, and C.A. Smith.

B21 *A study of night-time chemistry of HO_x radicals in the Northern and Southern Hemisphere*, R. Sommariva, Z. Fleming, D.E. Heard, J.D. Lee, P.S. Monks, M.J. Pilling, and L. Whitehouse.

A22 *Isomerization of 1-butoxy radicals*, M. Paulus and F. Zabel

B22 *Stereodynamics of the $H + D_2$ reaction: how the direction of the initial rotation does control the reactivity*, J. Aldegunde, J.M. Alvariño, M.P. de Miranda and F.J. Aoiz.

A23 *Photodissociation of ozone in the Hartley bands: conical intersections, potential energy surfaces and dynamics*, E. Baloitcha and G.G. Balint-Kurti.

B23 *Ion imaging studies of photon-initiated bimolecular reactions,* M.J. Bass, M. Brouard, R. Cireasa and C. Vallance.

A24 *The reactions $H + H_2O$ and $H + D_2O$: stereodynamics and new values for the integral cross-sections*, M. Brouard, S. Marinakis, L. Rubio and C. Vallance.

B24 *Dynamics of HCCO and CH_2 radical formation from the reaction $O(^3P) + C_2H_2$ in crossed beams using soft electron impact ionization for product detection*, G. Capozza, F. Leonori, E. Segoloni, G. G. Volpi, and P. Casavecchia.

A25 *The dynamics of prototype insertion reactions: crossed beam experiments versus quantum and quasiclassical trajectory scattering calculations on ab initio potential energy surfaces for $C(^1D) + H_2$ and $N(^2D) + H_2$*, N. Balucani, G. Capozza, E. Segoloni, L. Cartechini, R. Bobbenkamp, P. Casavecchia, L. Bañares, F. J. Aoiz, P. Honvault, B. Bussery-Honvault, J.-M. Launay.

B25 *Crossed molecular beam studies of radical-radical reactions: $O(^3P) + C_3H_5$ (allyl)*, G. Capozza, F. Leonori, E. Segoloni, N. Balucani, D. Stranges, G. G. Volpi, and P. Casavecchia.

A26 *Ab initio calculations of the first absorption band of N_2O and dynamical prediction of diffuse vibrational structures,* M.N. Daud, A. Brown and G.G. Balint-Kurti.

B26 *Optical triple-resonance study of non-adiabatic processes*, R.J.Donovan, T.Ridley, K.P.Lawley and A.M.Sjodin.

A27 *Vibrational excitation of the O_2 reagent in the reaction $H + O_2 \Leftrightarrow OH + O$*, R.J. Duchovic and M.A. Parker.

B27 *The photodissociation of the t-butyl radical, C_4H_9*, M. Zierhut, W. Roth and I. Fischer.

A28 *Photodissociation of O_2 in the Schumann-Runge band into spin-orbit substates*, T. Jeranko and G.G. Balint-Kurti.

B28 *Photodissociation and ionisation of two-photon aligned states of HCl and HBr*, S. Manzhos, C. Romanescu, H.-P. Loock and J. Underwood.

A29 *Theoretical study of structures and relative stabilities of 4-methylphenol water complexes*, F. Louis.

B29 *Quasiclassical trajectory study of the collision-induced dissociation of CH_3SH^+ + Ar*, E. Martínez-Núñez, S.A. Vázquez, and J.M.C. Marques.

A30 *Time-dependent and time-independent stereodynamics of the H + D_2 reaction*, R.A. Pettipher and M.P. de Miranda.

B30 *Polarization effects in laser quantum control of chemical processes,* Q. Ren, G.G. Balint-Kurti, F.R. Manby, H. Rabitz, and M. Artamonov.

A31 *Rovibrational distributions of HF in the photodissociation of vinyl fluoride at 193 nm: A direct MP2 quasiclassical trajectory study*, S. Vázquez and E. Martínez-Núñez.

B31 *Photodissociation studies of state-selected $BrCl^+$ molecular ions by velocity map ion imaging*, O.P.J. Vieuxmaire, N. Hendrik Nahler, J.R. Jones, R.N. Dixon, and M.N.R. Ashfold.

A32 *Ultraviolet photofragmentation dynamics of pyrrole studied by H (Rydberg) atom photofragment translational spectroscopy*, B. Cronin, M.G.D. Nix, R.H. Qadiri and M.N.R. Ashfold.

B32 *Time resolved FTIR emission studies of molecular dynamics*, G. Hancock, M.D. Morrison and M.J. P. Saunders.

A33 *H-atom abstraction reactions between Cl atoms and organic molecules*, C. Murray, J.K. Pearce, P.N. Stevens and A.J. Orr-Ewing.

B33 *Product study of the reaction between thiophene and nitrate radical,* M.T. Baeza, B. Cabanas, M.P. Martin, S. Salgado, F. Villanueva, E. Monedero and K. Wirtz.

A34 *REKIN, an experiment to study the oxidation of metal vapors: first experiments with $Zn_{(g)}$ and O_2*, I. Alxneit and P.Bodek.

B34 *What we have learned about the stabilities of cyclopropane and cyclopropene group 14 ring analogues, through gas phase kinetic studies of cycloaddition reactions of heavy methylenes (silylene and germylene) combined with quantum chemical (ab initio) studies*, R. Becerra, S.E. Boganov, M.P. Egorov, V.I. Faustov, I.V. Krylova, O.M. Nefedov, V.M. Promyslov, N.D. Zelinsky, and R. Walsh.

A35 *X-ray free-electron lasers: requirements for the UK?* R.J. Donovan.

B35 *Low temperature reactions of OH radicals with unsaturated hydrocarbons*, B. Hansmann.

A36 *Mechanism of the oxidation of hydrocarbons transplanted from gas-phase conditions to solution chemistry*, I. Hermans, T.L. Nguyen, P.A. Jacobs, J. Peeters.

B36 *Dependence of water on the kinetics of the self reaction of HO_2*, N. Kanno, M. Uetake, K. Tonokura, A. Tezaki and M. Koshi.

A37 *UV absorption spectra and kinetics of methyl substituted hydroxycyclohexadienyl radicals*, L.N. Krasnoperov, D. Johnson, R. Lesclaux.

B37 *A kinetic analysis of the effect of O_2 on the reactions of atomic bromine with some hydrocarbons and ethers*, L.M. Anthony and J.M. Roscoe.

A38 *Ultraviolet CO chemiluminescence in $CH(X^2\Pi)$ and $CH(a^4\Sigma^-)$ reactions with atomic oxygen at 298 K*, G.L. Vaghjiani.

B38 *The β bond dissociation reactions of "biallyl" type of radicals*, M. Szori, I.G. Csizmadia, and B. Viskolcz.

A39 *How can very different chemical kinetic models produce similar results?* I. Gy. Zsély, J. Zádor and T. Turányi.

B39 *Which rate parameters should be measured more precisely to improve complex kinetic models?* J. Zádor, I. Gy. Zsély, and T. Turányi.

A40 *Trajectory simulations of polyatomic-polyatomic collisions*, V. Bernshtein and I. Oref

B40 *Measurement of relaxation of orientation and alignment in inelastic collisions by polarisation spectroscopy*, M.L. Costen, H.J. Crichton, K.G. McKendrick and G. Richmond.

A41 *State-to-state collisional energy transfer in electronically excited CH/D radicals*, G. Richmond, M. L. Costen and K. G. McKendrick.

B41 *Interrogation of nitrogen plasmas using diode lasers*, B. Bakowski, G. Hancock, R. Peverall, S. E. Prince, G. A. D. Ritchie and L. Thornton.

A42 *Investigating hydrocarbon radicals with synchrotron radiation*, T. Schüssler, C. Alcarez, M. Elhanine, H.J. Deyerl, W. Roth and I. Fischer.

B42 *Absolute rate measurements and product distribution study of the reactions of electronically excited $CF_2(^3B_1)$ with O_2 and NO*, B. Dils, R.M.I. Elsamra, T.L. Nguyen, S.A. Carl and J. Peeters.

A43 *The mechanism of NO_x formation in the plasma treatment of waste gas streams*, A.M. Harling, J.C. Whitehead and K. Zhang.

B43 *Shock-tube investigations of the unimolecular decompositions of benzene and the phenyl radical*, B. R. Giri, H. Hippler, M. Olzmann, and O. Welz.

A44 *Ion–molecule reactions and TPEPICO spectroscopy of HCFCs – a comparison*, C.R. Howle,

D.J. Collins, C.A. Mayhew and R.P. Tuckett.

B44 *Formaldehyde yields in the OH + C_2H_4 reaction*, H. Hippler, S. Nasterlack, M. Olzmann and F. Striebel.

A45 *Measurement of adiabatic burning velocity in flat premixed flames of CO + H_2 + O_2 + N_2 to validate kinetic mechanisms*, A.A. Konnov and I.V. Dyakov.

B45 *Destruction of three freons (CH_2F_2, CH_2FCl and CH_2Cl_2) in dielectric barrier discharge: kinetics and mechanistic implications*, L.G. Krishtopa and L.N. Krasnoperov.

A46 *Absolute rate measurements and product distribution study of the reactions of electronically excited $CF_2(^3B_1)$ with several hydrocarbons*, B. Dils, R.M. Kulkarni, S.A. Carl and J. Peeters.

B46 *Quenching rates of field-ionising Rydberg states of Ar in a fast flow glow discharge plasma*, R.S. Mason, I.P. Mortimer, and N.A. Dash.

A47 *Reactions of H/SO_2 adducts with atomic hydrogen*, X. Hu and P. Marshall.

B47 *Experimental and detailed chemical kinetic modelling study of the mutual sensitisation of the oxidation of nitric oxide and methane over extended temperature and pressure ranges*, P. Dagaut and A. Nicolle.

A48 *The effect of SO_2 on SNCR: experimental and detailed chemical kinetic modelling study*, P. Dagaut and A. Nicolle.

B48 *Cavity ring-down spectroscopy of a DC arcjet diamond depositing plasma*, C.J. Rennick, J.A. Smith, M.N.R. Ashfold and A.J. Orr-Ewing.

A49 *Recent work on the $OH/CH_3OCH_3/O_2$ system including isotopic studies*, T.J. Still, M.A. Blitz, K. McKee and P.W. Seakins.

B49 *Formation pathway of HO_2 in the reaction of methoxymethyl with molecular oxygen*, K. Suzaki, N. Kanno, K. Tonokura, M. Koshi and A. Tezaki.

A50 *Ab initio study of allylic hydrogen abstraction from polyalkenes*, M. Szori, B. Viskolcz.

B50 *The oxidation of carbon soot in a non-thermal, atmospheric pressure plasma: experiment and modelling*, A.R. Martin, J.T. Shawcross, and J.C. Whitehead.

A51 *Detailed chemical kinetic modelling of the gas-phase processes during straw combustion*, T. Perger, I. Gy. Zsély, and T. Turányi.

B51 *Tropopause chemistry revisited: HO_2 initiated oxidation as a major acetone sink,* I. Hermans, T.L. Nguyen, P.A. Jacobs, and J. Peeters.

A52 *Rate coefficients for removal of $CN(X^2\Sigma^+, v = 2)$ from selected rotational levels between $N_i = 0$ and 57 in collisions with N_2 and C_2H_2*, K.M. Hickson, C.M. Sadowski, and I.W.M. Smith.

B52 *Kinetic study of the temperature dependence of the OH initiated oxidation of dimethyl sulphide*, M. Albu, I. Barnes, and R. Mocanu.

A53 *Kinetics study of the reaction $OH + NO_2 + M$: pressure and temperature dependent falloff parameters*, S. Valluvadasan, D.B. Milligan, W.J. Bloss, and S.P. Sander.

Abstracts of Plenary Lectures and Contributed Talks

The uptake of meteoric metal atoms on polar mesospheric clouds

John M. C. Plane[1], Benjamin J. Murray[1], Tomas Vondrak[1], Stephen R. Meech[2]

[1]School of Environmental Sciences, [2]School of Chemical Sciences and Pharmacy, University of East Anglia, Norwich NR4 7TJ, United Kingdom

Email: j.plane@uea.ac.uk

Polar mesospheric clouds (PMCs) occur at high latitudes during mid-summer, over the height range 82 – 86 km. The clouds overlap in altitude with the layers of metal atoms (Na, K, Fe etc.) that are produced by the ablation of meteoroids entering the atmosphere. This paper will examine several of the probable interactions between PMCs and metals. The lidar technique has been employed to observe both the metal layers (by resonance fluorescence scattering) and the PMCs (by Mie scattering), with fine height resolution. Observations at South Pole show that essentially all of the Fe atoms in the vicinity of a strong PMC disappear. Lidar observations at various Arctic locations have shown that Na and K atoms are substantially removed below 90 km in the high-latitude summer mesosphere, and the undersides of these layers exhibit extremely small scale-heights. These features indicate that the metals are removed rapidly from the gas phase by uptake on the ice particles, at a rate that exceeds their replenishment by meteoric ablation and vertical transport. It has been speculated that the incorporation of these metals into the ice lowers the photoelectric work function sufficiently to explain the occasional observation of positively-charged ice particles. The electrical environment of these particles is important because they give rise to strong radar backscatter (termed Polar Mesospheric Summer Echoes).

In this paper we will report new laboratory studies of the uptake of Na, K and Fe on low-temperature ice, using a fast flow tube technique. Na and K stick on ice (amorphous or cubic crystalline) at essentially every collision, over the temperature range 100 – 160 K. Uptake of Fe is also very efficient, although the uptake coefficient falls below 0.1 below 130 K. An atmospheric model incorporating the experimental results will be used to show that the metal depletions observed in the mesosphere are explained by heterogeneous uptake. An important conclusion is that there appears to be a permanent layer of small (less than 20 nm) particles above 85 km throughout mid-summer at high latitudes.

We will also report measurements of the photo-electric work function of Na in ice, using a pulsed laser technique with electron time-of-flight spectroscopy. This shows that ice with freshly-deposited Na has a low work function (< 2.8 eV) and a very large cross-section for photo-electric emission. Although the majority of Na atoms appear to react (presumably to form NaOH) on a time-scale of minutes even at temperatures of 130 K, photo-electric emission is much faster. These results indicate that when turbulence, for instance at a wind shear, mixes Na atoms from above 87 km with ice particles below 86 km, every particle on which a Na atom adsorbs will become positively charged, with significant consequences for the radar backscatter.

Near-IR Kinetic Spectroscopy of Peroxy Radical Reactions

L. S. Alconcel*, D. J. Robichaud†, M. Okumura†, S. P. Sander*

** Jet Propulsion Laboratory, 4800 Oak Grove Dr M/S 183-901, Pasadena, CA 91109-8099, USA*
† California Institute of Technology, M/S 127-72, 1200 E. California Blvd, Pasadena, CA 91125, USA

Hydroperoxy (HO_2) and alkylperoxy (RO_2) radicals are key intermediates in the formation of tropospheric ozone. Accurate measurements of the rates of the reactions of these short-lived radical species are needed to model the clean and polluted atmosphere. While kinetic data for reactions of peroxy radicals have improved in recent years, there are still numerous uncertainties. For example, the previously measured temperature dependencies of the self and cross-reactions rates of some of the peroxy radicals are contradictory. The current study addresses the deficiencies in the kinetic data for this class of reactions with a unique experimental approach. Monitoring of the HO_2 radical signal via near-IR diode laser frequency modulation (FM) spectroscopy and the RO_2 radical signal via UV absorption spectroscopy permits unique characterization of the peroxy species. It is important that both spectroscopies be used simultaneously and that the rate constants are measured under a range of conditions, since the radical chemistry is complex: the self-reaction of ethylperoxy ($C_2H_5O_2$) radicals, for instance, can lead to the secondary formation of HO_2 radicals. Preliminary studies of the HO_2 + $C_2H_5O_2$ reaction indicate that this technique is capable of operating over a wide dynamic range, from 30:1, of initial $[HO_2]_0$:$[RO_2]_0$. The rate constant measurements of HO_2 + RO_2 reactions, including CH_3O_2 and $C_2H_5O_2$, provided by this technique represent a significant step towards generating more accurate atmospheric models, particularly for the remote troposphere and the stratosphere, where NO is not the dominant sink for RO_2 radicals.

Experimental Studies on the Reactions of Peroxy Radicals with NO_2

Carl Percival, Teresa Raventos-Duran, Asan Bacak, and Max Bardwell.

Department of Physics, University of Manchester Institute of Science and Technology, Sackville Street, PO Box 88, Manchester, M60 1QD. UK.

The formation of tropospheric ozone is strongly dependent on the level of NO_x as a consequence of its reaction with RO_2 (peroxy radicals). It is therefore important to characterise the coupling of NO_x and RO_2 to understand the tropospheric ozone budget. Model studies have shown that in the mid to upper troposphere both HO_2NO_2 and $CH_3O_2NO_2$ may well constitute a significant fraction of NO_y (~ 20%). Despite the importance of these species, there are little or no experimental data available on their formation at the actual temperatures that pertain upper troposphere. A turbulent flow chemical ionisation mass spectrometer has been used to provide kinetic and mechanistic data on the reactions of RO_2 (where R = H or CH_3) with NO_2 over the pressure range 70 – 700 Torr and temperature range 180 – 300 K.

Initial experiments have been carried out to study the reaction of $CH_3O_2 + NO_2$. Experiments were performed under pseudo first order conditions with $[NO_2]$ being at least an order of magnitude than $[CH_3O_2]$ and the kinetic information being provide by monitoring the CH_3O_2 concentration time profiles. Figure 1 shows the pressure dependence of the rate coefficient at 223K. The results represent an extension in the range of temperatures over which the reaction $CH_3O_2 + NO_2$ has been studied experimentally and are in excellent agreement with the values recommended by DeMore et al. Further work on the reaction of $HO_2 + NO_2$ will be reported.

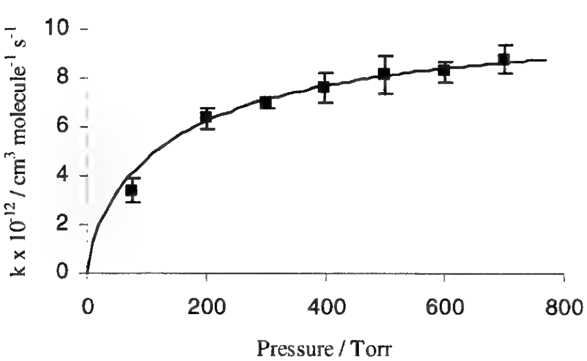

Figure 1 Pressure dependence of the reaction of CH_3O_2 + NO_2 at 223 K

Study of the Atmospherically Important Reaction - Cl_2 with Dimethylsulphide

M.V. Ghosh, D.E. Shallcross[(a)] and J.M. Dyke

Department of Chemistry, University of Southampton, Southampton, UK, SO17 1BJ
(a) Department of Chemistry, University of Bristol

A progress report will be given on a project which is aimed at interfacing a differentially pumped flow-tube to a photoelectron spectrometer and using it to study the kinetics of gas-phase reactions. A rate constant for the Cl_2 + DMS reaction has been measured at room temperature with this apparatus and a summary of the measurements will be presented. This study has been supported by infrared and ultraviolet absorption measurements in a closed cell. The emphasis of this talk, which is the first of two talks, will be on summarizing the kinetics measurements that have been made.

There are numerous processes of atmospheric relevance that need investigation in the DMS oxidation process, but the motivation of this present work was to study the products and mechanism of the reactions $Cl_2 + CH_3SCH_3 \rightarrow product.$ and $Cl + CH_3SCH_3 \rightarrow products.$ The experiments performed at Southampton on the Cl_2 +DMS and Cl + DMS reactions, using a flow-tube inlet system connected to a photoelectron spectrometer, showed that these reactions take place by a number of steps.

In the Cl_2+DMS reaction, an intermediate (Me_2SCl_2) is produced which has a lifetime of several tens of milliseconds before it decomposes to CH_3SCH_2Cl and HCl. Calculations at the MP2/6-31++G** level of theory carried out at Southampton University confirmed the PES results.

In the case of the DMS+Cl reaction, the experimental evidence suggested two possible pathways. In the first one, the first step is hydrogen abstraction which produces the unstable radical CH_3SCH_2. Further reaction with Cl or Cl_2 gives rise to either HCl, CH_3 and HClCS. The second channel gives CH_3SCl and the radical CH_3 directly.

Kinetics, Spectroscopy, and Thermochemistry of the Cl–DMSO Adduct

P.H. Wine,[1,2] J.M. Nicovich,[1] M.L. McKee,[3] K.M. Kleissas,[1,4] S. Parthasarathy,[2] F.D. Pope,[1,5] and A.T. Pegus[1,6]

[1]*School of Chem. & Biochem., Georgia Inst. of Technology Atlanta, GA 30332-0400, USA*
[2]*School of Earth & Atmos. Sci., Georgia Inst. of Technology, Atlanta, GA 30332-0340, USA*
[3] *Dept. of Chemistry, Auburn University, Auburn, AL 36849, USA*
[4] *Now at Dept. of Chemistry, Bucknell University, Lewisburg, PA 17837, USA*
[5] *Now at School of Chemistry, University of Bristol, Bristol BS8 1TS, UK*
[6] *Now at Dept. of Chemistry, University of Sussex, Falmer, Brighton BN1 9QJ, UK*

Dimethylsulfoxide (DMSO) is an important intermediate in the atmospheric oxidation of dimethylsulfide (DMS). As a result, the atmospheric chemistry of DMSO plays a potentially important role in global climate modification (or regulation). We have carried out the most detailed kinetic and mechanistic study of the Cl + DMSO reaction reported to date. This reaction plays a minor role as an oxidation pathway for DMSO under marine boundary layer conditions, and is also of interest for developing a detailed understanding of reactivity trends in H–transfer reactions, adduct formation and dissociation reactions, and adduct bimolecular reactions in radical + organosulfur compound systems.

In one set of experiments, detection of Cl atoms by time-resolved atomic resonance fluorescence spectroscopy has been coupled with laser flash photolysis of $Cl_2CO/DMSO/N_2$ mixtures to investigate Cl + DMSO kinetics over a wide range of temperature and pressure. At T < 300K, the Cl + DMSO rate coefficient is found to have both pressure-independent and pressure-dependent channels. At T = 298 K and P = 600 Torr, the overall rate coefficient is $\sim 1 \times 10^{-10}$ $cm^3 molec^{-1} s^{-1}$ with the pressure-dependent adduct formation channel accounting for 85-90% of the observed reactivity. At T > 400 K, only the pressure-independent pathway is observed, and rate coefficients are considerably slower than those measured at T < 300K. At an intermediate temperature of 330 K, non-exponential Cl atom decays are observed that are attributable to Cl atom regeneration via the adduct dissociation reaction. The observed double exponential decays are analyzed to obtain both the Cl + DMSO addition rate coefficient and the Cl–DMSO unimolecular decomposition rate coefficient; hence, the equilibrium constant for Cl + DMSO $\leftrightarrow$ Cl–DMSO is determined. The experimental equilibrium data are employed in a "third law analysis" to obtain a value of 73±10 kJ mol^{-1} for the 298 K bond dissociation energy of Cl–DMSO; this adduct appears to be less strongly bound than Cl–DMS, but more strongly bound than OH–DMS, OH–DMSO, Br–DMS, and Br–DMSO.

In a second set of experiments, time-resolved UV-visible spectroscopy has been coupled with laser flash photolysis of $Cl_2CO/DMSO/N_2$ mixtures to make the first observations of the gas phase UV-visible absorption spectrum of Cl–DMSO. A broad, unstructured spectrum is observed with $\lambda_{max} \sim 390$ nm and $\sigma_{max} \sim 5 \times 10^{-17}$ $cm^2 molec^{-1}$; the observed gas phase spectrum is almost identical to the aqueous phase spectrum reported by Kishore & Asmus [*J. Phys. Chem.* **1991**, *95*, 7233]. Using adduct absorption at 390 nm as the kinetic probe, 298 K rate coefficients have been measured for reactions of Cl–DMSO with O_2, NO, and NO_2. The measured rate coefficients in units of $cm^3 molec^{-1} s^{-1}$ are $k_{O2} < 1 \times 10^{-18}$, $k_{NO} = 1.6 \times 10^{-11}$ and $k_{NO2} = 2.0 \times 10^{-11}$; these rate coefficients are very similar to those we have reported previously for reactions of the Cl–DMS adduct with O_2, NO, and NO_2 [Urbanski & Wine, *J. Phys. Chem. A* **1999**, *103*, 10935].

Reactivity trends in OH, Cl, Br reactions with DMS and DMSO will be discussed, as will the likely atmospheric fate of Cl–DMSO.

Kinetics of the ClO + ClO and the ClO + BrO Reactions

Gavin Boakes and David M. Rowley

Department of Chemistry, University College London, Christopher Ingold Laboratories, 20 Gordon Street, London WC1H 0AJ, U.K.
d.m.rowley@ucl.ac.uk

The reactions of gaseous halogen monoxide free radicals participate in catalytic cycles which destroy atmospheric ozone. The ClO + ClO association reaction, followed by the solar photolysis of the ClO dimer, Cl_2O_2, is known to be the principal mechanism for massive Springtime stratospheric ozone loss (the ozone 'holes') observed each year over Polar regions. The ClO + BrO reaction couples stratospheric chlorine and bromine chemistries and provides (in one channel) a route to stratospheric OClO. In order to model this atmospheric chemistry accurately, high quality channel specific kinetic data are required for these reactions under appropriate conditions of temperature and pressure.

In this work the kinetics of the ClO association self-reaction and the ClO + BrO bimolecular reaction have been studied as a function of temperature (210-298 K) and pressure (100-760 Torr) using flash photolysis with time resolved UV absorption spectroscopy. The time-honoured method of monitoring peaks in the characteristic vibronic ($A \leftarrow X$) absorption spectrum of the halogen monoxide species has been applied. However, uniquely in this work, a charge coupled device (CCD) has been used to record broadband absorption spectra of reacting gas mixtures at sequential time points during the radical reactions. Spectral deconvolution techniques have allowed the accurate and unequivocal monitoring of multiple UV absorbing species in reactions, constraining kinetic data and providing direct channel specific kinetics for the OClO producing channel of the ClO + BrO reaction.

The results indicate that the ClO + ClO association reaction is more rapid than most previous studies indicate, but in broad agreement with a recent study by Bloss *et al.*[1] The ClO + BrO reaction kinetics and OClO branching ratio are in broad agreement with previous studies. No evidence for any pressure dependence or transient absorptions attributable to a stabilised $BrClO_2$ species was found in the BrO + ClO reaction. The atmospheric implications of these results will be briefly discussed.

---

1. W.J. Bloss *et al.*, *J. Phys. Chem. A.*, **105**, 11226, (2001).

Laser-induced fluorescence detection of $O(^1S)$ atom from O_3 photolysis and its application for kinetic study of the reaction of $O(^1S)$ with atmospheric molecules

Kenshi Takahashi†, Tomoki Nakayama, and Yutaka Matsumi

Solar-Terrestrial Environment Laboratory and Graduate School of Science, Nagoya University (3-13 Honohara, Toyokawa, Aichi, 442-8507, Japan) † kent@stelab.nagoya-u.ac.jp

A new method for direct detection of $O(^1S)$ atom using a technique of laser-induced fluorescence (LIF) at 121.8 nm is presented. The $O(^1S)$ atom was produced from 193 nm photolysis of O_3. The tunable coherent radiation around 121.8 nm as probe laser light was generated by two-photon resonance four-wave difference frequency mixing in Kr/Ar mixture. The limit of detection of our system was estimated to be 1×10^9 atoms cm^{-3}. The sensitivity of this new detection method is high enough to determine the quantum yield for $O(^1S)$ formation from O_3 photolysis at 193 nm to be $(2.5 \pm 1.1) \times 10^{-3}$.

Our study shows a direct evidence of the $O(^1S)$ formation in the UV photodissociation reaction of O_3 for the first time, while there have been many reports on the $O(^1D)$ and $O(^3P)$ formation in this reaction. The contribution for the OH radical production from the reaction of H_2O with $O(^1S)$ produced from O_3 photolysis relative to that from the well-known $O(^1D)$ + H_2O reaction has been estimated as a function of altitude in the stratosphere, using the photolytic $O(^1S)$ quantum yield value obtained in this study and the available rate coefficients for $O(^1S)$ reactions. The maximum contribution of the $O(^1S)$ reaction to the OH production was found to be a 14 %-fraction of that from the $O(^1D)$ reaction at 40 km altitude at mid-latitudes, assuming the spin-forbidden dissociation process, $O(^1S)$ + $O_2(X^3\Sigma_g^-)$, for the formation of $O(^1S)$ in the photolysis of O_3.

Using the new method we have developed, the kinetic study investigating the gas-phase reaction of $O(^1S)$ with atmospheric molecules such as O_2, O_3, CO_2, and H_2O, has also been performed at 295 ± 2 K. Gas mixtures of O_3 with which of O_2, CO_2, and H_2O are irradiated at 193 nm laser light. The $O(^1S)$ atoms are produced from 193 nm photolysis of O_3 and monitored using the LIF method. The reaction rate coefficients are compared with the available literature data on those reactions, in which techniques of the emission observation at 557 nm associated with the forbidden $O(^1S \rightarrow {}^1D)$ transition were used in the former studies. We demonstrate that the LIF technique is a powerful tool to investigate both photodissociation of small molecules to yield $O(^1S)$ and kinetics of the $O(^1S)$ reactions.

Ab initio Modelling of Atmospheric Oxidation Reactions

Jeremy N. Harvey

School of Chemistry and Centre for Computational Chemistry, University of Bristol, Cantock's Close, Bristol BS4 3NQ

Atmospheric oxidation of volatile organic compounds plays an important role in ozone production. Especially for heavier VOCs, it can lead to formation of dicarboxylic acids and other involatile species which can precipitate to form aerosol. In order to understand when this will occur, it is necessary to know the oxidation mechanism, which is frequently highly complex. Computational methods are increasingly used to help understand oxidation mechanisms. In this talk, we will present results of computations on the oxidation mechanism of nopinone, the primary product in the atmospheric oxidation of α- and β-pinene, two monoterpenes which are among the most abundant VOCs emitted by vegetation.

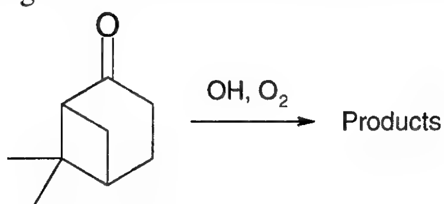

Nopinone

Nopinone is a bicyclic ketone which does not have any carbon-carbon double bonds, so its oxidation is mostly initiated by hydoxyl radical hydrogen atom abstraction. This can occur at one of seven different sites on the molecule. We will describe *ab initio*, density functional theory, and transition state theory computations aimed at predicting the individual rate coefficients, and thereby the overall oxidation rate and the site selectivity, and will compare our results with those derived from empirical rules such as the structure-activity relationships of Atkinson *et al.* We will also discuss the reliability of the computed rate coefficients.

Alternative Spectroscopic Probes of Collisional Energy Transfer

K. G. McKendrick

School of Engineering and Physical Sciences, Heriot-Watt University, Edinburgh, EH14 4AS, UK
e:mail: k.g.mckendrick@hw.ac.uk

The theme of this lecture will be the extraction of information on collisional energy transfer using optical methods. Recent developments in the field will be surveyed. Interest will be focussed on ubiquitous small free radicals of relevance to combustion and atmospheric chemistry, illustrated with examples from the author's own group and elsewhere.

The conceptually simplest approaches are based on well-established linear spectroscopies. These methods nevertheless continue to produce new and interesting information. As a typical example, dispersed laser-induced fluorescence (LIF) is often an effective way of getting information on collision-induced rotational (RET) and vibrational (VET) energy transfer within electronically excited states. In suitable cases, where there happen to be at least two near-degenerate excited states with allowed optical transitions to a lower-lying state, then the method can also be used to study electronic energy transfer (EET). Both intra- and inter-electronic state transfer will be illustrated with recent work on the CH $A^2\Delta$ and $B^2\Sigma^-$ states. New observations on the collision-partner dependence of absolute rates of RET and the efficiency of EET will be discussed.

Optical double-resonance methods in which both steps involve linear absorption (or less commonly, stimulated emission) have also been exploited. However, the generality of these methods is quite restricted by the requirement for the molecule of interest to have suitable combinations of several bound, optically connected excited states.

As an alternative strategy, non-linear optical methods based on variants of four-wave mixing (FWM) are now being developed. In principle, the collision-number dependence of the intensity of the non-linear signal beam provides a direct probe of a number of collisional phenomena. Some of these (e.g. electronic dephasing) are perhaps not of mainstream chemical interest, but with the correct choice of FWM spectroscopy they include the key inelastic processes of RET, VET and EET. In particular, the particular variant of Polarisation Spectroscopy (PS) has been shown to be sensitive not only to these inelastic processes, but also to depolarising collisions that cause realignment of the plane of molecular rotation. This polarisation information, which is difficult to obtain by other methods, provides a new and highly sensitive probe of the anisotropy of the intermolecular potential. More sophisticated double-resonant variants of PS also allow the collisions of ground and excited electronic states to be studied separately. Progress in this field will be illustrated with recent PS-based observations of the collisional behaviour of the OH radical in the $A^2\Sigma^+$ and $X^2\Pi$ states.

Mechanisms for Quenching $^1CH_2$ – Reactive, Nonreactive and Combinations thereof.

M.A. Blitz, N. Choi, T. Kovacs, M.J. Pilling and P.W. Seakins
School of Chemistry, University of Leeds, Leeds, LS2 9JT, UK.

The methylene radical (CH_2) plays an integral role in combustion and has been suggested as a major precursor to soot formation. Ground state $^3CH_2$ has a close lying electronically excited singlet state, $^1CH_2$, with a separation of only 38 kJ mol^{-1}. The proximity of the states and the widely differing reactivities of the two states mean that interconversion must be considered in combustion systems. Despite the importance of CH_2, relatively little is known about the mechanisms for quenching $^1CH_2$, exceptions being extensive room temperature measurements on relaxation by inert species[1] and the temperature dependence of singlet removal by argon.[2] Data are especially lacking for reactions where there is the possibility for both relaxation and reaction. In this contribution we shall present results on the temperature dependence of $^1CH_2$ removal by He, H_2 and O_2. The results show that quenching mechanisms are complex and vary substantially between different classes of reagent.

$^1CH_2$ + He: The removal of $^1CH_2$ has been studied by laser flash photolysis (of ketene at 308 nm)/laser induced fluorescence as a function of temperature from 300–680 K. Agreement with previous room temperature work is good but the temperature dependence of the reaction ($k = (2.1\pm0.4)\times10^{-12}\ T^{2.1\pm0.3}$ cm^3 molecule^{-1}s^{-1}) is significantly stronger than argon ($T^{0.93\pm0.12}$).[2] Such behaviour can be rationalised by a Parmenter Seaver (PS) correlation – where the rates of quenching by inert gases are strongly correlated with an attractive well. The overall temperature dependence of the quenching process has a positive and essentially reagent independent temperature component from a proposed 'rotational gateway' mechanism,[3] and a negative component from the attractive well. As the well depth in the He-CH_2 system is significantly shallower than Ar-CH_2 this negative component is almost absent with the He quencher. Studies on other noble and inert gas systems are currently in progress and will be presented.

$^1CH_2$ + H_2: The rate of removal of $^1CH_2$ by H_2 is much greater than for the noble gases. For H_2, reaction (forming CH_3 and H) as well as relaxation is possible. Previous determinations of the reactive component of the reaction in this laboratory[4] yield a quenching rate coefficient significantly greater than that predicted by a PS correlation. This suggestion of an alternative quenching mechanism has been confirmed by recent experiments observing the temporal dependence of the [H] (via VUVLIF) produced by reaction of either $^1CH_2$ with H_2, or on a longer timescale via quenched $^3CH_2$ and NO. Room temperature results agree with our earlier work ($f_{reaction}$ = 0.85), but as the temperature is raised the quenching component ***decreases*** and at 500 K $f_{reaction}$ = 1.0. The implications of these results on quenching mechanisms with reactive species and soot formation will be discussed.

$^1CH_2$ + O_2: Many highly exothermic channels exist for this reaction, and the $^1CH_2$ removal rate is higher than the PS prediction, suggesting reactive removal. However, the room temperature temporal profile of the H atom product (again observed by VUVLIF) matches production from triplet methylene with no fast component corresponding to singlet methylene reaction[5]. This suggests that collisions of $^1CH_2$ with O_2 lead solely to relaxation. Our interpretation of the low reactivity of $^1CH_2$ with O_2 is that formation of exothermic intermediate complexes (equivalent to CH_4 in the $^1CH_2 + H_2$ system) is spin forbidden and therefore there is a barrier to product formation. Results from current experiments on the temperature dependence of the $^1CH_2 + O_2$ reaction may shed further light on this important reaction.

[1] M.N.R. Ashfold, M.A. Fullstone, G. Hancock, G.W. Ketley, Chem. Phys. 55 (1981) 245.
[2] G. Hancock, M.R. Heal, J. Phys. Chem. 96 (1992) 10316.
[3] U. Bley, F. Temps, J. Chem. Phys. 98 (1993) 1058.
[4] M.A. Blitz, M.J. Pilling, P.W. Seakins, Physical Chemistry Chemical Physicis 3 (2001) 2214.
[5] M.A. Blitz, K.W. McKee, M.J. Pilling, P.W. Seakins, Chem. Phys. Lett. 372 (2003) 295.

Investigations of collisional energy transfer of highly vibrationally excited *trans*-stilbene

T. Lenzer, H. Frerichs, M. Hollerbach, K. Luther
Institut für Physikalische Chemie, Universität Göttingen, Tammannstr. 6,D-37077 Göttingen, Germany, E-mail: tlenzer@gwdg.de

The development of advanced measurement techniques has opened up new possibilities to accurately determine central quantities of collisional energy transfer at the typically very high densities of states of larger molecules, relevant, *e.g.*, to combustion systems. In addition, previously inaccessible parameters like higher moments of energy transfer and distributions of collisional transition probabilities have been determined.[1,2] As the number of systems investigated is constantly growing, it becomes increasingly possible to identify systematic tendencies of important energy transfer parameters.

In this contribution, the collisional energy transfer of *trans*-stilbene in the gas phase has been investigated by applying the method of "Kinetically Controlled Selective Ionization (KCSI)" developed in our group. All measurements can be described by a three-parameter-form of the energy transfer probability $P(E',E) \propto \exp[-\{(E-E')/(C_0+C_1 \cdot E)\}^Y]$ (for $E' < E$, with the upward wing given by detailed balance), which was recently proposed by us, and in the meantime has also been theoretically confirmed by statistical models.[3] The shape parameter Y shows a systematic increase with the size of the collider, ranging from $Y < 1$ for helium up to $Y > 1$ for n-heptane. This corresponds to an increased or decreased amplitude of highly efficient collisions compared to a monoexponential model ($Y = 1$), respectively. Comparisons with our earlier experiments on toluene[1] and azulene[2] show, that in the case of small colliders the deactivation of the larger *trans*-stilbene molecule is considerably more efficient, as it might be expected due to the larger number of low frequency modes in *trans*-stilbene. Surprisingly, for large colliders this difference in energy transfer efficiency is much less pronounced. Possible reasons like incomplete IVR during the collision or vibrational resonances will be discussed to explain this strikingly different behavior.

[1] T. Lenzer, K. Luther, K. Reihs, and A.C. Symonds, J. Chem. Phys. **112**, 4090 (2000).
[2] U. Hold, T. Lenzer, K. Luther, and A.C. Symonds, J. Chem. Phys. **119**, 11192 (2003).
[3] D. Nilsson, S. Nordholm, T. Lenzer, and K. Luther, Phys. Chem. Chem. Phys., submitted.

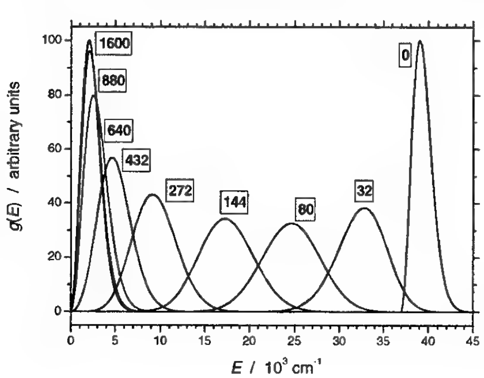

Collisional deactivation of a highly vibrationally excited trans-stilbene population by helium, as determined from a master equation analysis of the KCSI results. The numbers in the plot denote the number of collisions experienced by the respective vibrational population distribution during relaxation.

Trajectory simulations of polyatomic-polyatomic collisions

V. Bernshtein , I. Oref

Department of Chemistry, Technion-Israel institute of Technology, Haifa 32000, Israel
E-mail: chr21vb@technion.ac.il

In the present work the mechanism of collisional energy transfer (CET) between polyatomic systems was systematically explored by classical trajectory calculations. The investigations focused on benzene, toluene, azulene, and pyrazine collisions.

CET quantities like average energy transfer, <ΔE>, collision duration, <τ>, and probability density function, P(E,E'), were evaluated from trajectory calculations as a function of bath temperature, photon excitation, and potential energy surface. The contributions of individual vibrational modes and groups of modes to CET as well as collisions with frozen rotational degrees of freedom were examined.

The CET mechanism in polyatomic bath consists, unlike monatomic bath, of direct as well as chattering collisions in which the bath molecule gains energy by repeatedly banging into the excited molecule (see figure).

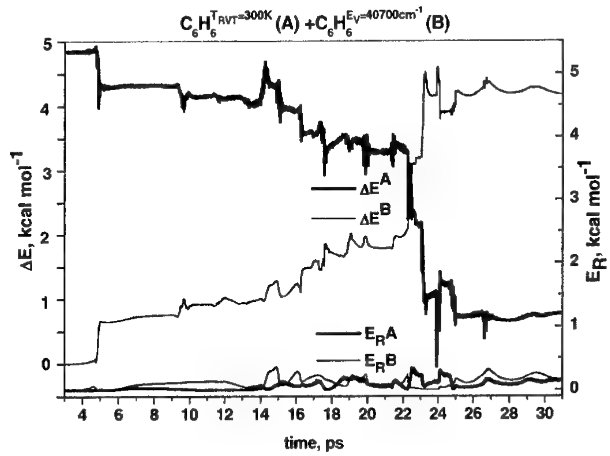

It was found that mainly vibration to vibration energy transfer affect CET and there is hardly any rotational energy transfer. However, it was found that there is a significant intra-collision rotational energy flux. Moreover, freezing the rotations increases <τ> by factor of 3, and causes an increase in the absolute value of <ΔE> up to 50%. It comes about from the fact that the molecular rotations destabilize the van der Waals collision complex.

Supercollisions were found and they do occur in collisions with long complex lifetimes. There is no specific gateway mode or group of modes that are more efficient in CET. These results are supported by experimental work and indicate surprising differences in CET between polyatomic-polyatomic collisions and polyatomic-monatomic collisions. The mechanism of CET in polyatomic-monatomic systems was studied in great details [1]. It shows CET mediated by rotations with a low frequency dominant gateway mode and a CET probability density function with a high ΔE tail, part of which can be assigned to supercollisions. The present results produce mechanistic insight into CET of polyatomic bath collider.

[1] V. Bernshtein and I. Oref, *J.Phys.Chem. A*, **105**,10646 (2001).

The Role of van der Waals Radical Complexes in Combination Reactions of Polyatomic Radicals at High Pressures

Kentaro Sekiguchi, Changyoul Lee, Kawon Oum, Klaus Luther and Jürgen Troe

Institut für Physikalische Chemie, Universität Göttingen, Tammannstr. 6, D-37077 Göttingen, Germany: Tel: +49 551 39 12598; Fax: +49 551 39 3150; Email: koum@gwdg.de.

The rate of combination of two radicals depends on pressure, temperature and the nature of the solvent molecules. While smooth "fall-off" curves are expected according to the conventional energy transfer mechanism, deviations from this simple behaviour occur if an alternative reaction path of combination via the radical-complex mechanism gains in importance. Such a situation can be found even in reactions involving large polyatomic radicals. As a consequence, the enhancement of rate constants is observed at pressures where the constant "high pressure limit" (k_∞) of the energy transfer mechanism is predicted. A likely explanation of such observations is based on the abundance of the radical-solvent van der Waals complexes at medium solvent densities.

In this presentation, we discuss the combination reactions CCl_3 + CCl_3 (+M) $\rightarrow$ C_2Cl_6 (+M) (k_1), CCl_3 + Br (+M) $\rightarrow$ CCl_3Br (+M) (k_2), and $C_6H_5CH_2$ + $C_6H_5CH_2$ (+M) $\rightarrow$ $C_{14}H_{14}$ (+M) (k_3) over the pressure range 0.01-1000 bar at temperatures from 250 to 400 K. He, Ar, Xe, N_2, CO_2, CF_3H, CF_4 and SF_6 were employed as bath gases. Radicals were generated by UV photolysis of precursors and the absorption of radicals was monitored by transient UV absorption. The limiting "high pressure" rate constants within the energy transfer mechanism were determined from the constant values at pressures near 1-10 bar, as $k_{1,\infty}(T) = (1.0 \pm 0.2) \times 10^{-11} (T/300\ \mathrm{K})^{-0.17}$, $k_{2,\infty}(T) = (2.0 \pm 0.2) \times 10^{-11} (T/300\ \mathrm{K})^{-0.13}$ and $k_{3,\infty}(T) = (4.1 \pm 0.2) \times 10^{-11} (T/300\ \mathrm{K})^{-0.3}$ $\mathrm{cm^3\ molecule^{-1}\ s^{-1}}$. The reactions became increasingly faster when the pressure was further raised until they finally started to slow down at densities where diffusion-controlled kinetics takes over. Such a peculiar density dependence of combination rate constants was seen in all three reaction systems, but both starting point and the degree of enhancement of rate constants depend on the strength of radical-bath gas interaction and temperatures of the medium. Possible origins of these pressure effects, such as the influence of the radical-complex mechanism and the density dependence of electronic quenching, are discussed. The measured rates are further analysed in terms of SACM / CT theory, resulting in a consistent trend of the enhancement of rate constants for radical-complexes due to larger rigidity factors.

Experimental and Theoretical evidence for Homogeneous Catalysis in the Gas-Phase Reaction of SiH_2 with H_2O (and D_2O). A combined Kinetic and Quantum Chemical Study.

Matthew J. Almond, Nicola Goldberg, Robin Walsh
School of Chemistry, University of Reading, Whiteknights, Reading, UK.

Rosa Becerra
Instituto de Quimica-Fisica 'Rocasolano', C.S.I.C., Madrid, Spain

J. Pat Cannady
Dow Corning Corporation, Midland, MI, USA

J. Steven Ogden
Department of Chemistry, University of Southampton, Highfield, Southampton, UK

Time-resolved kinetic studies of the reaction of silylene, SiH_2, with H_2O and with D_2O have been carried out in the gas phase at 297 K and at 345 K, using laser flash photolysis to generate and monitor SiH_2. The reaction was studied over the pressure range 5-400 Torr with SF_6 as bath gas. Experiments of two kinds were carried out (i) with variable $[H_2O]$ and $[D_2O]$ at constant SF_6 (5 Torr) and (ii) with constant $[H_2O]$ (or $[D_2O]$) and variable SF_6. The pseudo first order rate constants, k_{obs}, for $[SiH_2]$ decay gave good fits to the quadratic equation:

$$k_{obs} = k_a + k_b[H_2O] + k_c[H_2O]^2$$

Furthermore the rate constant k_b was found to be highly pressure (SF_6) dependent. Rate constants (both k_b and k_c) at 345 K were about half those at 297 K. Isotope effects, k_{bH}/k_{bD}, were in the range 1.0–1.15, suggesting no involvement of H- (or D-) atom transfer in the rate determining step. Values for k_{cH}/k_{cD} were larger. The mechanism proposed to account for these results involves the initial formation of the zwitterionic donor-acceptor complex, $H_2Si{\cdots}OH_2$ in a vibrationally excited state which can either be stabilised by collision with SF_6 or react further with H_2O (or D_2O). RRKM modelling shows that the reaction is close to the low pressure limit for this third body assisted association reaction.

Quantum chemical (*ab initio*) calculations at the G3 level support this mechanism and show that, whereas $H_2Si{\cdots}OH_2$ is unable to undergo unimolecular isomerisation to silanol, SiH_3OH, due to a high energy barrier, the catalysed reaction in the presence of H_2O, is a barrierless process. This is the first example of a gas phase catalysed reaction of a silylene.

Full details of the kinetics and theoretical calculations will be given at the meeting.

Time-resolved absorption studies of radical-radical reactions involving $NCO(X^2\Pi)$ and simple alkyl radicals: $H(^2S)$, $CH_3(X\ ^2A_2'')$, and $C_2H_5(X^2A'')$

Y. Gao and R. G. Macdonald

Argonne National Laboratory Chemistry Division 9700 South Cass Ave. Argonne, IL 60439
Email: rgmacdonald@anl.gov

There is an increasing effort to reduce NOX emissions from combustion sources, and the NCO radical plays a critical role in NO_X chemistry. It is involved in both the chemistry leading to the formation of NO_X and various strategies for its reduction through the addition of chemical additives to exhaust gases. However, there is still a lack of detailed knowledge of NCO chemistry, particularly its reactions with transient species, atoms and radicals. The determination of rate constants for radical-radical reactions is difficult because of the necessity to monitor the temporal concentration of either one or two transient species. Another important aspect of radical-radical chemistry is product identification. In the current study, the strategy adopted to tackle these two problems was to accurately monitor the temporal concentration profiles of as many of the molecular species as possible. The detection technique was high-resolution time-resolved infrared absorption spectroscopy in the 2.7 to 3.4 micron spectral region. Rate constants involving the initial transient species and secondary reaction processes were determined by comparison of the various experimental concentration profiles to those generated by a detailed-chemical model of the system under investigation. The multiple species and high signal-to-noise of the concentration temporal profiles constrained the influence of secondary chemistry on the results. The transient species were generated by the 248 nm laser photolysis of ClNCO and subsequent reaction of the Cl atom with RH, where R was H, CH_3, or C_2H_5. The $NCO(X^2\Pi)$ radical was detected using the combination band (1011) ← (0010) near 3.16 microns and the other species from fundamental infrared transitions. For each system, the primary product channel and species detected are summarized as follows:

$NCO(^2\Pi) + H(^2S) \rightarrow NH(^3\Sigma) + CO$; NCO, NH(v=0,1), HCl

$NCO(^2\Pi) + CH_3(^3A_2'') \rightarrow CH_3NCO(^1A')$; NCO, CH_3, HCN, HNC, NH, HCl

$NCO(^2\Pi) + C_2H_5(^2A'') \rightarrow C_2H_4$ or $H_3CCH(^3A'') + HNCO$
; NCO, HCN, HNCO, C_2H_4, HCl

Reactions of hyperthermal atomic oxygen: surprising reaction mechanisms, intersystem crossing effects and collisional energy transfer processes

George C. Schatz

Department of Chemistry, Northwestern University, Evanston IL 60208-3113 USA

Recent advances in experimental techniques, primarily by Tim Minton at Montana State, have made it possible to study the dynamics of reactions of $O(^3P)$ with small molecules at hyperthermal energies in the 1-5 eV range. The results of these experiments are not always easy to interpret, however in this talk I will show that the use of direct dynamics classical trajectory simulations make it possible to provide a detailed understanding of the hyperthermal reaction dynamics, leading to the discovery of many new features of atomic oxygen chemistry that are largely unknown at lower energies. These include the presence of new reaction mechanisms in which the O atom adds to saturated hydrocarbons to form oxy radicals, the first ever observation of triplet/singlet crossing effects in the reaction of O with H_2, and observation of the squeezed atom effect (leading to anomalously large collisional energy transfer) in collisions of O with ethane. I also hope to describe studies of O atom reactions with fluorinated hydrocarbons, where collisions induced dissociation is important, and related studies of O atom reactions with alkane thiol self-assembled monolayers on gold surfaces. This work has been done in collaboration with Diego Troya.

Exploring radical-radical reaction dynamics

Jong-Ho Choi

Department of Chemistry and Center for Electro- and Photo Responsive Molecules
Korea University, 1, Anam-dong, Seoul 136-701, Korea

The reaction dynamics of ground-state atomic oxygen [$O(^3P)$] with propargyl (C_3H_3) has first been investigated by applying laser induced fluorescence (LIF) spectroscopy in a crossed beam configuration.[1-5] Several new exothermic channels (1)-(4) were observed.

$$O(^3P) + C_3H_3 \rightarrow C_3H_2 + OH \quad (1)$$
$$\rightarrow C_3H_2O + H \quad (2)$$

We also performed *ab initio,* RRKM (Rice-Ramsperger-Kassel-Marcus) and *prior* calculations to characterize the reaction mechanisms and energy partitioning, and found out that the barrier height, reaction enthalpy and the number of intermediates involved along the reaction pathway are of extreme importance in understanding such reactive scattering processes. We hope this work sheds some light on the gas-phase atom-radical dynamics at the molecular level, which has been unexplored so far.

References
1. H.C. Kwon, J.H. Park, H. Lee, H.K. Kim, Y.S. Choi and J.H. Choi, J. Chem. Phys. **116**, 2675 (2002).
2. J.H. Park, H. Lee, H.C. Kwon, H.K. Kim, Y.S. Choi and J.H. Choi, J. Chem. Phys. **117**, 2017 (2002).
3. J.H. Park, H. Lee and J.H. Choi, J. Chem. Phys. **119**, 1-13 (2003)
4. H. Lee, S.K. Joo, L.K. Kwon and J.H. Choi, J. Chem. Phys. **119.**, 1-14 (2003).

5. H. Lee, S.K. Joo, L.K. Kwon, and J.H. Choi*, J. Chem. Phys. **120**, 2215 (2004).
6. S.K. Joo, L.K. Kwon, H. Lee, and J.H. Choi*, J. Chem. Phys. **120**, 7976 (2004).

Crossed molecular beam studies of the $O(^3P) + C_2H_4$ reaction using "*soft*" electron impact ionization: Primary products, reaction dynamics and branching ratios

G. Capozza, E. Segoloni, G. G. Volpi, and P. Casavecchia
Dipartimento di Chimica, Università di Perugia, 06123 Perugia, Italy

Our understanding of the dynamics of bimolecular reactions has benefited greatly of the "*universal*" capability of the Crossed Molecular Beams (CMB) scattering technique with Electron-Impact (EI) mass spectrometric detection and time-of-flight analysis [1]. In principle, all reactions products can be detected by this technique. However, one of the main limitations of EI is known to reside in the dissociative ionization - of reagents, products, and background gases. This can greatly complicate, and even prohibit the identification of products, particularly for multiple channel polyatomic reactions. To overcome this problem, in our laboratory we have very recently introduced, for the first time, the *soft* EI ionization for product detection [2]. Rather than resorting to soft photoionization (PI) with tunable (5-30 eV) VUV radiation from a synchrotron, we use EI ionization with tunable (7-100 eV) electrons from a hot filament. This is an attractive alternative to the use of PI by synchrotron radiation, and offers the added bonus that branching ratios can be derived because EI ionization cross sections are known or can be estimated. A first application was to the reaction $O(^3P)+C_2H_2$ for which we have determined the dynamics of the competing CH_2+CO and HCCO+H channels and the branching ratio [3].

Here we report on the investigation of the reaction $O(^3P)+C_2H_4$, which plays a key role, besides in the combustion of ethylene itself, in the overall mechanism for hydrocarbon combustion. There are five exoergic channels:

$$O(^3P) + C_2H_4 \rightarrow H + CH_2CHO \qquad \Delta H^\circ_0 = -13 \text{ kcal/mol} \qquad (2a)$$
$$\rightarrow H + CH_3CO \qquad \Delta H^\circ_0 = -25 \text{ kcal/mol} \qquad (2b)$$
$$\rightarrow H_2 + CH_2CO \qquad \Delta H^\circ_0 = -85 \text{ kcal/mol} \qquad (2c)$$
$$\rightarrow CH_3 + HCO \qquad \Delta H^\circ_0 = -27 \text{ kcal/mol} \qquad (2d)$$
$$\rightarrow CH_2 + HCHO \qquad \Delta H^\circ_0 = -7 \text{ kcal/mol} \qquad (2e)$$

Since the pioneering work of Cvetanovic in the mid 1950s many research groups have investigated this reaction, employing a variety of experimental techniques under different conditions of pressure and temperature, identifying only some of the possible products, which has given rise to uncertainties and controversy. On the other hand, for modeling combustion systems, detailed knowledge of all primary reaction products, their rate coefficients, and their branching ratios are needed.

By using "*soft*" EI ionization, we have been able to unambiguously detect the following radical and molecular products, CH_2CHO, CH_3CO, CH_2CO, CH_3, and CH_2, corresponding to the five reaction pathways (2a-e). From a detailed series of angular and velocity distribution measurements at *m/e*=42, 15, and 14 using different electron energies, and from measurements of fragmentation patterns, it was possible to characterize the reaction dynamics of all five competing channels and determine their branching ratios [4]. We believe that *soft* EI ionization, making the so-called *universal* detection possible, represents a cornerstone in the field and will contribute to establishing a closer link between the kinetics and dynamics of elementary gas-phase chemical reactions.

[1] P. Casavecchia, *Rep. Prog. Phys.* **63** (2000) 355, and references therein.
[2] P. Casavecchia, G. Capozza, and E. Segoloni, "Crossed molecular beam reactive scattering: towards *universal* product detection by *soft* electron-impact ionization", in "Modern Trends in Chemical Reaction Dynamics", *Advanced Series in Physical Chemistry*, Ed. by K. Liu and X. Yang (World Scientific, Singapore, 2004), in press.
[3] G. Capozza, E. Segoloni, F. Leonori, G. G. Volpi, P. Casavecchia, *J. Chem. Phys.* **120**, 4557 (2004).
[4] G. Capozza, E. Segoloni, G. G. Volpi, and P. Casavecchia, in preparation.

The H + D_2 Reaction: A Challenge for Experiment and Theory

F. Ausfelder, A. E. Pomerantz, R. N. Zare
Department of Chemistry, Stanford University, Stanford, CA 94305-5080, USA

S. C. Althorpe
Department of Chemistry, University of Exeter, Stocker Road, Exeter EX4 4QD, *UK*

F. J. Aoiz L. Bañares J. F. Castillo
Departmento de Química Física, Facultad de Química,
Universidad Complutense, 28040 Madrid, Spain

The H + D_2 reaction has been investigated experimentally using resonance enhanced multiphoton ionisation (REMPI). HD(v'=2,3, j') product rotational distributions have been recorded as a function of collision energy. The experimental distributions are compared with state-of-the-art time-dependent and time-independent quantum-mechanical calculations. Systematic deviations are found between the experimental results and the theoretical predictions in the HD(v'=3, j') distributions. The experimental distributions approach the statistical limit with increasing collision energy much faster than the theoretical ones. However, experiment and theory agree well for the HD(v'=2, j') distributions at all energies. Additionally, the inelastic channel of the title reaction was investigated and the resulting D_2(v'=1,2, j') distribution measured as a function of collision energy. The experimental results were compared with time-dependent calculations and agree very well. The results show a markedly different behaviour as a function of collision energy than the reactive results. A simple model is proposed to explain the difference in behaviour between reactive and inelastic results.

Recent studies of the state-to-state stereodynamics of elementary reactions

Marcelo P. de Miranda and Robert A. Pettipher

Department of Chemistry, University of Leeds, Leeds LS2 9JT, United Kingdom

We will report recent results from theoretical studies of the quantum stereodynamics of atom-exchange reactions, obtained with time-dependent and time-independent methods. These will include:

• Correspondence between quantum and classical polarization moments. We have used minimum-uncertainty polarized states[1] to obtain a rigorous quantum expression for continuous probability density functions of angular momenta. This expression, in which the function $P(\theta_j,\phi j)$ is written in terms of quantum polarization moments and spherical harmonics, allows for a rigorous and unambiguous determination of the correspondence between quantum and classical polarization moments. It is found that statements frequently found in the literature (e.g., that probability density functions are Fourier transforms of density matrices, or that in the correspondence principle limit the quantum term $2j + 1$ must be replaced by the solid angle 4π) are incorrect, and that the direct comparison between quantum and classical results, just as the interpretation of experimental data, requires consideration of a Clebsch-Gordan coefficient that has been ignored in previous studies.

• Near-side and far-side reactions. We have developed a simple model for the stereodynamics of atom-diatom reactions mediated by a collinear collision complex, examples of which include $H + D_2$ and the resonance-mediated $F + H_2$ reaction. Consideration of our model shows that the polarization moment that gives most insight into the stereodynamics of such reactions is a measurable alignment moment that up to now has received little attention. It allows one to distinguish near-side from far-side mechanisms, and also gives insight into the relative contributions of the total angular momentum and bending vibration of the collinear complex to the reaction (stereo)dynamics. The validity of the model for the $H + D_2$ reaction is considered by comparison of its predictions to results from exact time-dependent and time-independent quantum calculations either with or without use of the nearside/far-side decomposition of the scattering amplitude suggested by Connor and coworkers.[2]

1. F. T. Arecchi, E. Courtens and R. Gilmore, Phys. Rev. A 6 (1972) 2211.
2. A. J. Dobbyn, P. McCabe, J. N. L. Connor and J. F. Castillo, PCCP 6 (1999) 1115.

From Vibrationally Cold to Vibrationally Mediated Ozone Photodissociation: Probing Orientation and Alignment of the Singlet Oxygen Products.

Gus Hancock, Sophie J. Horrocks, Paul J. Pearson, Grant A. D. Ritchie, Daniel F. Tibbetts.

Physical and Theoretical Chemistry Laboratory, Oxford University, South Parks Road, Oxford, OX1 3QZ, UK.

Angular momentum polarization of the O_2 (a $^1\Delta_g$) product from photolysis of ozone has been measured as a function of wavelength (270 – 300 nm) *via* REMPI time of flight mass spectrometry. A lambda-doublet dependent angular momentum alignment is observed at 270 nm and seen to persist at longer photolysis wavelengths. A decrease in the magnitudes of angular momentum orientation and alignment moments is observed and discussed in terms of an impulsive dissociation which is modified to a varying extent by parent rotations and vibrations.

The translational anisotropy of the product molecule, independent of lambda-doublet state, initially decreases as the kinetic energy of the photofragments decreases, before rising in magnitude as the thermodynamic limit for dissociation of vibrationally cold ozone is approached. The transition to a vibrationally mediated dissociation is accompanied by a marked reduction of the translational anisotropy and this threshold region is investigated further through studies on the orientation and alignment of the atomic O (^{1}D) fragment.

Orbital polarization effects in molecular photodissociation

Mark Brouard, Raluca Cireasa, Andrew P. Clark, Timothy J. Preston and Claire Vallance

The Physical and Theoretical Chemistry Laboratory, Department of Chemistry, University of Oxford, South Parks Road, Oxford OX1 3QZ, United Kingdom

Laser pump-probe techniques have been used to study electronic angular momentum polarization effects in the $O(^3P_J)$ products of triatomic molecular photodissociation systems. The experiments employ polarized photolysis radiation coupled with resonantly enhanced multiphoton ionisation (REMPI) and velocity-map ion-imaging. We have recently characterized the $O(^3P_J)$ photofragments generated in the spin-forbidden photodissociation of N_2O at 193nm:

$$N_2O + h\nu \rightarrow N_2 + O(^3P_J)$$

The dependence of the ion-images, and integrated image intensities, on laser pump-probe polarization geometry has enabled us to determine the electronic alignment of the ground state O-atom photofragments [1]. The data have been used to help identify the electronic channel responsible for spin-forbidden dissociation in this atmospherically important molecular system.

Similar experiments have now been conducted on the 193nm photodissociation of SO_2:

$$SO_2 + h\nu \rightarrow SO + O(^3P_J)$$

Unlike the case in N_2O, the coproduct of the ground state O atom is this time an open shell $SO(^3\Sigma^-)$ species. However, in spite of this added complexity, the O atoms still possess electronic angular momentum alignment. The data are again used to help to identify which electronic state(s) are populated during molecular fragmentation.

[1] M. Brouard, A.P. Clark, C. Vallance, O.S. Vasyutinskii, *J. Chem. Phys.* in press (2003).

* email address: mark.brouard@chemistry.ox.ac.uk

One- and Two-photon Processes in the Hydroxyl Radical

Mark P. J. van der Loo and Gerrit C. Groenenboom
Institute of Theoretical Chemistry, University of Nijmegen, Toernooiveld 1, 6525 ED Nijmegen, The Netherlands

Dragana Č. Radenović, André J. A. van Roij, Dmitri A. Chestakov, André T. J. B. Eppink, J. J. ter Meulen, and David H. Parker
Department of Molecular and Laser Physics, University of Nijmegen, Toernooiveld 1, 6525 ED Nijmegen, The Netherlands

Margaret E. Greenslade and Marsha I. Lester
Department of Chemistry, University of Pennsylvania, Philadephia, Pennsylvania 19104-6323

The hydroxyl radical plays a crucial role in atmospheric chemistry, in combustion processes, and in astrochemical processes, and it is receiving considerable attention in recent cold molecule research. The experimental study of OH is difficult because all of the electronic transitions originating from the ground state, except for the well known A–X transition, lie in the vacuum ultraviolet. A new experimental setup is employed by Dave Parker and co-workers for the (one photon) photodissociation and the (2+1) REMPI (resonance enhanced multiphoton ionization) study of OH and OD. In these experiments the jet-cooled radical is prepared with a hexapole state selector in the upper Λ-doublet level of its X $^2\Pi_{3/2}$ electronic ground state.

In photodissociation experiments at 226 and 243 nm both the $O(^3P_2)$ and $D(^2S)$ photofragments were recorded with the velocity mapped ion imaging technique. The observed peaks in the total kinetic energy release were interpreted to arise from the $1^2\Sigma^-{}_{1/2} \leftarrow X^2\Pi_{3/2}(v)$ transitions of highly vibrationally excited OD with v up to six. To support this interpretation we performed time independent photodissociation cross section calculations with the renormalized Numerov method. In these calculations we employed potentials and R-dependent transition dipole moments obtained from new, high level ab initio calculations (CASSCF+MRCI, aug-cc-pV6Z basis set, using the MOLPRO package). The first results of this study were reported in a rapid communication [Radenović et al., J. Chem. Phys. **119**, 9141 (2003)]. Ongoing experimental and theoretical work concerns the $O(^3P_{2,1,0})$ fine-structure distribution, electronic alignment, and photodissociation anisotropy parameters.

The (2+1) REMPI experiment was done in the 220-246 nm region, probing the $D^2\Sigma^-(v')$ $X^2\Pi(v'')$ and $3^2\Sigma^-(v') \leftarrow X^2\Pi(v'')$ transitions in OH. New vibrational levels of the $D^2\Sigma^-$ and $3^2\Sigma^-$ Rydberg states were identified. The observed transitions involve ground state vibrational levels with $v'' \leq 3$ and $v' \leq 3$ for the $D^2\Sigma^-$ state and $v' = 0, 1$ for the $3^2\Sigma^-$ state. We also studied these two-photon transitions theoretically. For this purpose we also computed the potential energy curves of the Rydberg states. In addition we computed the relevant R-dependent transition dipole moments involving the (repulsive) $1^2\Sigma^-$ state, which is expected to be the dominant intermediate state giving intensity to the two-photon transitions. Since in the literature we could not find a description of a method to compute the intensity of a bound-bound two-photon transition with a repulsive intermediate state we developed a new method for this problem. We employ a Green's function formalism implemented in the Seideman Miller ABC-DVR, absorbing boundary conditions discrete variable representation. The experiment provides only limited information about the intensities of the transitions. Still, the pattern of observed transitions matches very well with the computed intensities. This gives us confidence in our understanding of this REMPI process and our ability to predict the feasibility of REMPI detection in similar situations.

Gas-phase kinetics and dynamics at very low temperatures: Obtaining data for astrochemistry

Ian R. Sims

PALMS – UMR 6627 du CNRS, Equipe Astrochimie Expérimentale, Université de Rennes 1, Bâtiment 11c, Campus de Beaulieu, 35042 Rennes Cedex, France;
Electronic mail: ian.sims@univ-rennes1.fr

Chemistry at very low temperatures – and, in particular, the study of collisional processes in the gas phase – is a fascinating area of research, both for its fundamental interest and for its application to such diverse environments as the atmospheres of Earth and other planets, and the synthesis of a wide range of molecular species within dense interstellar clouds (ISCs). In this lecture I will review the experimental techniques available for studying gas phase reactive and inelastic processes at very low temperatures, and give a detailed description of the CRESU (Cinétique de Réaction en Ecoulement Supersonique Uniforme, or Reaction Kinetics in Uniform Supersonic Flow) technique. I will give an overview of the results obtained in collaboration with Ian W.M. Smith, Bertrand Rowe and co-workers in the CRESU apparatuses in Rennes and Birmingham (now transferred to Rennes), and attempt to highlight some general trends in reactivity at low temperatures. I will then focus on the results of some recent studies of (1) inelastic collisions and (2) reactive collisions:

(1) Inelastic collisions. Infrared – vacuum ultraviolet double resonance experiments (IRVUVDR) experiments have been implemented in CRESU apparatus to measure total and state-to-state rotational energy transfer rate coefficients for CO – He collisions at temperatures down to 15 K. The results are shown to be in remarkably good agreement with those obtained in *ab initio* scattering calculations by Cecchi-Pestellini *et al.*[1] Very recently, we have also measured total removal rate coefficients for CO in specific rotational states in collision with H_2 at room temperature and at 6.6 K. These results are of significant astrochemical interest, concerning collisions between the two most abundant molecules in interstellar space. We have also made similar measurements for $C(^3P_J)$ in specific spin orbit states.

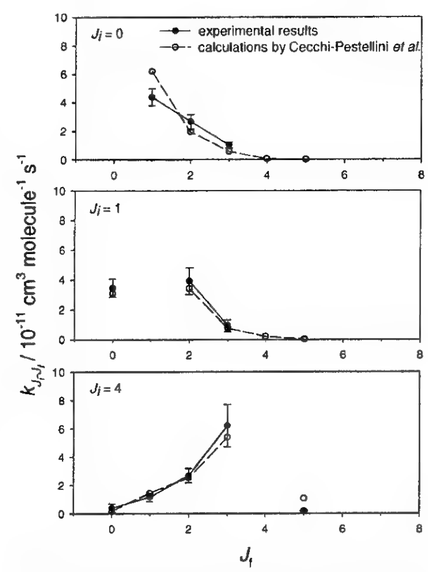

FIG. 1. Experimental state-to-state rate coefficients for rotationally inelastic collision between CO ($X^1\Sigma^+$, $v = 2$, $J_i = 0$, 1 and 4) and He at 15 K compared with theoretical results of Cecchi-Pestellini *et al.*

(2) reactive collisions. The reaction $O + OH \rightarrow O_2 + H$ is the principal source of interstellar O_2, and hitherto has not been studied below ca. 160 K. We use a novel VUV co-photolysis technique to produce both unstable reactants within the CRESU flow and obtain rate coefficients which are at substantial variance with those used in current astrochemical models. I will present the new technique and the results obtained to date. Experiments are currently underway to study the kinetics of the C_2 radical at low temperatures. This species thought to play a role in the synthesis of hydrocarbons both in interstellar space and in the atmospheres of planets such as Titan. No measurements of rate coefficients for reactions involving C_2 at low temperatures have been made to date, and I hope to present preliminary results from new experiments carried out in Rennes.

[1] C. Cecchi-Pestellini, E. Bodo, N. Balakrishnan, and A. Dalgarno, Astrophys. J. **571**, 1015 (2002).

H Atom Branching Ratios from CN + C_2H_2, C_2H_4 Reactions as a function of Temperature and Pressure.

Namil Choi, Mark Blitz, Mike Pilling, Liming Wang and P.W. Seakins
School of Chemistry, University of Leeds, Leeds, LS2 9JT

The reaction of CN radicals with ethene has three possible channels:

$$\begin{aligned} CN + C_2H_4 &\rightarrow CNC_2H_3 + H \\ &\rightarrow HCN + C_2H_3 \\ &\xrightarrow{M} (CN)H_2CCH_2 \end{aligned}$$

For the corresponding reaction with ethyne only the addition/elimination and stabilization channels are open. The reactions are of relevance for formation of long chain nitrogen containing molecules in the atmospheres of the giant planets and their satellites. The Cassini mission to Titan provides a new impetus to such studies.

We have used VUV laser induced fluorescence to monitor H atom production from the title reactions. The use of a calibration reaction with a 100% conversion of CN to H removes the need for absolute calibrations of CN and H signals.

$$\mathbf{CN} + H_2 \rightarrow HCN + \mathbf{H}$$

The temporal dependence of both CN removal and H atom production can be followed during the same experiment to ensure that the observed H atoms do originate from the desired reaction and not any secondary processes.

Results at room temperature show 100% production of H for the title reactions over the range 10 – 100 Torr [1]. This result is in contrast to earlier work by Monks et al [2] who observed a much lower yield of CNC_2H_3 from the CN + C_2H_4 reaction and inferred significant production of HCN + C_2H_3. For the CN + C_2H_2 reaction, the result is in good agreement with Huang et al [3], who where unable to observe any other non atomic product than CNC_2H.

However, preliminary results and calculations for lower temperatures, more relevant to the outer planets suggest that the yield of H atoms falls as a function of pressure as shown in Fig 1. Further experiments are currently in progress over a wider range of temperatures and pressures. Theoretical surfaces have been calculated for the reactions and will be used to interpret the pressure and temperature dependencies.

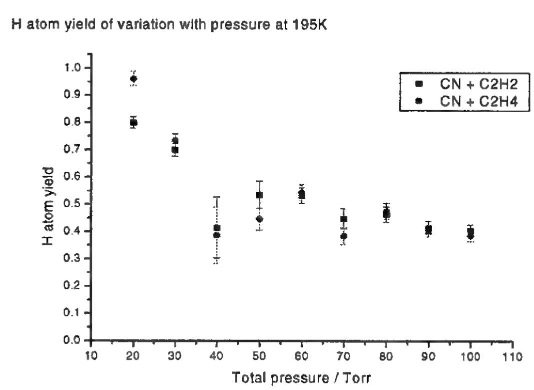

Figure 1

The implications of the results for modelling the atmospheres of the outer planets will be presented.

[1] N. Choi, M.A. Blitz, K.W. McKee, M.J. Pilling, P.W. Seakins, Chem. Phys. Lett. 384 (2004) 68.
[2] P.S. Monks, P.N. Romani, F.L. Nesbitt, M. Scanlon, L.J. Stief, Journal of Geophysical Research 98 (1993) 17115.
[3] L.C.L. Huang, O. Asvany, A.H.H. Chang, N. Balucani, S.H. Lin, Y.T. Lee, R.I. Kaiser, Y. Osamura, J. Chem. Phys. 113 (2000) 8656.

Outer Planets' Atmospheric Chemistry: Rate Constant for the CH_3 C_2H_5 Reaction at Low Temperatures and Pressures

R. J. Cody[1], A. S. Pimentel[1], W. A. Payne[1], and F. L. Nesbitt[1,2]

[1] *Laboratory for Extraterrestrial Physics, NASA Goddard Space Flight Center, Greenbelt, MD, USA*

[2] *Department of Chemistry, Catholic University of America, Washington, DC; also at Coppin State College, Baltimore, MD, USA*

The ethyl radical, C_2H_5, is predicted by photochemical modeling to be one of the most abundant C_2 species in the atmospheres of Jupiter and Saturn. The reaction $CH_3 + C_2H_5$ (1) is expected to be one of the important loss processes for C_2H_5 and an important source of C_3H_8 in these atmospheres. There have been four direct studies of the rate constant for Reaction 1 but none at the lower temperatures and pressures needed for the modeling studies of the atmospheres of the Outer Planets. Therefore, we are measuring the rate constant at T = 295 and 202 K, and P = 0.4, 1 and 2 Torr. The measurements are performed in a discharge - fast flow system under pseudo-first order conditions with $[C_2H_5] / [CH_3] = 10 - 110$. Pre-mixed gases of CH_4 and C_2H_6 in helium are added through a movable injector to the main gas flow containing a discharged mixture of fluorine atoms and molecular fluorine in helium. The radicals CH_3 and C_2H_5 are formed by the reactions of F atoms with CH_4 and C_2H_6, respectively. We monitor the decay of the CH_3 radical via low-energy (10 ev) electron impact mass spectrometry. Because of complications from secondary chemistry, the rate constants for Reaction 1 are derived by a one-parameter fitting of the rate constant decay curve to a numerical simulation of the reaction system using the Facsimile program. The results thus far show moderate dependence upon both temperature and pressure. The rate constants for the reaction $CH_3 + C_2H_5$ are k(295K, 1 Torr) = $(1.8\pm0.3)\times10^{-11}$, k(295K, 2 Torr) = $(3.0\pm0.6)\times10^{-11}$, k(202K, 1 Torr) = $(2.6\pm0.6)\times10^{-11}$, and k(202K, 2 Torr) = $(3.3\pm0.8)\times10^{-11}$, all in units of cm^3 $molecules^{-1}$ s^{-1}. A comparison will be made with previous measurements.

Acknowledgements. This research is being supported by the NASA Planetary Atmospheres Program. ASP thanks the National Academy of Science for the award of a research associateship.

Unexpected branching ratios in astrophysically important dissociative recombination reactions

W. D. Geppert,[a] F. Hellberg,[a] A. Ehlerding,[a] F. Österdahl,[b] R.Thomas,[a] J. Semaniak,[c] M. Kamińska,[c] A. Al-Khalili,[a] M. af Ugglas,[d] N.Djurić,[e] A. Paál[d] and M. Larsson[a]

[a] *Department of Physics, Stockholm University, Alba Nova, SE-106 91, Stockholm Sweden.*
[b] *Department of Physics, Royal Institute of Technology, Alba Nova, SE-106 91 Stockholm, Sweden.*
[c] *Institute of Physics, Świętokrzyska Academy, ul. Świętokrzyska 15, PL-25406 Kielce, Poland.*
[d] *Manne Siegbahn Laboratory, Frescativägen 24, SE-104 05 Stockholm, Sweden.*
[e] *JILA, University of Colorado 440 UCB Boulder, CO 80309-0440, USA.*

Cross sections and branching ratios for the dissociative recombination (DR) reactions of $DOCO^+$, the isoelectronic DON_2^+ and SO_2^+ at reactant kinetic energies from 1 to 1000 meV have been measured using the CRYRING ion storage ring facility at the Manne Siegbahn Laboratory at Stockholm University. The grid technique[1] has been employed to investigate the branching ratios of the different product channels. In the DR of $DOCO^+$ the following channels are possible at a relative kinetic energy of the reactants of 0 eV:

$$
\begin{array}{lllll}
DOCO^+ + e^- & \rightarrow & D + CO_2 & + 7.92\ \mathrm{eV} & (1a) \\
 & \rightarrow & DO + CO & + 6.86\ \mathrm{eV} & (1b) \\
 & \rightarrow & COD + O & + 3.80\ \mathrm{eV} & (1c) \\
 & \rightarrow & CO + D + O & + 2.47\ \mathrm{eV} & (1d) \\
 & \rightarrow & CD + O_2 & - 0.04\ \mathrm{eV} & (1e)
\end{array}
$$

From the measured fragment mass spectrum (Fig.1) the branching ratios of these different channels can be obtained.

Analysis yields the unexpected result that channel (1a) amounts to only 6 ± 4 %, whereas the three-body break-up (1d) by far dominates (67 ± 2 %), which is contrary to the theory of Bates according to which elimination of the deuterium atom should be favoured and three-body processes were ruled out.[2] The branching ratio of channel (1b) was determined as 27 ± 2 %, which is in very good agreement with earlier flowing afterglow measurements.[3] Pathways (1c) and (1e) were found to be negligible. With the isoelectronic DON_2^+ ion an analogous pattern was observed. In this reaction, the dominating channels were those leading to $DO + N_2$ (46 %) and $D + O + N_2$ (40 %). In the case of SO_2^+ all three possible fragmentation pathways are exoergic:

$$
\begin{array}{lllll}
SO_2^+ + e^- & \rightarrow & SO + O & + 6.94\ \mathrm{eV} & (2a) \\
 & \rightarrow & S + O_2 & + 6.40\ \mathrm{eV} & (2b) \\
 & \rightarrow & S + 2O & + 1.24\ \mathrm{eV} & (2c)
\end{array}
$$

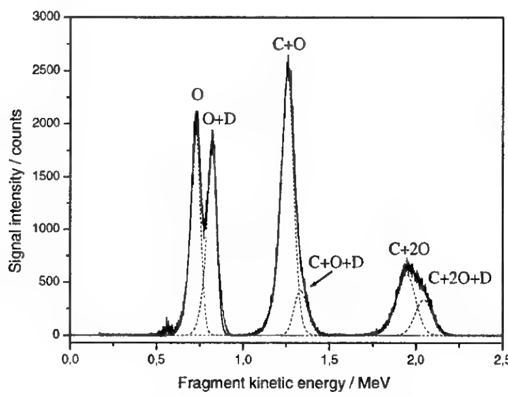

Fig. 1 Energy spectrum of the neutral fragments from the dissociative recombination of $DOCO^+$ with the grid in place. The solid line shows the data, whereas double-Gaussian fitting curves of the peaks are shown as dashed lines and the total fit as dotted line.

Whereas the branching ratio of the most exoergic channel (2a) is only 61 ± 5%, the three-body pathway (2c) accounts for the remaining flux (39 ± 5%). Energy dependencies of the cross sections between 1 and 1000 meV have also determined. From these cross sections thermal reaction rates could be obtained, which are described by $k = 1.2 \pm 0.3 \times 10^{-6}\ (T/300)^{-0.64\pm0.01}\ cm^3s^{-1}$, $k = 1.4 \pm 0.3 \times 10^{-6}\ (T/300)^{-0.74\pm0.01}\ cm^3s^{-1}$ and $k = 4.7 \pm 1.4 \times 10^{-7}\ (T/300)^{-0.50\pm0.02}\ cm^3s^{-1}$ for $DOCO^+$, DON_2^+ and SO_2^+, respectively. The present results are compared with DR branching ratios of other isoelectronic ions and astrophysical implications, especially on the chemistry of dark clouds and the ionosphere of Jupiter's satellite Io are discussed.

1 A. Neau, A. Al-Khalili, S. Rosen, A. Le Padellec, A. M. Derkatch, W. Shi, L. Vikor, M. Larsson, M. B. Nagard, K. Andersson, H. Danared, M. af Ugglas, *J. Chem. Phys.*, 2000, **113,** 1762

2 D. R. Bates, *Astrophys. J.*, 1986, **306,** L45; D. R. Bates, Interstellar Cloud Chemistry revisited in "Modern Applications of Atomic and Molecular Processes" (ed. A. E. Kingston, London, Plenum)

3 C. R. Herd, N. G. Adams, D. Smith, 1990, *Astrophys. J.* **349**, 388

An Experimental and Theoretical Investigation of the $C_2H + NH_3$ Reaction

S. A. Carl, H. M. T. Nguyen, R. M. I. Elsamra, R. M. Kulkarni, M. T. Nguyen, J. Peeters

Katholieke Universiteit Leuven, Celestijnenlaan 200F, B-3001 Leuven, Belgium

Most gas-phase reactions of radicals with closed-shell molecules face sizable energy barriers and thus have negligible rate constants at the low temperatures ($10\ K \leq T \leq 100\ K$) found in interstellar regions where the chemistry is dominated by barrier-less reactions governed by long-range attractive forces. A notable exception to this is the reaction of CN with NH_3 having $k(100\ K) \approx 1 \times 10^{-10}\ cm^3\ s^{-1}$.[1]

Isoelectronic with CN is the C_2H radical that has been detected in interstellar regions and in planetary atmospheres. and since it is isoelectronic with CN the rate constant for its reaction with NH_3 might also be large at low temperatures. Here we present the first experimental and theoretical study of the $C_2H + NH_3$ reaction.

The absolute rate constants for $C_2H + NH_3 \rightarrow$ products were experimentally determined over the temperature range 295 – 765 K at a pressure of 10 Torr (He) and over the pressure range 5 - 30 Torr at 295 K. The pressure-independent rate constant is indeed large and exhibits a pronounced negative temperature dependence: $k_1(T) = (3.9 \pm 0.4) \times 10^{-11}(T/295\ K)^{-0.75 \pm 0.10}\ cm^3\ s^{-1}$ both unusual for reaction of a radical with a saturated molecule. The predicted rate constant at 100 K is $k(100\ K) = (8.8 \pm 3.0) \times 10^{-11}\ cm^{-3}\ s^{-1}$. The (extrapolated) high rate constant both at interstellar temperatures and combustion temperatures should make this reaction important in those environments.

We have also investigated portions of the $C_2H + NH_3$ potential energy surface. Calculations at the CCSD(T)/6-311++G(3df,2p) + ZPE level show that the $C_2H + NH_3$ reaction has two main entrance channels: H-abstraction and condensation. The relative energies (kcal/mol) along the H-abstraction pathway are as follows: **1** $C_2H + NH_3$ (0) $\rightarrow$ pre-reaction complex **CO2** (-2.9) $\rightarrow$ **TS** (-1.8) $\rightarrow$ post-reaction complex **CO3** (-28.4) $\rightarrow$ HCCH + NH_2 (-26.6). This channel thus begins with the formation of a weakly bound complex HCC...H_3N, which after H-atom transfer gives rise to a second weakly bound complex, HCCH...NH_2. The condensation pathway leads to H_2N-CCH + H (-14.2) but has a high point of +4.3 kcal/mol. H-abstraction is therefore expected to be the only channel at interstellar temperatures and to dominate condensation even at combustion temperatures.

1. Sims, I. R.; Queffelec, J. -L.; Defrance, A.; Rebrion-Rowe, C.; Travers, D.; Bocherel, P.; Rowe, B. R.; Smith I. W. M. *J. Chem. Phys.* **1994**, *100*, 4

Dissociative photoionisation of hydrocarbon radicals

W.Roth[1], T. Schüßler[1], C. Alcaraz[2], and I. Fischer[1]

[1] *Institute of Physical Chemistry, University of Wuerzburg, D-97074 Wuerzburg*
[2] *LURE, Bât. 209, BP 34, Centre Universitaire Paris-Sud, F-91898 Orsay*

The VUV photochemistry of the radicals allyl, C_3H_5, propargyl C_3H_3, and ethyl, C_2H_5, is investigated using synchrotron radiation. The radicals are produced by flash pyrolysis from the corresponding iodides and bromides, respectively. The onset of dissociative ionisation is determined by photoelectron-photoion coincidence (PEPICO). Like in most hydrocarbons, loss of H_2 is the major reaction channel in the allyl and ethyl cation. However, dissociative ionisation of propargyl is associated with loss of a hydrogen atom, leading to formation of c $C_3H_2^+$. The process sets in around 12.6 eV, in agreement with computations. The results are of relevance for the chemistry of dense interstellar clouds, where the reaction $C_3H^+ + H$ plays a major role. Our results show that the channel leading to c-$C_3H_2^+ + H$ is exothermic relative to the entrance channel, in agreement with some earlier experiments, but in contrast to calculations.

Time-Resolved Cavity Ringdown Measurements of Fast Reactions: Retrieving Rate Constants from Non-Exponential Ringdown Signals

G. Friedrichs, M. Fikri, Y. Q. Guo, J. Neumann, F. Temps

Institut für Physikalische Chemie, Christian-Albrechts-Universität zu Kiel, Olshausenstr. 40, 24098 Kiel, Germany

gfriedr@phc.uni-kiel.de, temps@phc.uni-kiel.de

Cavity ringdown spectroscopy (CRDS) is a highly sensitive and quantitative absorption method. Moreover, in contrast to emission techniques such as laser induced fluorescence, CRDS is insensitive to predissociation or collisional quenching processes, which facilitates the investigation of pressure dependent reactions. Until recently, the kinetic applications of CRDS were limited to relatively slow reactions with lifetimes of the measured species longer than the ringdown time of typically several tens of μs. In this case, the concentration of the reactive species can be easily extracted from the single-exponential decay profile and the complete transients can be obtained by varying the delay between the photolysis or pump laser and the ringdown probe laser. For fast reactions which occur on the same time scale as the ringdown, however, the ringdown becomes non-exponential due to the convolution with the concentration change. Here, the so-called Simultaneous Kinetics and Ringdown (SKaR) model developed by Brown et al. (*J. Phys. Chem. A* **104** (2000) 7044) can be applied.

However, when the probe laser linewidth is comparable to or exceeds the absorption linewidth of the detected species, as it is common with conventional pulsed dye lasers, multi-exponential overall ringdown signals are obtained even without any reactions due to the "bandwidth effect". We recently presented an extended SKaR model (eSKaR) that takes this bandwidth effect into account and allows us to extract rate constants from non-exponential ringdown profiles originating from the convolution of the bandwidth effect and the kinetics (Guo et al., *Phys. Chem. Chem. Phys.* **5** (2003) 4622). We employed the eSKaR model to measure the kinetics of the reaction $SiH_2 + O_2$ and several other SiH_2 reactions under pseudo-first order conditions and were able to extract the rate constant directly from the *Ratio* function, which is the ratio of the ringdown signal with reaction to that measured without absorber. Of course, for an accurate extraction of the reaction rate constant the absorption linewidth and the probe laser bandwidth have to be known.

In order to further verify the eSKaR model and to assess the influence of absorption linewidth effects we now extended our measurements to the reaction of amino radicals with nitric oxide at pressures up to 600 mbar. The reaction NH_2 + NO serves as a well defined test system since pressure broadening coefficients of NH_2 are known from narrow-bandwidth absorption studies and the rate constant of this reaction was repeatedly measured at room temperature.

The Glow Discharge Plasma is a Rydberg Gas

Rod S Mason, Ifor P Mortimer, Dave J Mitchell and Neil A Dash

Chemistry Department, University of Wales Swansea, Swansea SA2 8PP, UK
r.s.mason@swan.ac.uk

Often described as the fourth state of matter, the gaseous plasma is classically defined as a 'dense' medium of ions and electrons, overall electrically neutral, which also contains many excited state species. The glow discharge has served as a model for the electrical plasma for the past 100 years. However, there are many unexplained anomalies. Not least is the difficulty of detecting ions from the plasma boundary furthest away from the cathode, by mass spectrometry, when sampling at distances greater than a few mm from the cathode. We have studied this phenomenon extensively using a fast flow technique to isolate the Ar/Cu plasma from the method of its formation and can show that relatively very few ions are carried into the flowing plasma. However ions are very easily generated from species leaving the plasma, to be detected by mass spectrometry, by field-ionisation. The spectrum depends on the strength of the field. Thus with a field of 2000V cm^{-1}, Ar^+ is generated in abundance. With a low field of 100 V cm^{-1}, it is mostly Cu^+ in the mass spectrum and very little Ar^+ is detected. To become focussed the ionisation of the excited states must be very rapid, it is therefore inferred that the ions produced are from Rydberg atoms. If so, the lifetimes are very long (10^{-4} – 10^{-3} s) and are stabilised in the plasma environment. Their concentration is estimated to be similar to that expected for the plasma density. The ionising states of Ar are rapidly quenched by adding H_2 to the afterglow plasma. Cu ionisation is first boosted and then quenched and there is little evidence of the ion-molecule reaction chemistry expected in the presence of free ions. In some circumstances free Ar^+ ions can be released by (for example) the reaction:

$$Ar^R + CCl_4 \rightarrow Ar^+ + CCl_3 + Cl^-$$

In other circumstances free electrons can be released by (for example) the reaction:

$$Ar^R, Ar^* + NO \rightarrow Ar + NO^+ + e^-$$

Experiments conducted include Fast Flow Glow Discharge mass spectrometry, plasma potential and conductivity measurements and plasma reaction chemistry studies, in both the flowing afterglow mode described above and in the fast flowing full discharge. Although the Langmuir model of the glow discharge plasma has been the accepted model for 70 years, we are proposing that the model of this important cold plasma needs a rethink. This (proposed) talk will present a summary of evidence.

The Long Way from Reaction Kinetics Experiments to Rate Data Usable in Technological Applications

Jürgen Warnatz

Interdisciplinary Center of Scientific Computing,Heidelberg University, Im Neuenheimer Feld 368, D-69120 Heidelberg, Germany.

1. Compilation of original rate data: This first step is providing T- and p-dependent rate data of elementary steps potentially involved in applications in technology, determining "best" values. The main problems here are multi-channel radical-radical reactions due to the difficult experiments.

2. Generation and validation of working reaction mechanisms: The output of the first step is not yet suitable to run a CFD computer code, due, e. g., to lacking data or incorrect rates or product specifications. Therefore, these rate data are tested with the help of experimental results on typical, but simple, (0D, 1D geometry) combustion situations: ignition, flame propagation, flame structure, quenching, pollutant formation. It is anticipated that rate coefficients can then be changed within the range of their error limits to reproduce the experiments listed. More critical is it, if missing reactions using estimated rate coefficients have to be added.

3. Computer generation of reaction mechanisms: For larger hydrocarbons, there are no data available for many reactions. Therefore, rule-determined computer generation of reaction mechanisms has to be used to get reaction mechanisms, starting from an initial set of species to be specified.

4. Reduction of the reaction mechanism: Normally, detailed reaction mechanisms are so large, that they cannot be handled by 2D or 3D CFD codes. Thus, a reduction of the reaction mechanism has to be performed in a given parameter space, preferable using suitable mathematical techniques, basing on time-scale splitting.

5. Tabulation of reaction rates: The final step is the tabulation of reaction rates and averaged (with a pdf approach, presumed or computed pdf) reaction rates for the description of the interaction of turbulent flow field and chemical reaction.

Synchrotron Photoionization Molecular-Beam Mass Spectrometric Characterization of Intermediates in Rich Flames

Craig A. Taatjes, Tina Kasper, Andrew McIlroy
Combustion Research Facility, Mail Stop 9055, Sandia National Laboratories, Livermore, CA 94551-0969

Terrill A. Cool, Koichi Nakajima, Juan Wang
School of Applied and Engineering Physics, Cornell University, Ithaca, NY 14886

Matthew E. Law, Aude Morel, Phillip R. Westmoreland
Department of Chemical Engineering, University of Massachusetts, Amherst, MA 0100

Lionel Poisson, Darcy S. Peterka, and Musahid Ahmed
Chemical Sciences Division, Lawrence Berkeley National Laboratory, Berkeley, CA 94720

Control of pollutant emissions, while also promoting the more efficient use of fossil fuels and the introduction of renewable fuels, requires a close insight into the chemical processes involved in combustion. Low-pressure flames are important model systems for the investigation of combustion mechanisms because they can be designed to exhibit nearly one dimensional variations in species concentration and temperature, and because the reduced pressure increases experimental spatial resolution. In the last year at the ALS, low-pressure flames of ethane, propane, ethene, and propene have been investigated to illuminate key pathways to the formation of adverse combustion emissions, especially soot. The formation of small aromatic structures from linear unsaturated compounds (e.g. C_2H_2, C_3H_3, ...) is a major step in the mechanism towards polyaromatic hydrocarbon (PAH) and soot production at high temperatures. Reliable concentration profiles of these species may help to identify and distinguish the routes to benzene and subsequent PAH formation in different fuels. As the lower alcohols are known to suppress the formation of soot when added to hydrocarbon fuels, rich ethanol and propanol flames have also been investigated. Concentration profiles of a variety of stable and reactive species are measured *in situ* by molecular beam mass spectrometry, using a time-of-flight mass spectrometer in combination with single-photon ionization. The ionization energies of most stable species and radicals present in flames range from 5 eV to 15 eV; the ALS is an excellent source for the required VUV radiation because of its ease of tunability and high brightness. A scan over a range of photon energies allows the identification of species by their appearance energies. This capability is especially important when more than one chemical species or isomer may be assigned to a signal in the mass spectrum. In the present case the energy resolution of the ALS has allowed determination of the concentrations of the C3H4 isomers allene and propyne in fuel rich hydrocarbon flames, and permitted characterization of the novel intermediate species ethenol (vinyl alcohol), observed in flames for the first time at the ALS.

This work is supported by the Division of Chemical Sciences, Geosciences, and Biosciences, the Office of Basic Energy Sciences, the U. S. Department of Energy. Sandia is a multi-program laboratory operated by Sandia Corporation, a Lockheed Martin Company, for the National Nuclear Security Administration under contract DE-AC04-94-AL85000.

Systematic, automated model construction for high-conversion ethane pyrolysis

David M. Matheu,[a] Anthony M. Dean,[b] Jeffrey M. Grenda,[c] William H. Green, Jr.[d]

Advancement in the understanding and design of such important gas-phase processes as hydrocarbon pyrolysis, combustion, and partial oxidation hinges, in part, on the development of correct, detailed chemical kinetic models. But the size and complexity of the required chemical mechanisms makes them extremely difficult to construct by hand. Chemists and engineers have thus turned to software tools that attempt to build these large mechanisms automatically, but these tools suffer from many limitations, including the inability to treat pressure-dependence, and the arbitrary termination of mechanism growth.

We present a new, elementary-step-based mechanism generation algorithm which combines an integrated approach to pressure-dependent reactions with a rational, flux-based criteria for truncating mechanism growth. Applications to the difficult-to-understand, highly pressure-dependent methane and high-conversion (>98%) ethane pyrolysis systems reveal important new pathways, not previously considered by other researchers, that may explain the experimentally observed behavior. We conduct a thorough study of the generated kinetic models, which includes reaction pathway diagrams, sensitivity analysis, equilibrium calculations, brute-force parameter variation analysis, and a study of the importance of our systematic pressure-dependence treatment to the predictions of the minor species concentrations. This examination reveals a set of highly complex, interconnected, parallel reaction pathways that control the formation and destruction of acetylene, butadiene, propylene, and benzene (all of which are believed to be important as pyrolytic carbon precursors).

[a]National Institute of Standards and Technology
Physical and Chemical Properties Division
100 Bureau Dr. Stop 8380
Gaithersburg, MD 20899-8380
david.matheu@nist.gov

[b]Department of Chemical Engineering
Colorado School of Mines
451 Alderson Hall
Golden, CO 80401
amdean@mines.edu

[c]ExxonMobil Research and Engineering Company
1545 Rt. 22 East
Annandale, NJ, 08801
jeffrey.m.grenda@exxonmobil.com

[d]Department of Chemical Engineering
Massachusetts Institute of Technology
77 Massachusetts Ave. Room 66-448
Cambridge, MA 02139
whgreen@mit.edu

The thermal unimolecular decomposition of HCO

H. Hippler, N. Krasteva, F.Striebel

Institut f. Phys. Chemie, Lehrstuhl f. Molekulare Physikalische Chemie
Universität Karlsruhe, Kaiserstr. 12, 76128 Karlsruhe, Germany

Formyl radicals are formed in combustion processes in the course of the oxidation of hydrocarbons. Their fate is than determined by the competition between unimolecular decomposition, which yields H-atoms and is thus a chain carrier, and reactions which H, OH or O_2, which yield H_2, H_2O and HO_2, respectively, and are thus chain terminating processes. For a reliable modeling of the combustions process an accurate knowledge of the rate constants for all reactions mentioned above is needed. Additionally, there is interest in the title reaction from a fundamental point of view: HCO radicals are known to decompose *via* isolated resonances. The decay of these isolated resonances has been characterized in detail both experimentally as well as theoretically and it has been found that the decay rates (k(E)) show marked fluctuations. The effect of the fluctuations of k(E) on the thermal rate constant (k(T,p)), however, has so far not been studied in detail. It has rather been assumed that the thermal rate constant is in the low pressure regime under combustion conditions and a second order rate constant has been used for modeling purposes. This fact motivated us to investigate the title reaction under a wide range of conditions to check the validity of the above mentioned assumption. We have done experiments at temperatures between 590 and 800 K and pressures ranging from 1 to 150 bar of helium. Additionally, experiments at 700 K and N_2 as bath gas have been performed. Formyl radicals have been generated by pulsed laser photolysis of acetaldehyde and they have been detected using laser induced fluorescence. We find i) that the above mentioned assumption is not correct and ii) that the experimentally observed pressure dependence of the rate constant is not in agreement with the results of RRKM and master equation computations. We are, however, able to describe the observed pressure dependence with a Lindemann-Hinshelwood-type calculation based on the resonance lifetimes calculated by Schinke and co-workers (H.-M. Keller et al., J Chem. Phys. 105 (1996), 4983). These calculations show that the falloff curves are much broader than expected: At pressures as low as a few mbar the rate constant is no more in the low pressure regime while at 150 bar it is still more than one order of magnitude smaller than the predicted high pressure rate constant.

Acknowledgement: Financial Support by the Deutsche Forschungsgemeinschaft (SFB 606: 'Instationäre Verbrennung: Transportphänomene, Chemische Reaktionen, Technische Systeme') is gratefully acknowledged.

The products of the NH + CO_2 and H_2O reactions. Practical and fundamental aspects

Arthur Fontijn and Sayed M. Shamsuddin
High-Temperature Reaction-Kinetics Laboratory, The Isermann Department of Chemical and Biological Engineering, Rensselaer Polytechnic Institute, Troy, New York 12180-3590

Paul Marshall
Department of Chemistry, University of North Texas, Denton, TX 76203-5070

William R. Anderson
AMSRL-WM-BD, U.S. Army Research Laboratory, Aberdeen Proving Ground, MD 21005-5060

The reactions of NH with CO_2 and H_2O have been studied by Rohrig and Wagner in the 1200 to 1900 K temperature range.[1] They assumed HNO + CO and HNO + H_2 to be the respective products. However, introduction of their rate coefficients with these products into models of NO reduction in NO/CO/H_2 mixtures and of dark zone lengths in nitrate ester propellant combustion led to orders of magnitude differences with the observations.

We have re-investigated the NH + CO_2 reaction and confirm the magnitude of their rate coefficients. This leads to the conclusion that HNO + CO are not the products. This has been confirmed by *ab initio* calculations that show the barriers for formation of these products to be much larger than the measured activation energies. As other product combinations are too endothermic, it is assumed that an intermediate adduct forms. *Ab initio* calculations have identified several possible adducts. These are insufficiently stable to be the probable end products and are thought to undergo further, not yet identified, reactions.

Rohrig and Wagner had used a shock tube to produce NH by HN_3 dissociation. In the present work a high-temperature photochemistry reactor was used, where the NH was produced by the 193 nm 2-photon photolysis of NH_3. We measured $k(415 - 1225\ K) = 8.5 \times 10^{-32} (T/K)^{5.87} \exp(1000\ K/T)\ cm^3\ molecule^{-1} s^{-1}$.

In further work we have re-measured the NH + H_2 reaction rate coefficients, which gave excellent agreement with those of Ref. 1. This indicates that it must be assumed that their rate coefficients for the H_2O reaction are also substantially correct and that HNO + H_2 can not be the products of that reaction. *Ab initio* investigation of the NH + H_2O system is underway.

1. M. Rohrig, H.Gg. Wagner, Proc. Comb. Inst. 25, 975 (1994)

Work supported by ARO, NSF, and the Welch Foundation.

The reaction of $CH_3 + O_2$: Experimental determination of the rate coefficients for the product channels at high temperatures

John T. Herbon, Ronald K. Hanson, Craig T. Bowman, and David M. Golden

Department of Mechanical Engineering, Stanford University

The reaction of methyl radicals (CH_3) with molecular oxygen (O_2) has been investigated in high-temperature shock tube experiments from 1570 to 2710K. The overall reaction rate coefficient, $k_1 = k_{1a} + k_{1b}$, and individual rate coefficients for the two high-temperature product channels (channel (1a) producing CH_3O+O and channel (1b) producing CH_2O+OH) were determined in ultra-lean mixtures of CH_3I and O_2 in Ar/He. Narrow-linewidth UV laser absorption at 306.7nm was used to measure OH concentrations, for which the normalized rise time is sensitive to the overall rate coefficient k_1 but relatively insensitive to the branching ratio of the individual channels and to secondary reactions. Atomic resonance absorption spectroscopy measurements of O-atoms were used for a direct measurement of channel (1a). Through the combination of measurements using the two different diagnostics, rate coefficient expressions for both channels were determined. The overall rate coefficient is in close agreement with a recent *ab initio* calculation and one other shock tube study, while comparison of k_{1a} and k_{1b} to these and other experimental studies yields mixed results. In contrast to one recent experimental study, reaction (1b) is found to be the dominant channel over the entire experimental temperature range.

Formation and decomposition of chemically activated c-C_5H_9O radicals in the gas phase

Walter Hack[1], Karlheinz Hoyermann[2], Jörg Nothdurft[2], Matthias Olzmann[3], Thomas Zeuch[2]

[1]*Max-Planck-Institut für Biophysikalische Chemie, Am Fassberg, D-37077Göttingen, Germany*
[2]*Institut für Physikalische Chemie, Universität Göttingen, Tammannstr. 6, D-37077 Göttingen, Germany; jkupfer@gwdg.de*
[3]*Institut für Physikalische Chemie, Universität Karlsruhe, Fritz-Haber-Weg 4, D-76128 Karlsruhe, Germany*

Saturated cyclic hydrocarbons like c-C_5H_{10} and c-C_6H_{12} are components of typical gasolines thus attention has been paid to their oxidation mechanisms. As the primary attack of c-C_5H_{10} by atoms (H, O) and radicals (OH, CH_3) leads to c-C_5H_9 radicals, their further reactions are of interest. Here the reaction of cyclo-pentyl radicals with oxygen atoms was studied experimentally and theoretically with respect to the primary products and the unimolecular reactions of the intermediate c-$C_5H_9O^*$, especially in regard to ring opening.

The experimental arrangement of laser flash photolysis combined with quantitative FT-IR spectroscopy allowed the determination of the stable products at different pressures (4mbar, 1 bar). The radicals were formed via the reaction c-C_5H_{10} + Cl with Cl atoms stemming from the photolysis of $CFCl_3$ and the atomic oxygen from the photolysis of SO_2.

The main reaction products identified and quantified were c-C_5H_8O (cyclopentanone), 4-C_4H_7CHO (pentenal), C_2H_4, and CO. Minor products were C_3H_6 (propene) and C_2H_3CHO (2-propenal). No c-C_5H_8, 3-C_4H_7CHO, c-C_4H_8, and 1-C_4H_8 were detected. The products are explained by a mechanism in terms of the formation and subsequent reactions of a chemically activated cyclopentoxy radical.

$$\begin{array}{lcl} \text{c-}C_5H_9 + O & \rightarrow & \text{c-}C_5H_9O^* \\ \text{c-}C_5H_9O^* & \rightarrow & \text{c-}C_5H_8O + H \\ & \rightarrow & \text{4-}C_4H_7CHO + H \\ & \rightarrow & 2C_2H_4 + CO + H \end{array}$$

The branching ratios at low and high pressure are listed in the table

	c-C_5H_8O + H	4-C_4H_7CHO + H	$2C_2H_4$ + CO + H
4mbar	0.23	0.42	0.35
1 bar	0.25	0.52	0.24

The experimental branching fractions are analyzed in terms of statistical rate theory with molecular and transition-state data from quantum chemical calculations. The specific rate coefficients for the decomposition and isomerization reactions of the chemically activated intermediates are calculated from RRKM theory, and the threshold energies are adjusted so as to reproduce the relative product yields observed. By using these optimized values, high-pressure limiting Arrhenius parameters for the unimolecular reactions of cyclo-C_5H_9O are predicted and recommendations for the use in combustion modeling are given.

Addition reactions of sulfur species: S + NO, O + SO_2, and S + N_2O

A. Goumri, Jacinth Naidoo, Elizabeth Mitchell, Yide Gao and Paul Marshall*

Department of Chemistry, University of North Texas, P.O. Box 305070, Denton, Texas 76203-5070, USA

*marshall@unt.edu

Sulfur is known to influence NOx formation in flames but the mechanism is unknown. There may be direct sulfur-nitrogen interactions, or sulfur may affect the overall radical pool. In this context the title reactions have been studied by the laser photolysis – resonance fluorescence technique, at temperatures up to 1000 K and pressures of Ar bath gas up to 800 mbar.

In the case of

$$S + NO + Ar \rightarrow \text{products} \qquad (1)$$

simple third order kinetics are observed (contrary to prior experiments, made at room temperature, which suggested fall-off behavior). The third-order recombination rate constant drops with increasing temperature. Using an ab initio potential energy surface, RRKM modeling of this process via flexible TST gives excellent accord with our experiments. ONS is the likely dominant product. The ab initio calculations also reveal other slightly less stable isomers of ONS, and other reaction paths such as abstraction and addition of S to the oxygen end of NO are discussed.

Ab initio studies of the potential energy surface for

$$S + N_2O\ (+Ar) \rightarrow \text{products} \qquad (2)$$

indicate the possibility of several addition/elimination and abstraction pathways, leading to both NS and SO formation. The former is significant because routes to NS, a species observed in flames, are not well-established. Preliminary kinetic measurements confirm high barriers proposed for these reactions.

Our extended T and p measurements on the spin-forbidden process

$$O + SO_2 + Ar \rightarrow SO_3 + Ar \qquad (3)$$

reveal for the first time (a) a predicted maximum in the recombination rate constant at about 800 K, and (b) fall-off behavior. The results can be rationalized in terms of Troe's approximate master equation formalism, and extrapolated to yield the high-pressure limit. The addition reaction occurs over a significant barrier. Several proposed detailed mechanisms are discussed, which differ as to the relative location of the barrier and the singlet-triplet curve intersection, and thus as to how the probability of intersystem crossing influences the kinetics. We present new ab initio information about the potential energy surfaces involved, particularly our characterization of a new bound triplet state for SO_3.

Quantum reaction dynamics of polyatomic molecules

David C. Clary

Department of Physical and Theoretical Chemistry
University of Oxford, South Parks Rd, Oxford OX1 3QZ
david.clary@chem.ox.ac.uk

Quantum dynamics calculations provide results on chemical reactions that can be compared in detail with experiment. They have the advantage that quantum effects such as tunnelling and zero-point energy are dealt with accurately. If the potential energy surfaces are accurate then experimentalists can have confidence in the predictions.

Reactions of atoms with diatomic molecules represent the simplest chemical reactions and have been the subject of many accurate quantum-dynamics calculations on good potential surfaces. Reactions of polyatomic molecules are also now receiving attention and offer the interesting opportunity to examine how different types of vibrational modes affect a chemical reaction. It is difficult to include all the degrees of freedom in such calculations and methods that reduce the problem to the key modes in the chemical reaction become useful. This is the "reduced dimensionality" approach we have been following.

In this talk a general reduced dimensionality method will be described that combines accurate quantum chemistry calculations of a small number of key points on the potential energy surface with a quantum dynamical treatment of the bonds being broken and formed in a chemical reaction. Recent applications of the method, by Dr Boutheina Kerkeni in our group at Oxford, to the reactions of H atoms with polyatomics such as CH_4, C_2H_6 and CH_3OH will be described. The results demonstrate significant tunnelling in these reactions and the calculated rate constants compare favourably with experiment. The promising results suggest that this will be a general procedure for making accurate predictions on the reaction kinetics and dynamics of larger polyatomic molecules.

Do we know how to think about surface chemistry? Electronically non-adiabatic interactions in molecule metal-surface scattering.

Alec M. Wodtke

Dept. of Chemistry and Biochemistry, University of California, Santa Barbara, California 93106

When molecules with low levels of vibrational excitation collide with metal surfaces, vibrational induced excitation of the metal's electrons is not strong unless incidence energies are high. Furthermore, theoretical studies suggest that elementary steps in surface reactions, like trapping, diffusion and desorption are not strongly influenced by coupling between adsorbate nuclear motion and metallic electrons, i.e the Born-Oppenheimer approximation is valid. There have been only a limited number of studies that attempt to test the importance of electronically non-adiabatic influences for large amplitude intramolecular adsorbate motion characteristic of passing through a chemical transition state. These studies provide accumulating evidence that coupling of large amplitude molecular vibration to metallic-electron degrees-of-freedom can be quite strong. Recently, we observed electron emission for a solid metal surface when highly vibrationally excited nitric oxide molecules are scattered from a low work function metal surface. These results give direct evidence that interactions between a metal surface and molecules undergoing large amplitude intramolecular nuclear motion can promote strong non-adiabatic coupling to excited electronic states of the metal. These results suggest that theoretical approaches relying on the Born-Oppenheimer approximation may not accurately reflect the nature of transition-state traversal in reactions at metal surfaces and point to the need to account for strong electronically non-adiabatic influences in theories of heterogeneous catalysis.

Gas-liquid interfacial reaction dynamics between $O(^3P)$-atoms and squalane

Sven P. K. Köhler, Mhairi Allan, Hailey Kelso, David A. Henderson, Kenneth G. McKendrick

School of Engineering and Physical Sciences, Heriot-Watt University, Edinburgh EH14 4AS, UK

We report the first measurements of internal energy distributions in the gas phase produced by reactive scattering at a gas-liquid interface. In particular, we recorded rotationally resolved laser-induced fluorescence (LIF) spectra of hydroxyl radicals which are the main gas phase product of the reaction between $O(^3P)$ atoms and the liquid hydrocarbon squalane $C_{30}H_{62}$/ $C_{30}D_{62}$.

$O(^3P)$ atoms are created by laser photolysis of NO_2 at 355 nm above a continually refreshed liquid hydrocarbon surface generated using a wheel that rotates through a temperature-controlled bath of liquid squalane. Hydroxyl radicals are detected under collision-free conditions by LIF. The detected hydroxyl radicals unambiguously originate from the surface because their time-of-flight profile correlates with different surface–laser distances (see figure).

The rotational populations derived are sensitive to the surface temperature. This implies that the hydroxyl radicals at least partially relax at the surface. However, measurements at –10°C and +80°C give gas-phase rotational temperatures that only differ by ~30 K. This indicates that relaxation is not complete. The rotational temperature in (v'=1) is colder than in (v'=0), as would be expected for a direct abstraction mechanism. On the other hand, this temperature difference is not as large as expected from previous gas-phase results. We therefore conclude that the reaction proceeds *via* two different mechanisms: one component is a direct abstraction mechanism as observed in the gas phase, whereas the other is a trapping-desorption mechanism that generates rotationally relaxed hydroxyl radicals. This is supported by Monte-Carlo simulations of the observed time-of-flight profiles, and by previous complementary molecular beam scattering experiments.

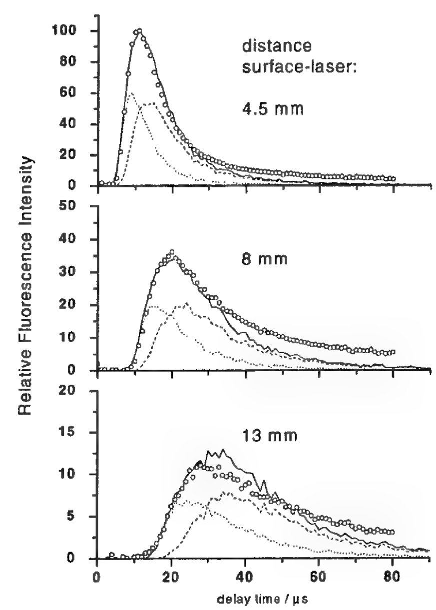

Hydrogen Atom Production from the Photolysis of Water Ice Particles

Masahiro Kawasaki* and Hiroto Tachikawa+

* *Department of Molecular Engineering, Kyoto University, Kyoto 615-8510, Japan*
+ *Department of Molecular Chemistry, Hokkaido University, Sapporo 060-8628, Japan*

Several experimental studies on VUV photodissociation of water adsorbed on cold surfaces have been reported. At around 200 nm, there has been no experimental study because it has been believed that the ice is completely opaque for photons of longer than 160 nm. Dressler and Schnepp, however, reported in *J. Chem. Phys.* (1960) a region of weak and continuous absorption extended from 180 to 210 nm. In the present experiment we have investigated the UV photodissociation dynamics of water ice at 193 nm. Our purpose is directly to observe the formation of hydrogen atoms and estimate its influence on the mesosphere ozone depletion (Fig.1) since there are appreciable amounts of small water-ice particles including the noctilucent clouds (NLCs) in the high-latitude polar mesopause region and the solar radiation at 200 nm is much stronger than at Lyman-α line.

According to our theoretical calculation, a water molecule on ice surface may have a character similar to a water molecule attached to a $(H_2O)_6$ cluster, which absorbs 200 nm photon. (Fig.2). Actually we have directly observed H atoms signals in the 193 nm photodissociation of water ice films with the REMPI technique.

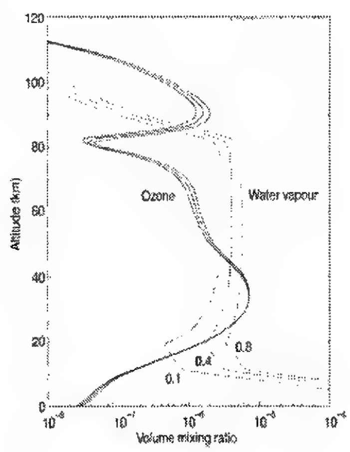

About atmospheric implication of the present results, we have estimated relative contribution of NLCs photolysis to the hydrogen atom formation near the mesopause region, comparing with that of water vapor;

$$\frac{H_{ice}}{H_{vapor}} = \frac{\int d\lambda\, \sigma_i(\lambda)\times P_i(\lambda)\times \phi_i(\lambda)\times C_i}{\int d\lambda\, \sigma_v(\lambda)\times P_v(\lambda)\times \phi_v(\lambda)\times C_v} \leq 0.5$$

where H stands for the amount of H atoms,σ:absorption cross section, P: solar flux, φi: quantum yield = 0.01, C: concentration. The photodissociation of NLCs could be another important source of H atoms by solar irradiation.

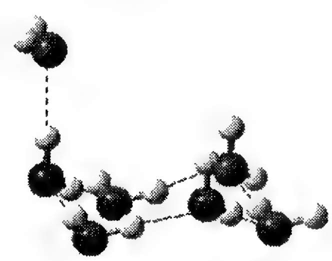

Fig.2 Optimized structure of the $(H_2O)_{6+1}$ water cluster. A water molecule is hydrogen-bonding to a model crystalline surface $(H_2O)_6$.

Acknowledgment The authors thank Dr. B. Murrell and Prof. J. Plane for stimulation discussion.

Publication A. Yabushita et al., *J. Chem. Phys.* **120**, 5463 (2004)

Reversible Gas Adsorption in Coated Wall Flow Tube Reactors. Model Simulations and Application to the Uptake of Acetone on Ice around 200 K.

P. Behr, A. Terziyski, U. Scharfenort and R. Zellner

Institute of Physical and Theoretical Chemistry, University of Duisburg-Essen, D-45117 Essen, Germany
e-mail: reinhard.zellner@uni-essen.de

A kinetic model has been developed to simulate reversible gas adsorption in coated wall flow tube reactors (CWFTs) with moveable injectors. The motivation of this work is to generate a theoretical dynamical framework for adsorption studies of atmospheric trace gases on ice surfaces at temperatures around 200 K using the CWFT technique. It is shown in this model that for higher uptake rates and enthalpies of adsorption in the order of 50 kJ/mol, as typical for oxygenated organics on ice surfaces, the observed adsorption is reversible and the resulting kinetic profiles with respect to laboratory time of gas phase concentrations depend on the detailed operations of the flow system and the injector. The predictions of the model with respect to gas and surface concentrations as a function of operational variables will be demonstrated.

The kinetic model has been applied to adsorption studies of acetone on ice surfaces at temperatures between 190 – 223 K. It is found that in this temperature range the adsorption on ice may described by an uptake coefficient of $\gamma \sim 6 \cdot 10^{-3}$, independent of temperature. The desorption, on the other hand, is found to be strongly temperature dependent with an activation energy of $E_a = 46.0$ kJ/mol and a pre- exponential factor of $A = 1.5(\pm 0.5) \cdot 10^{12}\ s^{-1}$. Modelling of the kinetic profiles also indicates that at temperatures between 190 and 203 K an additional surface removal process takes place which is not consistent with reversible adsorption but rather by diffusion into the bulk ice phase. The nature and the rate of this process will be described in detail.

Uptake Measurements of Phenolic Compounds by Water Droplets and Determination of their Henry's Law Constants Over the Temperature Range 278-303 K: Implications for Tropospheric Multiphase Chemistry

Florent Louis*[a)], Gontrand Leyssens[a)], Jean-Pierre Sawerysyn[a)], Valérie Feigenbrugel[b)], Stéphane Le Calve [b)], and Philippe Mirabel [b)]

a) Physico-Chimie des Processus de Combustion et de l'Atmosphère (PC2A), UMR CNRS 8522, Bât. C11, Université des Sciences et Technologies de Lille, 59655 Villeneuve d'Ascq, France
b) Centre de Géochimie de la Surface (CGS), UMR CNRS 7517, Université Louis Pasteur, 67084 Strasbourg, France
* florent.louis@univ-lille1.fr

Phenols constitute a class of organic substances of particular environmental interest. Due to their widespread discharge into the environment and their toxicity to many living organisms, phenol and its alkyl derivates are presently found on most priority lists (Mackay, 1991). Once released or produced in the atmosphere by gas phase photo-oxidation of alkylbenzenes, these compounds, due to their high solubilities in water, are expected to be efficiently scavenged from the gas phase by rain and fog. The partitioning of phenolic compounds between aqueous and gaseous phases has to be investigated in order to better define their fate, their transport, and their removal in the troposphere.

In this talk, we report the laboratory determination of the temperature-dependent mass accommodation coefficients (α) and Henry's Law constants (HLC) using respectively a wetted-wall flow tube technique and a dynamic equilibrium system. The obtained data (α, HLC) were then used to estimate the fractions of phenolic compounds in atmospheric aqueous phase and their resulting atmospheric lifetimes under clear sky and cloudy conditions. Results will be presented and discussed.

Reference:

Mackay, D., 1991. Multimedia Environmental Models. The Fugacity Approach. Lewis Publishers, Chelsea, MI.

Towards Examining Single Aerosol Particle Dynamics

J.P. Reid, R.M. Sayer, R. Symes, R. Gilham, R. Hopkins and A. Cotterill

School of Chemistry, University of Bristol, Cantock's Close, Bristol BS8 1TS, UK

Optical techniques for probing the evolving size, composition and morphology of single particles can provide a powerful approach to study the chemistry and physics of atmospheric aerosols. Using a combination of non-linear optical techniques, such as cavity enhanced Raman scattering, experiments will be described that yield a spectroscopic fingerprint of a single particle with a single laser shot. From such a fingerprint, the size and composition of the particle can be accurately determined. Results from experiments designed to characterise the non-linear cavity enhanced droplet spectroscopy of aqueous aerosol particles will be presented. An application of cavity enhanced droplet spectroscopy to measurements of the evaporation rates of multicomponent organic/aqueous droplets by probing evolving size and composition simultaneously will be described. Finally, new methods for sampling and isolating single particles for controlled laboratory experiments will be presented.

Atmospheric Degradation of Fluorotelomer Alcohols: A Significant Global Source of Perfluorinated Acids?

T. J. Wallington[1], M. P. Hurley[1], M. P. Sulbaek Andersen[1], J. C. Ball[1], D. A. Ellis[2], J. W. Martin[2], and S. A. Mabury[2]

[1] *Ford Motor Company, SRL 3083, P.O. 2053, Dearborn, Michigan, 48121 – 2053.*
[2] *Department of Chemistry, University of Toronto, Toronto, ON, Canada, M5S 3H6*

Humans and animals in urban and remote locations are contaminated with persistent and bioaccumulative perfluorinated carboxylic acids (PFCAs) [1-3]. The source of this ubiquitous PFCA pollution is unknown. Fluorotelomer alcohols (FTOHs) are a class of industrially important chemicals with the general formula $C_xF_{2x+1}CH_2CH_2OH$ that have been observed in the atmosphere. The atmospheric oxidation of FTOHs is a potential source of PFCAs. Smog-chamber studies of the kinetics and mechanism of the OH radical initiated degradation of FTOHs have been conducted [4]. It was observed that reactions of HO_2 with $C_xF_{2x+1}C(O)O_2$ radicals formed during FTOH oxidation are a source of PFCAs [5]. The likelihood that FTOHs contribute significantly to the observed global dissemination of PFCAs will be discussed.

References

1. Masunaga, S., Kannan, K., Doi, R. Nakanishi, J. Giesy, J.P. Levels of perfluorooctane sulfonate (PFOS) and other related compounds in the blood of Japanese people. *Organohalogen Compounds (Dioxin 2002).* **59**, 888 – 891 (2002).
2. Martin, J.W., Smithwick, M.M., Braune, B.M., Hoekstra, P.F., Muir, D.C.G., Mabury, S.A. Identification of Long-chain Perfluorinated Acids in Biota from the Canadian Arctic. *Environ. Sci. Tech.* (Submitted 2003).
3. Kannan, K Choi, J-W., Iseki, N., Senthilkumar, K., Kim, D.H., Masunaga, S., Giesy, J.P. Concentrations of perfluorinated acids in livers of birds from Japan and Korea. *Chemosphere*. **49**, 225 – 231 (2002).
4. Ellis, D.A., Martin, J.W., Mabury, S.A., Hurley, M.D., Sulbaek Andersen, M.P., Wallington, T.J. Atmospheric lifetime of fluorotelomer alcohols. *Environ. Sci. Tech.* **37**, 3816-3820 (2003).
5. Sulbaek Andersen, M.P., Hurley, M.D., Wallington, T.J., Martin, J.W., Ellis, D.A., Mabury, S.A. Atmospheric chemistry of C_2F_5CHO: mechanism of the $C_2F_5C(O)O_2 + HO_2$ reaction. *Chem. Phys. Lett.* **381**, 14-21 (2003).

Tropospheric oxidation of terpenes and isoprene: Ring closure in unsaturated oxy- and peroxy radicals

Luc Vereecken and Jozef Peeters

Katholieke Universiteit Leuven, Celestijnenlaan 200F, B-3001 Leuven, Belgium
Luc.Vereecken@chem.kuleuven.ac.be

Oxy- and peroxy radicals play a pivotal role in the atmospheric oxidation of most volatile organic compounds (VOCs). The traditional view is that peroxy radicals react with NO or with other (hydro-)peroxy radicals, depending on NO-pollution levels, while oxy radicals decompose, undergo an H-shift, or react with O_2. For isoprene and the monoterpenes, by far the most abundant non-methane VOCs emitted in the atmosphere, the (per)oxy radicals formed are unsaturated, i.e. they contain a C=C double bond. This allows for an intramolecular addition reaction of the (per)oxy radical on the double bond, leading to a cyclic peroxide or ether structure. These ring-closure reactions were never observed in laboratory experiments, but a computational kinetic study revealed that (per)oxy ring-closure reactions can be important pathways in atmospheric conditions. Some indirect evidence for the importance of these ring closure reactions is available: the low yield of acetone in the OH-initiated oxidation of β-pinene, 2-15% experimentally, can only be rationalized by strong competition against the acetone formation channel by the ring closure reactions.

The rate of ring closure depends on structural properties of the VOC studied, making it difficult to predict *a priori* whether the ring closure reaction will be competitive. For isoprene, the peroxy radicals, formed after OH-addition on the inner carbons (appr. 10 %) and addition of O_2, will react with NO or $HO_2/R'O_2$ in typical experimental conditions, but over 90% of these peroxy radicals are predicted to undergo ring closure followed by rapid reaction with O_2 in the pristine environment where isoprene is emitted most. Many of the monoterpenes also contain two or more double bonds, and can therefore react similarly.

The most ubiquitous terpenes α- and β-pinene bear only one double bond, but we have shown earlier[1] that the four-membered ring is prone to breaking promptly after initial addition of an OH radical, forming hydroxymenthenylperoxy radicals after reaction with O_2. For α-pinene, this mechanism has been identified[2] as the dominant route to acetone formation. For the peroxy radicals formed here, peroxy ring closure outruns the reaction with NO even at moderately polluted levels of 1 ppbv NO, both for α- and β-pinene, affecting acetone formation in low NO-conditions. In elevated NO-concentrations those peroxy radicals will react with NO to form oxy radicals, which in turn can potentially undergo ring closure, forming a cyclic ether. For α-pinene, ring closure is too slow to compete effectively, such that the oxy radicals will react as predicted and measured in numerous earlier studies. For β-pinene, however, it was found that ring closure in the HO-menthenoxy radicals can outrun both decomposition and H-shift reactions. This oxy ring closure is important in high NO-conditions, as well as in low NO-conditions where RO_2+$R'O_2$ reactions also yield these alkoxy radicals. This reaction chain contributes some hitherto uninvestigated reaction products (formates, esters, multi-oxygenated compounds) in the oxidation of β-pinene, for which only 50% of the final oxidation products have been identified so far, compared to the near 100% for α-pinene.

1. J. Peeters, L. Vereecken, G. Fantechi, Phys. Chem. Chem. Phys., 3, 5489-5504, 2001.
2. L. Vereecken, J. Peeters, Phys. Chem. A, 104, 11140-11146, 2000.

Investigations of high-temperature gas phase systems

Katharina Kohse-Höinghaus

Physikalische Chemie I, Universität Bielefeld
Universitätsstraße 25, D-33615 Bielefeld, Germany
kkh@pc1.uni-bielefeld.de

In many high-temperature systems, the complex interplay of gas phase reactions has a significant influence on process performance. The presentation will highlight combustion and CVD systems. In both environments, detailed diagnostics is necessary to analyse important parameters of influence. Often, quantitative information on species concentration is needed, and calibration issues play a crucial role. Laser spectroscopy and mass spectrometry are typically used to provide the necessary information, which may then be combined with surface analysis in CVD systems. Some recent examples will be discussed, and related strategies and suggestions for future research will be given.

High-T Measurements in Reflected Shock Waves of Rate Constants for $CH_3 + O_2$

J. V. Michael, M.-C. Su, J. W. Sutherland, and N. Srinivasan

Chemistry Division, Argonne National Laboratory, 9700 S. Cass Ave., Argonne, IL 60439, USA

About four years ago, we measured rate constants at high temperature for the reaction,

$$CH_3 + O_2 \rightarrow CH_3O + O, \qquad (1)$$

using O-atom atomic resonance absorption spectrometry (ARAS) as the method of detection.[1] Since the ARAS method is so sensitive, the reaction rate was measured under essentially chemical isolation conditions. The result could be expressed in Arrhenius form over the range 1600-2100 K, as:

$$k_1 = 3.9 \times 10^{-11} \exp(-16858\ K/T)\ cm^3\ molecule^{-1}\ s^{-1}. \qquad (2)$$

In this earlier work, the need for including the molecular process,

$$CH_3 + O_2 \rightarrow CH_2O + OH, \qquad (3)$$

was found to be negligible. Instead, we proposed the direct reaction,

$$CH_2O + O_2 \rightarrow HO_2 + HCO, \qquad (4)$$

followed by the thermal decompositions of both HO_2 and HCO, yielding H-atoms which are instantaneously converted to O-atoms through $H + O_2 \rightarrow OH + O$, to give the excessive amounts of [O] found at the later stages of reaction at the highest temperatures. This proposal of a negligible molecular reaction has drawn criticism from several workers.

In an attempt to reconcile the need for reaction (3) in combustion kinetics, we have fitted our shock tube with a White cell operating at 308 nm (source is a microwave lamp in H_2O/Ar) using 32 passes (2.8 m). This configuration gives a signal to noise ratio of unity at 5×10^{11} radicals cm^{-3}. Hence, kinetics experiments can be performed at $[OH] < 1 \times 10^{13}$ radicals cm^{-3}, and this high sensitivity reduces secondary chemistry substantially thereby allowing us to form an opinion about reaction (3). OH profiles were measured and analyzed in the initial stages of reaction. The results are shown in Fig. 1. Clearly reaction (3) has a well defined rate and is competitive with (1). We have therefore reanalyzed the earler O-atom profiles,[1] giving the Arrhenius plot shown in Fig. 2 and a new updated value for the rate constants for reaction (1):

$$k_1 = 3.06 \times 10^{-12} \exp(-12006\ K/T)\ cm^3\ molecule^{-1}\ s^{-1}. \qquad (5)$$

This latter result is a slight increase over our original estimate and now agrees almost perfectly with the values of Braun-Unkhoff et al.[2] The implications of the rate constants for both reactions (1) and (3) will be discussed.

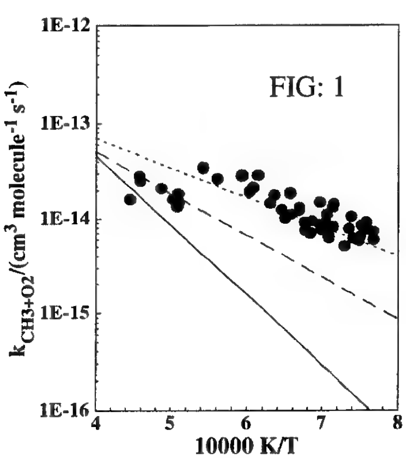

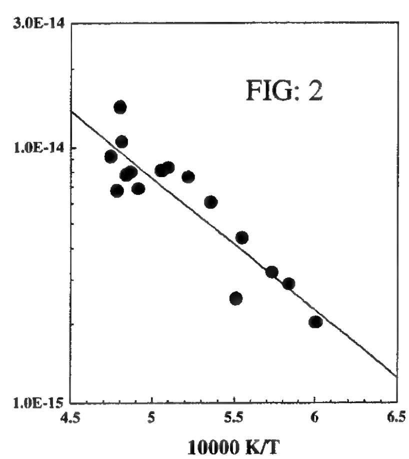

This work was supported by the U.S. Department of Energy, Office of Basic Energy Sciences, Division of Chemical Sciences, Geosciences, and Biosciences under Contract No. W-31-109-ENG-38.

1. J. V. Michael, S. S. Kumaran, and M.-C Su, J. Phys. Chem. A **103**, 5942 (1999).
2. M. Braun-Unkhoff, C. Naumann, and P. Frank, in *Shock Waves*, Brun, Raymond, Cumitrescu, Lucien (Eds.); Nineteenth International Symposium on Shock Waves; Springer: Berlin, Germany, 1995; Vol. 2, p 203.

High-temperature kinetics of propyne and allene: decomposition vs. isomerization

T. Bentz, R. X. Fernandes, B. R. Giri, H. Hippler, and M. Olzmann

Institut für Physikalische Chemie, Universität Karlsruhe (TH), Kaiserstr. 12, D-76128 Karlsruhe, Germany

Olzmann@chemie.uni-karlsruhe.de

The thermal decomposition reactions of propyne and allene are of crucial importance in pyrolysis and combustion systems. Both reactions have been investigated several times, the results, however, are contradictory. Whereas Hidaka et al. [1] obtained rate coefficients for the decomposition of propyne, which are two times higher than those for the decomposition of allene, Scherer et al. [2] observed the opposite. Moreover, Kiefer et al. [3] found only slightly differing rates but observed an unusual falloff behaviour, which could be explained by assuming hindered pseudo-rotations in C_3H_4.

In our contribution we report on shock-tube investigations of the thermal decomposition reactions of allene and propyne in the temperature range from 1500 to 2100 K and at pressures between 0.25 and 4 bar. We used H-ARAS as a sensitive probe for H-atoms and obtained rate coefficients for the allene and propyne decomposition, which are virtually identical and, moreover, exhibit the same temperature and pressure dependence. This is a strong evidence for a fast isomerization preceding the decomposition step.

We rationalize our results in terms of statistical rate theory using a SACM approach for the decompositon reactions with appropriately averaged sums and densities of states. The pressure dependence is analyzed by a master equation, and kinetic parameters for combustion modeling are recommended. Additionally, we discuss our model in view of recent C_3H_4 photodissociation experiments [4].

1. Y. Hidaka, T. Nakamura, A. Miyauchi, T. Shiraishi, and H. Kawano, *Int. J. Chem. Kinet.* **21**, 643 (1989).
2. S. Scherer, Th. Just, and P. Frank, *Proc. Combust. Inst.* **28**, 1511 (2000).
3. J. H. Kiefer, P. S. Mudipalli, S. S. Sidhu, R. D. Kern, B. S. Jursic, K. Xie, and H. Chen, *J. Phys. Chem. A* **101**, 4057 (1997).
4. R. H. Qadiri, E. J. Feltham, N. H. Nahler, R. P. Garcia, and M. N. R. Ashfold, *J. Chem. Phys.* **119**, 12842 (2003).

The Isomerisation of Simple Alkoxyl Radicals: New Temperature-Dependent Rate Data and Structure Activity Relationship

David Johnson, Paola Cassanelli and R. Anthony Cox

Centre for Atmospheric Science, University Chemical Laboratory, University of Cambridge, Lensfield Road, Cambridge, CB2 1EW, UK

Relative-rate experiments have been carried out, at several different temperatures between 240 and 340 K, to determine the Arrhenius rate parameters for the isomerisation of the 1-pentoxyl, 2-pentoxyl, and 5-methyl-2-hexoxyl radicals. Isomerisation rates were measured relative to the bimolecular reaction of each alkoxyl radical ($RO^{\cdot}$) with O_2. The order of reactivity, in terms of the rate of reaction for isomerisation, was 5-methyl-2-hexoxyl > 1-pentoxyl > 2-pentoxyl reflecting the relative-strengths of tertiary, secondary, and primary C-H bonds, *i.e.* the nature of the bond cleaved in the isomerisation process. Further to this, the measured Arrhenius activation barriers, and reported barriers for bimolecular reactions of the methoxyl radical with several simple hydrocarbons, are shown to correlate linearly with the bond strength of the cleaving C-H bond. The *A*-factors obtained for the three isomerisation processes also scale linearly with the number of available abstractable H atoms, with a value of 3.0×10^{10} s^{-1} per H atom. This value combined with the activation barrier correlation constitutes a structure activity relationship for the estimation of the kinetics of the isomerisation of simple alkoxyl radicals, at temperatures pertaining to the Earth's troposphere.

Reaction Kinetics of OH + C_2H_{2n} from 200-300K

Patricia Cleary, Kenny McKee, Mark Blitz, Paul Seakins, Liming Wang and Mike Pilling

School of Chemistry, University of Leeds, Leeds, LS2 9JT

Small hydrocarbons can play a large role in photochemical ozone production. Depending on their lifetimes in the atmosphere, they can also be used as tracers for air mass age and processing. For both applications, accurate rate constants are needed as a function of temperature and pressure. Many laboratory studies have focused on reaction kinetics of OH with C_2H_4 and C_2H_2 at 300K or above, typical of conditions at the Earth's surface. The kinetics of small hydrocarbons at lower pressures and temperatures, typical of conditions throughout the troposphere, are currently being investigated in order to better constrain models of regional air quality and global atmospheric chemistry.

The reaction rates of OH + C_2H_{2n} (+ M) were determined by laser flash photolysis-laser induced fluorescence. OH was generated by photolyzing HNO_3 at 248 nm. The OH was then observed via fluorescence at 308 nm following excitation at 283 nm. He, N_2 and O_2 have been studied as bath gases. The reactions have also been studied in SF_6, using laser flash photolysis/cavity ring down spectroscopy to investigate the high pressure limits; There is some disagreement in the literature about the high pressure limit for C_2H_2.

An attempt was also made to determine the high pressure limit for OH + C_2H_2, by measuring the rate of removal of OH(v=1,2). Provided that direct vibrational energy transfer is slow, and that intramolecular vibrational relaxation is fast, the rate constant should provide a direct measure of k_∞. It was found, however, that k(v=2) is almost twice k(v=1), suggesting a significant role for direct vibrational energy transfer. The rate coefficients show a complex T dependence, indicating a significant influence of the known van der Waals well, which has a depth of ~1000 cm^{-1}.

The combined rate data for OH(v=0-2) will be presented and analysed using the available data on the potential energy surfaces, including reaction channels other than adduct formation. The influence of the van der Waals well on the kinetics will be discussed, especially at the low temperatures found in the upper troposphere. The implications of the results for atmospheric oxidation and for chemical tracer studies will be presented.

Breakdown of Variational Transition State Theory in Barrierless Recombination Reactions of Large Radicals

Jürgen Troe

Institut für Physikalische Chemie, Universität Göttingen, Tammannstrasse 6, D-37077 Göttingen, GermanyTel.: +49-551-393121, Fax: +49-551-393150,
email: shoff@gwdg.de

Rate constants for barrierless recombination reactions in the high pressure limit often are calculated within the framework of variational transition state theory (VTST). It is well known that the canonical version of VTST (CVTST) has problems because thermal averaging is done before the variational step, while the correct order of the procedure should be the inverse. This defect is cured by using E,J-microcanonical VTST (μVTST) which, however, requires more computational effort. A further refinement is provided by a channel-resolved treatment in the statistical adiabatic channel model (SACM).

Comparing μVTST and CVTST with classical trajectory calculations (CT), differences where realized which were found to be up to about a factor of two. These differences were attributed to "recrossing trajectories". This talk discusses a more fundamental breakdown of VTST which is typical for recombination reactions of large radicals. Phase-space sampling along a reaction coordinate, being an essential element of VTST, implies adiabatic motion of the conserved and transitional modes of the system during the approach of the radicals. While this is mostly true for the conserved modes, this may not be the case for the transitional modes. Depending on the value of the Massey parameter of the system, being related to the ratio of the collision time and the rotational periods of the radicals, the dynamics may be located somewhere between adiabatic and sudden. The larger the radicals, the larger are the rotational periods such that the Massey parameters may decrease and the dynamics may be closer to sudden than to adiabatic. In this case, VTST is basically inapplicable. Instead we have suggested the use of an SACM/CT approach which handles the conserved modes adiabatically while the dynamics of the transitional modes is treated by CT calculations. This talk gives quantitative examples and traces the limits of applicability of adiabatic concepts like VTST.

An Efficient and Accurate Direct Transition State Theory Approach for Radical-Radical Associations

Stephen J. Klippenstein,[1] Yuri Georgievskii,[1] and Lawrence B. Harding[2]

[1]*Combustion Research Facility, Sandia National Laboratories, Livermore, CA, 94551-0969, USA*
[2]*Chemistry Division, Argonne National Laboratory, Argonne, IL, 60439, USA*

A procedure for directly obtaining variable reaction coordinate transition state theory predictions from modest quantum chemical simulations will be briefly summarized. Illustrative applications to a number of hydrocarbon radical-radical association reactions will be presented. This direct statistical procedure is based on the direct evaluation of the orientational contribution to the transition state partition function at the CASSCF/dz level. Higher level corrections are obtained from a correspondence between CASSCF/dz calculations for the system of interest along the minimum energy path and related and higher level calculations for the smallest chemically similar system. Results obtained for CH_3 + H, C_2H_5 + H, C_2H_3 + H, CCH + H, and CH_3 + CH_3 reactions illustrate the accuracy of the approach. New predictions for the C_2H_5 + CH_3, C_2H_5 + C_2H_5, iso-C_3H_7 + H, iso-C_3H_7 + CH_3, iso-C_3H_7 + C_2H_5, iso-C_3H_7 + iso-C_3H_7, tert-C_4H_9 + H, tert-C_4H_9 + CH_3, tert-C_4H_9 + C_2H_5, tert-C_4H_9 + tert-C_4H_9, C_6H_5 + H, C_6H_5 + CH_3, and $C_{10}H_7$ + H reactions illustrate the power of the approach. These predictions also illustrate a variety of steric effects.

Temperature-Dependent Rate Coefficients for Removal of OH (v = 1) by Several Species

David C. McCabe[1,2,3], B. Rajakumar[1,2], I. W. M. Smith[4], and A. R. Ravishankara[1,2,3]

[1]*NOAA Aeronomy Lab, 325 Broadway R/AL2, Boulder, CO USA*
[2]*CIRES, University of Colorado, Boulder, CO USA*
[3]*Department of Chemistry and Biochemistry, Univ. of Colorado, Boulder, CO USA*
[4]*School of Chemistry, University of Birmingham, Edgbaston, Birmingham, UK*

The rate coefficient for the removal of a vibrationally excited radical by a molecule has been used to approximate the high-pressure limiting rate coefficient for the association of the radical (in the vibrational ground state) with that molecule. This approach has been used to study many association reactions. However, there have only been a few measurements of the temperature dependence of the rate coefficients for the removal of vibrationally excited radicals. We have measured the temperature-dependent rate coefficients for the removal of OH (v = 1) by several species, among them H_2O, D_2O, O_2, CH_4, and N_2O. Pulsed laser photolysis of a suitable precursor was used to generate the vibrationally excited OH, which was then detected using pulsed laser-induced fluorescence. The rate coefficient for OH (v = 1) removal by methane is essentially temperature independent, because quenching occurs without complex formation. The rate coefficients for removal of OH (v = 1) by other molecules, however, have negative temperature dependences, with negative activation energies ranging from $E_a/R = (-160 \pm 20)$ K for the removal of OH (v = 1) by N_2O to $E_a/R = (-610 \pm 90)$ K for the removal of OH (v = 1) by D_2O. The relatively large negative E_a/R for several of these rate coefficients suggests that the vibrationally excited radical is lost by a mechanism involving formation of a complex between vibrationally excited OH and the quenching molecule. Once this complex is formed, dissociation of the complex to regenerate the vibrationally excited radical competes with randomization of the vibrational energy of OH into the other modes of the complex; this competition results in the negative temperature dependence. Included in this category is the removal of OH (v = 1) by O_2, where quenching was not previously assumed to proceed *via* complex formation. Additionally, we have measured the temperature-dependent rate coefficients for the quenching of OD (v = 1) by H_2O and D_2O; the differences in the quenching kinetics of these isotopomers gives further insight on the quenching mechanism. We will discuss the implications of these temperature-dependent rate coefficients.

Femtosecond Soft X-Ray Photoelectron Molecular Dynamics

Stephen R. Leone Astrid Müller, Jürgen Plenge, Louis Haber, and James Clark

Departments of Chemistry and Physics and Lawrence Berkeley National Laboratory
University of California, Berkeley, CA 94720
srl@cchem.berkeley.edu
http://www.cchem.berkeley.edu/leonegrp/

Many important kinetic phenomena have their origins in ultrafast dynamical processes that occur on femtosecond timescales. Ultraviolet photoelectron spectroscopy and x-ray core level photoelectron spectroscopy are two important methods used to study the electronic structure and energetics of neutral molecules, radicals, and surface processes. Until now, these methods have mainly been used for static spectroscopy or very slow kinetics. A laser method has been developed to obtain camera-like snapshots of ultrafast processes by measuring ultraviolet and soft x-ray photoelectron spectra of molecules during their dissociation and transformation. The method uses high order harmonic generation of a Ti:sapphire ultrafast laser in a rare gas jet to produce probe pulses of 20-100 eV photon energies. Such pulses are able to interrogate valence shell electrons and core level electrons and their chemical shifts as a molecule undergoes a transformation. Gaseous molecules are probed within a magnetic bottle time-of-flight electron spectrometer to energy analyze the electrons produced upon ionization, which delivers the photoelectron spectra. The time overlap of the soft x-ray probe pulse and a visible or ultraviolet pump pulse is obtained by detecting photoelectron cross correlations with above-threshold ionization side-band processes. Dissociation of bromine molecules is studied. The molecules are excited to a repulsive dissociative state by pulses of 400 nm light, and a selected harmonic is used to obtain time-resolved photoelectron spectra at various pump-probe time delays. Atomic-like photoelectron features appear extremely rapidly, within 40 fs. A wave packet on the dissociative state is also observed. In other investigations, the photoelectron spectra of short-lived bound excited states are studied. New information about the ionization cross sections of transient states and their photoelectron spectra are obtained. Details are presented on the technique, as well as studies of other molecules, coupled also with baseline high resolution spectra obtained at a synchrotron source to aid the interpretation. Results are also presented using high order harmonics to produce wave packet superposition states and on the kinetic modification of wave packet recurrences in the presence of fields. Many concepts for user facilities that produce ultrafast x-ray pulses are being pursued widely in the international scientific community. A brief description of the characteristics of one such source and possible applications will be outlined. These concepts pave the way for a general method to probe transient states in molecules by photoelectron spectroscopy, a method that has been very successfully employed for ground state analyses.

Photodissociation studies of state-selected molecular ions by velocity map ion imaging

N. Hendrik Nahler, Olivier P.J. Vieuxmaire, Josephine R. Jones, Michael G.D. Nix, Richard N. Dixon, and Michael N.R. Ashfold
University of Bristol, School of Chemistry, Bristol BS8 1TS, UK

High resolution ion imaging methods have been used to study the photodissociation of ground state Br_2^+ ($^2\Pi_g$) and $BrCl^+$ ($^2\Pi$) cations, with spin-orbit and vibrational state specification, monitoring the $^{79}Br^+$ and $^{35}Cl^+$ fragments as appropriate. The state-selected molecular ions are prepared by a 2+1 REMPI scheme and then dissociated by absorption of a single photon from a second tunable dye laser. Image analysis allows precise determination of the dissociation energies of Br_2^+ ($^2\Pi_{3/2,g}$), Br_2^+ ($^2\Pi_{1/2,g}$), $BrCl^+$ ($^2\Pi_{3/2}$), and $BrCl^+$ ($^2\Pi_{1/2}$) also providing values for the respective spin-orbit splitting constants. The values so derived for $BrCl^+$ are in excellent agreement with those obtained from complementary photoelectron imaging studies.

Photoexcitation of Br_2^+ at wavelengths just above the first dissociation threshold yields ground state Br^+ and Br fragments, the recoil anisotropy of which is found to be sensitively wavelength dependent. Careful measurements of the angular anisotropy (β-parameter) versus the dissociation wavelength reveals the presence of high frequency structure, in the region up to the first excited [$Br(^2P_{3/2}) + Br^+(^3P_1)$] dissociation limit; this we attribute to predissociating vibrational levels in an adiabatic potential converging to this excited limit. The structure has been rationalised by performing spin-orbit averaged *ab initio* electronic structure calculations for all ungerade excited states of Br_2^+ associated with the $\ldots\sigma_g\pi_u\pi_g{}^*\sigma_u{}^*$ valence space, incorporating spin-orbit effects semi-empirically, and then propagating wavepackets on the coupled diabatic potential energy curves so derived. The model calculations are able to reproduce all of the trends observed experimentally and provide much new insight into the non-adiabatic couplings amongst the various excited states of this text-book open-shell system.

The dissociation channels from $BrCl^+$ show predominantly parallel character. Branching ratios into the various Br^+ (^3P_J) and Cl (^2P_J) channels will be presented and discussed in the context of the various participating excited state potentials. Three photon excitation of BrCl resonance enhanced at the two photon energy by ($^2\Pi_{1/2}$)5sσ, v≥0 levels also generates super-excited BrCl molecules which dissociate to form $Br^{(*)}$ + Cl** products. The Cl** atoms are ionized by further photon absorption. The Br + Cl** products show angular distributions characterized by P_2, P_4, and P_6 terms; this we attribute to a $\Sigma\rightarrow\rightarrow\Pi\rightarrow\Pi$ transition in BrCl.

Adiabatic and non-adiabatic dissociation of rovibrationally excited acetylene and its homologues

Y. Ganot, A. Golan, X. Sheng, I. Bar and S. Rosenwaks

Department of Physics, Ben-Gurion University of the Negev, Beer-Sheva 84105, Israel

An extensive study of rovibrationally mediated photodissociation (VMP) of acetylene isotopomers is presented and work in progress on its homologues, propyne and 1-butyne, is reported. Direct visible (VIS) or near infrared (NIR) excitation efficiently prepared the rovibrational levels in the regions of three to five C-H stretch modes of C_2H_2 and C_2HD and UV photons at ~ 243 nm dissociated them. UV photons from the same laser or from an independent UV laser subsequently ionized the H or D photofragments via resonantly enhanced multiphoton ionization (REMPI). Detection of the H(D) photofragment yield *vs.* the VIS/NIR or UV laser wavelength resulted in VIS/NIR or UV dependent action spectra, representing rovibrational excitation or rovibronic absorption spectra, respectively. The rovibrational excitation generated large enhancement in C-H(D) bond rupture. Through comparison of the VIS/NIR action spectra with photoacoustic (PA) absorption spectra it has been established that the photodissociation efficacy is very much affected by the Franck-Condon (FC) overlap of the prepared vibrational wavefunction with the dissociating wavefunction. For that reason, combination bands that include bending are preferable in promoting dissociation in both isotopomers. Furthermore, monitoring H(D) production, demonstrates a very irregular rotational intensity pattern exhibiting significant differences in photodissociation propensities depending on the initially prepared rotational quantum state in a given vibrational state. This is attributed to the mixing of the prepared rovibrational states with dark states of bent character, revealing rotational state dependent selectivity in C_2HD bond fission. The photodissociation of initially prepared states in the region of three C-H stretches of C_2H_2 results in non-adiabatic dissociation from the bound part of the electronically excited $\tilde{A}\,{}^1A_u$ state of acetylene, whereas preparation of four or five C-H stretches results in adiabatic dissociation from its repulsive part. Bond-selectivity was not observed in propyne isotopomers and in 1-butyne where vibrational spectroscopy and intramolecular dynamics were studied via VMP and PA spectroscopies.

Kinetic and Mechanistic Studies of Product Isomer Branching in the Recombination of OH with NO_2

A.J. Hynes, L. D'Ottone, P. Campuzano-Jost and M. Fardy

Division of Marine and Atmospheric Chemistry, Rosenstiel School of Marine and Atmospheric Science, Miami, Fl, USA

The three-body recombination of OH with NO_2 (1) plays an important role in both tropospheric and stratospheric chemistry. In the troposphere, it can act as a major sink for OH, while in the stratosphere it acts to control partitioning among the HO_x and NO_x families with a consequent impact on catalytic ozone cycles. Reaction (1) has been the subject of a number of recent experimental and theoretical studies and, although it is now clear that the reaction proceeds via two channels producing both nitric and peroxynitrous acids, the relative importance of channel (1b) is unclear.

$$OH + NO_2 + M \rightarrow HNO_3 + M \quad (1a)$$
$$\rightarrow HOONO + M \quad (1b)$$

In this work we report studies of reaction (1) using both isotopically labeled and vibrationally excited OH which are designed to study the branching ratio between (1a) and (1b). Reaction (1c) offers a route to the high pressure limit for reaction (1a) if isomerization of $H^{18}ON^{16}O_2$ is rapid compared with decomposition of the energized adduct .

$$^{18}OH + N^{16}O_2 \rightarrow H^{18}ON^{16}O_2 \quad (1c)$$

We have measured the rate coefficient for reaction (1c) and monitored the appearance of the ^{16}OH from the decomposition of the isotopically scrambled $H^{18}ON^{16}O_2$. We find that isomerization is rapid producing a statistical mixture of $H^{18}ON^{16}O_2$ and $H^{16}ON^{18}O^{16}O$, hence we identify the rate coefficient for reaction (1c) as being 2/3 of the high pressure limit. We obtain a high pressure limit of $k_{\infty,1\alpha} = (1.5 \pm 0.2) \times 10^{-11}$ cm^3 molecule^{-1} s^{-1}. We have also measured the rate of vibrational deactivation of OH (v = 1-5) with NO_2 as a proxy for the sum of the high pressure limits of reactions 1a and 1b. We obtain a rate coefficient of $k_{deactivation}=(6.4 \pm 0.1) \times 10^{-11}$ cm^3 molecule^{-1}s^{-1}, independent of vibrational level. In addition we report the observation of non-exponential decays in reaction (1) which we identify as being due to the decomposition of HOONO. These results will be compared with the predictions of recent theoretical studies.

This work was supported by the National Science Foundation.

Formation of Nitric Acid or Its Isomer, Peroxynitrous Acid, in the Gas-Phase HO_2 + NO Reaction Studied by High Pressure Turbulent Flow Reactor/Chemical Ionization Mass Spectrometry

N. I. Butkovskaya, A. Kukui[#], N. Pouvesle and G. LeBras

CNRS, Laboratoire de Combustion et Systèmes Réactifs, 1C Av. de la Recherche Scientifique, 45071 Orléans Cedex 2, France; [#]CNRS, Service d'Aéronomie, Paris, France

The gas-phase HO_2 + NO (1) reaction plays a key role in ozone production in both troposphere and lower stratosphere. This reaction is also used in radical chemical amplifiers to convert low atmospheric concentrations of HO_2 into measurable NO_2 concentrations in a chain reaction. It was found that the presence of water in the amplifier results in a decrease of the chain length, and this effect was attributed, at least partially, to the formation of non-radical products (e.g., HNO_3) in reaction (1) [1]. Up to now, the only observed channel was $HO_2 + NO \rightarrow OH + NO_2$.

In the present work, a high pressure turbulent flow reactor coupled with chemical ionization mass-spectrometer was used to study the influence of water on the formation of HNO_3 or its isomer, HOONO, in the HO_2 + NO reaction. However, it was found that even under dry conditions nitric acid (or its isomer) is produced with a yield of about 0.1%. In the presence of water vapor a slight increase of the yield was observed. The experiments were carried out at T = 298 K and P = 200 Torr of carrier gas N_2. Sequential reactions $H + NO_2 \rightarrow OH + NO$ and $OH + NO_2 \rightarrow HNO_3$ in excess of known concentration of NO_2 were used to calibrate the HNO_3 signal. Two ion-molecule reactions were used to detect HNO_3: $HNO_3 + SF_6^- \rightarrow [HF{\cdot}NO_3]^- + SF_5$ and $HNO_3 + SiF_5^- \rightarrow [HNO_3{\cdot}SiF_5]^-$. It is not known whether these detection methods distinguish between HNO_3 and HOONO, but equal relative sensitivities obtained by two methods for HNO_3 from calibration system and for the acid product from reaction (1) suggest that the observed product is HNO_3. Since detection of HNO_3 from HO_2 + NO was complicated by the secondary $OH + NO_2 \rightarrow HNO_3$ reaction, OH radicals were scavenged either by adding cyclo-hexane, or working with sufficiently high concentrations of NO. In the former case a chain production of NO_2 and HNO_3 was observed. A detailed mechanism and atmospheric implications of the observed minor channel of reaction (1) will be discussed.

[1]. C. M. Mihele, M. Mozurkewich and D. R. Hastie, *Int. J. Chem. Kinet.*, **31**, 145 (1999).

Dynamics of the $OH + NO_2 \rightarrow HONO_2$ Recombination Reaction

John R. Barker [a,b], Yong Liu [a], and Lawrence L. Lohr [b]

[a] *Department of Atmospheric, Oceanic, and Space Sciences*
[b] *Department of Chemistry*
University of Michigan, Ann Arbor MI 48109-2143, USA
(e-mail: jrbarker@umich.edu)

The reaction of hydroxyl radicals with nitrogen dioxide is a prototypical recombination reaction producing two chemical isomers (HOONO and $HONO_2$). Nitric acid formation is one of the most important sinks for atmospheric OH and NO_x. Previously, extensive master equation simulations were carried out to fit the existing experimental data and to make extrapolations to atmospheric conditions [D. M. Golden, J. R. Barker, and L. L. Lohr, J. Phys. Chem. A 107, 11057 (2003)]. Currently, we are using quasi-classical trajectory calculations to investigate the $OH + NO_2$ recombination reaction as a function of temperature, vibrational energy, and potential energy surface parameters. Another important motivation for this work is to determine the quantitative relationship between k_∞ and the rate constant for vibrational deactivation of OH(v=1,2,3) by NO_2.

The model potential energy surface (PES) near the equilibrium structure of $HONO_2$ is based on analytical fits to the results of *ab initio* quantum chemical and density functional theory calculations, while the long-distance asymptotic PES is based on the known properties of OH and NO_2. In the intermediate distance regime, the PES is based on a family of "stiff" Morse oscillators. The reaction dynamics are being calculated on this family of model surfaces in order to ascertain the sensitivity of the results.

Preliminary results give rates of intramolecular vibrational redistribution (IVR) from the OH bond in $HONO_2$ that are in excellent agreement with the literature value. They also predict that the capture rate constant is practically identical with vibrational deactivation rate constant for OH(v) at room temperature (on one model PES). Except for the electronic partition function, the calculated capture rate constant *increases* with increasing temperature, even though the reaction is barrier-less. The results of these and the other calculations currently underway will be described.

HO_2NO_2 Thermal Decomposition Rate Coefficient Measurements and $\Delta_rH^o_{298K}$ Determination

Tomasz Gierczak[‡], Elena Jimenez[†], Veronique Riffault, James B. Burkholder, and A. R. Ravishankara

Aeronomy Laboratory, National Oceanic and Atmospheric Administration, 325 Broadway, Boulder, CO 80305-3328, USA

Rate coefficients for the thermal decomposition of HO_2NO_2 (peroxynitric acid, PNA) in the gas phase

$$HO_2NO_2 + M \rightarrow HO_2 + NO_2 + M \qquad (1)$$

were measured over the temperature range 328 – 363 K in 25 and 50 Torr of N_2. Rate coefficients were determined by monitoring the steady state concentration of the OH radical in a mixture of HO_2NO_2 and NO, where NO converts HO_2 to OH and OH reacts with HO_2NO_2 and other reactive impurities. The OH temporal profile (measured using pulsed laser induced fluorescence) following a perturbation of the steady state OH radical concentration yielded the rate coefficient for OH loss. Pulsed excimer laser photolysis of HO_2NO_2 at 248 nm

$$HO_2NO_2 + h\nu \rightarrow HO_2 + NO_2 \qquad (2a)$$
$$\rightarrow OH + NO_3 \qquad (2b)$$

provided the system perturbation. The measured thermal decomposition rate coefficients in combination with reported reaction rate coefficients for the $HO_2 + NO_2$ association reaction, k_{-1}, were used to derive $\Delta_rH^o_{298K}$ for reaction (1) and $\Delta_fH^o_{298K}(HO_2NO_2)$. These values will be presented and their implications discussed.

‡ Permanent Address: Dept. of Chemistry, Warsaw University, ul Zwirki i Wigury 101, 02-089, Warsaw, Poland.

† Current address: Departamento de Química Física. Facultad de Ciencias Químicas. Universidad de Castilla-La Mancha. Camilo José Cela, 10. 13071 Ciudad Real, Spain.

Laboratory Studies of Iodine Oxide Chemistry

Terry J Dillon, Dirk Hoelscher and John N Crowley

Max Planck Institute for Chemistry, Mainz, Germany.

Iodine oxide, IO, is a key intermediate in the iodine-catalysed destruction of ozone in the marine boundary layer.

$I + O_3$	$\rightarrow$	$IO + O_2$	in the MBL and in the lab
$O(^3P) + RI$	$\rightarrow$	$IO + R$	in the lab

Laser flash photolysis generation of the iodine oxide radical, IO, was coupled to the detection methods of optical absorption spectroscopy (for IO, OIO, I_2 and O_3), resonance fluorescence ($O(^3P)$ and I) and laser induced fluorescence (I_2) to investigate the key photochemical properties of IO. The quantum yields for IO formation in processes such as $O(^3P) + RI \rightarrow$ (IO + products), and its absorption cross-section (at 427.2 nm, used by LP-DOAS instruments in the field) were determined. In addition, the kinetics, products, and hence ozone-destroying potential of the IO self-reaction were investigated:

$IO + IO (+ M)$	$\rightarrow$	$(IO)_2 (+ M)$	
	$\rightarrow$	$O_2 + I_2$	
	$\rightarrow$	$OIO + I$	} only I-atom producing channels
	$\rightarrow$	$O_2 + 2I$	} result in catalytic in O_3 destruction.

Laboratory and field studies of the atmospheric oxidation of volatile organic compounds

Mario J. Molina, Keith Broekhuizen, Rainer Volkamer, and Luisa T. Molina

Massachusetts Institute of Technology, 77 Massachusetts Ave, Room 54-1814, Cambridge, MA 02139, USA

We have investigated in the laboratory the kinetics and mechanism of the atmospheric oxidation of propylene (C_3H_6), used as a proxy to larger hydrocarbons. We measured the rate coefficient for its reaction with OH at 100 Torr over the 235-305 K temperature range. In the atmosphere, the OH-propylene adduct rapidly reacts with oxygen to produce the hydroxy-propylperoxy radical ($CH_3CH(OO)CH_2OH$). We also measured the rate coefficient for the reaction of this radical with NO at 100 Torr over the 235-305 K temperature range.

In the Spring of 2003, a multinational team of atmospheric scientists from Mexican, US, and European institutions conducted an intensive, five-week field campaign in the Mexico City Metropolitan Area (MCMA). The overall goal of this effort was to contribute to the understanding of the air quality problem in megacities by conducting measurements and modeling studies of atmospheric pollutants in the MCMA, and more specifically to investigate the gas-phase chemistry of relevance to the formation of ozone and secondary organic aerosol. The state-of-the-art measurement instrumentation deployed in the MCMA included two open-path differential optical absorption spectrometers (DOAS). A special focus was paid to the quantification of speciated aromatic hydrocarbons, NO_2, SO_2 ozone, glyoxal, and the radical precursors HONO and HCHO. Preliminary results from the DOAS measurements will be presented in the context of the role that the oxidation of volatile organic compounds plays in the processing of pollutants in the MCMA.

A study into the kinetics of the reaction of IO with CH_3O_2

C.S.E. Bale, C.E. Canosa-Mas, and R.P.Wayne

Physical and Theoretical Chemistry Laboratory, University of Oxford, South Parks Road, Oxford, OX1 3QZ
(frin@physchem.ox.ac.uk)

Iodine monoxide (IO) is known to react with species such as HO_2 and NO_2 in cycles that catalytically destroy ozone. It has been suggested that IO could also react with peroxy radicals, such as methyl peroxy (CH_3O_2), in a similar manner. However, as yet there has been no investigation into these reactions. We present a discharge-flow study of the kinetics of the reaction between IO and CH_3O_2. Off-axis continuous-wave cavity-enhanced absorption spectroscopy (CEAS) has been employed to detect IO directly, and CH_3O_2 indirectly (*via* titration with NO and subsequent detection of the NO_2 produced). A violet laser diode centered at λ = 412 nm has been used to monitor both IO (σ_{412nm} = 1.28 H $10^{!17}$ cm^2 molecule$^{!1}$) and NO_2 (σ_{412nm} = 5.27 H $10^{!19}$ cm^2 molecule$^{!1}$). Because of the unavoidable secondary reactions that occur in the system, such as the reaction between IO and both CH_3O and HO_2 (which are formed alongside CH_3O_2) a simple *pseudo*-first order analysis could not be used. Instead, the measured IO decay in the absence and presence of CH_3O_2 was fitted to a numerical model to estimate the rate constant for the reaction of IO with CH_3O_2.

Deposition of nitric acid on to molecular and ionic sulfuric acid hydrate thin films

Suzanne B Couling and Andrew B Horn

School of Chemistry, University of Manchester, Oxford Road, Manchester, M13 9PL.

The uptake of nitric acid on to sulfuric acid aerosols is important in the formation of Polar Stratospheric Clouds (PSCs). However, despite the considerable effort made to characterise the formation processes and composition of PSC particles over the past two decades uncertainties still remain. In particular, the processes leading to the formation of solid PSC particles are not well understood. Laboratory experiments have suggested that supercooled binary solutions in equilibrium with water and nitric acid vapour will not freeze unless the temperature drops below the frost point[1]. The addition of even small amounts of H_2SO_4 (<5 wt% H_2SO_4) decreases the freezing temperature of nitric acid solutions and emulsions further. However the occurrence of solid phase PCS and observed denitrification early in the artic polar winter requires a freezing process that can occur above the ice frost point.[2,3] The identification of non-ionised meta-stable sulfuric hydrates on the surface of aerosol mimics[4] and during the formation of sulfuric acid aerosols[5] raises the question as to the effect these metastable species have on the uptake of HNO_3 and their impact on the freezing process. In recent work, the uptake of nitric acid onto thin films of molecular sulfuric acid hydrates has been compared with the uptake onto ionised films of over-hydrated sulfuric acid monohydrate (SAM). Nitric acid is observed to absorb onto and desorb from thin films of molecular sulfuric acid hydrate without triggering a change in structure or composition, whereas the absorption of nitric acid onto ionised over-hydrated SAM leads to the crystallisation of sulfuric acid tetrahydrate (SAT). The presence and location of molecular hydrates in realistic aerosol samples is discussed, and we suggest that this difference in behaviour between molecular and ionised hydrates may provide an explanation for the different freezing mechanisms observed in PSCs.

1 Chang H-Y A, Koop T, Molina L T and Molina M J. *J Phys Chem A*, **103**, 2673, 1999.
2 Drdla K, Schoeberl M R and Browell E V. *J Geophys Res*, **108**, D5, 8312, 2003.
3 Couling S B, Nash K L, Fletcher J, Vickerman J and Horn A B. *J Am Chem Soc*, **125**, 13038, 2003.
4 Couling S B, Sully K J and Horn AB . *J Am Chem Soc* **125** (7), 1994, 2003.
5 Couling S B, Fletcher J, Horn A B, Newnham D A, McPheat R A and Williams R G. *PCCP*, **5**, 4108, 2003.

Abstracts of Posters

A1

Temperature dependence of the reactions between a series of acetates and Cl atoms

Alberto Notario, Carlos A. Cuevas, Ernesto Martínez and José Albaladejo

Departamento de Química Física, Universidad de Castilla-La Mancha.
Avenida Camilo José Cela, nº 10, 13071 - Ciudad Real, Spain
E-mail: Jose.Albaladejo@uclm.es

Atomic chlorine is highly reactive with organic and inorganic compounds, so that relatively small concentrations can compete with the main tropospheric oxidants (OH, O_3 and NO_3),

playing a more important role in the oxidation of volatile organic compounds (VOCs), including the studied acetates, than previously thought (Finlayson-Pitts, 1993). The contribution of Cl to the oxidation of VOCs could be significant in areas where the concentration of Cl precursor species has been reported to be high, such as coastal boundary layer, and it may significantly contribute to the formation of ozone and other components of the photochemical smog in these areas.

Absolute rate coefficients have been measured for the gas phase reactions of chlorine atoms with a series of aliphatic acetates: methyl acetate (k_1), ethyl acetate (k_2), n-propyl acetate (k_3) and n-butyl acetate (k_4), using the Pulsed Laser Photolysis – Resonance Fluorescence technique (PLP-RF), over the temperature range 265-383 K. The obtained kinetic data were used to derive the Arrhenius expresions: $k_1 = (9.31 \pm 1.02) \times 10^{-12} \exp[-(359 \pm 70)/T]$; $k_2 = (4.35 \pm 0.65) \times 10^{-12} \exp[(342 \pm 92)/T]$; $k_3 = (2.22 \pm 0.2) \times 10^{-11} \exp[(217 \pm 58)/T]$; and $k_4 = (5.41 \pm 1.51) \times 10^{-11} \exp[(245 \pm 168)/T]$ (in units cm^3 $molecule^{-1}$ s^{-1}).

As far as we know, the results from this work constitute the first temperature dependence measurements for the reactions of Cl with the mentioned esters. These rate coefficients are compared with the previous studies carried out at 298 K (Notario, 1998), and with the reactivity of OH radicals (El Boudali, 1996). The atmospherics implications are also discussed.

El Boudali, A., Le Calvé, S., Le Bras, G. And Mellouki, A., **1996**. *Journal of Physical Chemistry*, 100, 12364-12368.

Finlayson-Pitts, B. J., **1993**. *Research on Chemical Intermediates*, 19, 235-249.

Notario A., Le Bras G., Mellouki A., **1998**. *Journal of Physical Chemistry*, 102, 3112-3117.

B1

Low pressure kinetic and mechanistic study of the reaction of Cl with acrolein

Alfonso Aranda, Yolanda Díaz de Mera, Ana Rodríguez, Diana Rodríguez, Lorena Morales, Ernesto Martínez, Elena Jiménez

Facultad de Químicas, Campus Universitario, s/n. 13071 Ciudad Real, Spain

Introduction

Acrolein (CH_2=CHCHO) is released into the environment from natural and anthropogenic sources. As an example, it is emitted by forest fires and the activities involving the combustion in incinerators, diesel motor… Several reactions of acrolein with different oxidants (OH, NO_3…) have been studied in different experimental conditions. In the marine boundary layer (MBL), the concentration of Cl atoms range from 5 to 15×10^3 atoms cm^{-3} and, so, the effect on the removal of acrolein can also be relevant.

Experimental, results and discussion

The kinetic experiments were carried out using the discharge-flow technique and a detection system based on mass spectrometry. The kinetics, mechanism and products of Cl atoms reactions with acrolein, over the temperature range 260-333 K and at low total pressure (0.5-3 Torr) have been studied under pseudo-first order kinetic conditions in excess of organic compound over Cl atoms. The study with the temperature shows no significant changes in the rate constant. The reaction rate is found to increase very slightly with increasing temperature, giving the following Arrhenius expression:

$$k = (9.3\pm9.7)\times10^{-11}\exp[(-149\pm297)/T] \quad cm^3 molecule^{-1} s^{-1} \qquad T = 260\text{-}333\ K$$

The obtained values at room temperature indicates that the reaction Cl + acrolein (1) is not sensitive to pressure changes within the limited range studied.

From the study of the formation and identification of products, the reaction (1) proceeds simultaneously through the two possible channels, abstraction and addition:

$$CH_2{=}CHCHO + Cl \rightarrow CH_2CHCO^* + HCl \qquad (1a)$$
$$CH_2{=}CHCHO + Cl \rightarrow [CH_2CHCHOCl]^* \qquad (1b)$$

The branching ratio for abstraction channel at 298 K and 1 Torr was determined as 0.83 ± 0.13 and led to HCl and CH_2CHCO^* radical. The temperature dependence of this abstraction channel has also been studied, giving the Arrhenius expression:

$$k\,(1a) = (5.4\pm2.0)\times10^{-10}\exp[(-748\pm110)/T] \quad cm^3 molecule^{-1} s^{-1} \qquad T = 260\text{-}333\ K$$

From these results, in the temperature and low pressure ranges studied, the major reaction channel is abstraction. For temperatures higher than 333 K and low pressure, the contribution of addition to the global rate constant may be considered as negligible.

Atmospheric implications are related with the production of significant amounts of the radical CH_2CHCO^*, which is expected to react predominantly with oxygen under atmospheric conditions.

Experimental study of the interaction of HO_2 radicals with soot surface

Y. Bedjanian, S. Lelievre, G. Le Bras

Laboratoire de Combustion et Systèmes Réactifs, CNRS
1C avenue de la Recherche Scientifique 45071 Orléans Cedex 2, France
bedjanian@cnrs-orleans.fr

Soot particles, issue from the incomplete combustion of fossil and biomass fuels, may influence the chemical composition of the atmosphere through reaction of atmospheric constituents at their surface. In particular, loss of the oxidant radical HO_2 on soot may change the oxidative capacity of the atmosphere, as well as tropospheric and stratospheric ozone budgets.

The reactions of HO_2 with toluene and kerosene flame soot were studied over the temperature range 240 to 350 K and at P = 0.5 – 5 Torr of helium using a flow reactor coupled to a modulated molecular beam mass spectrometer. Flat-flame burner was used for the preparation and deposition of soot samples from premixed flames of liquid fuels under well controlled and adjustable combustion conditions. Kinetic experiments were carried out with a coaxial configuration of the flow reactor, soot samples deposited on Pyrex rods being introduced into the reactor along its axis. The reaction rate was measured from decay kinetics of HO_2 generated in reaction of F atom with H_2O_2.

The uptake coefficient of HO_2 on soot was determined to be $\gamma = (7.5 \pm 1.5)\times10^{-2}$. This value was found to be independent of temperature in the range 240 – 350 K, type of fuel, flame richness, soot mass and concentrations of HO_2 and H_2O_2 used. No significant deactivation of soot surface during its reaction with HO_2 was observed. Experiments on soot ageing under ambient conditions showed that reactivity of aged soot is similar to that of freshly prepared soot samples.

Analysis of the results obtained for the HO_2 + soot reaction shows that the possible impact of this processes on HO_x budget in UTLS region of the atmosphere is negligible. On contrary, in the troposphere the HO_2 loss on soot can be a non negligible sink of HO_x species with a potential impact on photochemical ozone formation at least under urban conditions.

B2

Absorption Cross Sections for the Second and Third OH-Strectch Overtone of Pernitric Acid, Nitric Acid, and Hydrogen Peroxide

H. Stark[a)], M. Aldener, S. Brown[a)], J.B. Burkholder, and A.R. Ravishankara[a,b)]

National Oceanic and Atmospheric Administration, Aeronomy Laboratory, 325 Broadway, Boulder, CO 80305, USA

[a)] *Also associated with Cooperative Institute for Research in Environmental Sciences University of Colorado, Boulder, CO 80309, USA*

[b)] *Also associated with Department of Chemistry and Biochemistry, University of Colorado, CO 80309, USA*

HO_x ($OH+HO_2$) is a key oxidant in the atmosphere. In the troposphere, OH is mainly formed by ozone photolysis in the ultraviolet in the presence of water. At low UV conditions, e.g. dusk and dawn, OH formation via ozone photolysis is suppressed and, yet, significant HO_x concentrations are measured. OH production under these conditions can have an important influence on atmospheric oxidation processes (for example hydrocarbon oxidation). One possible additional HO_x formation pathway is direct overtone photolysis (DOP) in the visible and near-IR, a process involving overtone excitation of a chromophore (in this case the OH-stretch vibration), intramolecular vibrational energy transfer (IVR), and cleavage of a weak bond. Peroxynitric acid (HO_2NO_2, PNA) is a primary candidate for DOP production of HO_x in the atmosphere. We will present cavity ringdown (CRDS) measurements of the band strengths of the second and third overtone of PNA at 991 nm and 764 nm, respectively. We will also present low temperature measurements of the second overtone at 231 K. We will discuss the importance of the results for DOP and show model calculations to evaluate the importance of PNA for atmospheric HO_x production. For comparison, CRDS measurements of the cross sections for second and third overtone absorption by nitric acid (HNO_3) and hydrogen peroxide (H_2O_2) are also presented.

A3

Laboratory Measurements of Particle Nucleation in Monoterpene Ozonolysis

James B. Burkholder, Tahllee Baynard, Edward R. Lovejoy, and A.R. Ravishankara

Aeronomy Laboratory, National Oceanic and Atmospheric Administration, 325 Broadway, Boulder, CO, USA

Ozonolysis of monoterpenes, such as α- and β-pinene, in the atmosphere represents a potential source of "new" particle formation and secondary organic aerosol. The evaluation of this source and its possible impact on the radiative budget depends on the ability to model the source under the range of conditions found in the troposphere (for example: precursor concentrations, background surface area, and temperature). We have performed laboratory particle nucleation studies for α- and β-pinene ozonolysis in an attempt to address these issues.

Laboratory experiments were performed in a temperature regulated (275 to 335 K) small volume (~ 70 L) Teflon bag. Particle production and growth during the first ~1000 s of the ozonolysis reaction were measured by simultaneous sampling using condensation particle counters with 3 and 10 nm cutoffs. Representative experimental data illustrating the observed dependence of the particle production on precursor concentration, the OH radical, and temperature for both of the α- and β-pinene nucleation processes will be presented and compared with previous chamber studies.

A two-component particle nucleation model has been used to interpret and quantify the experimental observations. The model parameters include the thermodynamics for nucleation and growth, and the reaction product yields of a single nucleating species and a single condensing species. The nucleating and condensing species are not identified in this study and the modeled yields may represent the sum of multiple species. Using the results from this study, new particle and secondary aerosol formation in the atmosphere resulting from monoterpene oxidation will be evaluated.

B3

Atmospheric Chemistry of furans: Kinetic and Mechanism study of their reactions with NO_3 radicals and Cl-atoms.

B.Cabañas, M.T. Baeza, F. Villanueva, P. Martín, S. Salgado and E. Monedero

Universidad de Castilla-La Mancha. Departamento de Química-Física. Facultad de Químicas. Avda Camilo José Cela 10. 17071 Ciudad Real (Spain).

Furan and substituted furans have been identified in the atmospheric emissions from combustion of fossil fuel and biomass burning. Also they have been found to be a minor product of the OH radical-initiated degradation of hydrocarbons. To date there are some studies concerning the fate of furans in the atmosphere, a larger part of these studies are about their reaction with the OH radicals, being the night-time reaction of these compounds with NO_3 radicals, less studied and scarce the information about the Cl-atoms reactions.
In this work we presented the result of a kinetic and mechanism study for a series of methyl-substituted furans (furan, 2-methylfuran, 3-methylfuran, 2-ethylfuran and 2,5-dimethylfuran) with NO_3 radicals and Cl-atoms. The values of the rate constants for the studied reactions have been determined at (298 ± 1)K and atmospheric pressure by a relative technique using a gas chromatograph with flame ionisation (GC-FID) detector see Table. The product study has been carried out using the combined gas chromatography-mass-spectrometry (GC-MS) techniques. The obtained information is useful to get a better understanding of the role of these compounds in the atmospheric chemistry and to develop a reliable structure reactivity relationship for these compounds.

Compound	$k_{Cl}/10^{-10}$ *cm³ molecule⁻¹ s⁻¹*	$k_{NO_3}/10^{-11}$ *cm³ molecule⁻¹ s⁻¹*
Furane	***2.04±0.35***	***0.14±0.01***
2-methylfurane	***2.38±0.39***	***2.57±0.11***
3-methylfurane	***4.07±0.27***	***2.86±0.09***
2-ethylfurane	***5.14±0.75***	***2.10±0.08***
2,5-dimethylfurane	***5.69±0.53***	***5.78±0.10***

- R. Atkinson, J. Phys. Chem. Ref. Data Monogr. 1 (1989).
- R. P. Wayne, I. Barnes, P. Biggs, J. P. Burrows, C. E. Canosa-Mas, J. Hjorth, G. LeBras, G. K. Moortgat, D. Perner, G. Poulet, G. Restelli, H. Sidebottom, Atmos. Environ. Part A. 25 (1991) 1.
- R. Atkinson, J. Phys. Chem. Ref. Data Monogr. 2 (1994).
- Kind, I. Berndt, T., Boge, O; Rolle, W. Chem., Phys, Lett., 256, 679, 1996.

A4

Studying The Fundamentals Of The Uptake Of NH_3 Onto Micron Sized Acidified Water Droplets Using A Laser Induced Fluorescence Technique.

Andrew J. Cotterill, Jariya Buajarern, Robert M. Sayer and Jonathan P. Reid*

School of Chemistry, The University of Bristol, BS8 1TS
* E-mail: J.P.Reid@bristol.ac.uk

Our experiments are focused on obtaining a fundamental understanding of the uptake of ammonia, which is the dominant basic species in the atmosphere, onto acidified water droplets. This is the most important process in the atmosphere for the stabilisation of acidic aerosols.

Our micron-sized droplets are generated using a vibrating orifice aerosol generator (VOAG), which produces a monodisperse train of aerosol droplets into a custom-built aerosol chamber.

The droplets are seeded with a low concentration of the fluorescent dye acridine. The laser induced fluorescence (LIF) of acridine, when excited at 355nm from a pulsed laser source, is Ph sensitive between pH 4 and 7 thus the LIF spectrum of the acridine doped droplets can be used as a unambiguous method for the determination of the pH of the droplet and therefore as a direct in situ probe of the uptake of ammonia onto the droplet (1). This is in contrast to other measurements on the same system, which are not direct as they infer the NH3 uptake by measuring a gas phase depletion (2).

We measure the pH of the droplets in the chamber as a function of NH_3 partial pressure, Dg (diffusion coefficient of ammonia in air), exposure time, starting pH of the droplets, acridine concentration within the droplets, type of acid used to acidify the droplets (H_2SO_4 or HNO_3) and droplet size. This represents a very thorough study of this important atmospheric process.

The second set of experiments we have carried out is to assess the actual impact of the droplet train upon the measurements themselves. These experiments have been carried out using droplets of the same size and then varying the spacing between them at fixed chamber pressures and fixed partial pressures of NH_3, this should go some way towards helping us understand some of the discrepancies that currently exist in the measurement of mass accommodation coefficients of NH_3 onto acidified sulphuric aerosol droplets and surfaces (2,3) and also for uptake processes studied on droplet train apparatus in general.

1. R.M. Sayer, R.D.B. Gatherer and J.P. Reid, 'A Laser Induced Fluorescence Techniques for determining the pH of Water Droplets and Probing Uptake Dynamics'. *Phys. Chem. Chem. Phys.* **5** (2003) 3740.

2. Swartz, E.; Shi, Q.; Davidovits, P.; Jayne, J. T.; Worsnop, D. R.; Kolb, C. E. 'Uptake of Gas-Phase Ammonia. 2. Uptake by Sulfuric Acid Surfaces'. *J. Phys. Chem. A* **1999**, *103*, 8824-8833.

3. Hanson, D.; Kosciuch, E. 'The NH_3 Mass Accommodation Coefficient for Uptake onto Sulfuric Acid Solutions'. Journal of Physical Chemistry A (2003), 107(13), 2199-2208.

B4

Laser Induced Fluorescence Studies of Atmospheric Mercury Cycling: Ultra-Sensitive Detection and Laboratory Kinetics

Deanna Donohoue, Anthony J. Hynes and Dieter Bauer

Division of Marine and Atmospheric Chemistry, Rosenstiel School of Marine and Atmospheric Science, University of Miami, 4600 Rickenbacker Causeway, Miami, Fl 33149, USA

Until recently Hg(0) was thought to be unreactive in the gas phase under atmospheric conditions. New measurements of the rapid depletion of atmospheric mercury in the arctic have demonstrated that, at least under some circumstances, mercury can undergo fast atmospheric cycling . These depletion events correlate well with the depletion of atmospheric ozone that appears to be triggered by the photolysis of labile halogen species released from the snow pack after the arctic sunrise. The implications of this for atmospheric mercury chemistry on a global scale are unclear because the precise mechanism of the arctic depletion events is not known and very little data is available for rate coefficients of Hg(0) with halogens. We are attempting to study these kinetics under conditions which will allow the pressure and temperature dependence of the rate coefficients to be determined. In addition we are investigating the use of laser based excitation schemes for the rapid, ultrasensitive detection of gas phase elemental mercury and reactive gaseous mercury. We have examined the sensitivity of single and sequential two photon laser induced fluorescence (LIF) detection techniques for gas phase Hg(0) under atmospheric conditions. These techniques combine extremely high detection sensitivity, selectivity and very fast time response. Our kinetics studies are currently focused on the reactions of Br, Cl with Hg(0). Our technique uses laser photolysis to produce the radical of interest followed by detection with a second laser using laser induced fluorescence. We have studied the reactions of Hg(0) with Cl and Br using photolysis of Cl_2 and Br_2 monitoring the decay of Cl and Br in an excess of Hg(0).

$$Hg + Cl + M \rightarrow HgCl + M \qquad (1)$$

$$Hg + Br + M \rightarrow HgBr + M \qquad (2)$$

We performed measurements at 100 and 200 Torr in N_2. We saw no evidence for any reaction within the precision of our measurements. To ensure that our experimental approach was reasonable we monitored the decay of Cl atoms in a known concentration of C_2H_6 and obtained good agreement with the literature value for this reaction. Our results suggest that the rate coefficients for reactions (1) and (2) are slower than 5×10^{-13} cm^3 molecule^{-1} s^{-1} at 200 Torr. We are currently measuring the decay of Hg(0) in an excess of Cl and Br atoms monitoring both species by LIF. In addition we have photolyzed $HgCl_2$ and observed the LIF spectra of the $^2\Pi_{3/2}$- $^2\Sigma$ (1-0) and (0-0) transitions of HgCl. This is the first observation of this molecule using the laser induced fluorescence technique. The dispersed fluorescence signal, obtained by pumping the band heads of the (1-0) and (0-0) bands, shows vibrational progressions from the initially pumped $^2\Pi_{3/2}$ (1 or 0) level to a series of vibrational levels in the ground state. We are also attempting to quantify the factors limiting detection sensitivity of Hg(0) and RGM using sequential two photon LIF in conjunction with preconcentration on gold tubes (Hg(0)) and KCl denuders (RGM).

This research has been supported by a grant from the U.S. Environmental Protection Agency's Science to Achieve Results (STAR) program.

A5

The Contribution of Sea Salt to the Marine Submicron Aerosol Mode: Size Segregated and Total Seasalt Aerosol Distributions at a Coastal Marine Site

Deanna Donohoue, Pedro Campuzano-Jost, Hal Maring and Anthony J. Hynes

Division of Marine and Atmospheric Chemistry, Rosenstiel School of Marine and Atmospheric Science, University of Miami, Miami, FL, USA

The extent of the contribution of sea salt to the submicron range of the marine boundary layer has been a subject of debate for over 30 years. Most current models of the MBL assume that this fraction of the total marine aerosol load is made up almost exclusively of sulfate aerosol. In this size range, chemical measurements in the field are quite challenging, due to the low particle count and small total aerosol mass. However aerosol volatility techniques, have reported a significant sea salt contribution in the submicron range at moderate to high wind speeds. This again contrasts with most particle impaction measurements, which found negligible amounts.

Our Aerosol Sodium Detector (ASD) utilizes thermal emission in a flat, reducing, optically thin hydrogen/oxygen flame (~1700 K). The integrated emission response is calibrated against the response form synthetic NaCl aerosol produced by a Vibrating Orifice Aerosol Generator (VOAG). It is capable of measuring sea salt size distributions in near real time. Coupled with a DMA, it can also provide size-specific sea salt ratios for particles diameters between 100 and 300 nm, making it ideally suited not only to determine the sea salt contribution to marine aerosol but also the extent of internal mixing. The ASD was deployed for three weeks in January 2004 at a coastal marine site at Bellows Airforce Station on O'ahu, Hawai'i. In a collaboration with the Department of Oceanography of the University of Hawai'i, thermal volatility and MOUDI measurements were taken simultaneously to asses the response of these instruments to changing aerosol loading conditions. We alternated between two sampling points a)on UH's tower at 15 m above sealevel, high enough above the shorebreak and the treeline to be representative of marine background aerosol. b) 4 m above the beach, facing straight into the wind, about 70 m from the initial wave breaking.

In its current revision, the ASD is capable of measuring sea salt size distributions in short integration periods and, due to the mass-based technique, unmatched size accuracy over the operational range of 100 –1900 nm. Ease of calibration and stability make it suitable for long-term deployments at coastal sites or ships. It shows good agreement with APS data for the coarse mode, as well as reasonable agreement with data from thermal volatility measurements. In the marine background aerosol at Bellows, sea salt was a minor, although not insignificant, submicron component. At wind speeds between 7 and 10 m/s, it made a 10-15% contribution to number concentration in the range 100-150 nm. In the plume of the shorebreak, sea salt ratios were consistently higher (30%-50%), suggesting that even at moderate wind speeds sea salt might be the primary aerosol in the lower 10 m over the open ocean. Size segregated measurements were performed on both inlets, showing little evidence of substantial aerosol aging processes in the Bellows aerosol. The high accuracy of the measurements revealed a shift in size of yet unknown origin.

This work was supported by the Office of Naval Research

B5

Kinetics of the reactions of CH_2Br and CH_2I radicals with O_2 at atmospheric temperatures

Arkke Eskola[1], Dorota Wojcik[2], Emil Ratajczak[2], and Raimo Timonen[1]

[1]*Laboratory of Physical Chemistry, University of Helsinki, A.I. Virtasen aukio 1, FIN-00014 Helsinki, Finland*

[2]*Department of Physical Chemistry, Wroclaw Medical University, pl Nankiera 1, 50-140 Wroclaw, Poland*

The kinetics of the reactions of $CH_2Br + O_2$ and $CH_2I + O_2$ have been studied at temperatures between 220 and 450 K. Laser photolysis at 193 nm of the proper precursor (dibromomethane for CH_2Br and chloroiodomethane for CH_2I) along the laminar flow reactor was used to homogenously generate radicals of interest, whose decay in the presence of molecular oxygen was subsequently monitored in time-resolved experiments using **photoionization mass spectrometry (PIMS)**. The reaction rates of the CH_2Br radicals with O_2 were observed to depend on buffer gas density (typical for formation of peroxy-radicals) within the experimental range ($0.3 - 15 \times 10^{17}$ of He), see figure 1. No bath gas density dependence (within the experimental error) was, however, observed for the reaction rates of the CH_2I radicals with O_2 under the experimental conditions ($0.2 - 15 \times 10^{17}$ of He), in agreement with the previous investigation of this reaction[1] at room temperature.

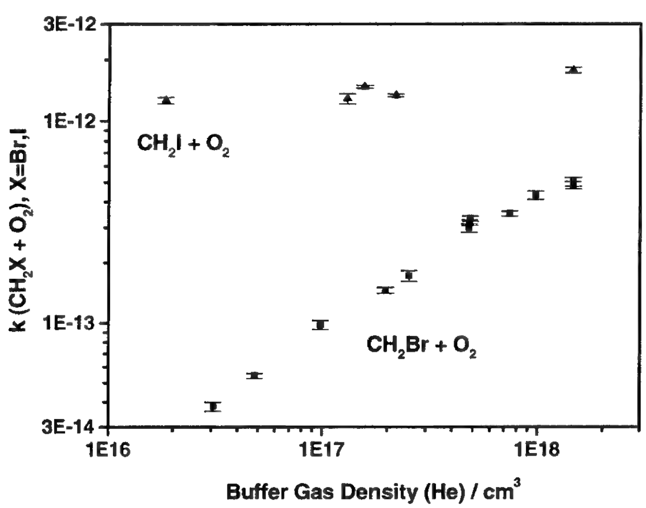

Figure 1. Buffer gas density dependence of the $CH_2I + O_2$ and $CH_2Br + O_2$ reactions at T = 298K.

(1) Masaki, A.; Tsunashima, S.; Washida, N. (1995) J. Phys. Chem., 99, 13126.

A6

A pulsed Laval nozzle apparatus for the study of kinetics at very low temperatures

Andrew Goddard, Dwayne E. Heard and Sally E. Taylor

School of Chemistry, University of Leeds, Leeds, LS2 9JT, UK

The use of Laval nozzles for studying chemical processes at low temperatures has been well documented in recent years.[1] There has been a recent trend toward using pulsed nozzles rather than continuous flow designs,[2] with the advantages of a smaller apparatus and pumping requirements. There is a reduced cost when using expensive gases as the carrier / buffer gas.

Laval nozzles allow an expansion in the form of a collimated supersonic flow that is uniform in Mach number, temperature and density. This flow provides a thermalised, super-saturated, effectively wall-less reaction vessel of well defined conditions. A pulsed system can achieve temperatures between 70 and 300K with densities of 10^{16} - 10^{18} cm^{-3}.

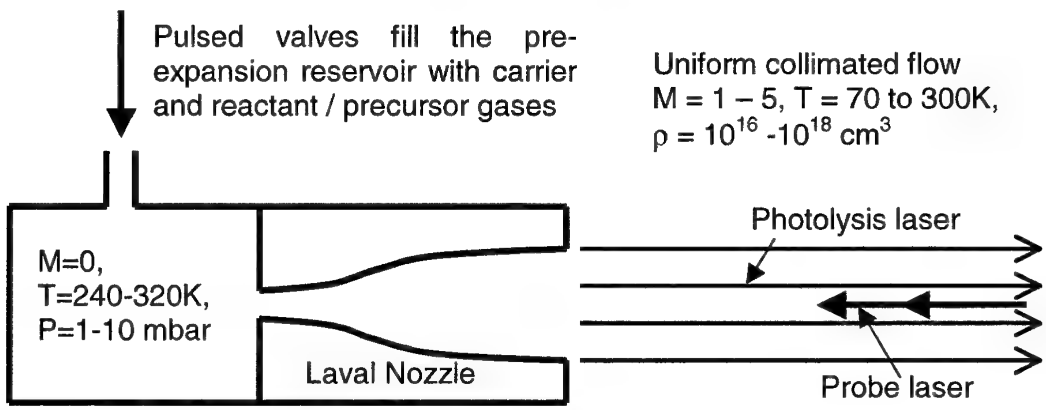

This paper will describe the operation and preliminary testing of a new pulsed Laval nozzle system currently under construction at the University of Leeds to study the kinetics of important reactions in the Earth's atmosphere and those of other planets. Initial studies will focus on the kinetics of reactions and energy transfer processes involving the hydroxyl radical at atmospherically relevant temperatures using detection by laser-induced fluorescence.

1. Smith M. A., *International Reviews in Physical Chemistry,* 1998, **17**, 35-63.
2. Atkinson D. B. and Smith M. A., *Rev. Sci. Instrum.*, **66**, 4434-4446.

Studies of Iodine Monoxide by Laser-Induced Fluorescence

Tom Gravestock, Mark A. Blitz, William J. Bloss and Dwayne E. Heard

Department of Chemistry, University of Leeds, Leeds, LS2 9JT.

Iodine monoxide, IO, is known to play an important role in catalytic ozone destruction in the marine boundary layer (MBL).[1] The chemistry of iodine oxides could also be important for other processes such as particle formation and halogen activation from sea-salt aerosol.

The reaction of IO + DMS was studied over the temperature range of 300 – 500 K and a pressure range of 10 – 300 Torr. Laser induced fluorescence (LIF) in the (2,0) band of the $A^2\Pi_{3/2} \leftarrow X^2\Pi_{3/2}$ electronic transition of IO was used to monitor the reaction post excitation at 445 nm. No pressure dependence was observed for the reaction and the room temperature rate constant was determined as 2.0 (± 0.4) × 10^{-14} $cm^3 molecule^{-1} s^{-1}$, an order of magnitude smaller than the most recent study[2] but in agreement with the previous literature. The rate of reaction was observed to increase with temperature and had an activation energy of ~ 10 kJ/mol. This suggests that the reaction is bimolecular (IO + DMS → DMSO + I), again in disagreement with the most recent study. Our results suggest that IO has little influence on the DMS budget in the marine boundary layer as it reacts too slowly with DMS to compete with OH and NO_3 oxidation.

The dispersed fluorescence from **v'** = 2 and **v'** = 0 in the $A^2\Pi_{3/2}$ excited state of IO has been measured for the first time by LIF at 445 nm and 465 nm respectively. The fluorescence from **v'** = 2 displayed vibrational structure and extended to ca. 650 nm (the (2,11) vibrational band). Although much weaker, dispersed fluorescence from **v'** = 0 was also observed.
Electronic quenching measurements of the $A^2\Pi_{3/2}$ state of IO in N_2 were performed. As this state is highly predissociative[3] it was thought unlikely that quenching would have a significant effect on the fluorescence signal. Although quenching of the short-lived **v'** = 0 level was not observed, the fluorescence intensity originating from **v'** = 2 was found to decrease by a factor of ~ 4 between 0 – 760 Torr after exciting at the (2,0) bandhead. The quenching effect of **v'** = 2 became less apparent with increasing ***J'***, in agreement with the ***J*** – dependent predissociation mechanism of this vibrational manifold.

These measurements are particularly useful for the development of an IO LIF field instrument.[4] The dispersed fluorescence spectrum of IO LIF assists optical filter design in order to maximise quantum efficiency of fluorescence collection whilst minimising interference from background solar radiation. The quenching data provides a means to evaluate the pressure dependence of instrumental sensitivity.

References

1. McFiggans, Gordon; Plane, John M. C.; Allan, Beverley J.; Carpenter, Lucy J.; Coe, Hugh; O'Dowd, Colin. **A modeling study of iodine chemistry in the marine boundary layer.** Journal of Geophysical Research, [Atmospheres] (2000), 105(D11), 14371-14385.
2. Nakano, Yukio; Enami, Shinichi; Nakamichi, Shinji; Aloisio, Simone; Hashimoto, Satoshi; Kawasaki, Masahiro. **Temperature and Pressure Dependence Study of the Reaction of IO Radicals with Dimethyl Sulfide by Cavity Ring-Down Laser Spectroscopy.** Journal of Physical Chemistry A (2003), 107(33), 6381-6387.
3. Newman, Stuart M.; Howie, Wendy H.; Lane, Ian C.; Upson, Mark R.; Orr-Ewing, Andrew J.. **Predissociation of the $A^2\Pi_{3/2}$ state of IO studied by cavity ring-down spectroscopy.** Journal of the Chemical Society, Faraday Transactions (1998), 94(18), 2681-2688.
4. Bloss, William J.; Gravestock, Thomas J.; Heard, Dwayne E.; Ingham, Trevor; Johnson, Gavin P.; Lee, James D. **Application of a compact all solid-state laser system to the in situ detection of atmospheric OH, HO_2, NO and IO by laser-induced fluorescence.** Journal of Environmental Monitoring (2003), 5(1), 21-28.

A7

Measurement of the chemical lifetime of OH in the atmosphere during TORCH

W. J. Bloss, J. Davey, D. E. Heard, T. Ingham, G. P. Johnson, M. J. Pilling, D. E. Self, S. C. Smith and J. Stanton

School of Chemistry, University of Leeds, Leeds, LS2 9JT

Many of the advances in our understanding of chemical oxidation in the atmosphere have come from comparison of field measurement data with the predictions of chemical models. For short-lived species, such as OH, concentrations are determined by chemistry alone, and zero-dimensional models that neglect transport are widely used to calculate free-radical concentrations for comparison with measurement. In polluted regions models often overpredict OH concentrations, possibly due to an underestimate of the OH sinks used to constrain the model, as it is not possible to measure all VOC species and their oxidation products. In steady-state, [OH] is given by [OH] = P / L, where $L = \Sigma_i k_i [i]$ (i = sink species, k_i = rate coefficient for reaction of i with OH), the reciprocal of its atmospheric lifetime, τ. Measurement of the lifetime, τ, allows an assessment of missing sinks in the model, and when combined with [OH], enables the production rate, P, to be calculated directly.

We have developed a field instrument to measure the lifetime of OH in the atmosphere, and have deployed it during the TORCH project. OH is generated by VUV photolysis of water vapour in humidified N_2 inside a sliding injector that can be translated within a larger diameter flowtube through which ambient air is drawn at a known (calibrated) velocity. After a distance downstream of the injector the flow is sampled by small pinhole and expanded into a low pressure chamber in which OH is detected with excellent sensitivity by laser-induced fluorescence spectroscopy, using a very high pulse repetition frequency laser at 308 nm and gated photon counting. The sensitivity of the system is calibrated to be $< 1 \times 10^7$ molecule cm^{-3}. By successively moving the injector away from the sampling nozzle, the reaction time between OH and its ambient sinks is increased, and an exponential decay is measured, as shown below for data taken during the TORCH 2003 campaign. After subtraction of the wall-loss, the atmospheric lifetime τ can be determined. OH data recorded in a short mixing region after the injector is not used in the analysis.

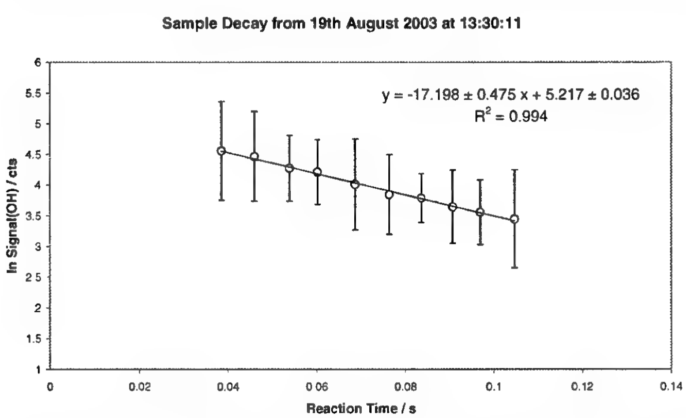

A large number of lifetimes were determined in the field (~ 5 mins required to measure a single lifetime), and have been compared with calculated lifetimes, using measured sinks (NO_2, non-methane hydrocarbons, oxygenated VOCs, and others), as well as model calculated degradation products that also react with OH, but are unmeasured. Care must be taken to understand fully the impact of any recycling of OH from reaction of HO_2 with NO.

The North Atlantic Marine Boundary Layer Experiment (NAMBLEX)

D. E. Heard and the NAMBLEX consortium
School of Chemistry, University of Leeds, Leeds, LS2 9JT

The NAMBLEX field campaign took place in the summer of 2002 at Mace Head, Ireland (53.2 N, 9.5 W), and involved over 50 scientists from 14 institutions. Vertically resolved measurements were made of the detailed structure of the boundary layer using a Doppler radar, sonic anemometers, a sodar and a small balloon. The chemical composition in the gas and aerosol phases was determined comprehensively using a variety of state-of-the-art instrumentation. Gas phase species measured included free-radicals (OH, HO_2, RO_2, IO, BrO, OIO, NO_3), halogen precursors (RX, I_2), nitrogen compounds (NO, NO_2, NO_y, HNO_3, organic nitrates), NMHC, o-VOCS, HCHO, peroxides, O_3, CO, and CH_4, together with spectrally resolved actinic flux to yield photolysis frequencies. Several species were measured using more than one technique enabling intercomparisons. Aerosol measurements included real-time size-dependent number distributions, hygroscopicity (to give realistic reactive surface areas) and chemical composition (using two aerosol mass spectrometers). The campaign was supported by measurements from a light aircraft. Several models of varying complexity, some based on the Master Chemical Mechanism, were used to study free-radical chemistry. This paper will provide an overview of the major results from the NAMBLEX campaign. A brief summary follows:

Chemical *and* dynamical measurements. Detailed chemical compositional measurements ran alongside detailed physical measurements of the structure of the boundary layer. Physical measurements were made using a balloon, SODAR, wind profiler and sonic anemometers.

New molecules measured. First measurements of I_2 and mid-latitude measurements of BrO. First measurements of OIO using broad-band cavity ring-down spectroscopy. Determination of NO_3 using two methods - long path and *in situ*. Highly detailed speciation of oxygenated VOCs using several instruments, measured continuously during the campaign.

New instruments deployed. A wind profiler, two aerosol mass spectrometers, upgraded FAGE and DOAS instruments, two CH_2O instruments, two peroxide instruments, a negative ion mass spectrometer for alkyl nitrates, speciated hydrocarbons and oxygenated VOCs using several GCS, a new broad-band cavity ring-down spectrometer, and a new MAX-DOAS instrument.

Comprehensive data sets during clean westerlies. Clean westerly trajectories were encountered over several weeks. Comprehensive measurements of many species, including NMHC, halogen precursors using GC-MS, o-VOCs, free-radicals (OH, HO_2, RO_2, NO_3, IO), and a wide range of supporting measurements of free-radical sources and sinks.

Real time aerosol composition as a function of aerosol diameter using two complementary mass spectrometry methods (Aerodyne AMS and TSI ATOFMS), single particle analysis. Real time size/number distributions, coupled with growth factors (hygroscopicity) enables a realistic reactive surface area to be calculated and CCN activity to be evaluated.

Role of halogens in controlling the HO_X budget. Coupling of HO_x/XO_x cylces clearly demonstrated in the troposphere (only demonstrated before in the stratosphere). Up to 40% of HO_2 loss is controlled by reaction with IO at low tide.

Role of iodine in production of new particles in the MBL. Co-measurements of organic iodine compounds (using GC-MS), radical intermediates (IO, OIO), and I_2, and measurement of aerosol phase iodine has aided the understanding of the formation of new particles in the marine environment, which can grow to CCN. Halogens are present in small particles formed from the interaction of seaweed with ozone/UV light. Model of aerosol nucleation developed.

Model comparisons - importance of oxygenates and halogens. Comparison of measurements of OH, HO_2 and RO_2 with predictions of box model based on the Master Chemical Mechanism. Modelled and measured HO_x and RO_x in much better agreement than previously observed at Mace Head, and better if oxygenated species (e.g. alcohols, acetylaldehye and acetone) included as sinks for OH. O-VOCs not measured before in the MBL under clean conditions. There are significant concentrations of HO_2 and total peroxy radicals at night, in good agreement with the model

Intercomparisons. For some species, e.g. CH_2O, peroxides, NMHC, measurements were made using more than one technique, enabling comparison of methods. In most cases agreement was excellent, enabling validation of instruments.

Reactions of partially oxidised hydrocarbons (POH) with OH

Dirk Hölscher, Terry J. Dillon and John N. Crowley

Max-Planck-Institute for Chemistry, Division of Atmospheric Chemistry, 55020 Mainz, Germany

Partially oxidised hydrocarbons (POH) are formed in the atmosphere by the degradation of biogenic and anthorpogenic hydrocarbons, in biomass burning and are directly emitted by vegetation. The POH of this study are hydroxyacetone ($CH_3C(O)CH_2OH$), glycolaldehyde ($HOCH_2CHO$), methanol (CH_3OH) and ethanol (C_2H_5OH) All these compounds are removed from the atmosphere via their reaction with the hydroxyl radical. Laser flash-photolysis of different suitable OH-precursors, coupled to laser induced fluorescence detection of OH was used to investigate the kinetics of the reactions:

$$OH + CH_3C(O)CH_2OH \rightarrow \text{products } (220 < T/K < 350)$$

$$OH + HOCH_2CHO \rightarrow \text{products } (230 < T/K < 350)$$

$$OH + CH_3OH \rightarrow \text{products } (210 < T/K < 350)$$

$$OH + C_2H_5OH \rightarrow \text{products } (216 < T/K < 368).$$

In situ optical determination (UV absorption spectroscopy) of the POH concentration enables accurate measurement of temperature dependent rate coefficients for each reaction. For $CH_3C(O)CH_2OH$ and $HOCH_2CHO$ these data are the first at low temperatures relevant e.g. for the upper troposphere, and enable calculation of relative rates of photolysis and reaction with OH in the atmosphere.

Using Pulsed Laser Techniques to Probe the Mass Transfer Dynamics of Multicomponent Aerosol Droplets

Rebecca J Hopkins, Robert M Sayer, Jonathan P Reid

School of Chemistry, University of Bristol, Cantock's Close, Bristol, BS8 1TS, U.K

In this work, the novel and non-intrusive spectroscopic technique, Cavity Enhanced Raman Scattering (CERS), is exploited to investigate the dynamics of micron size multicomponent droplets. CERS occurs as a result of droplets behaving as low loss optical cavities at wavelengths coinciding with whispering gallery modes thus providing a mechanism for optical feedback. It is possible to use the CERS technique to probe evaporation dynamics by monitoring size and compositional change.

Evaporation studies of ethanol, methanol and propanol containing droplets have been performed in a purpose built aerosol chamber by probing the composition change of droplets generated from a Vibration Orifice Aerosol Generator (VOAG) using the CERS technique. The CERS technique enables the extraction of size and composition data from a single spectrum for a single aerosol droplet.

The experiment is performed using a tightly focused Nd:YAG laser beam and illuminating single droplets on their edge. CERS spectra from many droplets are summed to give a spectrum that averages out the variation of the intensity of laser light coupled into the droplets. A ratio of the peak integrals of the ethanol/methanol/propanol and water Raman bands gives an indication of the chemical composition of the droplet. Using this strategy, a calibration plot can be obtained allowing the droplet composition to be determined.[1]

The calibration plot can then be utilised in an experiment where the exposure time of the droplets is varied and the compositional change is observed. The purpose built aerosol chamber allows the introduction of alcohol and water vapour so droplet equilibrium conditions can be reached. Equilibrium conditions can be perturbed allowing the study of evaporation dynamics in different environments.

Experiments are performed where the evaporative flux from the droplets is monitored as a function of chamber pressure. An increase in evaporative flux from the droplet is observed with decreasing gas pressure. This experiment is repeated for different droplet sizes and three different alcohol/water systems and this information is then used to measure aerosol droplet vapour pressure directly.

A method for measuring droplet temperature by examination of the O-H Raman stretching band is presented proving the CERS technique as a versatile technique enabling the examination of size, composition and temperature for aerosol droplets.

1. R J Hopkins, R Symes, R M Sayer, J P Reid, 'Determination of the size and composition of multicomponent ethanol/water droplets by cavity-enhanced Raman scattering.' Chemical Physics Letters 380 (2003) 665-672.

A9

The influence of inorganic iodine compounds on the oxidative capacity of the marine boundary layer

D. M. Joseph [1], S. H. Ashworth [2], J. M. C. Plane [1]

(1) School of Environmental Sciences, University of East Anglia, Norwich NR4 7TJ, U. K.,
(2) School of Chemistry & Pharmacy, University of East Anglia, Norwich NR4 7TJ, U. K.
m.joseph@uea.ac.uk

The biogenic formation and subsequent evasion of iodoalkanes and mixed haloalkanes by kelp and other coastal species has been well documented. The iodoalkanes, in particular, are photochemically labile, so that iodine atoms are rapidly formed during daylight and these consequently participate in ozone destruction cycles. While IO is produced in the reaction of I atoms with ozone and, after photolysis, continues a catalytic destruction cycle, both I atoms and IO can react with NO_x compounds present in polluted air masses. These reactions can produce reservoir compounds, which are more resistant to photolysis and thus alter the rates of catalytic cycles.

One suggested reservoir compound is iodine nitrate, $IONO_2$, which is formed as an adduct from IO and NO_2. The photolysis of iodine nitrate has been investigated using cavity ring-down spectroscopy and laser induced fluorescence to monitor complementary products in the two possible reaction channels. The formation of I + NO_3, as opposed to the reverse reaction to give IO + NO_2, has implications for the ozone concentration in the Marine Boundary Layer, as the products have different effects on the concentration of ozone and consequently the oxidizing capacity of the troposphere. In addition to determining the dominant product channel in the photolytic decomposition of $IONO_2$, attempts to measure its absorption cross-section have also been carried out by several optical techniques in the laboratory. The NO_3 detection limit of the cavity ring-down system has also confirmed, using N_2O_5 as a source of NO_3 through both photolytic and thermal decomposition.

B9

Reactions of halogen atoms and halogen monoxides with dimethyl sulfide

S. Enami, Y. Nakano, S. Hashimoto, S. Aloisio, and M. Kawasaki

Department of Molecular Engineering , Kyoto University, Kyoto 615-8510, Japan
* kawasaki@moleng.kyoto-u.ac.jp Fax -81-75-383-2573

Dimethyl sulfide (DMS) oxidation has a substantial impact on cloud formation over the oceans and hence influences the Earth's radiation balance and climate system. In this study, we have studied reaction kinetics of DMS with cavity ring-down spectroscopy (CRDS).

1. Reactions of DMS with Br and Cl

The reaction of Br atom with DMS proceeds via an association mechanism to form the Br-DMS adduct in the typical condition of troposphere.

$$Br + CH_3SCH_3 + M \rightleftarrows Br\text{-}DMS + M \qquad (1, -1)$$

The equilibrium constant and rates of the reaction are determined by CRDS. We conclude that the X-DMS adduct is not importance in atmospheric chemistry because of its rapid back-reaction.

2. Reactions of DMS with BrO and IO

In the reaction of IO and BrO with DMS, the reaction rate constants show a negative temperature and a positive pressure dependence:

$$IO + CH_3SCH_3 \rightarrow I + CH_3S(O)CH_3. \qquad (2)$$

The reaction has reached its high-pressure limit with a rate constant of 2.5×10^{-13} molecule^{-1} cm^3 s^{-1}. In light of these new data, DMS oxidation by IO can compete with oxidation by the OH radical in the marine boundary layer. Our estimates show that DMS oxidation by IO can account for discrepancies between modeled and measured rates.

3. A new source of IO in the atmosphere

Observing the CRDS spectrum of IO, we have found that the rate constants of the $CH_2I + O_2$ reaction are pressure-independent. The two-body reaction is dominant:

$$CH_2I + O_2 \rightarrow IO + HCHO \qquad (3)$$

The formation yield of IO from $CH_2I + O_2$ is estimated to be unity. In the troposphere, the major sources of CH_2I are both the photodissociation of dihalogen molecules CH_2IX (X = I, Br and Cl) and the reaction of CH_3I with OH. If CH_2I is oxidized by O_2 to generate an IO radical with 100% yield under the atmospheric conditions. Our results suggest that CH_3I could be a plausible candidate for another natural IO source.

Publications: 1. Y. Nakano *et al., J. Phys Chem.* A **105**, 11045 (2001), 2. Y. Nakano *et al., J. Phys. Chem.* A 107, 6381 (2003), 3. S. Enami *et al., J. Phys Chem.* A (submitted)

Kinetic Measurements of CH_3S Addition to Isoprene Between 213 and 373K

L.C. Koch and A.R. Ravishankara

National Oceanic and Atmospheric Administration, 325 Broadway, Boulder, Colorado, 80305, Department of Chemistry and Biochemistry, University of Colorado, Boulder, Colorado, 80309 and the Cooperative Institute for Research in Environmental Sciences, University of Colorado, Boulder, Colorado, 80309

Dimethylsulfide (DMS, CH_3SCH_3) and isoprene may coexist in coastal regions. In the gas phase, DMS is rapidly oxidized to CH_3S. Therefore, the reaction of CH_3S with isoprene may conjoin the natural sulfur and hydrocarbon oxidation mechanisms. The reaction of CH_3S with isoprene was studied using laser-induced fluorescence to detect CH_3S radicals, which were produced through pulsed laser photolysis of dimethyldisulfide, (CH_3SSCH_3), at 248 nm. Isoprene concentrations were determined through UV absorption at 213.9 nm. CH_3S temporal profiles were measured in the presence of differing amounts of isoprene, at temperatures between 213 and 373K. The rate coefficient for CH_3S reacting with isoprene, k_{1f}, is shown below in Arrhenius form.

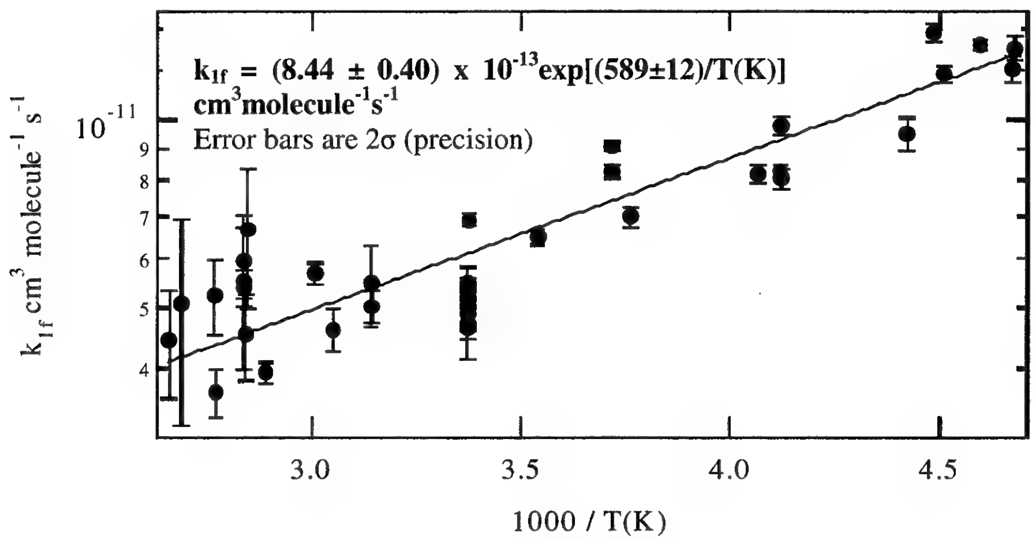

At temperatures between 213 and 330K, CH_3S temporal profiles were single exponential. However, at temperatures above 330K, CH_3S temporal profiles were biexponential. We attribute this behavior to the decomposition of an adduct that formed between CH_3S and isoprene. The rate coefficient for adduct decomposition, k_{1r}, was determined to be (1±12) x 10^{15}exp[(-10100±3800)/T(K)] s^{-1}, where error bars are 2σ (precision). The equilibrium coefficient, K_p, was ascertained from the quotient of k_{1f} and k_{1r}, as well as from fitting to biexponential profiles of CH_3S. Δ_rH^o for formation of the CH_3S-isoprene adduct was calculated to be approximately -19 kcal mol^{-1}. Biexponential CH_3S temporal profiles became single exponential upon addition of ~10^{17} molecules cm^{-3} of O_2. This outcome is consistent with a reaction between the CH_3S-isoprene adduct and O_2. The rate coefficient for reaction of the adduct with O_2 was determined to be (3±1) x $10^{-14} cm^3 molecule^{-1} s^{-1}$. We will discuss the oxidation of DMS in the presence of isoprene with consideration for these new measurements.

B10

Continuous wave diode laser cavity ring-down and cavity enhanced absorption spectroscopy for trace gas detection

Ruth E Lindley, Mikhail I Mazurenka, Alistair M Parkes, Ryuichi Wada, Alex Shillings and Andrew J Orr-Ewing.

School of Chemistry, University of Bristol, Cantock's Close, Bristol, BS8 1TS, U.K.

Continuous wave diode laser cavity ring-down spectroscopy (CRDS) and cavity enhanced absorption spectroscopy (CEAS) have been applied to the study of atmospherically relevant gases at low (pptv and ppbv) concentrations.

Use of a violet diode laser (λ ~410 nm) has enabled the detection of NO_2 at mixing ratios as low as 200 pptv with CRDS and around 8 ppbv using off-axis CEAS with lock-in detection. A blue diode laser (λ ~437 nm) is currently being employed for IO detection with a projected detection limit (based on the NO_2 measurements) in the region of 2 pptv using CRDS.

Near infrared distributed feedback diode lasers (λ ~ 1.5 μm) are being used for the measurement of C_2 hydrocarbons with detection limits for acetylene of the order of 1 ppbv (in the absence of pressure broadening) using both CRDS and 'on-axis' CEAS.

A comparison of CRDS and CEAS, including sensitivity, measurement time and stability considerations, will be presented and the advantages and disadvantages of each technique will be discussed. The development of field instruments, using CRDS and CEAS, for (near) real-time measurement of the trace gases mentioned above will also be presented.

A11

Mechanism of the ozonolysis of unsaturated compounds leading to SOA formation

Y. Ma and G. Marston

School of Chemistry, University of Reading, Whiteknights, PO Box 224, Reading RG6 6AD

The reactions of ozone with relatively large unsaturated compounds such as the terpenes are known to be important sources of secondary organic aerosol (SOA). However, the mechanisms of formation of the oxygenated products thought to lead to SOA are not well understood, with uncertainty in the mechanisms of formation of even the first-generation products. In this paper, experiments on the reactions of ozone with terpenes (and simpler model compounds) are described which have the aim of elucidating the mechanism of formation of some of these compounds. A static reaction chamber coupled with separation by gas chromatography and detection by mass spectrometry is used to examine the mechanism of formation of diacids from the reactions. These low volatility compounds have been proposed as the nucleating species in SOA creation. Detection of such compounds requires derivatisation to the dimethyl ester before injection into the GC/MS. Yields are measured as a function of initial reaction conditions (*e.g.* humidity, presence and nature of radical scavengers, presence and nature of Criegee intermediate scavengers, *etc.*), and the results of these experiments are used to provide mechanistic information about the reactions.

B11

Detection of the Criegee Intermediate by Fast Flow Coupled to FTIR

S.A. Kennedy, R. Walsh, G. Marston,

School of Chemistry, University of Reading, Whiteknights, PO Box 224, Reading RG6 6AD

R.J. Knight, K.M. Smith and R.G. Williams

Space Science and Technology Department, Rutherford Appleton Laboratory (RAL), Chilton, Didcot, Oxon OX11 0QX

The reactions of ozone with alkenes are important processes in the chemistry of the Earth's lower atmosphere, making important contributions to hydrocarbon oxidation, hydroxyl radical formation and the creation of secondary organic aerosol. The reactions are believed to occur *via* the formation of the Criegee intermediate (CI), a species of the general type R^1R^2COO. Despite the importance of the reactions and the key role played by this unusual intermediate, the CI has never been detected in the gas phase. In this paper, we describe experiments aimed at detecting the species by a combination of the high pressure fast flow technique with Fourier transform infrared (FTIR) spectroscopy at the RAL Molecular Spectroscopy Facility. The flow tube is coupled to the FTIR instrument using multi-pass optics, and preliminary experiments using precursor molecules (2,3-dimethylbut-2-ene and ozone) show that the arrangement works satisfactorily. The search for a signal due to the CI will use previous matrix and theoretical spectra as a guide combined with knowledge of its expected temporal profile based on the OH-formation work of Anderson and co-workers (J.H. Kroll, J.S. Clarke, N.M. Donahue, J.G. Anderson, K.L. Demerjian, *J. Phys. Chem. A*, **105**, 1554 (2001)).

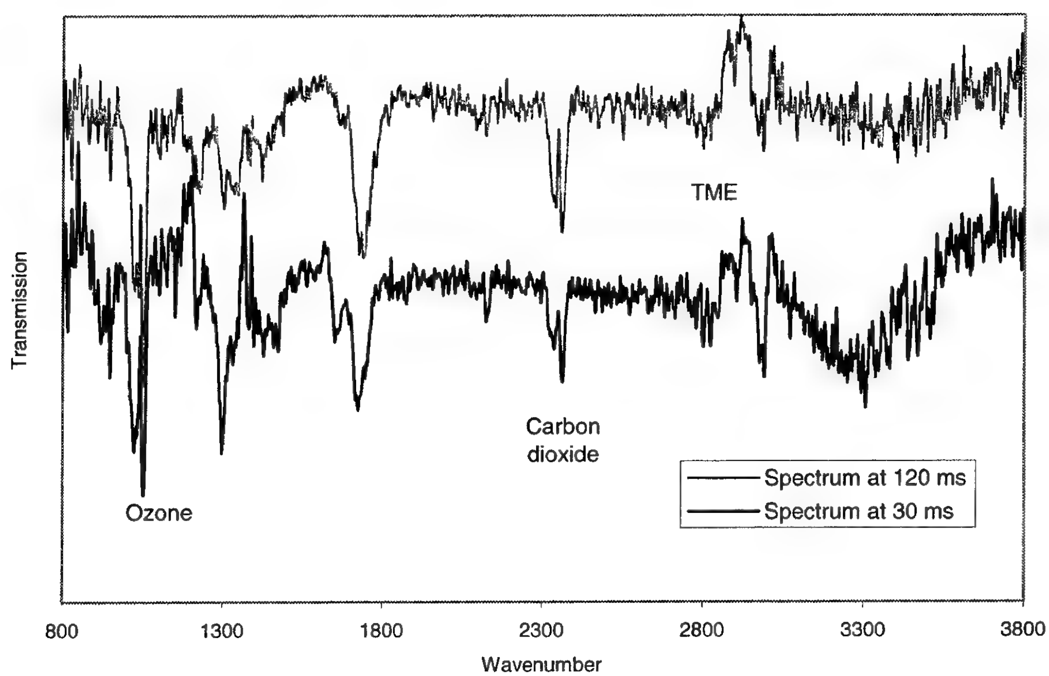

Fig. 1. Spectra obtained from the reaction of ozone with tetramethylethylene (TME).

A12

Formation of $O(^3P)$ atoms in the photolysis of N_2O at 193 nm and $O(^3P) + N_2O$ product channel in the reaction of $O(^1D) + N_2O$

Yutaka Matsumi, Satoshi Nishida, and Kenshi Takahashi
Solar-Terrestrial Environmental Laboratory and Graduate School of Science, Nagoya University, Honohara 3-13, Toyokawa, Aichi, 442-8507, Japan.
FAX : +81-533-89-5593
e-mail : matsumi@stelab.nagoya-u.ac.jp

The $O(^3P)$ atom produced in the 193 nm photolysis of N_2O has been detected by a technique of vacuum ultraviolet laser-induced fluorescence spectroscopy around 130 nm. The quantum yield value of the $O(^3P)$ atoms produced directly in the photolysis of N_2O at 193 nm at room temperature has been determined to be 0.005 ± 0.002. The $O(^3P)$ atom formation process in the reaction of $O(^1D) + N_2O$ is also studied and the channel branching ratio of $O(^3P) + N_2O$ has been determined to be 0.04 ± 0.02 among the product channels, 2 NO, $N_2 + O_2$ and $O(^3P) + N_2O$. Photodissociation processes of N_2O at 193 nm and reaction processes of $O(^1D) + N_2O$ system have been discussed based on the experimental results. Due to importance of the $O(^1D) + N_2O$ reaction in the stratosphere, impact of the experimental result of $O(^3P)$ formation from the $O(^1D) + N_2O$ reaction on the stratospheric chemistry is also studied by one-dimensional atmospheric model calculations.

B12

Accurate determination of the absolute quantum yield for $O(^1D)$ formation in the photolysis of ozone at 308 nm

Yutaka Matsumi, Kenshi Takahashi, Shinsuke Hayashi, and Takayuki Suzuki

Solar-Terrestrial Environment Laboratory and Graduate School of Science, Nagoya University, Honohara 3-13, Toyokawa, Aichi, 442-8507, Japan.
FAX : +81-533-89-5593
e-mail : matsumi@stelab.nagoya-u.ac.jp

The absolute $O(^1D)$ quantum yield from the photodissociation reaction of O_3 at 308 nm should be determined accurately with a high precision for its atmospheric significance. This is because it has been used as a reference in previous relative measurements to obtain the $O(^1D)$ quantum yields as a function of photolysis wavelength in the near ultraviolet (UV) region. In this study, the near-UV pulsed laser photolysis of O_3 with the direct detection of the $O(^1D)$ and $O(^3P)$ photofragments using a technique of vacuum UV laser-induced fluorescence has been applied to determine the absolute $O(^1D)$ quantum yield from O_3 photolysis. The absolute $O(^1D)$ quantum yield at 308.0 nm at room temperature (298 ± 2 K) is determined to be 0.804 ± 0.023 (95% confidence interval). The uncertainty is much smaller than the current recommendation value for atmospheric studies. The $O(^1D)$ quantum yield values at photolysis wavelengths between 307 and 311.5 nm are also presented.

A13

Reaction of hydroxyl radical with oxygenated organic compounds. A variational transition-state theory approach

Montserrat Ochando-Pardo,[†], Ignacio Nebot-Gil[†], Àngels González-Lafont,[‡], José M. Lluch[‡]

†Departament de Química Física and Institut de Ciència Molecular, Universitat de València, 46100 Burjassot, Spain, and ‡Departament de Química, Universitat Autònoma de Barcelona, 08193 Bellaterra, Barcelona, Spain

Isoprene is the most abundant nonmethane hydrocarbon emitted into the troposphere. Not only isoprene but also its reaction products play an important role in the photochemical production of ozone in urban and rural areas. Oxidation by the OH radical is the main degradation process of those compounds in the low atmosphere. A large number of experimental rate constants have been determined for the OH-initiated oxidation of several isoprene reaction products. However, theoretical calculations can help us to interpret experimental results, also providing a way to test the goodness of the most advanced electronic structure methods, and dynamical approaches.

In particular, in this work we have studied the reaction of OH radical with some oxygenated compounds which are oxidation products of isoprene: glycolaldehyde, methacrolein, and methyl vinyl ketone. All the reaction channels involved in those three oxidation processes have been analyzed by means of high-level electronic structure methods. Direct dynamics calculations have then been carried out to evaluate the overall rate constants within the frame of Variational Transition State Theory and its Canonical Unified Statistical extension. Multidimensional tunnelling corrections have also been included when necessary. The comparison of the three oxidation reactions will contribute to the understanding of the fate of isoprene reaction products in the atmosphere.

E-mail: Montserrat.Ochando@uv.es

B13

Examination of the OH formation mechanism in the reactions $CH_2CHO + O_2$ and $CH_3CHCHO + O_2$

T. Oguchi*, Y. Sato, and H. Matsui

Toyohashi University of Technology, Japan

The reactions of CH_2CHO and CH_3CHCHO radicals with O_2 have been investigated by laser-induced fluorescence method at room temperature. CH_2CHO and CH_3CHCHO are produced by a pulsed laser photolysis of precursor molecules. By conducting kinetic analyses, the rate constants for the reactions are found to show typical fall-off pressure dependence in the investigated pressure range (3–200 Torr, He buffer), which suggests the dominance of recombination processes to form peroxy radicals. OH radical is also confirmed to be a direct product in these reactions. The product yields of OH radicals are determined on the total pressure (10-200Torr). The mechanism of OH product channel is discussed by taking into consideration of H atom migration process in the five-membered structures of the chemically activated peroxy radicals formed from the initial reactions.

* to whom correspondence should be addressed.

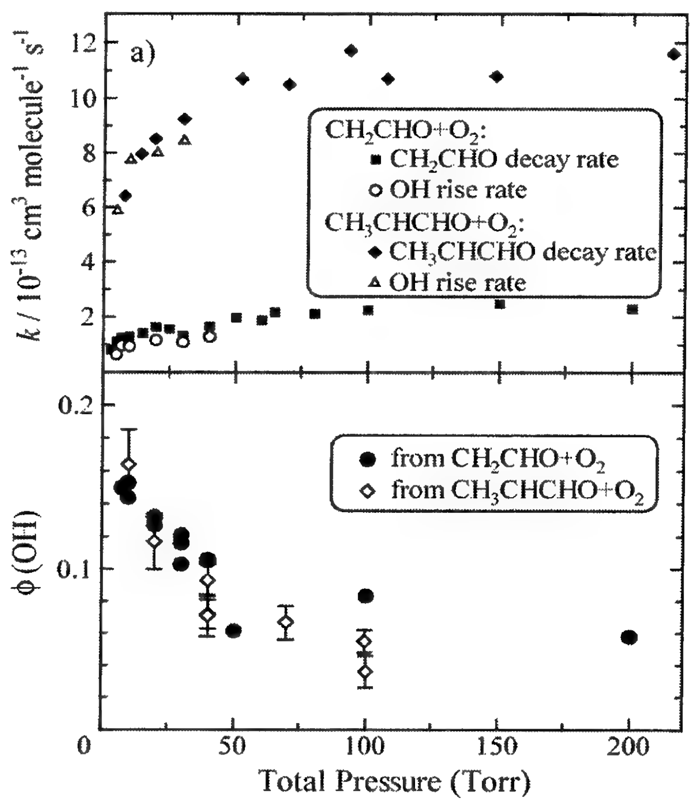

Fig. 1. Pressure dependence for the rate constants and the OH product yields of $CH_2CHO + O_2$ and $CH_3CHCHO + O_2$ reactions.

A14

Absolute Rate Determination and Mechanistic Analysis for the Reaction of Cl Atoms with CH_2I_2

V. G. Stefanopoulos, V.C. Papadimitriou, Y.G. Lazarou, and P. Papagiannakopoulos

Department of Chemistry, University of Crete, Heraklion 714 09, Crete, Greece

panosp@chemistry.uoc.gr Fax: +30-2810-393601

Iodine-containing compounds have been detected in significant amounts in ocean waters. Although CH_3I is the most abundant iodinated compound several iodocarbons, such as CH_2I_2, C_2H_5I, C_3H_7I and CH_2ICl are also presented, which are produced by biogenic processes (phytoplankton and macroalgae). These compounds have relative low solubility, and thus are transfered in high rates (1–2 Tg yr^{-1}) to the marine boundary layer (MBL). In general, iodinated compounds are very photolabile species and probably undergo efficient photodissociation in the troposphere. However, tropospheric degradation may also occur through the reaction with OH radicals, and probably in coastal areas with halogen atoms, where their concentrations are high. The present study investigates the gas phase reaction of Cl atoms with di-iodomethane CH_2I_2 under very low pressure conditions, by using the Very Low Pressure Reactor (VLPR) technique. The absolute rate coefficient at room temperature was found to be 2.19×10^{-11} $cm^3molecule^{-1}s^{-1}$, and the temperature dependence study (273 – 363 K) revealed that the Arrhenius pre-exponential factor and the activation energy for the reaction were $A = 3.3\times10^{-11}cm^3molecule^{-1}s^{-1}$ and Ea = 1.7 kJ/mol, respectively. Mass spectrometric analysis indicates that ICl and HCl are the primary reaction products, with no evidence of the iodine atom exchange reaction. Furthermore, oxidation experiments have shown that HCHO and HCOOH were the final products. Finally, theoretical calculations were also performed to elucidate the primary reaction mechanism.

Measurement of the Rate Constant for the Reaction H + C_2H_5 at Low Pressure and Low Temperature

A. S. Pimentel, [1] W. A. Payne, [1] F. L. Nesbitt, [1,2] R. J. Cody, [1] and L. J. Stief [1]

[1] *Laboratory for Extraterrestrial Physics, NASA/Goddard Space Flight Center, Greenbelt, MD, USA*

[2] *Department of Chemistry, Catholic University of America, Washington, DC; also at Coppin State College, Baltimore, MD, USA*

The reaction of H + C_2H_5 is predicted by photochemical modeling to be the most important loss process for ethyl radicals, C_2H_5, and a significant source of methyl radicals, CH_3, in the atmospheres of Jupiter [1] and Saturn [2]. The motivation for this study is that the available data [3, 4] is mostly indirect and not isolated from secondary chemistry. On the other hand, the results of this study show the primary reaction is essentially isolated from secondary chemistry. The measurements were performed in a discharge - fast flow system with the detection of the C_2H_5 radical by low-energy electron impact mass spectrometry under pseudo-first order conditions. [H] $\approx$ (3.1-5.7) times [C_2H_5]. Our experiments suggest negligible temperature and pressure dependencies. The rate constants for the reaction H + C_2H_5 are k(295K) = $(1.02\pm0.24)\times10^{-10}$, k(202K) = $(1.02\pm0.22)\times10^{-10}$ and k(150K) = $(0.93\pm0.21)\times10^{-10}$, all in units of cm^3 $molecule^{-1}$ s^{-1}. The rate constant for H + C_2H_5 measured at low pressure and temperatures can now be used in the photochemical models of the Jupiter and Saturn's atmospheres.

Acknowledgements. This research is being supported by the NASA Planetary Atmospheres Program. ASP thanks the National Academy of Science for the award of a research associateship.

[1] Gladstone, G. R., Allen, M., and Yung, Y. L. *Icarus* **119**, 1 (1996).

[2] Moses, J. I., Bezard, B., Lellouch, E., Gladstone, G. R., Feuchtgruber, H., and Allen, M. *Icarus* **143**, 244 (2000).

[3] Pratt, G. L. and Wood, S. W. *J. Chem. Soc. Faraday Trans I* **80**, 3419 (1984).

[4] Sillesen, A., Ratajczak, E., and Pagsberg, P. *Chem. Phys. Lett.* **201**, 171 (1993).

A15

Theoretical study of the OH addition to the β-pinene

Víctor Miguel Ramírez Ramírez

Universitat de València

In this work, we have investigated the gas-phase reaction between OH radical and the β-pinene, by means of *ab initio* calculations based on quantum theory. The four different possibilities for the initial OH addition to the double bond of β-pinene have been discussed. The energy barriers calculated at the QCISD(T)/6-31G(d) level of theory upon UMP2/6-31G(d) optimised structures, show that there are preferred orientations for the OH addition under atmospheric conditions of temperature and pressure. Precisely, the OH attack that leads to a tertiary radical and has less steric hindrance is the most favoured pathway.

The Master Chemical Mechanism – Latest Improvements (MCMv3.1)

S.M. Saunders[2], M.E. Jenkin[3], C. Bloss[1], V. Wagner[1], A.R. Rickard[1], L. Whitehouse[1], S. Pascoe[1] and M.J Pilling[1]

1. *School of Chemistry, University of Leeds, Leeds LS2 9JT, U.K.*
2. *Disciplines of Chemistry and Geography, University of Western Australia, Nedlands, 6009 Western Australia.*
3. *Imperial College London, Silwood Park, Ascot, Berkshire SL5 7PY, U.K.*

The MCM (Master Chemical Mechanism) is a near-explicit chemical mechanism describing the detailed gas phase degradation of a series of primary emitted VOCs. The mechanism is constructed according to a set of rules as defined in the latest mechanism development protocols (Saunders *et al.* [2003] and Jenkin *et al.* [2003]). Rate constants and product channel branching ratios are taken from the latest experimental data or are estimated from structure activity relationships (SARs). Strategic simplifications are applied in order to limit the number of reactions but retaining the essential elements of the chemistry. The latest version of the MCM, ***MCMv3.1*** has recently been made available on the MCM website:

http://www.chem.leeds.ac.uk/Atmospheric/MCM/mcmproj.html

The most important changes with regard to MCMv3.1 is an extensive update to the aromatic mechanisms and the addition of a number of new degradation schemes including MBO (2-methyl-3-buten-2-ol), an important biogenic hydrocarbon.

The degradation schemes of four aromatic systems; benzene, toluene, *p*-xylene and 1,3,5-trimethylbenzene, have been updated on the basis of new kinetic and mechanistic data from current literature and conference proceedings. The performance of these schemes concerning ozone formation from tropospheric aromatic oxidation has been evaluated using detailed environmental chamber datasets from the EU EXACT measurement campaigns which took place in the European Photoreactor (EUPHORE). Where appropriate, results from this database have been used to refine the mechanisms. The development work discussed on aromatic degradation schemes has been extended to update the degradation schemes of twelve other mono-aromatics in MCMv3.1 with saturated alkyl side chains.

As well as improvements to the MCM photochemical reaction schemes, ongoing work is also being carried out on the usability of the MCM website. New species look-up and SMILES look-up utilities increase the ease of navigation around the MCM and the subset assembler tool is extremely useful as the user can construct subset mechanisms straight from the MCM. A comprehensive up-to-date kinetic database for all reactions incorporated in the MCM, including literature channel branching ratios and rate constant citations along with estimations of their uncertainties is currently being constructed. This large database is linked directly to the relevant reactions on the MCM website. This facility will provide an extremely useful reference tool for the user and subject the MCM to a wider user group. Ongoing work is also being carried out in order to convert the MCM into FORTRAN and XML based versions making the MCM even more "user-friendly", particularly to the global/regional modelling communities.

Saunders, S. M., Jenkin, M. E., Derwent, R. G. and Pilling, M. J. (2003). Protocol for the development of the Master Chemical Mechanism, MCM v3 (Part A): tropospheric degradation of non-aromatic volatile organic compounds. *Atmos. Chem. Phys.* **3**, 161-180.

Jenkin, M. E., Saunders, S. M., Wagner, V. and Pilling, M. J. (2003a). Protocol for the development of the Master Chemical Mechanism, MCM v3 (Part B): tropospheric degradation of aromatic volatile organic compounds. *Atmos. Chem. Phys.* **3**, 181-193.

A16

The Development of a Novel Sodium Atom Chemiluminescence Technique for Measuring the Concentration of OH in the Atmosphere

Daniel E Self, John M C Plane[1], Dwayne E Heard and William J Bloss

School of Chemistry, University of Leeds, Leeds, LS2 9JT
[1] School of Environmental Sciences, University of East Anglia, Norwich

Measurements of OH concentrations are of central importance in understanding the chemistry of the troposphere. Due to the high reactivity of OH with many atmospheric constituents, it is only present at very low concentrations (typically around 10^6 molecule cm^{-3}) and is challenging to measure with accuracy. The most successful techniques currently used to measure OH in the field are FAGE – Fluorescence Assay with Gas Expansion, CIMS – Chemical Ionisation Mass Spectrometry and DOAS – Differential Optical Absorption Spectroscopy. However, these three techniques involve expensive equipment such as lasers and mass spectrometers and/or have limited sensitivity. The chemiluminescence technique proposed here should lead to a sensitive, cheap and compact field instrument.

The technique involves an oven, in which is contained Sodium metal (Na) and a heated injector to flow the entrained vapour into an air-sampling chamber. The sodium is partially in the form of a dimer, Na_2, reaction of which with OH produces excited $Na(^2P_J)^*$ atoms that emit at 589.0nm and 589.6nm. Hence the OH can be detected by photon-counting against a dark background through a narrowband filter, with a cooled PMT. The instrument could also measure atmospheric HO_2 radicals by converting them to OH using NO injection upstream of the detection region, as with the FAGE technique.

This research is a feasibility study into how well the technique should work, involving kinetic measurements of the reactions of Na_2 with atmospheric constituents O_2, H_2O, NO_2, NO, O_3 and OH and an estimate of the quantum yield of $Na(3\ ^2P_J)^*$ production from reaction with OH. Quantum *ab initio* calculations of enthalpies of important reactions are used in conjunction with measurements to determine potential interferences. The sodium oven has been adapted for the cell used for FAGE, in order to perform intercomparisons between the two techniques for calibrated and ambient OH samples.

Rate coefficients below were measured using LIF detection of Na_2 in a flow tube (units: cm^3 $molecule^{-1}\ s^{-1}$, errors: 1σ accuracy).

$$k(Na_2 + OH, 298K) = (1.01\ ^{+0.18}_{-0.19}) \times 10^{-10}$$
$$k(Na_2 + O_2, 298K) = (2.73 \pm 0.46) \times 10^{-11}$$
$$k(Na_2 + H_2O, 298K) < 1.4 \times 10^{-13}$$
$$k(Na_2 + NO_2, 298K) = (1.79\ ^{+0.51}_{-0.31}) \times 10^{-10}$$
$$k(Na_2 + NO, 298K) = (1.33\ ^{+0.13}_{-0.12}) \times 10^{-11}$$
$$k(Na_2 + O_3, 298K) = (1.25\ ^{+0.83}_{-0.46}) \times 10^{-10}$$

The quantum yield for production of $Na(3\ ^2P_J)^*$ from the Na_2 + OH reaction was measured to be $\sigma(Na(3\ ^2P_J)^*, 298K) = (0.33 - 3.1) \times 10^{-4}$.

B16

Kinetic studies of the reaction of R + O_2 (R = C_6H_5, C_2H_3)

Kenichi Tonokura,[1] Hiroshi Chishima,[2] and Mitsuo Koshi[2]
[1] *Environmental Research Center, The University of Tokyo, 7-3-1 Hongo, Bunkyo-ku, Tokyo 113-0033, Japan*
[2] *Department of Chemical System Engineering, The University of Tokyo, 7-3-1 Hongo, Bunkyo-ku, Tokyo 113-8656, Japan*

Reactions of hydrocarbon radicals (R) with oxygen molecules, O_2 are important processes during the oxidation of hydrocarbons in the chemistry of the urban atmosphere and combustion. Therefore, there have been numerous kinetic studies on R + O_2 reactions. In the present work, cavity ring-down spectroscopy coupled with pulsed laser photolysis has been used to study the kinetics of the reactions of C_6H_5 + O_2 and C_2H_3 + O_2 at 298 K in the pressure range of 10 – 120 Torr.

The absorption spectrum of vinylperoxy radical in the 439-465 nm wavelength range was observed after the 193 nm photolysis of $C_2H_3Br/O_2/Ar$ mixtures. Vinylperoxy radical has two isomers: a *trans* and a *cis* form. The electronic transition in the spectral range of 439-465 nm was assigned to a B ← X transition of the *cis*-isomer, as a result of calculations at the TD-UB3LYP/aug-cc-pVTZ level of theory. This spectrum is in agreement with that measured by Fahr *et al.*[1]

Pressure dependence of the vinylperoxy radical production was studied in the pressure range of 10-120 Torr (Figure 1). The vinylperoxy radical production was largely increased with increasing the total pressure, while the vinyl radical production was not affected by the total pressure. The total rate constants of the reaction of the vinyl radical with oxygen molecule have no pressure dependence in the current pressure range [2,3]. The experimental results suggest that the branching ratio of the vinylperoxy radical production in the C_2H_3 + O_2 reaction was increased because vinylperoxy radical was stabilized by the third-body M, as total pressure was increased. We also studied the C_6H_5 + O_2 reaction.

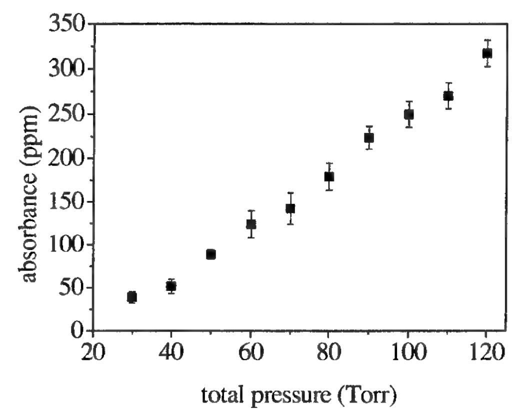

Figure 1: Pressure dependence of the vinylperoxy radical production

[1] A. Fahr *et al.* J. Phys. Chem. A **101**, 4879-4886 (1997)
[2] A.M. Mebel *et al.*, J. Am. Chem. Soc. **118**, 9759-9771 (1996)
[3] Y. Georgievskii, S.J. Klippenstein, J. Phys. Chem. A **107**, 9776-9781 (2003).

A17

Gas-Phase Reactions of the OH Radicals with Catechol

Estelle Turpin [1,2], Alexandre Tomas [1], Christa Fittschen [2], Nadine Locoge [1], Pascal Devolder [2]

1 Ecole des Mines de Douai, département Chimie-Environnement, 941, rue Charles Bourseul, 59500 Douai, France

2 Physico-chimie des Processus de Combustion et de l'Atmosphère, USTL, CNRS UMR 8522 59655 Villeneuve d'Ascq Cedex, France

Catechol or 1,2-dihydroxybenzene is a strong mutagenic and carcinogenic aromatic compound like benzene and has many sources. As primary emission sources, one can mention the chemical industry, in which catechol is used as antioxidant in many applications, as well as the photographic and cosmetic industries. It was also found in cigarette smoke. Yet, secondary emissions represent a major source, as the catechol is the major degradation product in the reaction of phenol with OH radicals (Olariu et al., 2002; Berndt et Böge, 2003). Because it is now recognised that phenol is the main primary degradation product in the benzene + OH reaction (Berndt et Böge, 2001; Volkamer et al., 2002), it follows that catechol is one of the most important ring-retaining product in the benzene OH-oxidation. As available literature data on the catechol atmospheric chemistry are very scarce (Olariu et al., 2000; Tomas et al., 2003), supplementary laboratory investigations on the atmospheric chemistry of this compound are needed in order to evaluate its environmental impact.

Reaction kinetics of catechol with OH radicals and Cl atoms were first investigated using a flexible Teflon smog chamber of about 300 L. OH radicals and Cl atoms were generated by the photolysis of CH_3ONO and Cl_2, respectively. Relative rate method was used to determine room temperature rate coefficients. Gas-phase reactants were sampled on activated charcoal cartridges and analysed by GC - FTIR technique. Rate coefficient values obtained (in units of cm^3 $molecule^{-1}$ s^{-1}) at (298 ± 2) K are $(1.1 \pm 0.2) \times 10^{-10}$ for the OH reaction and $(3.8 \pm 0.4) \times 10^{-10}$ for the Cl reaction. In a second part, experiments intending to identify the reaction products for both reactions were performed using the same setup as for the kinetic experiments. These two types of experiments aimed at differentiating the abstraction and the addition pathways in the first oxidation step. Preliminary results are presented and a mechanism for the reaction of OH with catechol is tentatively proposed.

References

Berndt T., Böge O. (2001), Phys. Chem. Chem. Phys. 3, 4946-4959
Berndt T., Böge O. (2003), Phys. Chem. Chem. Phys. 5, 342-350
Olariu R.I., Barnes I., Becker K.H., Klotz B. (2000) Int. J. Chem. Kin. 32, 696-702
Olariu R.I., Klotz B., Barnes I., Becker K.H., Mocanu R. (2002) Atmos. Environ. 36, 3685-3697
Tomas A., Olariu R.I., Barnes I., Becker K.H. (2003) Int. J. Chem. Kin. 35, 223-230
Volkamer R., Klotz B., Barnes I., Imamura T., Wirtz K., Washida N., Becker K.H., Platt U. (2002) Phys. Chem. Chem. Phys. 4, 1598-1610

B17

Discharge-flow studies of the kinetics of the reactions of NO_3 with CH_3O_2, $C_2H_5O_2$ and CF_3O_2

Stewart Vaughan, Carlos E. Canosa-Mas and Richard P. Wayne

Physical and Theoretical Chemistry, University of Oxford, South Parks Road, Oxford OX1 3QZ UK

The reactions of the nitrate radical, NO_3, with peroxy radicals, RO_2, are of atmospheric interest as the reactions may be an indirect source of OH radicals at night *via* the following reaction sequence:

$$NO_3 + RO_2 \rightarrow NO_2 + RO + O_2$$
$$RO + O_2 \rightarrow R'C(O)R'' + HO_2$$
$$HO_2 + O_3 \rightarrow OH + O_2 + O_2$$

A discharge-flow tube coupled with cavity-enhanced absorption spectroscopy (CEAS) detection systems for NO_3 and NO_2 at wavelengths of 662 nm and 404 nm, respectively, and resonance fluorescence (RF) detection of OH radicals was used to study the kinetics of the reactions $NO_3 + CH_3O_2$ (1), $NO_3 + C_2H_5O_2$ (2) and $NO_3 + CF_3O_2$ (3) at a $P \approx 5$ Torr and $T \approx 298$ K. Peroxy radicals were produced in the discharge-flow system, and their concentrations were monitored *via* titration with NO and measurement of the resultant NO_2 using the CEAS system at $\lambda = 404$ nm. The RF system for OH was used to indicate if any HO_2 radicals were present in the system. The values of [NO_2] and [OH] for various contact times were fitted to a numerical model to yield absolute values of the concentration of RO_2. The concentrations of NO_3 in the absence and presence of RO_2 were then measured and fitted to other numerical models containing the possible primary and secondary chemistry of the NO_3 and RO_2 radicals. These models give rate constants of $k_1 \approx 1 \times 10^{-12}$ cm^3 molecule^{-1} s^{-1}, $k_2 \approx 2 \times 10^{-12}$ cm^3 molecule^{-1} s^{-1} and $k_3 \approx 6 \times 10^{-13}$ cm^3 molecule^{-1} s^{-1} for the reactions of NO_3 with CH_3O_2, $C_2H_5O_2$ and CF_3O_2.

Atmospheric Chemistry of $CF_3CFHCF_2OCF_3$ and $CF_3CFHCF_2OCF_2H$: Reaction with Cl Atoms and OH Radicals, Degradation Mechanism, and Global Warming Potentials

T. J. Wallington[1], M. P. Hurley[1], M. P. Sulbaek Andersen[2], O.J. Nielsen[2]

[1] *Ford Motor Company, SRL 3083, P.O. 2053, Dearborn, Michigan, 48121 – 2053.*
[2] *University of Copenhagen, Universitetsparken 5, DK-2100 Copenhagen, Denmark*

FTIR smog chamber techniques were used to measure k($Cl+CF_3CFHCF_2OCF_3$) = (4.09±0.33) x 10^{-17}, k($OH+CF_3CFHCF_2OCF_3$) = (1.57±0.31) x 10^{-15}, k(Cl+ $CF_3CFHCF_2OCF_2H$) = (6.89±1.17) x 10^{-17}, and k(OH+ $CF_3CFHCF_2OCF_2H$) = (1.79±0.27) x 10^{-15} cm^3 $molecule^{-1}$ s^{-1}. The atmospheric lifetimes of $CF_3CFHCF_2OCF_3$ and $CF_3CFHCF_2OCF_3$ are 36 and 32 years, respectively. Chlorine atom initiated oxidation of $CF_3CFHCF_2OCF_3$ and $CF_3CFHCF_2OCF_3$ gives $CF_3C(O)F$ in molar yields of 82±5% and 96±5%, respectively. The 100 year time horizon global warming potentials of $CF_3CFHCF_2OCF_3$ and $CF_3CFHCF_2OCF_3$ relative to CF_3CFHCF_3 (HFC-227ea) are 1.24 and 1.29. All experiments were performed in 700 Torr of N_2/O_2 diluent at 296 K.

Laser Flash Photolysis Kinetics Study of the NO + O_3 Reaction

E.G. Estupinan,[1,2] J.M. Nicovich,[3] and P.H. Wine[1,3]

[1]*School of Earth & Atmos. Sci., Georgia Inst. of Technology, Atlanta, GA 30332-0340, USA*
[2] *Now at Combustion Chemistry Department, MS 9054, Combustion Research Facility, Sandia National Laboratories, Livermore, CA 94551-0969, USA*
[3] *School of Chem. & Biochem., Georgia Inst. of Technology Atlanta, GA 30332-0400, USA*

The reaction NO + $O_3 \rightarrow NO_2 + O_2$ (R1) is relatively easy to study in flow reactors. As a result, numerous studies of the kinetics of R1 were reported between 1964 and 1982, all of which employed flow tube techniques. Only one study of the kinetics of R1 has been reported since 1982 [Moonen et al., *J. Atmos. Chem.* **1998**, *29*, 299]. The value of k_{R1} at temperatures around 298 K is very well-established. However, there is considerable scatter in rate coefficients reported at temperatures typical of the lower stratosphere and, in fact, uncertainty in k_{R1} has been flagged as a major hindrance in quantitatively comparing measurements of lower stratospheric values of [NO_2] and j_{NO2} with model calculations of the same parameters [Del Negro et al., *J. Geophys. Res.* **1999**, *104*, 26687].

We have carried out the first flash photolysis study of the kinetics of R1. Our experimental approach employed NO as the excess reagent. O_3 was generated by 193 nm laser flash photolysis of $N_2O/N_2/O_2$/NO mixtures, and the temporal behavior of O_3 was monitored by time-resolved UV absorption spectroscopy at 254 ± 5 nm using a deuterium lamp as the probe light source. It was necessary to keep NO concentrations below 10^{16} per cm^3 in order to avoid interference from the NO + NO + O_2 reaction, thus limiting the range of pseudo-first order rate coefficients that could be measured to less than 30 s^{-1} at the lowest temperature investigated (210 K). However, this did not present a serious problem because O_3 loss in the absence of NO was dominated by (1) diffusion from the photolyzed region to fill the reactor (~1 s^{-1}) and (2) pump out from the reactor (~ 0.1 s^{-1}). At low temperatures (< 230 K), some interfering absorption from N_2O_4 and N_2O_3 was observed, but this interference could be corrected for quantitatively.

In agreement with several of the earlier studies, we observe non-Arrhenius behavior for R1. Our results over the temperature range 210 – 370 K are well-described using the following 3-parameter expression: $k_{R1}(T) = 1.6 \times 10^{-23} T^{3.85} \exp(-338/T)$ $cm^3 molec^{-1} s^{-1}$. We estimate the accuracy of the rate coefficients we have determined to be ±10% at T > 250 K, increasing to ±15% at T = 210 K. At temperatures typical of the lower stratosphere, we obtain rate coefficients that are a little faster than currently recommended by the NASA and IUPAC panels. It does not appear that our results will help to bring the field observations of [NO_2] and j_{NO2} reported by Del Negro et al. [*J. Geophys. Res.* **1999**, *104*, 26687] into agreement with model simulations, which suggests that the source of the difference may be a parameter other than k_{R1}.

A19

Negative-Ionization Mass Spectrometry Studies on the Reactions of Alkyl Peroxy Radicals with NO

Jia-Hua Xing, Yoko Nagai, Masayuki Kusuhara, and Akira Miyoshi

Department of Chemical System Engineering, Faculty of Engineering, The University of Tokyo, 7-3-1 Hongo, Bunkyo-ku, Tokyo, 113-8656, Japan

Organic peroxy radicals are important intermediates formed in the atmospheric degradation of hydrocarbons or in the low-temperature oxidation processes in combustion. In the troposphere, the title reactions are known to be a significant source of NO_2 leading to the formation of ozone:

$$ROO + NO \rightarrow RO + NO_2, \qquad (1)$$

$$NO_2 + O_2 \rightarrow NO + O_3.$$

In the present study a new method for kinetic measurements of peroxy radicals has been developed, in which real-time profiles of peroxy radicals are monitored by using a negative-ionization mass spectrometry coupled with laser-flash photolysis generation of reactant radicals. The rate constants for the gas-phase reaction of methyl- and ethylperoxy radicals with NO (1) have been studied at room temperature and 4-Torr total pressure. The alkyl peroxy radicals were generated by the recombination reactions of corresponding alkyl radicals with excess O_2, where alkyl radicals were prepared by laser photolysis of appropriate precursor molecules. The alkyl peroxy radicals are ionized by low-energy electron transfer from rare gas atoms in high Rydberg states. In this ionization technique, the target peroxy radicals can be detected at their parent mass numbers. The rate constants were determined to be: $k(CH_3O_2 + NO) = (9.9 \pm 1.5) \times 10^{-12}$ and $k(C_2H_5O_2 + NO) = (11.0 \pm 1.5) \times 10^{-12}$ cm^3 molecule^{-1} s^{-1} which are about a factor of 1.3 larger than the previous recommendations for the atmospheric modeling.

B19

Gas-phase Reaction of OH Radical with a Series of Linear Ketones: Kinetics and Temperature Dependence between 228 and 405 K

Elena Jiménez, Bernabé Ballesteros, Ernesto Martínez and José Albaladejo

Universidad de Castilla-La Mancha. Departamento de Química Física. Avda. Camilo José Cela, 10. 13071 Ciudad Real, Spain

Jose.Albaladejo@uclm.es

Ketones are emitted into the atmosphere from a variety of natural and anthropogenic sources. These organic compounds are also produced in the atmosphere during the oxidation of hydrocarbons such as alkanes and alkenes. The reaction with atmospheric radicals, such as OH, NO_3, and Cl atoms is expected to be the main loss process for these ketones in the troposphere.

In this work absolute rate coefficients for the reaction of OH (k_{OH}) with a series of linear ketones (2-butanone, 2-pentanone, 2-hexanone, and 2-heptanone) were determined at different temperatures (228-405 K) and pressures (50-600 Torr in Helium). Laser pulsed photolysis of gas-phase H_2O_2 was used to generate OH radicals and its laser induced fluorescence was employed to monitor OH concentration as a function of the reaction time. The measured rate coefficients were found to be pressure independent over the range studied. The temperature dependence of k_{OH} was different from 2-butanone and the rest of linear ketones studied. The rate coefficients for the OH + 2-butanone reaction shows an Arrhenius behaviour with a slightly positive temperature dependence (*i.e.*, k_{OH} increases when T increases). However, the temperature dependence for the reaction of OH with the rest of ketones studied here shows a markedly deviation from an Arrhenius behaviour over the temperature range studied. Furthermore, we observed the rate coefficients for OH + 2-pentanone, 2-hexanone, and 2-heptanone increased when temperature decreased for temperatures below 298 K.

The temperature dependence of the rate coefficient of the OH+2-butanone reaction has been previously measured by Wallington and Kurylo and LeCalvé *et al.* In contrast, the reaction of OH with higher ketones was performed only at room temperature (Wallington and Kurylo 1987, Atkinson 1988, Atkinson 2000). Thus, this work constitutes the first determination of the temperature dependence of the rate coefficients for the reaction of OH with 2-pentanone, 2-hexanone, and 2-heptanone. Our results will be compared when possible with previous studies. The temperature dependence of k_{OH} will be discussed in terms of the H-abstraction by OH radicals.

References

Wallington, T. J.; Kurylo, M. J. *J. Phys. Chem.* **1987**, *91*, 5050-5054.

Le Calve, S.; Hitier, D.; Le Bras, G.; Mellouki, A. *J. Phys. Chem. A,* **1998**, 102, 4579-4584.

Atkinson, R.; Aschmann, S. M. *J. Phys. Chem.* **1988**, 92, 4008-4008.

Atkinson, R.; Tuazon, E. C.; Aschmann, S. M. *Environ. Sci. Technol.* **2000**, 34, 623-631.

A20

Kinetic Studies on the Reactions of Hydroxyl Radicals with a Series of Alkoxy Esters

S. M. O'Donnell[1], H. W. Sidebottom[1], J. C. Wenger[2], A. Mellouki[3] and G. Le Bras[3]

[1] *Chemistry Department, University College Dublin, Dublin 4, Ireland*
[2] *Chemistry Department, University College Cork, Cork, Ireland*
[3] *Laboratoire de Combustion et Systèmes Réactifs, CNRS, 45071 Orléans, Cedex 2, France*

Gas-phase reaction with hydroxyl (OH) radicals is the principal, if not dominant, atmospheric fate of the vast majority of oxygenated VOCs. As a result there have been many kinetic studies of the reactions of hydroxyl radicals with monofunctional oxygenated compounds such as ethers, alcohols, ketones and esters. In contrast only a limited number of studies have been performed on the reactivity of oxygenated compounds bearing more than one functional group, with recent efforts focussing for example on diethers and hydroxyethers. However, little attention has been given to alkoxy esters, another important group of multifunctional oxygenated VOCs that are increasingly being used in many solvent applications. In addition, alkoxy esters are the major atmospheric oxidation products of diethers which are also employed as solvents and have great potential for use as fuel additives.

The aim of this work was to investigate the kinetics of hydroxyl radical reactions with a series of alkoxy esters of structure $RC(O)O(CH_2)_nOR'$, where R = H, CH_3, R′ = CH_3, C_2H_5 and n = 1, 2. Rate coefficients were determined at room temperature using the relative rate technique and over the temperature range 263-372 K using the absolute rate technique of pulsed laser photolysis-laser induced fluorescence. The kinetic data were used to derive Arrhenius expressions for the reactions and tropospheric lifetimes for the alkoxy esters. The rate coefficients will be discussed in terms of structure-activity relationships and compared to the values obtained for other oxygenated hydrocarbons.

B20

Kinetics of the OH radical reaction with amides

G. Solignac[1], A. Mellouki[1], G. Le Bras[1], I. Barnes[2]

[1] *LCSR-CNRS, 1C Avenue de la recherche scientifique 45071 Orléans cedex 02-France*
[2] *Bergische University Wuppertal,Fachbereich C - Physikalische Chemie, Gauss Strasse 20, D-42097 Wuppertal, Germany*

Reaction with OH radicals is a major sink for most of the organic pollutants in the atmosphere. Amides are widely used in industries as organic solvents. Up to now very few studies have been conducted on amides and the available structure activity relationships are based only on a few amines and no amides. The aim of this work was to measure the rate constants of the reactions of the OH radical with a series of amides and to investigate the mechanism. Three compounds have been investigated so far: N-methylformamide ($HC(O)NHCH_3$), N,N-dimethylformamide ($HC(O)N(CH_3)_2$) and N,N-dimethylacetamide ($CH_3C(O)N(CH_3)_2$). The experiments have been performed in a 480L glass photoreactor using in situ FTIR analysis. The data were obtained at room temperature (298 ± 2)K and atmospheric pressure using the relative rate method. The results will be presented and discussed in terms of structure-activity relationships and atmospheric impact of the studied amides.

A21

Photochemistry of formaldehyde

M.N.R. Ashfold, A.J. Orr-Ewing, F.D. Pope, D.E. Shallcross, C.A. Smith.

School of Chemistry, University of Bristol, Bristol BS8 1TS, UK
F.Pope@bristol.ac.uk

The HO_x family (OH and HO_2) is central to the photochemistry of the atmosphere. Recent measurement campaigns have revealed HO_x concentrations greater than predicted by current models. Formaldehyde is recognized as an important source of HO_x in the upper troposphere.

The photodissociation of formaldehyde by sunlight can occur through two distinct and competing channels:

$$H_2CO + h\nu \rightarrow H_2 + CO \qquad (\lambda<370\text{ nm})$$
$$H_2CO + h\nu \rightarrow HCO + H \qquad (\lambda<330\text{ nm})$$

Both the products from the second channel produce HO_x molecules after the reaction with O_2:

$$HCO + O_2 \rightarrow HO_2 + CO$$
$$H + O_2 \rightarrow HO_2$$

This project investigates the HO_x production due to the photochemistry of formaldehyde. To achieve this, high resolution absorption cross section data for formaldehyde and quantum yields for the production of HCO from formaldehyde are needed over the wavelength range and conditions of temperature and pressure appropriate to the upper troposphere. To measure formaldehyde's radical quantum yield the concentration of formaldehyde and its radical products are measured concurrently. The cavity ring down technique is used to monitor the relative production of HCO subsequent to the UV photolysis. Measurement of the formaldehyde concentration is achieved using multipass absorption spectroscopy. Due to absorption cross sections for HCO being unreported, this method only produces a relative radical quantum yield. Calibration of the relative yield to get an absolute yield is done using the technique of REsonant MultiPhoton Ionisation (REMPI). The comparison of the REMPI signal of a compound with a known quantum yield (e.g. HI) compared to formaldehyde's less than unity quantum yield signal will give the information necessary for the calibration.

The data produced will be introduced into atmospheric models to assess the importance of formaldehyde in the upper tropospheric region.

B21

A study of night-time chemistry of HO_x radicals in the Northern and Southern Hemisphere

R. Sommariva[1], Z. Fleming[2], D.E. Heard[1], J.D. Lee[3], P.S. Monks[2], M.J. Pilling[1], L. Whitehouse[1]

[1] *Department of Chemistry, University of Leeds, Leeds, UK*
[2] *Department of Chemistry, University of Leicester, Leicester, UK*
[3] *Department of Chemistry, University of York, York, UK*

Recent measurements by Laser Induced Fluorescence and PERCA during the NAMBLEX campaign (Mace Head, Ireland, July-September 2002) showed comparatively high concentrations of peroxy radicals (HO_2 and RO_2), during the night under unpolluted conditions, while OH was always below the instrumental detection limit.

A simple model, constrained to measured values of CO, CH_4, O_3, HCHO, NO_x, H_2O and temperature was used to study the night-time chemistry of HO_x during a case-study night (31st August – 1st September). Results were compared to a similar study for the night 15th – 16th February made during the SOAPEX-2 campaign in Cape Grim, Tasmania, January-February 1999.

The rates of production and destruction of the key species in the model were calculated to show the relative importance of the reactions driving the night-time chemistry at the two sites during those nights.

The analysis of the system was conducted by calculating the eigenvalues and the eigenvectors of the Jacobian matrix to study the lifetimes of the modes within the system and to investigate the coupling of the key species and the dynamics of the chemical system.

Isomerization of 1-Butoxy Radicals

M. Paulus and F. Zabel
Institut für Physikalische Chemie, Universität Stuttgart, Pfaffenwaldring 55, D-70569 Stuttgart; e-mail: f.zabel@ipc.uni-stuttgart.de

Alkoxy radicals are important reactive intermediates in the atmospheric degradation of volatile organic compounds. In the atmosphere, they undergo either unimolecular transformation (decomposition/isomerization, k_{uni}) or reaction with O_2 (k_{O2}):

(1a) thermal decomposition ($k_{uni} = k_{dis}$, → aldehyde/ketone + alkyl/H)
(1b) isomerization ($k_{uni} = k_{iso}$, → hydroxyaldehyde/hydroxyketone)
(2) reaction with O_2 (k_{O2}, → aldehyde/ketone + HO_2)

Depending on the ratio $k_{uni}/(k_{O2}\times[O_2])$, different products are formed with different effects on atmospheric chemistry. The 1-butoxy radical is a model compound for large alkoxy radicals where fast isomerization via a six-membered transition state is possible. If (1b) and (2) are the only important loss reactions of 1-butoxy the rate constant ratio k_{iso}/k_{O2} can be determined from the product yields of reaction channels (1b) and (2):

$$\frac{k_{uni}}{k_{O_2}} \approx \frac{k_{iso}}{k_{O_2}} = \frac{\Delta[\text{4-hydroxybutanal}]\times[O_2]}{\Delta[n\text{-butanal}]}$$

However, identification of 4-hydroxybutanal (Niki et al., 1981; Atkinson et al., 1996) was not very straightforward so far, and the temperature dependence of $k_{uni}/(k_{O2}\times[O_2])$ is not well established.

The main aim of this work is:

(i) to identify 4-hydroxybutanal as a product of reaction (1b);
(ii) to determine the ratio k_{iso}/k_{O2} for 1-butoxy as a function of temperature.

Experiments were performed in a temperature controlled photochemical reaction chamber from quartz (v = 209 L) on time scales from 10 to 1000 s and at temperatures between 282 and 311 K. 1-Butoxy radicals are prepared by stationary photolysis of mixtures of 1-iodobutane, O_2, NO, and N_2 at 254 nm. Reaction mixtures are analyzed *in situ* by long path (29 m) FT-IR spectrometry. The following results were obtained:

(i) The product IR spectra indicate the presence of a compound featuring both a carbonyl and an OH band. These bands were assigned to the expected product 4-hydroxybutanal. This product, however, was transformed, on a time scale of seconds, to the isomeric compound 2-hydroxytetrahydrofuran which was identified by its IR spectrum.

(ii) The product 4-hydroxybutyl nitrate was identified by its IR spectrum. Allowance was made for the formation of both 4-hydroxybutyl nitrate and 2-hydroxytetrahydrofuran in the evaluation of k_{iso}/k_{O2}.

(iii) Similar to our previous results on other alkoxy radicals, the measured ratio k_{iso}/k_{O2}, i.e. $(k_{iso}/k_{O2})_{eff}$, depends on the partial pressure of oxygen. This effect may originate from the formation of a certain fraction of chemically activated alkoxy radicals.

(iv) From the O_2 dependence of the measured $(k_{iso}/k_{O2})_{eff}$, k_{iso}/k_{O2} for a thermal system can be deduced. For 298 K and 200 mbar O_2, $(k_{iso}/k_{O2})_{eff}$ is equal to experimental values of Cox et al. (1987) where 1-butoxy was also obtained from 1-butylperoxy+NO (i.e. chemically activated), and k_{iso}/k_{O2} is equal to (i) an experimental value obtained using a thermal source of 1-butoxy and (ii) a value derived from an *ab-initio* result for k_{iso} from Somnitz and Zellner (2000) combined with k_{O2} from Atkinson (1997), both of which are applicable to thermal systems.

(v) Work on the temperature dependence of k_{iso}/k_{O2} is in progress.

Conclusions of this work are:

4-Hydroxybutanal is probably the major gas phase product of the isomerization of 1-butoxy radicals in the atmosphere. Either in the gas phase or on the surface and in the interior of aerosol droplets, however, 4-hydroxybutanal may be converted to 2-hydroxytetrahydrofuran. For atmospheric applications, chemical activation of the 1-butoxy radicals has possibly to be taken into account.

B22

Stereodynamics of the H+D_2 reaction: how the direction of the initial rotation does control the reactivity

J. Aldegunde and J. M. Alvariño
Departamento de Química Física, Facultad de Química, Universidad de Salamanca, 37009 Salamanca, Spain

M. P. de Miranda
School of Chemistry, University of Leeds, Leeds LS2 9JT, United Kingdom

F. J. Aoiz
Departamento de Química Física, Facultad de Química, Universidad Complutense 28040 Madrid, Spain

We have investigated the influence of D_2 rotational alignment on the dynamics of the H + $D_2(v = 0, j = 2) \rightarrow HD(v', j') + D$ reaction, considering two- and three-vector correlations (namely, $\boldsymbol{k}$-$\boldsymbol{j}$ and $\boldsymbol{k}$-$\boldsymbol{j}$-$\boldsymbol{k}'$, where $\boldsymbol{k}$ and $\boldsymbol{k}'$ are the reactant-approach and product-recoil directions, respectively).

The quantum and quasiclassical formalisms we have used are analogous to those previously employed in studies of product rotational polarisation, and is adequate for the analysis of the influence of reactant polarisation on both integral and differential reactive cross sections.

Quantum and quasiclassical data agreed very well, and showed that the product state distribution and differential cross sections can be controlled to a considerable extent by varying the direction chosen for the alignment of the D_2 molecule.

J.A. thanks the Ministry of Science and Technology of Spain (BQU2002-04462-C02-01) for financial support.

A23

Photodissociation of ozone in the Hartley bands: conical intersections, potential energy surfaces and dynamics.

Ezinvi Baloitcha and Gabriel Balint-Kurti
University of Bristol, U.K.

We present the results of extensive ab initio multi-reference CI calculations for the singlet even symmetry (1A') low lying potential energy surfaces of Ozone. We show, for the first time, that there is at least one, non-symmetry related conical intersection between the excited state surfaces which will play an important role in the photodissociation dynamics giving rise to of the Hartley bands. The transition dipole moments and the diabatic coupling potential energies between the diabatic surfaces are also presented. The electronic natures of the wavefunctions in the vicinity of crossings are discussed. Absorption total cross section corresponding to Hartley bands are calculated.

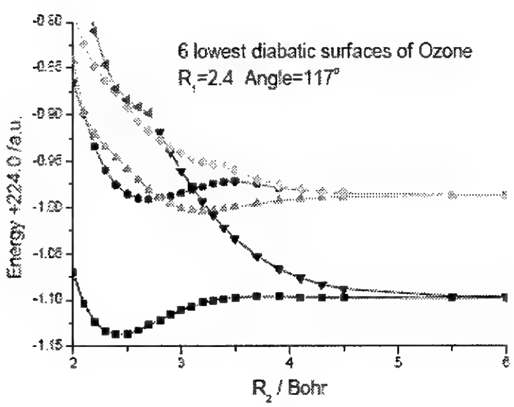

Cut through the lowest 6 diabatic potential energy surfaces.

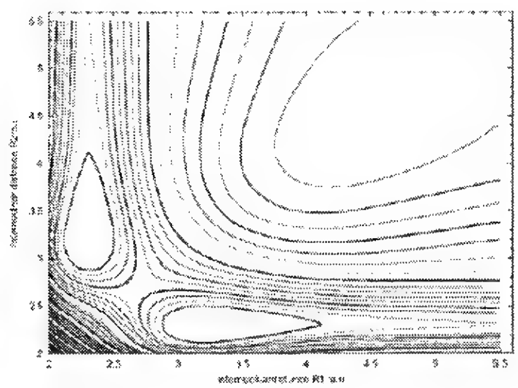

Two dimension contour plot of the B^1A' second diabatic excited state for the bound angle of $\theta=117^o$.

B23

Ion imaging studies of photon-initiated bimolecular reactions

Mark J. Bass, Mark Brouard, Raluca Cireasa, and Claire Vallance

The Physical and Theoretical Chemistry Laboratory, Department of Chemistry, University of Oxford, South Parks Road, Oxford OX1 3QZ, United Kingdom

The photon-initiated reaction technique [1], coupled with state resolved product detection using resonantly enhanced multiphoton ionisation (REMPI) and velocity-map ion-imaging, is used to study of the bimolecular reaction

$$Cl + CH_4 \rightarrow HCl + CH_3$$

The experiments were performed in a coexpansion of molecular chlorine and methane, with the atomic Cl reactants generated by polarized laser photodissociation of Cl_2 at 308nm. The methyl radical products were detected using (2+1) REMPI *via* the 0^0_0 vibronic band. In agreement with previous work by Kandel and Zare [2], a sensible fit to the data could only be achieved by assuming that a significant fraction of the product signal arises from reaction of Cl with vibrationally excited methane reactants, assumed to be thermally populated in low frequency modes. Differential cross-sections are presented for the reactions of Cl with CH_4, CD_4 and CH_3D, involving both ground state and bend- or torsion-excited reactants. Cross-section enhancements associated with excitation of these modes are also estimated. The new data will be compared with previous experimental and theoretical work on this and related reactions.

[1] M. Brouard, P. O'Keeffe, C. Vallance, *J. Phys. Chem. A*, **106**, 3629, (2002).
[2] S.A. Kandel and R.N. Zare, *J. Chem. Phys.* **109**, 9719 (1998).

* email address: mark.brouard@chemistry.ox.ac.uk

A24

The reactions $H + H_2O$ and $H + D_2O$: Stereodynamics and new values for the integral cross-sections

M. Brouard, S. Marinakis, L. Rubio and C. Vallance

The Physical and Theoretical Chemistry Laboratory, Department of Chemistry, University of Oxford, South Parks Road, Oxford OX1 3QZ, UK.

The reaction $H+H_2O$ and its isotopically substituted analogues serves as a prototype polyatomic reaction for experimental and theoretical research in the field of gas-phase reaction dynamics [1, 2]. The aim of this study is to probe the dependence of the scattering dynamics on product $OD(^2\Pi_\Omega)$ spin-orbit state. In the past, Doppler-resolved LIF spectroscopy of $OD(^2\Pi_{1/2},v'=0,N'=1,A')$ products [3,4], has been employed to determine the product angular and kinetic energy release distributions. In order to reveal the dependence of the scattering dynamics on product spin-orbit state, the present study probes the $OD(^2\Pi_{3/2},v'=0,N'=1,A')$ products at 2.48 eV. The angular distributions show scattering over a wide range of angles, with a preference towards the forward direction. The kinetic energy release distributions indicate that the HD co-products are born with significantly more internal excitation than at 1.43 eV. Both angular and kinetic energy release distributions from this study show almost identical scattering behaviour as their spin-orbit excited $OD(^2\Pi_{1/2})$ counterpart. In this study the product spin-orbit effects in the $H+D_2O$ reaction are discussed with reference to the $H+CO_2$ reaction and simple models are invoked to explain the different behaviours. The results are also compared with QCT calculations employing the most recently developed PES. For the reaction $H+H_2O \rightarrow OH+H_2$ at 1.21 eV, the OH rotational populations in both spin-orbit states are presented and for low rotational levels are shown to deviate from the statistical limit.

In addition, absolute values of the cross-section for the $H+D_2O$ abstraction reaction have been determined experimentally at mean collision energies of 1.83 eV and 2.48 eV. The data support the recently reported [2] value for the $H+H_2O$ cross-section at 2.46 eV which was considerably lower than earlier measurements and reveal that previous experiments [5] also overestimated the cross-section for the $H+D_2O$ isotopic reaction. The new measurements agree to within a factor of three with theoretical calculations. The kinetic isotope effect for the reaction, and its dependence on the collision energy, is also discussed.

References:

1) D. H. Zhang, M. A. Collins, S. – Y. Lee, Science 290, 961-963 (2000).
2) M. Brouard *et al.*, Phys. Rev. Lett. 90, 093201 (2003).
3) M. Brouard, I. Burak, D. M. Joseph, G. A. J. Markillie, D. Minayev, P. O' Keeffe, and C. Vallance, J. Chem. Phys. 114, 6690 (2001).
4) M. Brouard, *et al.*, J. Chem. Phys. 118, 1162 (2003).
5) S. Koppe *et al.*, Can. J. Chem. 72, 615-624 (1994).

email address: mark.brouard@chemistry.ox.ac.uk

Dynamics of HCCO and CH_2 Radical Formation from the Reaction $O(^3P)$ + C_2H_2 in Crossed Beams using *Soft* Electron Impact Ionization for Product Detection

G. Capozza, F. Leonori, E. Segoloni, G. G. Volpi, and P. Casavecchia

Dipartimento di Chimica, Università di Perugia, 06123 Perugia, Italy

We have recently introduced, for the first time, the concept of *"soft"* electron-impact (EI) ionization by tunable electrons (7-100 eV) for product detection in crossed molecular beams (CMB) reactive scattering experiments with mass spectrometric detection [1,2]. Analogously to when using *"soft"* photo-ionization (PI) by tunable VUV synchrotron radiation [3], by tuning the electron energy below the threshold of the dissociative ionization of interfering species, one can often eliminate background signal that would normally prohibit experiments using classic, i.e., "*hard*" (with 60-200 eV electrons), EI ionization (the latter is plagued by the well known problem of the "dissociative ionization", which leads to extensive fragmentation). Soft EI ionization is crucial for disentangling the dynamics of complex polyatomic reactions. In addition, because absolute EI ionization cross sections can be reliably estimated, branching ratios can also be determined.

The first reaction to the investigation of we have applied this approach is $O(^3P) + C_2H_2$, of considerable importance in combustion chemistry. Two main pathways are energetically open at thermal energies:

$$O(^3P) + C_2H_2 \rightarrow HCCO + H \qquad \Delta H^0_0 = -19.5 \text{ kcal/mol} \qquad (1a)$$

$$\rightarrow CH_2 + CO \qquad \Delta H^0_0 = -47.1 \text{ kcal/mol} \qquad (1b)$$

We have studied the reaction at two collision energies, E_c=9.5 kca/mol and E_c=13.1 kcal/mol (the latter was obtained by crossing the two same reactant beams at 135° rather than at 90°, which affords a higher angular and time-of-flight (TOF) resolution). This reaction was previously studied in CMB at E_c= 6 kcal/mol [4] using ^{18}O to be able to detect $C^{18}O$ in TOF measurements. In our experiments, by using 17 eV electrons for product ionization we have been able to detect CH_2 radicals from channel *1b* with nearly no background and, most important, without contribution from interfering signals (arising from C_2H_2, HCCO, and N_2 fragmentation). From product angular and TOF distributions in the lab, product angular and translational energy distributions in the center-of-mass were derived for both channels *1a* and *1b*. The branching ratio was also derived [1] and found to be in excellent agreement with the most recent, accurate kinetic determinations. Information on the ionization threshold of HCCO (ketenyl) with a well-defined internal energy content was obtained by measuring its EI efficiency curve down to 9 eV.

References

[1] - G. Capozza, E. Segoloni, F. Leonori, G. G. Volpi, and P. Casavecchia, *J. Chem. Phys.* **120**, 4557 (2004).

[2] - P. Casavecchia, G. Capozza, and E. Segoloni, in "Modern Trends in Chemical Reaction Dynamics", *Advanced Series in Physical Chemistry*, Ed. by K. Liu and X. Yang (World Scientific, Singapore, 2004), in press.

[3] - X. Yang, J. Lin, Y.T. Lee, D.A. Blank, A.G. Suits, A.M. Wodtke, *Rev. Sci. Instrum.* **68**, 3317 (1997).

[4] - A.M. Schmoltner, P.M. Chu, and Y.T. Lee, *J. Chem. Phys.* **91**, 5365 (1989).

A25

The Dynamics of Prototype *Insertion* Reactions: Crossed Beam Experiments versus Quantum and Quasiclassical Trajectory Scattering Calculations on *Ab Initio* Potential Energy Surfaces for $C(^1D) + H_2$ and $N(^2D) + H_2$

N. Balucani,[1] G. Capozza,[1] E. Segoloni,[1] L. Cartechini,[1] R. Bobbenkamp,[1] P. Casavecchia[1]
L. Bañares,[2] F. J. Aoiz,[2] P. Honvault,[3] B. Bussery-Honvault,[3] J.-M. Launay[3]

[1]*Dipartimento di Chimica, Università di Perugia, 06123 Perugia, Italy*
[2]*Departamento de Química Física, Universidad Complutense, E-28040 Madrid, Spain*
[3]*PALMS/SIMPA-UMR 6627 du CNRS ,Université de Rennes I, 35042 Rennes, France*

In order to deepen our understanding of the dynamics of *insertion* reactions [1,2], we have recently extended our crossed beam investigations beyond $O(^1D)+H_2$ to two other prototypical reactions, $N(^2D)+H_2$ and $C(^1D)+H_2$, which occur on a PES with a deep well associated with the strongly bound species NH_2 and CH_2, respectively. We exploit the capability of generating continuous supersonic beams of $N(^2D)$ and $C(^1D)$ atoms [1,2]. We have studied $C(^1D)+H_2$ at two collision energies, E_c=1.86 and 3.8 kcal/mol, and the isotopic variant $C(^1D)+D_2$ at E_c=3.6 kcal/mol by measuring product angular and velocity distributions in crossed beam experiments with mass spectrometric detection and time-of-flight analysis. The results at E_c=1.86 kcal/mol, which were previously compared with statistical predictions [2], have been compared with exact quantum-mechanical (QM) as well as quasiclassical trajectory (QCT) scattering calculations carried on a new *ab initio* PES [3]. For the higher E_c of 3.8 kcal/mol and for $C(^1D)+D_2$ the experimental results have been compared with the results of QCT calculations.

Following on studies of the isotopic variant $N(^2D)+D_2$ at E_c=15.9 and 21.3 kJ/mol, and comparisons with QCT calculations on an accurate *ab initio* ground state $1^2A''$ PES [4], we have investigated the reaction $N(^2D) + H_2(j=0\text{-}3) \rightarrow NH + H$, at E_c=15.9 kJ/mol and compared the results with those of QM and QCT calculations. The good agreement between QM predictions and experiment assess the quality of the *ab initio* ground state PES. Small, but significant discrepancies between QCT and QM calculations suggest the occurrence of quantum effects - tunneling through the combined potential and centrifugal barrier, similarly to what seen for abstraction reactions [6].

Acknowledgments: R. Bobbenkamp acknowledges a fellowships within the EC Research Training Network REACTION DYNAMICS (contract HPRN-CT-1999-00007).

References

[1] P. Casavecchia, N. Balucani, G. G. Volpi, *Annu. Rev. Phys. Chem.* **50**, 347 (1999); P. Casavecchia, *Rep. Prog. Phys.* **63**, 355 (2000); K. Liu, *Annu. Rev. Phys. Chem.* **52**, 139 (2001); X. Liu, J. J. Lin, S. Harich, G. C. Schatz, X. Yang, *Science* **289**, 1536 (2000).

[2] Bergeat, L. Cartechini, N. Balucani, G. Capozza, L.F. Phillips, P. Casavecchia, G.G. Volpi, L. Bonnet, J.-C. Rayez, *Chem. Phys. Lett.* **327**, 197 (2000).

[3] B. Bussery-Honvault, P. Honvault and J. M. Launay, *J. Chem. Phys.* **115**, 10701 (2001).

[4] N. Balucani, M. Alagia, L. Cartechini, P. Casavecchia, G.G. Volpi, L.A. Pederson. G.C. Schatz, *J. Phys. Chem. A* **105**, 2414 (2001).

[5] P. Honvault and J. M. Launay, *J. Chem. Phys.* **111**, 6665 (1999); *ibid.* **114**, 1057 (2001).

[6] N. Balucani, L. Cartechini, G. Capozza, E. Segoloni, P. Casavecchia, G. G. Volpi, F. J. Aoiz, L. Banares, P. Honvault, J.-M. Launay, *Phys. Rev. Letters* **89**, 013201-1 (2002); and in preparation.

B25

Crossed molecular beam studies of *radical-radical* reactions: $O(^3P) + C_3H_5$ (allyl)

G. Capozza, F. Leonori, E. Segoloni, N. Balucani, D. Stranges*, G. G. Volpi, and P. Casavecchia

Dipartimento di Chimica, Università di Perugia, 06123 Perugia, Italy

** Dipartimento di Chimica, Universita` di Roma "La Sapienza", Roma, Italy*

The Crossed Molecular Beams (CMB) scattering technique with "universal" electron-impact (EI) mass-spectrometric detection and time-of-flight (TOF) analysis has been central in the development of our understanding of reaction dynamics [1]. While reactive differential cross sections (DCSs) have been measured using this technique for a great variety of atom (radical) + molecule reactions over the past 40 years [1], very little has been done on radical-radical reactions. This is mainly due to the difficulty of generating beams of two radical species of sufficient intensity to carry out angular and velocity distribution measurements. We record only an earlier study in 1997 by Lee's group [2] using the CMB method, aimed at determining DCSs for a radical-radical reaction: $C(^3P)$ + propargyl (C_3H_3) was investigated using a pulsed supersonic $C(^3P)$ atom beam obtained by laser ablation of graphite and a pulsed supersonic beam of propargyl radicals obtained by laser photolysis of propargyl bromide. From TOF measurements at a few selected angles, the lab angular distribution of the C_4H_2 product was obtained and the center-of-mass DCS derived. There are also a few reports on dynamical studies of radical-radical reactions in crossed beams by using LIF detection. In 1991 Dagdigian and coworkers [3] reported OD product rovibrational distributions for $O(^3P)+ND_2$ in pioneering crossed beam work by using a MW generated $O(^3P)$ beam and a pulsed ND_2 beam obtained from laser photolysis of ND_3. Very recently, Choi and coworkers [4] reported OH product rovibrational distributions from the reactions $O(^3P)$+propargyl (C_3H_3) and $O(^3P)$+allyl (C_3H_5) in unskimmed pulsed jet experiments by generating the $O(^3P)$ beam by pulsed laser photolysis of NO_2 and the alkyl radical by pulsed "flash pyrolysis" [5] of suitable alkyl halide precursors.

In order to investigate the dynamics of radical-radical reactions using the CMB technique with "continuous" mass spectrometric detection it is desirable to use "continuous" supersonic beams of the radical species, so that one can measure readily the product angular distributions by modulating one of the two beams for background subtraction. Then, from also product TOF distribution measurements, one can derive the double reactive DCS in the center-of-mass system. In our laboratory we are generating since a number of years "continuous" supersonic beams of a variety of simple radicals [$O(^3P,^1D)$, $N(^4S,^2D)$, $C(^3P,^1D)$, $Cl(^2P)$, $OH(^2\Pi)$, and $CN(^2\Sigma^+)$] by using a high-pressure radio-frequency discharge quartz nozzle beam source [1]. Very recently, we have also developed a radical source, based on the "flash pyrolysis" in a SiC nozzle of a suitable precursor, for generating "continuous" supersonic beams of alkyl radicals (CH_3, C_2H_5, C_3H_3, C_3H_5, etc.). The availability of these sources for producing "continuous" supersonic beams of a variety of radical species, coupled with a sensitive CMB apparatus exploiting the "*soft*" electron impact ionization for product detection [6], is permitting us to undertake the investigation of the dynamics of a variety of radical-radical reactions.

Here we report on the first measurements of product angular and velocity distributions for the radical-radical reaction $O(^3P)$ + allyl (C_3H_5), of great relevance in combustion chemistry.

References

[1] P. Casavecchia, *Rep. Prog. Phys.* **63**, 355 (2000), and references therein.
[2] R. I. Kaiser, W. Sun, A. G. Suits, and Y. T. Lee, *J. Chem. Phys.* **107**, 8713 (1997).
[3] D. Patel-Misra, D. G. Sauder, and P. J. Dagdigian, *J. Chem. Phys.* **95**, 955 (1991).
[4] S. -K. Joo, L.-K. Kwon, H. Lee, and J.-H. Choi, *J. Chem. Phys.* **120**, 7976 (2004); ibid. **119**, 9337 (2003).
[5] D. W. Kohn, H. Clauberg, and P. Chen, *Rev. Sci. Instrum.* **63**, 4003 (1992).
[6] G. Capozza, E. Segoloni, F. Leonori, G. G. Volpi, P. Casavecchia, *J. Chem. Phys.* **120**, 4557 (2004).

A26

Ab Initio calculation of the first absorption band of N_2O and dynamical prediction of diffuse vibrational structures

Mohammad Noh Daud, Alex Brown and Gabriel G. Balint-Kurti

Centre for Computational Chemistry, University of Bristol, Bristol BS8 1TS, U.K.

The ultraviolet absorption spectrum of N_2O in the range 160nm to 220nm with a maximum near 182 nm exhibits a broad gaussian-shaped continuum with a number of diffuse structures. The diffuse structures are likely to be due to predissociation arising from some avoided crossing of upper excited states. However, experimental studies of photodissociation of N_2O by REMPI spectroscopy of N_2, Doppler spectroscopy of $O(^1D_2)$, and 2D ion imaging of $O(^1D_2)$ have not clearly revealed the non-adiabatic dissociation pathway. In an effort to understand photodissociation of N_2O especially in the first absorption band we have undertaken an improved *ab initio* study of the adiabatic potential energy surfaces together with their associated transition dipole moments. We present the five lowest adiabatic surfaces and discuss the role of curve crossings in the photodissociation. Of particular interest is the location of the crossing point of the $2^1A'$ and $3^1A'$ states in the collinear geometry. The diabatic potential energy surfaces corresponding to the two lowest excited $^1A'$ electronic states are also presented. In future work the new surfaces will be used to carry out time-dependent quantum calculations of the photodissociation dynamics of N_2O.

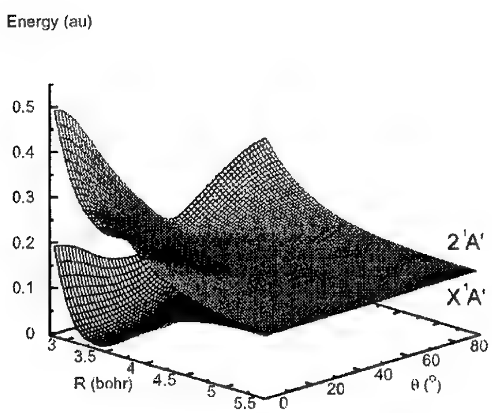

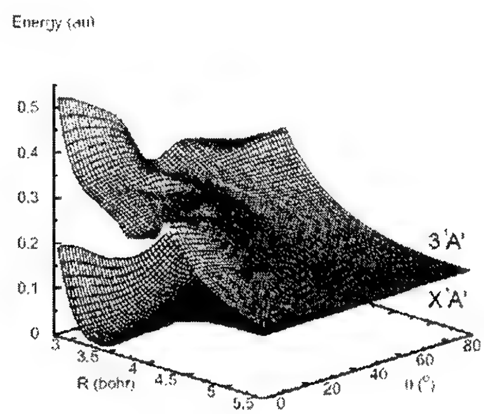

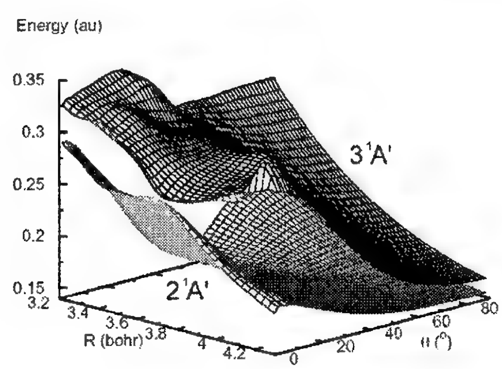

Optical Triple-Resonance Study of Non-Adiabatic Processes

R.J.Donovan, T.Ridley, K.P.Lawley and A.M.Sjodin

School of Chemistry, University of Edinburgh, West Mains Rd., Edinburgh. EH9 3JJ

Coupling in the near-adiabatic region between Rydberg and charge-transfer (ion-pair) states has been studied extensively in diatomic molecules (eg. double minima and shelf-states in H_2 and Na_2). However, relatively little is known about the fundamental aspects of similar couplings in polyatomic molecules, although it is even more commonplace, due to the increased number of degrees of freedom and the higher density of states. Indeed, it is this increased complexity that hinders the detailed study of polyatomic systems and makes the interpretation of their spectra extremely challenging. An alternative approach to gaining a fundamental understanding of non-adiabatic processes, in systems with a high density of states, is to explore regions where the density of states is high in diatomic molecules. One such region is just below the dissociation threshold for free ion-pair formation,where the density of vibrational states approaches infinity.

We have recently shown[1] that all of the observed Rydberg states, above the lowest charge-transfer dissociation limit of I_2, are coupled to continua producing free-ion-pairs, i.e.

$$X_2 + h\nu \rightarrow X_2^* \text{ (Ry)} \rightarrow X^+ + X^-$$

Just below the free ion-pair dissociation limit, long-lived (ca 2 μs) states are observed which undergo dissociation when a delayed pulse electric field is applied. It was suggested that these states are accessed through coupled Rydberg/ion-pair, *doorway*, states. These excited doorway states evolve into highly extended charge transfer states(v~1000) which are directly analogous to zero kinetic energy (ZEKE) Rydberg states and they are thus referred to as zero ion kinetic energy (ZIKE) states.[2]

We are now engaged in work to identify the Rydberg states of I_2 that act as ZIKE doorway states and we have used *optical triple-resonance* (OTR), employing three independently tunable dye lasers, to approach the ZIKE region from lower energies, where well defined Rydberg series are observed. We have observed long vibrational progressions in two Rydberg states and a region where strong Rydberg ion-pair mixing is evident. An analysis of these spectra is currently in progress.

1. K.P.Lawley, A.C.Flexen, R.J.Maier, A.Manck, T.Ridley and R.J.Donovan, Phys. Chem. Chem. Phys.(2002),**4,** 1398.
2. T.Ridley, M.de Vries, K.P.Lawley, S.Wang and R.J.Donovan, J. Chem. Phys. (2002), **117**, 7117.

A27

Vibrational Excitation of the O_2 Reagent in the Reaction $H + O_2 \Leftrightarrow OH + O$

Ronald J. Duchovic and Marla A. Parker[a]

Department of Chemistry, Indiana University Purdue University Fort Wayne, Fort Wayne IN 46805-1499

Quasi-classical trajectories have been computed on the Melius-Blint (MB) Potential Energy Surface (PES) and on the Double Many-Body Expansion (DMBE) IV PES of Varandas *et al.* describing the $H + O_2 \Leftrightarrow OH + O$ reaction with the non-rotating (J = 0) O_2 reagent vibrationally excited to levels v = 6, 7, 8, 9, 10 at four temperatures: 1000 K, 2000 K, 3000 K, and 4000 K. The vibrational energy levels were selected using a semi-classical Einstein-Brillouin-Keller (EBK) quantization procedure while the relative translational energy was sampled from a Boltzmann distribution. The rate coefficient for the formation of the OH + O products is seen to increase monotonically with quantum number and nearly monotonically with temperature. On the MB PES, at T = 1000 K, the total rate coefficient increases by a factor of 5.2 as the initial vibrational quantum number of the O_2 diatom increases from $v = 6$ to $v = 10$. For T = 2000 K, this factor drops to 3.3, to 2.9 for T = 3000 K, and to 2.5 for T = 4000 K. On the DMBE IV PES, at T = 1000 K the total rate coefficient increases by a factor of 4.1 as the initial vibrational quantum number of the O_2 diatom increases from $v = 6$ to $v = 10$. For T = 2000 K, this factor drops to 3.5, to 2.1 for T = 3000 K, and to 2.0 for T = 4000 K. The less-direct group of trajectories is sensitive to the initial O_2 vibrational excitation in several different temperature ranges, apparently retaining the effect of reagent vibrational excitation. The more-direct group of trajectories does not exhibit this behavior. Reagent vibrational excitation does not increase the total rate coefficients for the title reaction more than the increase due to a simple temperature increase. The simple expectation that the more-direct trajectories would be less-likely to violate the Zero-Point Energy (ZPE) constraint is not supported by this study on both the MB PES and the DMBE IV PES. The less-direct and more-direct groups of trajectories differ in their contribution to the rate coefficient for the title reaction. In particular, at T = 4000 K, the two PESs used in this work differ dramatically in the roles of the less-direct and more-direct trajectories, suggesting different effects of the deep HO_2 potential energy well on the two surfaces. This work utilizes the recently introduced PES Library, POTLIB 2001, that made the comparisons between the two PESs discussed in this work possible in a very straightforward way.

[a]Student Research Assistant, Department of Chemistry, Indiana University Purdue University Fort Wayne, Fort Wayne IN 46805-1499

B27

The photodissociation of the t-butyl radical, C_4H_9

M. Zierhut, W.Roth, and I. Fischer

Institute of Physical Chemistry, University of Wuerzburg, Am Hubland, D-97074 Wuerzburg

The dissociation dynamics and kinetics of alkyl radicals is of considerable importance for the combustion community. We report the observation of the kinetics and dynamics in the photodissociation of the t-butyl radical, C_4H_9, upon excitation in the 3s Rydberg state around 330 nm, and the 3p state at 266 nm. The radicals are formed by pyrolysis of Azobutan, t-C_4H_9-NN-t-C_4H_9, and studied under isolated conditions in a molecular beam. At all wavelength investigated t-butyl loses a hydrogen atom, which is detected by [1+1'] photoionisation, leading to the formation of iso-butene, C_4H_8. H-loss at excitation wavelengths above 330 nm is described reasonably well by RRKM theory. Interestingly the dissociation rate slows down significantly at wavelengths shorter than 330 nm and the width of the H-atom Doppler profiles increases. Possible explanations as well as implications for the photochemistry and photophysics of alkyl radicals in general will be discussed.

A28

Photodissociation of O_2 in the Schumann-Runge band into spin-orbit substates

Timo Jeranko and Gabriel Balint-Kurti

Centre for Computational Chemistry, University of Bristol

O_2 photodissociation is a key atmospheric reaction. The oxygen molecule has been studied for several decades, yet the details of its photodissociation are not yet fully understood. Two transitions occur in the atmosphere, the weak Herzberg band and the strong Schumann-Runge band. Schumann-Runge transitions are responsible for formation of $O(^1D)$, the first excited atomic state possessing a different atmospheric chemistry to the main ground state product $O(^3P)$. A large number of avoided crossings characterises the Schumann-Runge transition.

The research aim is the accurate prediction of branching ratios into the $O(^1D)$ and $O(^3P)$ states as well as their spin-orbit substates using ab initio methods. Potential energy curves are obtained ab initio from variational calculations. State averaged complete active space self consistent field (CASSCF) calculations using aug-cc-pV5Z basis sets are performed to obtain accurate orbitals. Multireference configuration interaction (MRCI+Q) calculations using a 10 orbital active space then yield accurate Born-Oppenheimer potentials and properties such as transition dipole moments and spin-orbit matrix elements. A small empirical correction is applied to match the correct long-range spin-orbit limits.

The ground state wave function is computed from an accurate ground state potential by means of the Fourier Grid Hamiltonian method. Basis set extrapolation to the complete basis set limit yields vibrational energy spacings for the fundamental within 3 cm^{-1} of experimental values. Multiplication by a computed transition dipole moments for each state produces the initial excited state wave packets. These are then propagated in time using the time-dependent Schrodinger equation. Cross sections are obtained from Fourier transforms of the wavepackets in the long-range region[1].

Research has focused on the more accurate calculation of transition dipole moments (they converge more slowly than energies), convergence problems around intersections, better understanding of potentials in the long range, and adaptation of the propagation code for a many-state problem.

Future work will concentrate on accurate prediction of anisotropic quantities such as alignment and polarisation parameters.

[1] G.G. Balint-Kurti, Adv. Chem. Phys. **128**, 249 (2003)

Photodissociation and -ionisation of two-photon aligned states of HCl and HBr

Sergei Manzhos, Constantin Romanescu, and Hans-Peter Loock
Dept of Chemistry, Queen's University, Kingston, ON, K7L 3N6, Canada

Jonathan Underwood
Department of Physics and Astronomy, The Open University, Walton Hall, Milton Keynes, UK

The velocity-map imaging technique was used to record photoelectron and photofragment ion images of HCl and HBr following two-photon excitation of different $^1\Sigma^+(0^+)$ states and subsequent ionization/dissociation. The images allowed us to determine the branching ratios between autoionization and dissociation channels for the different intermediate states. These branching ratios can be explained quantitatively on the basis of intermediate state electron configurations, since the configuration largely prohibits direct ionization in a one-electron process, and competition between autoionization and dissociation into H* (n = 2) + Cl and H + Cl* (4s, 4p, 3d) is observed.

We also were able to calculate the angular distribution of the H-atom photofragment following multiphoton excitation of HCl and HBr. Here, the two-photon intermediate state was the rotationally selected $E^1\Sigma^+(0^+)$-state for HCl or $H^1\Sigma^+(0^+)$-state for HBr. The angular distributions of the resultant photoelectrons and photoions depend on the nature of all intermediate states and are an effective probe of the selection-rule induced alignment on the two photon level which is understood using the density matrix formalism and angular momentum theory. Consequently, the model can be used for pathway identification - in particular, when different virtual intermediate states compete in a two photon excitation.

A29

Theoretical Study of Structures and Relative Stabilities of 4-Methylphenol Water Complexes

Florent Louis

Physico-Chimie des Processus de Combustion et de l'Atmosphère (PC2A), UMR CNRS 8522, Bât. C11, Université des Sciences et Technologies de Lille, 59655 Villeneuve d'Ascq, France

The study of hydrogen bonding between water molecules and organic systems is important to understand the solvation of these systems and therefore their chemical reactivity in aqueous solution. Some relatively simple molecular structures can be considered as model systems in this type of studies. One of them is the 4-methylphenol. Uptake measurements of phenolic compounds (Louis, 2004) were performed to provide experimental values for a theoretical approach of its incorporation into a water droplet.

The aim of the present work is to provide an extensive theoretical study of the structures and relative stabilities of the hydrogen-bonded 4-methylphenol-water complexes. We therefore chose 4-methylphenol surrounded by n water molecules in various geometrical arrangements. The hydrogen-bonded complexes have been investigated with semi-empirical methodology and density functional theory methods combined using different basis sets. The first step in our study was to determine the most stable structures of hydrogen-bonded 4-methyl-phenol water complexes, secondly to study the nature of the hydrogen bonding in these complexes, and finally to estimate their thermochemical properties taking into account basis set superposition error, and zero-point energy corrections. Results will be presented and discussed.

Reference:

Louis F., Leyssens G., Sawerysyn J.-P., Feigenbrugel V., Le Calvé S., and Mirabel P. "Uptake Measurements of Phenolic Compounds by Water Droplets and Determination of their Henry's Law Constants Over the Temperature Range 278-303 K: Implications for Tropospheric Multiphase Chemistry", 18th Symposium on Gas Kinetics, Bristol, August 2004.

B29

Quasiclassical trajectory study of the collision-induced dissociation of CH_3SH^+ + Ar

Emilio Martínez-Núñez and Saulo A. Vázquez
Departamento de Química Física, Universidad de Santiago de Compostela, 15706 Santiago de Compostela, Spain

Jorge M. C. Marques
Departamento de Química, Universidade de Coimbra, 3004-535 Coimbra, Portugal

Quasiclassical trajectory calculations were carried out to study the dynamics of energy transfer and collision-induced dissociation (CID) of CH_3SH^+ + Ar at collision energies ranging from 4.34 to 34.7 eV. The relative abundances calculated for the most relevant product ions are found to be in good agreement with experiment, except for the lowest energies investigated. In general, the dissociation to form CH_3^+ + SH is the dominant channel, even though it is not among the energetically favored reaction pathways. The results corroborate that this selective dissociation observed upon collisional activation arises from a more efficient translational to vibrational energy transfer for the low-frequency C–S stretching mode than for the high-frequency C–H stretching modes, together with weak couplings between the low- and high-frequency modes of vibration. The calculations suggest that CID takes place preferentially by a direct CH_3^+ + SH detachment, and more efficiently when the Ar-atom collides with the methyl group-side of CH_3SH^+.

A30

Time-dependent and time-independent stereodynamics of the $H+D_2$ reaction

Robert A. Pettipher and Marcelo P. de Miranda

Department of Chemistry, University of Leeds, Leeds LS2 9JT, United Kingdom

Assuming it to be mediated by a collinear collision complex, we have developed a simple model for the stereodynamics of the $H + D_2$ reaction. Consideration of our model shows that the polarization moment that gives most insight into the reaction stereodynamics is a measurable alignment moment that up to now has received little attention. It allows one to distinguish near-side from far-side mechanisms, and also gives insight into the relative contributions of the total angular momentum and bending vibration of the collinear complex to the reaction (stereo)dynamics. The validity of the model is examined by comparison of its predictions to results from exact timedependent and time-independent quantum calculations either with or without use of the near-side/far-side decomposition of the scattering amplitude suggested by Connor and coworkers.[1]

1. A. J. Dobbyn, P. McCabe, J. N. L. Connor and J. F. Castillo, PCCP 6 (1999) 1115.

B30

Polarization Effects in Laser Quantum Control of Chemical Processes

Qinghua Ren , Gabriel G. Balint-Kurti, Fred R. Manby
School of Chemistry, University of Bristol, Bristol BS8 1TS, UK

Herschel Rabitz, Tak-san Ho and Max Artamonov
Princeton University

A novel method for incorporating polarization effects of the strong electric field into the optimal control calculations is presented. A Born-Oppenheimer like separation, which we refer to as the electric Born-Oppenheimer approximation, is introduced in which both the nuclear motion and the fluctuations of the external electric field are assumed to be slow as compared with the speed at which the electronic wavefunction responds to these changes. This assumption permits the definition of a new type of potential energy surface that depends not only on the geometry of the nuclei, but also on the electric field strength and on the orientation of the molecule with respect to the static electric field. The range of validity of the approximation is discussed in the paper. As an illustration of the method, it is applied to the optimal control of the vibrational excitation of a hydrogen molecule aligned with the field direction. *Ab initio* full configuration interaction calculations with a large orbital basis set are used to compute the H--H interaction potential in the presence of the electric field. The time dependent motion of the H2 molecules under the influence of the field is computed by solving the time-dependent Schrödinger equation. The time-dependent electric field within a short laser pulse is successfully optimized to create pulses which excite H2 from its ground state to its first and second vibrationally excited states with an efficiency of 98.6% and 98.7% respectively. The motions of the molecular wavefunctions during the action of the laser pulses and the frequency analsys of the pulses is also presented.

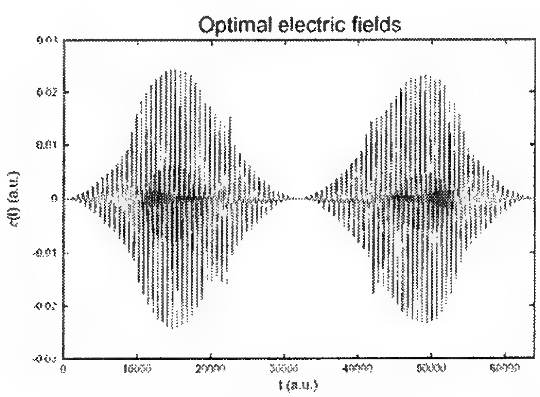

Optimsed laser pulse for $H_2(v=0) \rightarrow H_2(v=1)$

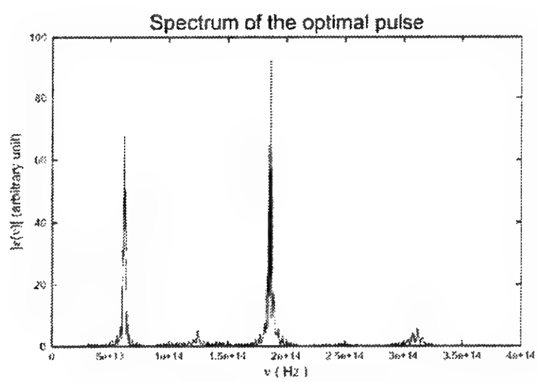

Spectrum of pulse

A31

Rovibrational distributions of HF in the photodissociation of vinyl fluoride at 193 nm: A direct MP2 quasiclassical trajectory study

Saulo Vázquez and Emilio Martínez-Núñez

Departamento de Química Física, Universidade de Santiago de Compostela, 15782, Santiago de Compostela, Spain.

Quasiclassical trajectory calculations were performed to calculate rovibrational distributions of the nascent HF fragment in the photodissociation of vinyl fluoride at 193 nm. The trajectories were initiated at the transition states of the four-center (4C) and three-center (3C) HF elimination channels, using a microcanonical, quasiclassical normal-mode sampling. In general, the calculated distributions are in reasonably good agreement with experiment. In particular, the trajectory distributions show bimodal character, although not as pronounced as that observed experimentally. The calculations predict that the 3C and 4C distributions are rather similar to each other, which suggests that the low-J and high-J components of the rotational distributions cannot be specifically assigned to each of these channels.

Photodissociation studies of state-selected $BrCl^+$ molecular ions by velocity map ion imaging

Olivier P. J. Vieuxmaire, N. Hendrik Nahler, Josephine R. Jones, Richard N. Dixon, and Michael N.R. Ashfold
University of Bristol, School of Chemistry, Bristol BS8 1TS, UK

Following the demonstrative study for the homonuclear diatomic Br_2^+ cation[1], high-resolution ion imaging methods have been applied to the photodissociation of the heteronuclear $BrCl^+$ molecular ion by monitoring both the $^{79}Br^+$ and $^{35}Cl^+$ photofragments.

One colour excitation of jet-cooled BrCl molecules at 30807.6 cm^{-1}, chosen so as to be resonant at the two photon energy with the $[^2\Pi_{1/2}]5s\sigma$, v'=0 intermediate Rydberg level, yields $BrCl^+$ parent and Br^+ fragment ions.

Velocity distributions for the $^{79}Br^+$ ions and photoelectrons, obtained from analysis of one-colour $^{79}Br^+$ and electron images, confirm that these fragments arise by one photon dissociation of $BrCl^+$ molecular ions, primarily in their $^2\Pi_{1/2,\, v=0}$ state, but with some 16% in the $^2\Pi_{3/2,\, v=0}$ state.

The state-selected $BrCl^+$ cations so obtained are then dissociated by absorption of a single photon from a second tunable dye laser. Analysis of two-colour images of the resulting Br^+ fragment ions measured in the range $370 \leq \lambda_{phot} \leq 436$ nm provides a detailed view of the number and nature of the available fragmentation pathways, and allows precise determination of the dissociation energies of $BrCl^+$ ($^2\Pi_{3/2}$) and $BrCl^+$ ($^2\Pi_{1/2}$), thereby providing an accurate value for the spin-orbit splitting constant as well as for the ionization potential of BrCl.

Cl^+ photofragments observed in one-colour images are found to arise via two distinct pathways:

(1) photodissociation of $BrCl^+$ ions as for the Br^+ fragments above. The higher ionisation potential of Cl means that this requires photons of higher energy than for Br^+ formation, and
(2) dissociation of a superexcited state formed by three photon excitation of BrCl and ionisation of the resulting excited Cl* atomic fragments.

The angular distributions of the fragments generated in the latter mechanism necessitates fitting with 2nd, 4th and 6th order Legendre polynomials. By calculating the recoil anisotropy following multiphoton excitation through different resonant states, the observed anisotropy is attributed to a $\Sigma \rightarrow \rightarrow \Pi \rightarrow \Pi$ transition in BrCl.

1. M. Beckert *et al., Phys. Chem. Chem. Phys,* 2003, **5**, 308-314

Ultraviolet photofragmentation dynamics of pyrrole studied by H (Rydberg) atom photofragment translational spectroscopy

Brid Cronin, Michael G.D. Nix, Rafay H. Qadiri and Michael N.R. Ashfold
School of Chemistry, University of Bristol, Bristol BS8 1TS, U.K.

H(D) atom loss channel(s) from pyrrole-h_5 and various of its partially and fully deuterated isotopomers following photoexcitation at various wavelengths in the range 230 - 193.3 nm have been investigated by H(D) Rydberg atom photofragment translational spectroscopy (PTS). As in the one previous PTS study of this molecule (at 193 nm and 248 nm)[1] and in a recent ion imaging study of the 243.1 nm photolysis of pyrrole-h_5,[2] we observe the total kinetic energy release (TKER) spectra of the H (and D) atoms to show two maxima, centred at ~2000 cm^{-1} and ~7000 cm^{-1}. Studies of the ways in which the TKER spectra depend on the relative alignment of electric ($\boldsymbol{\varepsilon}$) vector of the photolysis radiation with respect to the time-of-flight detection axis reveal that the slow H(D) atoms are formed with an isotropic recoil velocity distribution, while the faster H(D) atom peak has an associated angular anisotropy characterised by $\beta \sim -0.5$. TKER spectra obtained by monitoring H atoms from pyrrole-h_5 and D atoms from pyrrole-d_5 at any given photolysis wavelength are very similar, but studies involving the pyrrole-1D isotopomer, for example, show the fast peak to be relatively much enhanced when monitoring D and much reduced when monitoring H atom products.

Such behaviour is understandable within the framework of the most recent *ab initio* electronic structure calculations of the low lying excited states of pyrrole.[3,4] Photo-excitation at ~210 nm results in population of a $^1B_2(\pi^*\leftarrow\pi)$ excited state – the transition moment for which lies in the plane of the pyrrole molecule along the y (C_{2v} axis) and thus perpendicular to the breaking N–H(D) bond. The diabatic $^1B_2$ potential energy surface (PES) is bound with respect to N–H(D) bond fission, but out-of-plane motion enables efficient vibronic coupling with the first excited $^1A_2\,(3s/\sigma^*\leftarrow\pi)$ state. As in NH_3, this first excited state evolves from being predominantly a Rydberg (3s) state at small N–H bond lengths, to an anti-bonding valence state at larger R_{N-H}, whereupon it also experiences a conical intersection (CI) with the ground (X^1A_1) state PES. Photo-excited pyrrole molecules that dissociate directly on the $^1A_2$ PES are responsible for the fast H(D) atom peak in the TKER spectrum; their observed recoil anisotropy reflects the perpendicular nature of the $^1B_2$–X^1A_1 excitation (relative to the breaking N–H(D) bond). The isotropic distribution of H(D) atoms formed with low TKER are assumed to arise from that fraction of the dissociating molecules that avoid the CI at large R_{N-H} during an N–H bond extension phase. These have insufficient energy to dissociate on the excited (adiabatic) PES and can thus transfer to the ground state PES during a subsequent N–H bond compression, and thereby have the opportunity to sample large portions of the phase space associated with the ground state, and undergo substantial intramolecular vibrational redistribution (IVR) prior to eventual unimolecular decay.

Financial support from the EPSRC (via the pilot portfolio partnership LASER) and the European Union (BC, under contract no. HPRN-CT-2002-00183 PICNIC) is gratefully acknowledged, as is the support and encouragement of this study provided by Dr N.H. Nahler and K.N. Rosser.

1. D.A. Blank, S.W. North and Y.T. Lee, *Chem. Phys.*, **187**, 35 (1994)
2. J. Wei, A. Kuczmann, J. Riedel, F. Renth and F. Temps, *Phys. Chem. Chem. Phys.* **5**, 315 (2003)
3. B.O. Roos, P.-A. Malmqvist, V. Molina, L. Serrano-Andres and M. Merchan, *J. Chem. Phys.* **116**, 7526 (2002).
4. A.L. Sobolewski., W. Domcke, C. Dedonder-Lardeux and C. Jouvet, *Phys. Chem. Chem. Phys.* **4**, 1093 (2002) and references therein.

B32

Time Resolved FTIR Emission Studies of Molecular Dynamics

G. Hancock, M. Morrison, M. Saunders

Physical and Theoretical Chemistry Laboratory, University of Oxford, South Parks Road, Oxford, OX1 3QZ, UK

We report here a number of time resolved FTIR emission measurements involving the dynamics of free radical reactions. Firstly, 193 nm photolysis of N_2O produces $O(^1D)$ which subsequently reacts with N_2O:

$$O(^1D) + N_2O \rightarrow NO + NO$$
$$\rightarrow N_2 + O_2$$

The first reaction channel produces NO that is vibrationally excited (v = 1-16) and has been exploited to obtain the rates of collisional deactivation of NO(v) by a number of atmospherically important species, including O_2 and NO. Excellent agreement has been found with literature data, and approximately forty new rate constants are reported here. In particular the newly measured NO self quenching rates fill the gap between previous measurements at low v (where the rate constants decrease with increasing v) and high v (where they show the opposite trend).

Secondly, the photodissociation of NO_2/N_2O_4 at 193 nm has been investigated. NO and NO_2 nascent products have been observed and the nascent vibrational distribution of the NO product measured using both the fundamental and overtone bands of NO. The distribution peaks at $v = 5$, in agreement with lower energy studies, but also has a secondary maximum at $v = 14$, possibly due to dissociation via a crossing to another potential energy surface.

Thirdly, the reaction of $O(^1D)$ with fluoromethanes has been studied. A number of reaction products have been observed, including H_2CO and F_2CO, and particular attention has been paid to the nascent vibrational energy distribution of the HF product. The fate of the $O(^1D)$ reactant has also been investigated to determine the relative disposal of energy via reaction and energy transfer, particularly with respect to $O(^1D) + CF_3H$.

H-atom abstraction reactions between Cl atoms and organic molecules

Craig Murray, Julie K. Pearce, Paul N. Stevens and Andrew J. Orr-Ewing
School of Chemistry, University of Bristol, Cantock's Close, Bristol BS8 1TS, UK

Recently, our group has undertaken a series of experimental and theoretical investigations of the influence of functional groups on the dynamics of H-atom abstraction reactions between ground spin-orbit state $Cl(^2P_{3/2})$ atoms and a range of organic molecules, RCH_2OR', where R, R′ = H, CH_3 and CH_3X, where X = F, Cl, Br, I and NH_2. Experimentally, reaction was initiated by laser photolysis of molecular chlorine and the nascent HCl ($v' = 0$, J') products were detected by 2+1 resonance-enhanced multiphoton ionization in a time-of-flight mass spectrometer. Theoretical work involved the characterization of stationary points on the potential energy surface (PES) and "direct dynamics" trajectory calculations. Invariably, the nascent HCl rotational state distributions following abstraction from C-atoms adjacent to functional groups are hotter than those observed for reactions involving simple alkanes, and we attribute this enhanced rotational excitation to anisotropic, dipole-dipole interactions in the products region of the PES. Here, we report the results of recent studies on the dynamics of the reactions between $Cl(^2P_{3/2})$ atoms and the cyclic molecules ethylene oxide (C_2H_4O) and ethylene sulphide (C_2H_4S).

B33

Product study of the reaction between thiophene and nitrate radical

M.T. Baeza, B, Cabanas, M.P. Martin, S. Salgado, F. Villanueva, E. Monedero, and K. Wirtz

Departamento Quimica-Fisica, Facultad de Quimicas de Ciudad Real, Universidad de Castilla la Mancha, Campus Universitario s/n, Ciudad Real 13071, Spain

Products of the gas-phase reaction of NO_3 radical with thiophene have been investigated using different experimental systems. On one hand, experiments have been conducted in our laboratory using two different methods, a Teflon static reactor coupled to a gas chromatographer combined with mass-spectrometry (GC-MS) and a discharge flow tube with direct MS spectroscopic detection. A qualitative analysis in these cases indicates as possible products for the studied reaction at room temperature the followings: sulphur dioxide, acetic and formic acids, a short-chain aldehyde, 2-nitrothiophene and 3-nitrothiophene. On the other hand, quantitative experiments have been performed in the European Photoreactor (EUPHORE) in Valencia, Spain. In this case, the major products were: HNO_3 (≈80%), nitrothiophenes (≈30%), SO_2 (≈20%), propanal (3%) and a fraction of particles (≈10%). The obtained results indicate that at least 70% of the reaction of NO_3 reaction with thiophene proceeds by an H-abstraction process at room temperature. The mechanism of the reaction studied is proposed on base of experimental results.

A34

REKIN, an Experiment to Study the Oxidation of Metal Vapors: First Experiments with Zn(g) and O_2

Ivo Alxneit and Piotr Bodek
Paul Scherrer Institute, CH-5232 Villigen PSI, Switzerland. ivo.alxneit@psi.ch

With the aim to harvest sun light the conversion of concentrated solar radiation into storable and transportable energy carriers, so called "solar fuels" is a major activity of PSI's general energy research department. One attractive chemical process to produce hydrogen, the prototypical solar fuel, is the splitting of water. The direct thermal splitting of water, however, requires ultra high temperatures of about 3000 K and an effective technique to separate hydrogen from oxygen. Technologically somewhat less demanding are thermochemical cycles that separate the formation of oxygen and hydrogen in two distinct chemical reactions. At PSI a two-step cycle based on zinc oxide is studied for this purpose.[1] In a first step under concentrated solar radiation, zinc oxide is thermally decomposed into zinc and oxygen at 2300 K. The product, metallic zinc, is reacted with water in a second step yielding hydrogen and again zinc oxide. Of prime importance for the high temperature step is the separation of zinc and oxygen at the exit of the chemical reactor in order to avoid substantial reoxidation of zinc, formally the combustion synthesis of zinc oxide. Currently the separation of zinc and oxygen is implemented as a rapid quench. To design an effective quenching device, information on the path of the reaction and the associated rate constants must be known.

Only little information about the reaction of metal vapors with oxygen is available from the literature. The rate constant of the oxidation of magnesium vapor with oxygen was deduced from spatially resolved temperature measurements during the combustion of $Mg_{(g)}$ [2] and the reaction of transition metal atoms with oxygen at ambient temperatures was studied by fluorescence spectroscopy.[3] However, none of these studies are performed under conditions prevailing at the exit of a solar reactor.

REKIN was designed and built with the purpose to establish the reaction scheme and the kinetics of the oxiation of zinc vapor with oxygen under conditions similar to the ones in the high temperature solar process. REKIN implements a confined coaxial jet. Zinc vapor, optionally diluted with inert gas, leaves the central nozzle and is confined in a stream of (diluted) oxygen stemming from the annular nozzle. Gases are preheated to temperatures up to 1000 K. The concentration of species such as zinc atoms in the reaction zone are probed, spatially resolved, by planar laser-induced fluorescence (PLIF).

Here, we report on the characterization of the flow behavior of REKIN's coaxial nozzle and on first tests on the system $Zn_{(g)}$ / O_2. The two flows in the coaxial jet were visualized at room temperature using acetone as tracer and measuring its distribution by PLIF (λ_{ex} = 280 nm, λ_{det} = 540 nm). We found that no macroscopic eddies develop if flow velocities of the annular and the core flow respectively differ moderately, i.e. for moderate shear forces between the flows. We conclude that under these conditions the mixing of the two flows predominantly occurs by diffusion.

Financial support by the Swiss Federal Office of Energy (BFE) is gratefully acknowledged.

[1] Haueter P., Moeller S., Palumbo R. and Steinfeld A. (1999). The Production of Zinc by Thermal Dissociation of Zinc Oxide — Solar Chemical Reactor Design; Solar Energy 67 161.
[2] Kashireninov O.E., Kuznetsov V.A. and Manelis G.B. (1975). Kinetic Study by the Diffusion Flame Method of the Gas-phase Reaction Between Magnesium and Oxygen; Russ. J. Phys. Chem. 49, 520.
[3] Campbell M.L. (1998). Temperature Dependent Study of the Gas-Phase Kinetics of Zr (a3F2) and Hf (a3F2); J. Chem. Soc., Farad. Trans. 94, 1687 and references therein.

What we have learned about the Stabilities of Cyclopropane and Cyclopropene Group 14 Ring Analogues, through Gas Phase Kinetic studies of Cycloaddition Reactions of Heavy Methylenes (Silylene and Germylene) combined with Quantum Chemical (*Ab Initio*) Studies.

Rosa Becerra
Instituto de Quimica-Fisica 'Rocasolano', C.S.I.C., Madrid, Spain

Sergey E. Boganov, Mikhail P. Egorov, Valery I. Faustov, Irina V. Krylova, Oleg M. Nefedov, Vladimir M. Promyslov
N.D. Zelinsky Institute of Organic Chemistry, Russian Academy of Sciences, Moscow, Russian Federation

Robin Walsh
School of Chemistry, University of Reading, Whiteknights, Reading, UK.

The addition of silylene, SiH_2, and germylene, GeH_2 to ethylene and acetylene results in the initial formation of 3-membered ring heterocycles (silirane, silirene, germirane and germirene) just as methylene forms cyclopropane and cyclopropene in the analogous additions. This study will report the findings of gas-phase laser flash photolysis investigations of these systems (including isotopic variants). The studies are all supported by Potential Energy Surface calculations not only of the addition process, but also of potential further rearrangements of the heterocycles themselves.

The findings include:

- That, whereas methylene reacts to produce chemically activated rings which isomerise further, the heavy methylenes form the rings in third body assisted association reactions.
- The heterocycle rings are labile such that they can undergo rapid reversible interconversions with their ring opened alkyl (or alkenyl) heavy carbene isomers (eg silirane to ethylsilylene) under addition conditions.
- Unique amongst this set of heterocycles, germirene has a low energy decomposition pathway:

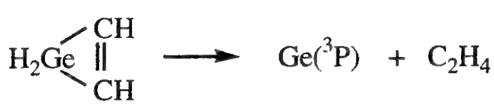

A35

X-Ray Free-Electron Lasers: Requirements for the UK ?

R.J.Donovan

School of Chemistry, University of Edinburgh, West Mains Rd., Edinburgh. EH9 3JJ

Partial funding for an X-ray free-electron laser ($\lambda \geq 1$ Å) has been agreed by the German Government and partners are now being sought. The poster will outline the present status of the project and present technical aspects.

Discussion on the requirements for the UK science community is invited.

B35

Low Temperature Reactions of OH Radicals with unsaturated hydrocarbons

Bjoern Hansmann

Institut für Physikalische Chemie, Universität Göttingen

The kinetics of the reaction of OH radicals with acetylene, ethylene propene, isoprene and benzene in the bath gas N_2 have been studied in a laval nozzle expansion. Laser induced fluorescence of OH radicals produced by photodissociation of hydrogen peroxide has been measured. The reaction rate of OH radicals with an excess of the unsaturated hydrocarbons has been determined in concentration ranges covering at least one order of magnitude to extract the bimolecular reaction rate. The rate constants have been found to show differing temperature dependence. In general the rates increase below room temperature, except acetylen, which has a no significant temperature dependence. Isoprene and propene show a turnover behavior from negative to positive temperature dependence when the temperarure is lower then 100 K. The role of the nature of the activation barrier and the influence of long-range electrostatic potentials for the reactions is discussed.

A36

Mechanism of the oxidation of hydrocarbons transplanted from gas-phase conditions to solution chemistry

Ive Hermans[a,b], Thanh Lam Nguyen[a], Pierre A. Jacobs[b], Jozef Peeters[a]*

[a] : *Division of Physical and Analytical Chemistry, Department of Chemistry, KULeuven, Celestijnenlaan 200F, B-3001 Heverlee – Belgium*

[b] : *Centre for Surface Science and Catalysis, Department of Interphase Chemistry, KULeuven, Kasteelpark Arenberg 23, B-3001 Heverlee – Belgium*

Based on quantum chemical potential energy surfaces, rate constants of primary as well as secondary radical-chain propagation steps were evaluated using Canonical Transition State Theory. It is found that α-hydrogen abstractions from cyclohexylhydroperoxide and cyclohexanol by the peroxyl radical chain carriers are much faster than H-abstraction from cyclohexane, and that these reactions of cyclohexylhydroperoxide and cyclohexanol result in their conversion to cyclohexanone. Alternative mechanisms for such conversions are also discussed under thermal conditions in solutions and chemically activated in gas-phase. On the other hand, but again contrary to current assumptions, cyclohexanone is found to be only slightly more susceptible to (α-)hydrogen abstraction than cyclohexane itself. In liquid phase an equilibrium between hydroperoxyl radicals and cyclohexanone, and α-hydroxy-cylohexylperoxyl radicals will be established.

* jozef.peeters@chem.kuleuven.ac.be, fax : +32 (0)16 327992

Dependence of water on the kinetics of the self-reaction of HO_2

Nozomu Kanno,[1] Masanori Uetake,[1] Kenichi Tonokura,[2] Atsumu Tezaki[3] and Mitsuo Koshi[1]

[1]*Department of Chemical System Engineering, The University of Tokyo*
[2]*Environmental Science Center, The University of Tokyo*
[3]*Department of Mechanical Engineering, The University of Tokyo*

The self-reaction of hydroperoxy (HO_2) radicals has been studied by near-IR two-tone frequency modulation spectroscopy in the spectral region of 1.43 μm. The depletion of HO_2 and the formation of hydrogen peroxide (H_2O_2) as the reaction product were observed at each absorption lines ($A'\tilde{A} \leftarrow A''\tilde{X}$ 000 – 000 band of HO_2 and $\nu_1 + \nu_5$ combination band of H_2O_2) without any interference on each other. The dependence of the reaction rate constant and signal intensities on addition of water was measured at 297 – 350 K and total pressure of 50 Torr nitrogen diluent. As shown in fig. 1, the decay rate of HO_2 is accelerated with adding water, notably at lower temperature. To correct the detection sensitivity change caused by the collision broadening, we measured spectral shapes of HO_2 at various pressures of N_2 and H_2O at room temperature, and converted to conventional absorption spectra. In fig. 2, retrieved peak area is slightly decrease with increasing water concentration at 50 Torr in diluent of N_2, indicating the formation of HO_2-H_2O complex. At the symposium, we will discuss the kinetics of the reaction between HO_2 and the HO_2-H_2O complex.

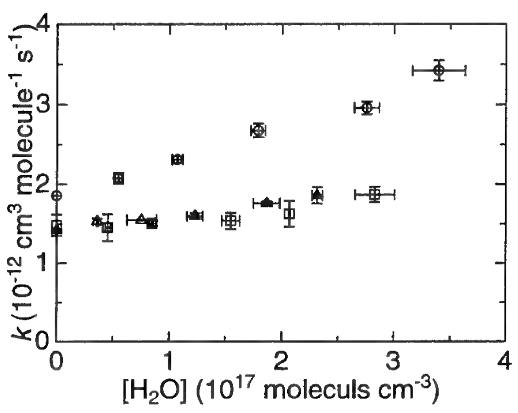

Fig. 1 Rate enhancement effect on water at 297 K (circle), 325 K (triangle), and 350 K (box).

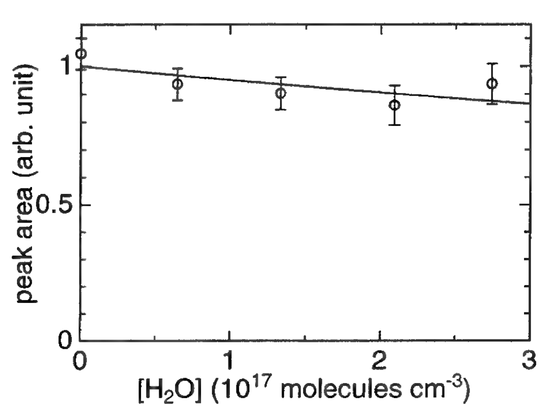

Fig.2 Water vapor dependence of retrieved peak area of HO_2 at 296 K.

A37

UV Absorption Spectra and Kinetics of Methyl Substituted Hydroxycyclohexadienyl Radicals

Lev N. Krasnoperov,[1] David Johnson,[2] Robert Lesclaux.[2]

[1]*Department of Chemistry and Environmental Science, New Jersey Institute of Technology, University Heights, Newark, NJ 07102, krasnoperov@adm.njit.edu*
[2]*LPCM, UMR 5803 CNRS, Universite Bordeaux I, 33405 Talence Cedex, France, lesclaux@cribxl.u-bordeaux.fr*

UV absorption cross-sections of hydroxycyclohexadienyl radical as well as several methyl substituted hydroxycyclohexadienyl radicals were measured using laser photolysis combined with transient UV absorption spectroscopy. Mixtures of hydrogen peroxide, benzene or methyl substituted benzenes and oxygen in nitrogen as a carrier gas were photolyzed at 248 nm (KrF excimer laser). The hydroxycyclohexadienyl radicals were formed in the addition reaction of OH to benzene or a substituted benzene (toluene, ortho-, meta-, and para-xylene, and 1,3,5-trimethylbenzene). The cross-sections were determined relative to the known cross-section of ethyl peroxy radical, in photolysis of gas mixtures with the aromatic compound replaced with ethane. In addition, limited kinetic data on the reactions of the substituted hydroxycyclohexadienyl radicals (self-reaction and reaction with molecular oxygen) as well as on the quenching of the triplet states of the aromatic compounds were also obtained.

UV absorption spectra are characterized by two poorly resolved peaks centered around 280 – 300 nm and 315 – 325 nm. The maximum absorption cross-sections for these peaks are summarized in Table 1.

Table 1. UV absorption cross-sections of hydroxycyclohexadienyl and methyl substituted hydroxycyclohexadienyl radicals.

Radical	λ_1 / nm	σ_1 / 10^{-18} cm^2 $molecule^{-1}$	λ_2 / nm	σ_2 / 10^{-18} cm^2 $molecule^{-1}$
Benzene-OH	282 ± 5	8.3 ± 0.3	315 ± 5	5.4 ± 0.3
Toluene-OH	290 ± 5	9.2 ± 0.3	317 ± 5	9.7 ± 0.3
m-Xylene-OH	-	-	320 ± 3	17.4 ± 0.5
o-Xylene-OH	285 ± 5	6.4 ± 0.3	317 ± 5	9.5 ± 0.3
p-Xylene-OH	300 ± 10	8.6 ± 0.3	325 ± 5	7.6 ± 0.5
Mesitylene-OH	277 ± 3	9.8 ± 0.3	225 ± 3	24.7 ± 0.5

B37

A Kinetic Analysis of the Effect of O_2 on the Reactions of Atomic Bromine With Some Hydrocarbons and Ethers

Lori M. Anthony and John M. Roscoe

Department of Chemistry, Acadia University, Wolfville, Nova Scotia B4P 1L4

The reactions of atomic bromine with ethene, 2-methyl propane, dimethyl ether and diethyl ether have been studied kinetically at 298 K in a 70 Litre photochemical reaction chamber using the relative rate method. The work was motivated in part by the observation that the rate constant for reaction of Br with diethyl ether at ambient temperature is comparable to that for the reaction of Br with ethene[1] while the rate constants for reactions of Br with saturated hydrocarbons are generally very much smaller than that for the reaction of Br with ethene[2].

The effects of bromine and oxygen partial pressures on the numerical value of the rate constants have been evaluated for several combinations of reactants. When ethene was used as the reference reactant, the experimental values of the rate constant ratio showed a strong dependence on the O_2 concentration as expected[3]. However, the experimental rate constant ratios obtained with mixtures of diethyl ether and dimethyl ether also showed a significant and unexpected dependence on the O_2 concentration. The dependence on O_2 concentration was analysed to obtain limiting values of the rate constant ratio that are independent of the concentration of O_2, using a method that does not depend upon a specific mechanism for the overall reaction. Rate constant ratios obtained using mixtures of dimethyl ether or diethyl ether with 2-methyl propane were independent of the O_2 concentration.

The measured rate constant ratios at 298 K for the reactions of Br with dimethyl ether and with diethyl ether can be put on an absolute basis using the well established absolute rate constant for the reaction of Br with 2-methyl propane[4] as the primary reference. This analysis gives for Br + $(CH_3)_2O$, $k_{298} = 9.43\times10^5 \pm 2\%$ L mol^{-1} s^{-1} and for Br + $(C_2H_5)_2O$, $k_{298} = 1.41\times10^7 \pm 6\%$ L mol^{-1} s^{-1}. With these rate constants as secondary reference values, the following rate constants were obtained: Br + $(C_2H_5)_2O$, 1.27×10^7 L mol^{-1} s^{-1} ± 8% (referenced to $(CH_3)_2O$); Br + C_2H_4, $k_{298} = 9.0\times10^7 \pm 25\%$ L mol^{-1} s^{-1} (referenced to $(C_2H_5)_2O$).

The role of O_2 is to compete with Br_2 for the free radicals produced in the system. In the case of ethene, in which FTIR spectra indicate the formation of little or no HBr, the reaction is initiated by addition of Br to ethene and the essential reactions to consider are

[1] $$C_2H_4 + Br \leftrightarrows C_2H_4Br$$

[2] $$C_2H_4Br + Br_2 \rightarrow C_2H_4Br_2 + Br$$

[3] $$C_2H_4Br + O_2 \rightarrow C_2H_4BrO_2 \rightarrow \text{Oxidation Products}$$

In the case of the ethers, FTIR spectra indicate formation of substantial amounts of HBr. If an adduct analogous to C_2H_4Br is formed in these reactions, it must decompose rapidly to HBr and an organic free radical.

1. Wallington, T. J.; Skewes, L. M.; Siegl, W. O.; Japar, S. M. *Int. J. Chem. Kinet.*, **21**, 1069 (1989).
2. Westley, F.; Herron, J. T.; Frizzell, D.; Hampson, R. F.; Mallard, W. J. *NIST Standard Reference Database 17-2Q98*, (1998).
3. Barnes, I.; Bastian, V.; Becker, K. H.; Overath, R.; Tong, Z. *Int. J. Chem. Kinet.*, **21**, 499 (1989). Yarwood, G.; Peng, N.; Niki, H. *Int. J. Chem. Kinet.*, **24**, 369 (1992).
4. Seakins, P. W.; Pilling, M. J.; Niiranen, J. T.; Gutman, D.; Krasnoperov, L. N. *J. Phys. Chem.*, **96**, 9847 (1992).

Ultraviolet CO Chemiluminescence in $CH(X^2\Pi)$ and $CH(a^4\Sigma^-)$ Reactions With Atomic Oxygen at 298 K

Ghanshyam L. Vaghjiani

ERC, Inc., Air Force Research Laboratory, AFRL/PRSP, 10 E Saturn Blvd, Edwards AFB, CA 93524, USA
Tel: 661 275 5657
Fax: 661 275 6245
Email: ghanshyam.vaghjiani@edwards.af.mil

Production of ultraviolet CO chemiluminescence has been observed for the first time in the gas-phase pulsed laser photolysis of a trace amount of $CHBr_3$ vapor in an excess of O-atoms. O-atoms were produced by dissociation of O_2 or N_2O in a cw-microwave discharge cavity in 2.0 torr of He at 298 K. Temporal profiles of the excited state products that formed in the photo-produced precursor + O-atom (or O_2) reaction were measured by recording their time-resolved chemiluminescence in discrete vibronic bands. The CO 4th Positive transition ($A^1\Pi$, v'=0 $\rightarrow$ $X^1\Sigma^+$, v"=2) near 165.7 nm, the CO Cameron band transition ($a^3\Pi$, v'=0 $\rightarrow$ $X^1\Sigma^+$, v"=1) near 215.8 nm and the OH band transition ($A^2\Sigma^+$, v'=1 $\rightarrow$ $X^2\Pi$, v"=0) near 282.2 nm was monitored in this work to deduce the decay kinetics of the chemiluminescence in the presence of various added substrates. From this the second-order rate coefficient values were determined for reactions of these substrates with the photo-produced precursors. Measured reactivity trends suggest that the prominent precursors responsible for the chemiluminescence are the methylidyne radicals, $CH(X^2\Pi)$ and $CH(a^4\Sigma^-)$, whose production requires the absorption of at least 2 laser photons by the photolysis mixture. The O-atom reactions with brominated precursors, which also form in the photolysis, are shown to play a minor role in the production of the CO chemiluminescence. However, the CBr_2 + O-atom reaction was identified as a significant source for the ultraviolet Br_2 chemiluminescence that was also observed in this work.

B38

The β bond dissociation reactions of "biallyl" type of radicals

M. Szori, I.G. Csizmadia, B. Viskolcz*

Department of Chemistry, Faculty of Education, University of Szeged
H-6701 Szeged, P. O. Box 396, Hungary

The allyl type of radical can be formed in different in high- and low temperature combustion reactions. The large stability of the allyl type of radical predetermines a crucial role in the oxidative stress or the aging process in living cells. The different non conjugated systems such polyunsaturated fatty acid chains or cycloheptatrienes contain the following pattern: [-CH=CH-CH_2-CH=CH-]

From such patterns high stability radicals can be formed, where 5 electrons are delocalized on 5 C-atoms. To model such systems the theoretical study on the thermal decomposition of the CH_3-CH=CH-CH_2-CH=CH-CH_3 molecules and the radicals formed by H atom dissociations were calculated by different levels of MO theory.

$$(CH3\text{-}CH{=}CH)_2\text{-}CH_2 \xrightarrow{-H} (CH3\text{-}CH{=}CH)_2\text{-}CH\bullet \xrightarrow{-H} CH_3\text{-}CH{=}CH\text{-}CH{=}CH\text{-}CH{=}CH_2$$

In the second step of the above reactions the total conjugated system (1,3-polyenes, like Vitamin A or beta-carotene) will be formed. The allyl type radicals can be found between the non conjugated and total conjugated stages. The nature of the delocalization of unpaired electrons as well as the overall kinetics will be discussed.

How can very different chemical kinetic models produce similar results?

I. Gy. Zsély, J. Zádor and T. Turányi

Department of Physical Chemistry, Eötvös University (ELTE)
H-1518 Budapest, P.O. Box 32, Hungary
Fax: +36-1209-0602, e-mail: turanyi@elte.hu

It is widely known that detailed reaction mechanisms with identical reaction steps but using very different significant rate parameters may provide similar simulation results. This phenomenon is related to the similarity of the local sensitivity functions $\partial Y_i(z)/\partial p_k$ of the chemical kinetic models [1], [2], where $Y_i(z)$ is a model output, p_k is a parameter and z is the independent variable (time or distance). Three types of similarity have been found: (i) *local similarity:* ratio $\lambda_{ij}(z)=(\partial Y_i(z)/\partial p_k)/(\partial Y_j(z)/\partial p_k)$ is equal for any parameter k; (ii) *scaling relation:* ratio $\lambda_{ij}(z)$ is equal to $(\mathrm{d}Y_i(z)/\mathrm{d}z)/(\mathrm{d}Y_j(z)/\mathrm{d}z)$; (iii) *global similarity:* ratio $\mu_{ikm}=(\partial Y_i(z)/\partial p_k)/(\partial Y_i(z)/\partial p_m)$ is constant in a range of the independent variable z.

Similarities can be detected by determining the ratios above or, in a more efficient way, via the investigation of the correlation of the sensitivity vectors [3] by calculating the scalar product of the corresponding vectors normalized to unit length. Local similarity may be a consequence [1] of the existence of low-dimensional slow manifolds in the space of variables of the model. Scaling relation may be present, if the dynamics of the system is controlled by a one-dimensional slow manifold. A general feature of all high temperature combustion models is that a rapid transition occurs from the unburnt state to the burnt state and this transition has a self-accelerating nature. The latter characteristic and local similarity together implies global similarity. Therefore, global similarity also seems to be a general feature of such models.

Global similarity means that the effect of the simultaneous change of several parameters can be fully compensated *for all variables, in a wide range of the independent variable* by changing a single parameter. In the case of empirical models, the only task of the model is to provide a good description of the observations. Presence of global similarity means that different parameter sets can provide the same simulation results. In the case of physical models, all parameters are assumed to have a 'true' value, which can be unambiguously determined in independent experiments. If a physical parameter is determined in a system of global similarity by fitting to experimental data, error in the fixed parameter values cause the obtained parameter to become erroneous. However, the fitted model perfectly reproduces all experimental data, even if the values of several variables are measured at several time points (or distances).

The statements are illustrated by numerical examples related to the simulation of homogeneous explosions and adiabatic burner-stabilized laminar flames of stoichiometric methane–air mixtures.

[1] I. Gy. Zsély, J. Zádor, T. Turányi, Similarity of sensitivity functions of reaction kinetic models. *J. Phys. Chem. A*, **107**, 2216-2238 (2003)
[2] I. Gy. Zsély, T. Turányi, The influence of thermal coupling and diffusion on the importance of reactions: The case study of hydrogen-air combustion. *Phys. Chem. Chem. Phys.*, **5**, 3622–3631(2003)
[3] J. Zádor, I. Gy. Zsély, T. Turányi, Investigation of the correlation of sensitivity vectors of hydrogen combustion models. *Int. J. Chem. Kinet.*, **36**, 1–15 (2004)

Which rate parameters should be measured more precisely to improve complex kinetic models?

J. Zádor, I. Gy. Zsély, and T. Turányi

Department of Physical Chemistry, Eötvös University (ELTE)
H-1518 Budapest, P.O. Box 32, Hungary
Fax: +36-1209-0602, e-mail: turanyi@elte.hu

Computer modelling plays a crucial part in the understanding of complex chemical kinetic processes. The parameters of the models are usually determined in independent experiments and are always associated with uncertainties. Two typical examples of complex chemical kinetic systems are the combustion of gases and the photochemical processes in the atmosphere. In this study, local uncertainty analysis [1], [2], the Morris method [3], and Monte Carlo analysis with Latin hypercube sampling [3] were applied to a tropospheric kinetic and to a combustion model.

The tropospheric kinetic model described the photochemical degradation of ethene, as it had been implemented in the Master Chemical Mechanism version 3 (MCMv3) [4]. The submechanism of ethene degradation contained 141 reactions of 45 chemical species. The effect of the uncertainty of all kinetic parameters on the calculated concentration of O_3 and HCHO was investigated and the results were compared with measurements made in the European Photoreactor (EUPHORE) at Valencia, Spain. In a similar study, the combustion of methane described by the Leeds Methane Oxidation Mechanism [5] (175 reactions of 37 species) was investigated. The effect of the uncertainty of all kinetic parameters and heats of formation of species were investigated on several results of premixed laminar flame calculations in a wide range of fuel-to-air ratio. In the cases of both models, the uncertainty of surprisingly few parameters caused most of the uncertainty of all model results. These critical kinetic and thermodynamic parameters were identified and their role in these two chemical kinetic systems was discussed.

The presented methods provide a general methodology for the identification of critical rate parameters and thermodynamic data that should be determined by smaller uncertainty; knowing more precise values of these parameters leads to a much more reliable complex chemical kinetic model.

Acknowledgement: This work was supported by the European Union project IALSI, contract No. EVR1-CT-2001-40013.

[1] T. Turányi, Sensitivity analysis of complex kinetic systems - tools and applications. *J. Math. Chem.*, **5**, 203-248(1990)

[2] T. Turányi, L. Zalotai, S. Dóbé, T. Bérces, Effect of the uncertainty of kinetic and thermodynamic data on methane flame simulation results. *Phys. Chem. Chem. Phys.*, **4**, 2568-2578(2002)

[3] A. Saltelli, E. M. Scott, K. Chen (eds.), *Sensitivity analysis*. Wiley, Chichester, 2000.

[4] S. M. Saunders, M. E. Jenkin, R. G. Derwent, M. J. Pilling. Protocol for the development of the master chemical mechanism, MCM v3 (part a): Tropospheric degradation of non-aromatic volatile organic compounds. *Atmos. Chem. Phys.*, **3**, 161-180(2003)

[5] K. J. Hughes, T. Turányi, A.R. Clague, M.J. Pilling, Development and testing of a comprehensive chemical mechanism for the oxidation of methane.*Int. J. Chem. Kinet.,* **33**, 513-538 (2001)

Trajectory simulations of polyatomic-polyatomic collisions

V. Bernshtein, I. Oref
Department of Chemistry, Technion-Israel institute of Technology, Haifa 32000, Israel
E-mail: chr21vb@technion.ac.il

In the present work the mechanism of collisional energy transfer (CET) between polyatomic systems was systematically explored by classical trajectory calculations. The investigations focused on benzene, toluene, azulene, and pyrazine collisions.

CET quantities like average energy transfer, $\langle \Delta E \rangle$, collision duration, $\langle \tau \rangle$, and probability density function, P(E,E'), were evaluated from trajectory calculations as a function of bath temperature, photon excitation, and potential energy surface. The contributions of individual vibrational modes and groups of modes to CET as well as collisions with frozen rotational degrees of freedom were examined.

The CET mechanism in polyatomic bath consists, unlike monatomic bath, of direct as well as chattering collisions in which the bath molecule gains energy by repeatedly banging into the excited molecule (see figure).

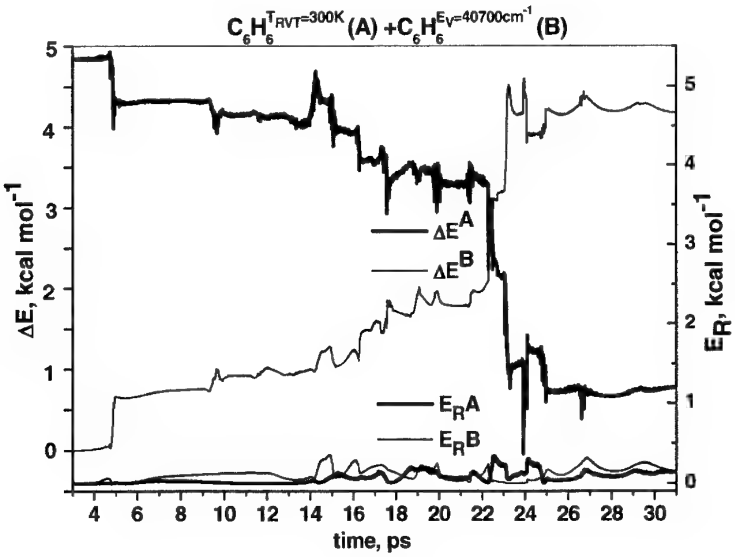

It was found that mainly vibration to vibration energy transfer affect CET and there is hardly any rotational energy transfer. However, it was found that there is a significant intra-collision rotational energy flux. Moreover, freezing the rotations increases $\langle \tau \rangle$ by factor of 3, and causes an increase in the absolute value of $\langle \Delta E \rangle$ up to 50%. It comes about from the fact that the molecular rotations destabilize the van der Waals collision complex. Supercollisions were found and they do occur in collisions with long complex lifetimes. There is no specific gateway mode or group of modes that are more efficient in CET. These results are supported by experimental work and indicate surprising differences in CET between polyatomic-polyatomic collisions and polyatomic-monatomic collisions. The mechanism of CET in polyatomic-monatomic systems was studied in great details [1]. It shows CET mediated by rotations with a low frequency dominant gateway mode and a CET probability density function with a high ΔE tail, part of which can be assigned to supercollisions. The present results produce mechanistic insight into CET of polyatomic bath collider.

References

[1] V. Bernshtein and I. Oref, *J.Phys.Chem. A*, **105**,10646 (2001).

Measurement of Relaxation of Orientation and Alignment in Inelastic Collisions by Polarisation Spectroscopy

M. L. Costen, H. J. Crichton, K. G. McKendrick and G. Richmond
School of Engineering and Physical Sciences,
Heriot-Watt University, Edinburgh, EH14 4AS, UK

We describe an alternative approach to the study of collisional energy transfer based on Polarisation Spectroscopy (PS). PS is an established spectroscopic technique, but is relatively unexploited in the field of collisional energy transfer [1,2]. A polarised pump laser beam resonant with a transition introduces non-equilibrium m_J distributions in the ground and excited states. A relatively weak linearly polarised probe beam co-propagates through the sample. When this is also resonant with the induced polarisation a weak signal beam of opposite polarisation is generated, which may be detected through a crossed polariser. PS is sensitive to collisions because they may either transfer population out of the initially prepared levels or cause a change in their polarisation state.

We will present results for collisional relaxation of orientation and alignment of small free radicals, e.g. NO or OH in collision with a controlled pressure (≤ 1 Torr) of suitable collider gas, e.g. He, Ar, N_2, CO, CO_2. Pump and probe pulses are produced from two independent Nd:YAG pumped dye lasers with conventional ~10 ns pulse lengths. The effect of collisions on PS may be measured by varying the delay between pump and probe pulses, an example of which for the OH radical is shown in figure 1.

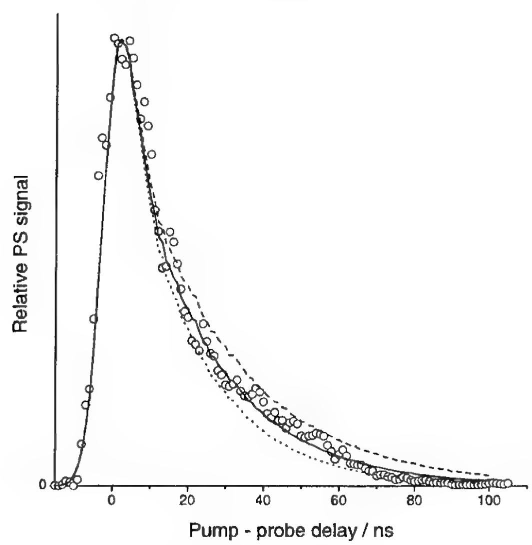

Fig. 1. PS signal as a function of pump-probe delay for OH (A-X) $Q_1(2)$, linear pump, 0.6 Torr He, with example simulations.

We interpret the PS signals with a theoretical description in an angular momentum spherical tensor formalism that emphasises the dynamical orientation and alignment we wish to measure [3].

References

[1] C. Wieman and T. W. Hänsch, *Phys. Rev. Letts.*, **36** (1976) 1170
[2] A. A. Suvernev, R. Tadday and T. Dreier, *Phys. Rev. A*, **58** (1998) 4102
[3] M. L. Costen, H. J. Crichton and K. G. McKendrick, *J. Chem. Phys*, **120** (2004) 7910

A41

State-to-State Collisional Energy Transfer in Electronically Excited CH/D Radicals

G. Richmond, M. L. Costen and K. G. McKendrick

School of Engineering and Physical Sciences, Heriot-Watt University, Edinburgh, UK
email: k.g.mckendrick@hw.ac.uk

Electronically inelastic collisions of excited CH radicals in the $A^2\Delta$ and $B^2\Sigma^-$ states have been studied. Previous work[1,2] found that collisions with CO_2 efficiently promotes electronic transfer between the $A^2\Delta$ and $B^2\Sigma^-$ states. This has been expanded to include other colliders such as He, Ar, H_2, N_2 and CO.

The CH radicals are generated by multiphoton photolysis of $CHBr_3$ at 266 nm. After a delay to allow decay of spontaneously produced excited state CH, selected rovibrational levels in either the $A^2\Delta$ or $B^2\Sigma^-$ state are prepared by a tuneable dye laser pulse. Transfer between the excited electronic states is detected by time-resolved dispersed fluorescence. Rate constants and product state branching ratios were determined for the transfer processes between B (v = 0) and A (v = 0/1). There is a general correlation between the efficiency of electronic state changing collisions and long-range attractive forces. Interestingly, it is uncorrelated with the probability of removal through chemical reaction, which is efficient for some partners, e.g. H_2 and CO. This implies that different regions of the potential surface are explored by electronically inelastic and chemically reactive collisions.

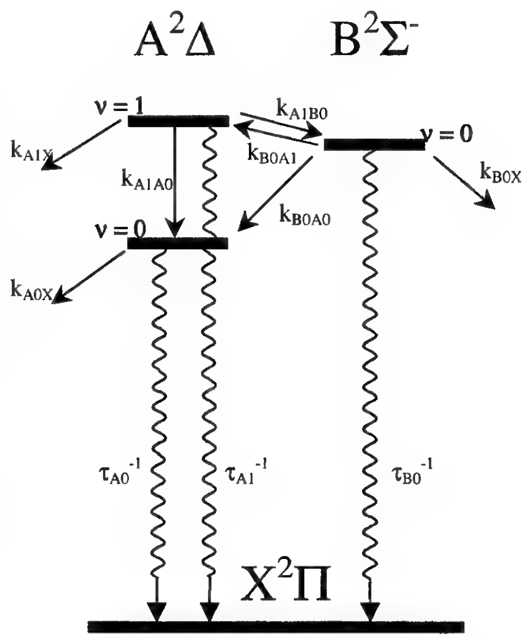

Fig 1. Four-level kinetic scheme describing the energy transfer processes between the $A^2\Delta$ and $B^2\Sigma^-$ states of CH.

A recent extension to this work is to investigate the effect of changing to the deuterated isotope of CH. The relative positions of the vibronic energy levels of interest are changed significantly in CD compared to CH, due to the difference in reduced mass. The B (v = 0) level now resides ~500 cm^{-1} above the A (v = 1) level as opposed to ~250 cm^{-1} below. Also, the energy gap between the A (v = 0/1) is reduced which may have an effect on any vibrational relaxation processes.

1. C. J. Randall, C. Murray and K. G. McKendrick, *Phys.Chem.Chem.Phys.*, **2**, 461 (2000).
2. C. Murray, C. J. Randall and K. G. McKendrick, *Phys.Chem.Chem.Phys.*, **2**, 5553 (2000).

Interrogation of nitrogen plasmas using diode lasers

B. Bakowski, G. Hancock, R. Peverall, S. E. Prince, G. A. D. Ritchie and L. Thornton

The Physical and Theoretical Chemistry Laboratory, The University of Oxford, South Parks Road, Oxford OX1 3QZ

As a consequence of the energetic nature of plasma, many varied and exotic processes occur. Only by quantitative measurements of different species or species in different quantum states can an understanding of the physicochemical properties of the plasma be achieved. This can be problematic because many excited species exist in low number densities but have a disproportionate effect on the plasma chemistry. In this contribution we present observations of metastable and ionic species produced in a molecular nitrogen plasma. Initial attempts to model the kinetic processes occurring in the plasma to reproduce the observations are also presented.

Cavity enhanced diode laser absorption spectroscopy is used to detect the low concentrations of both the ground state of N_2^+ and the metastable A-state of N_2 in an inductively coupled nitrogen plasma. The ICP chamber has been characterised using standard ion flux and optical emission techniques and obvious transitions to the inductively coupled regime are observed. The $v = 0$ and the $v = 1$ levels of the $A^3\Sigma_u^+$ state of N_2 have been probed directly using diode laser based cavity enhanced spectroscopy via the (3,0) and (3,1) bands of the $B\ ^3\Pi_g \leftarrow A^3\Sigma_u^+$ transition at 686 nm and 770 nm to determine absolute concentrations and temperatures. These were found to be dependent on plasma parameters; for example in a 10 mTorr discharge $T_{rot} \approx T_{tr}$, varying from ~ 300 K at 5 W to ~ 450 K at 400 W applied power. The overall population in the $v = 0$ level is found to be $(1.19 \pm 0.07) \times 10^{10}$ cm^{-3} under typical conditions of 100 W rf power and 10 mTorr pressure, corresponding to a discharge efficiency for the production of this level of ~ 10^{-5}. The rotational and translational modes of this electronically excited species are found to be in thermodynamic equilibrium at all powers and pressures used in this study. N_2^+ is probed on the Meinel band (the (2,0) band of the $A^2\Pi_u$ – $X^2\Sigma^+_g$ system) and yields number densities of approximately 10^9 cm^{-3} for $v = 0$. This is in good agreement with ion flux measurements at 100 W and 10 mTorr which give a flux of 1.8 $\times 10^{18}$ m^2 s^{-1}, from which a N_2^+ ion density of ~ 2×10^9 cm^{-3} was inferred. A reasonable kinetic model with good qualitative results for pressure and power dependence has been provided; the trends in the observations have been rationalised in terms of N atom chemistry and vibrational excitation.

A42

Investigating hydrocarbon radicals with synchrotron radiation

T. Schüßler[1], C. Alcaraz[2], M. Elhanine[2], H.-J. Deyerl[3], W.Roth[1], and I. Fischer[1]

[1] *Institute of Physical Chemistry, University of Wuerzburg, D-97074 Wuerzburg*
[2] *LURE, Bât. 209, BP 34, Centre Universitaire Paris-Sud, F-91898 Orsay*
[3] *Research Center for Communication and Optics, DTU Kopenhagen, DK-2800 Kgs. Lyngby*

Investigating the VUV photochemistry of pyrolytically produced hydrocarbon radicals poses considerable challenges, because a pulsed radical source has to be combined with a continuous light source. In an accompanying oral contribution we discuss the dissociative photoionization of the radicals allyl, C_3H_5, propargyl C_3H_3, and ethyl, C_2H_5. In this poster we want to focus on some additional experiments and want to discuss in particular how the experimental conditions influence the pyrolysis process. We show that bimolecular reactions in the pyrolysis nozzle become important and lead to the formation of background signals that have to be considered in the analysis of the experiment. We will also present threshold photoelectron spectra and photoion yield curves of hydrocarbon radicals.

Absolute rate measurements and product distribution study of the reactions of electronically excited $CF_2(^3B_1)$ with O_2 and NO

Bart Dils, Rehab M. I. Elsamra, Thanh L. Nguyen, Shaun A. Carl and Jozef Peeters

Katholieke Universiteit Leuven, Celestijnenlaan 200F, B-3001 Leuven, Belgium

Although the kinetics of gas phase reactions of fluorine containing compounds have been widely investigated due to their important role in the chemistry of plasma-etching, a critical step in the production of integrated circuits –several fluorinated compounds are still virtually unexplored. One potentially important species in etching plasmas, on which there is only limited information, is $CF_2(^3B_1)$, a long lived electronically excited biradical, which, apart from its reactions with other plasma gases, likely also plays a role in the formation of etch inhibiting $(C_xF_y)_n$ polymer films.

Using the photodissociation of C_2F_4 with an excimer laser pulse at 193 nm to generate $CF_2(^3B_1)$ –as opposed to the chemical generation through the C_2F_4 + O reaction used by other groups– we were able to straightforwardly determine the absolute rate constants of gas phase reactions of $CF_2(^3B_1)$ with reactants such as O_2 and NO, this over a broad temperature range between 288 K and 600 K:

$$CF_2(^3B_1) + O_2\text{: } k(T) = (6.7 \pm 1.9) \times 10^{-12} \exp[-(200 \pm 100)\text{K}/T] \text{ cm}^3 \text{ s}^{-1} \text{ molecule}^{-1}$$

$$CF_2(^3B_1) + NO\text{: } k(T) = (9.7 \pm 2.5) \times 10^{-12} \exp[+(545 \pm 80)\text{K}/T] \text{ cm}^3 \text{ s}^{-1} \text{ molecule}^{-1}$$

No pressure dependence of the rate constants was observed in the 1–20 Torr range.

Additional to these experimental determinations, quantum mechanical calculations were performed at the G2M//B3LYP/6-311+G(3df) and CASSCF/CASPT2 level of theory. It was found that for the reaction of $CF_2(^3B_1)$ with O_2 the main products under our low pressure conditions are FCO_2 + F and $F_2CO(^1A_1)$ + $O(^3P)$ depending on whether the reaction proceeds via the singlet or triplet surface. In the case of the $CF_2(^3B_1)$ + NO reaction, the main products are $CF_2(^1A_1)$ + NO (up to 99%) which amounts to quenching through a chemical process.

A43

The Mechanism of NO_x Formation in the Plasma Treatment of Waste Gas Streams

Alice M. Harling, J. Christopher Whitehead and Kui Zhang

Department of Chemistry, University of Manchester, Manchester M13 9PL.

Non-thermal, atmospheric pressure plasma processing is now accepted as a proven environmental clean-up technology for the removal of small concentrations of pollutants (e.g. NOx, particulates, solvents, CFC's etc.) from waste gas streams. It is a viable competitor to the more established technologies of catalysis, pyrolysis, adsorption and condensation. Plasma reactors at atmospheric pressure typically produce reactive species such as atomic oxygen and nitrogen, hydroxyl radicals and electronically-excited species which then chemically destroy the pollutants converting them into benign compounds that be safely vented to atmosphere or that can be safely removed and possibly recycled.

A problem encountered with destroying pollutants in gas streams containing oxygen is that high levels of the oxides of nitrogen (NO, NO_2 and N_2O) may also be formed as a consequence of the processing. The perceived wisdom at present is that the mechanism of formation of these nitrogen oxides is essentially decoupled from that for the destruction of the pollutant in the plasma discharge. Although, it is recognised that there are situations where peroxy radicals can effectively convert NO into NO_2

$$RO_2 \quad + \quad NO \quad \rightarrow \quad RO \quad + \quad NO_2.$$

We have studied the formation of NOx and N_2O during the plasma destruction of a range of compounds including a range of hydrocarbons (methane, toluene, acetic acid, acetone, diethyl ether, ethyl acetate, formic acid and methanol) and halogenated species (CH_2Cl_2, $CHCl_3$, CCl_4, CCl_2F_2, CF_4, $CHBr_3$, CH_3I) with air as the carrier gas. Using the plasma destruction of pure air as a baseline, it is found that the amount of NOx formed is unaffected by the addition of a few hundred ppm of the simple hydrocarbons (e.g. methane). However, in the case of the halogenated species (e.g. dichloromethane and CFC-12), we find a marked increase in the ratio of NO_2 to NO produced from ~ 1 for the non-halogenated species to ~2-3 for the halogenated methanes.

We also present the results of kinetic modelling studies which attempt to rationalise these experimental observations.

B43

Shock-tube investigations of the unimolecular decompositions of benzene and the phenyl radical

B. R. Giri, H. Hippler, M. Olzmann, and O. Welz

Institut für Physikalische Chemie, Universität Karlsruhe (TH), Kaiserstr. 12, D-76128 Karlsruhe, Germany

olzmann@chemie.uni-karlsruhe.de

The reactions of aromatic hydrocarbons and the related radicals are of crucial importance for the chemistry of combustion processes. In particular these reactions govern the kinetics of soot formation.

In our contribution, we report on shock-tube investigations of the unimolecular decompositions of benzene and the phenyl radical (c-C_6H_5) at temperatures ranging from 1500 – 2250 K and at pressures between 0.25 and 1.2 bar. Iodobenzene was used as precursor for c-C_6H_5, and the rate coefficients were obtained from a time-resolved measurement of the H-atom concentration by atomic resonance absorption.

Our results are discussed in terms of 2 different mechanisms for the phenyl decomposition namely, i) the route via ring opening to l-C_6H_5 and subsequent formation of l-C_6H_4 + H and l-C_4H_3 + C_2H_2 followed by l-$C_4H_3 \rightarrow C_4H_2$ + H [1,2] and ii) the route via ortho-benzyne (o-C_6H_4) + H with subsequent decomposition of o-C_6H_4 to give C_4H_2 + C_2H_2 and further C_4H + C_2H_2 + H [3-5]. It turns out that our observed H atom time profiles over the entire parameter range can be more adequately reproduced by mechanism ii. Kinetic parameters are derived and consequences for combustion modelling are discussed.

1. S. H. Bauer and C. F. Aten, *J. Chem. Phys.* **39**, 1253 (1963).
2. M. Braun-Unkhoff, P. Frank, and Th. Just, *Proc. Combust. Inst.* **22**, 1053 (1988).
3. H. Wang and M. Frenklach, *J. Phys. Chem.* **98**, 11465 (1994).
4. L. K. Madden, L. V. Moskaleva, S. Kristyan, and M. C. Lin, *J. Phys. Chem. A* **101**, 6790 (1997).
5. H. Wang, A. Laskin, N. W. Moriarty, and M. Frenklach, *Proc. Combust. Inst.* **28**, 1545 (2000).

Ion–molecule reactions and TPEPICO spectroscopy of HCFCs – a comparison

Chris R. Howle [a], Daniel J. Collins [b], Chris A. Mayhew [c] and Richard P. Tuckett [a]

[a] *School of Chemistry, University of Birmingham, Edgbaston, Birmingham B15 2TT, UK*
[b] *Department of Physics, Reading University, Reading, RG6 2AF, UK*
[c] *School of Physics and Astronomy, University of Birmingham, Edgbaston, Birmingham B15 2TT, UK*

The measurement of ion-molecule reaction rates and product distributions is of fundamental interest. These reactions are also of interest to the industrial plasma community, where a need exists for a detailed understanding of interactions occurring within plasmas that can lead to improvements in processing techniques. A better understanding of the mechanism of charge transfer (CT), vital to plasma modelling, can be obtained from ion-molecule reaction studies.

A long-range CT mechanism implies that the cation and neutral exert a mutual charge-induced dipole attraction, and an electron 'jumps' at a critical separation where the potential energy curves of $A^+ + BC$ and $A + BC^+$ cross. In the simple case where the potential can be expressed solely as a function of the charge-induced dipole interaction, the critical separation is inversely proportional to the difference between the recombination energy of the ion and the energy provided in ionising the neutral. This means that, for a CT process to occur at long range (defined as ≥ 5 Å), the recombination energy of the ion must be resonant with the energy required to ionise the neutral molecule BC either into the ground state or, more usually, into a vibronically excited state of BC^+. If long-range CT is unlikely, then two possibilities exist. Either the proximity of the reactants causes a perturbation in their potential energy curves which could allow a curve crossing much like the long-range mechanism, or the reactants form an ion-molecule complex in which chemical bonds are formed and broken or charge transfer occurs; i.e. chemical and CT processes can be in competition.

In order to investigate the nature of CT processes, studies into ion-molecule reactions using a selected ion flow tube (SIFT) apparatus can be compared to the fragmentation patterns of cationic products resulting from photoionisation of a neutral molecule via the observation of threshold photoelectron-photoion coincidences (TPEPICO). The branching ratios associated with the cations formed by long-range CT should correlate closely to those of the ion fragments produced by ionisation of the neutral with a photon energy equivalent to the recombination energy of the reactant ion. Any differences in ion product branching ratios would suggest that perturbation of the initial states has occurred. The neutral molecules that are focus of these studies are all hydrochlorofluorocarbons (HCFCs), namely $CHCl_2F$, $CHClF_2$ and CH_2ClF. HCFCs are widely accepted as temporary replacements for the ozone depleting CFC molecules, as their intrinsic hydrogen atoms make them vulnerable to OH attack in the troposphere, thereby greatly reducing the possibility of reaction between liberated chlorine atoms and stratospheric ozone.

Formaldehyde yields in the OH + C_2H_4 reaction

H. Hippler, S. Nasterlack, M. Olzmann, F. Striebel

Institut f. Phys. Chemie, Lehrstuhl f. Molekulare Physikalische Chemie, Universität Karlsruhe, Kaiserstr. 12, 76128 Karlsruhe, Germany.

Reactions of OH radicals with unsaturated hydrocarbons are important steps in atmospheric chemistry as well as combustion processes. At low and moderately elevated temperatures the initial steps of these reactions is the addition of OH to the hydrocarbon and thus the formation of a chemically activated hydroxyl alkyl radical. This chemically activated species can them eother re-dissociate, undergo further reactions or be stabilized by collisions with bath gas molecules. At higher temperatures, H-atom abstraction reactions become competitive. For modelling purposes, not only the total rate coefficients have to be known, but also the product spectra. So far, however, experimental studies on the title reaction have been devoted mainly to the determination of total rate constants. To our knowledge, only one study has been aimed at the experimental determination of product yields in this reaction: Hoyermann and cowrokers (Bartels et al. Proc. Symp. (Int.) Combust. 19, 61, (1982)) determined the formaldehyde yield to be 44% at 300 K and a total pressure of 3 mbar of helium. Moreover, they determined a yield of 35% for a C_2H_4O-species, which was assigned to be acetaldehyde. The aim of the present study is to determine formaldehyde yields in the OH + C_2H_4 reaction as a function of temperature and pressure. Initial experiments at room temperature and pressures ranging from 25 to 400 mbar seem to support the results of Hoyermann et al. The pressure dependence of the rate constant reported in the literature (see Fulle et al., Ber. Bunsenges Phys. Chem. 101, 1433 (1997) and literature cited therein), however, seems to be contradictory to these findings as are the most recently reported *ab initio* calculations of the stationary points on the potential energy surface (H. Hippler, B. Viskolcz, Phys. Chem. Chem. Phys. 2, 3591 (2000)). Further studies are underway to resolve the currently existing inconsistencies.

Acknowledgement: Financial support by the Deutsche Forschungsgemeinschaft (SFB 606: 'Instationäre Verbrennung: Transportphänomene, Chemische Reaktionen, Technische Systeme') is gratefully acknowledged.

Measurement of Adiabatic Burning Velocity in Flat Premixed Flames of CO + $H_2 + O_2 + N_2$ to Validate Kinetic Mechanisms

Alexander A. Konnov and Igor V. Dyakov

Department of Mechanical Engineering, Vrije Universiteit Brussel, 1050 Brussels, Belgium
akonnov@vub.ac.be

Contemporary reaction mechanisms for H_2/O_2 and $CO/H_2/O_2$ systems have been reviewed and evaluated. New accurate measurements of the elementary reaction rates and updates in the thermodynamic data require its extensive validation. The contemporary choice of the reaction rate constants is presented with the emphasis on their uncertainties. Then the predictions of ignition, oxidation, flame burning velocities and flame structure of hydrogen + oxygen + inert mixtures are shown. Modeling range covers ignition experiments from 950 to 2700 K from subatmospheric pressures up to 5 atm; hydrogen oxidation in a flow reactor at temperatures around 900 K from 0.3 up to 15.7 atm; flame burning velocities in $H_2 + O_2$ + inert mixtures from 0.35 up to 4 atm; hydrogen flame structure at 1 and 10 atm. Generally very good agreement was found between the modeling and experiments except in rich flames of H_2.

To extend the basis for the validation of the detailed reaction mechanism dedicated experiments in carbon monoxide + hydrogen + oxygen + nitrogen mixtures have been performed. Adiabatic burning velocities of the premixed flat flames are reported. The equimolar mixture of CO and H_2 was used as a fuel. The oxygen contents $O_2/(O_2 + N_2)$ in the artificial air was varied from 7 to 9 %. Non-stretched flames were stabilized on a perforated plate burner at 1 atm. A Heat Flux method was used to determine burning velocities under conditions when the net heat loss of the flame is zero. Earlier measurements of the adiabatic burning velocity in carbon monoxide + hydrogen + air and new results from the similar but diluted flames (Fig.) were compared with the predictions of the updated detailed reaction mechanism. It is demonstrated that recent modification of the recommended enthalpy of formation of OH radical only slightly affects calculated burning velocity. The updated mechanism over-predicts burning velocities in rich flames, however the difference between experiments and modeling is still comparable to the scattering of the measurements. This disagreement in similar flames highly diluted by nitrogen is much more pronounced (Fig.). It is concluded therefore that recent updates in the H/O reaction subset and in the thermodynamic data call for further revision of the H_2/CO kinetic mechanism. Possible modifications in the kinetic mechanism leading to general improvement of the accuracy of the modeling are demonstrated and discussed.

Financial support of this work by the EC within the "Safekinex" Project EVG1-CT-2002-00072 is gratefully acknowledged. The NATO is gratefully acknowledged for the grant to I.V.Dyakov.

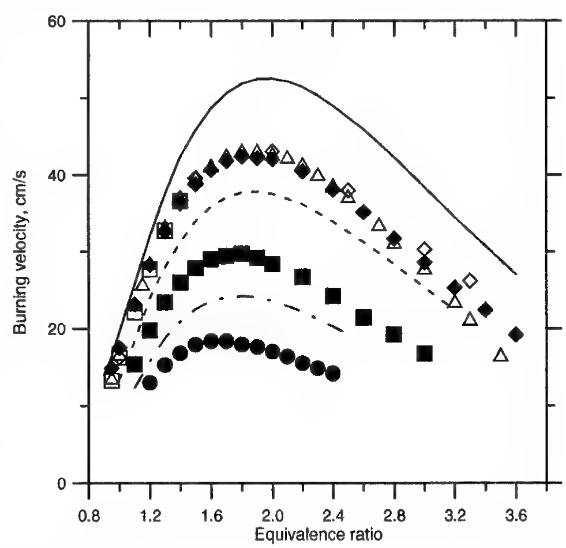

Fig. Measured (points) and calculated (lines) laminar burning velocities for hydrogen (50%) + carbon monoxide (50%) + oxygen + nitrogen flames at standard temperature and pressure. Circles and dash-dot line: oxygen contents $D = O_2/(O_2 + N_2)$ in the artificial air

Destruction of Three Freons (CH_2F_2, CH_2FCl and CH_2Cl_2) in Dielectric Barrier Discharge: Kinetics and Mechanistic Implications

Larisa G. Krishtopa[a] and Lev N. Krasnoperov

Department of Chemistry and Environmental Science,
[a) Material Characterization Laboratory,
New Jersey Institute of Technology, Newark, NJ 07102. U.S.A.
krasnoperov@adm.njit.edu

This study was designed to discriminate between several plausible mechanisms of hydrocarbon destruction in dielectric barrier corona discharges. A set of molecules was chosen based on their ionization energy: 12.71 eV, 11.71 eV and 11.32 eV for CH_2F_2, CH_2FCl and CH_2Cl_2. Kinetics of the destruction of these three chlorofluorocarbons in a dielectric barrier discharge was studied over the concentration range 10 - 1000 ppm using a tubular coaxial AC dielectric barrier flow reactor coupled to a MS and a GC-MS. The first molecule, CH_2F_2, has the ionization energy above that of molecular oxygen ($IP(O_2) = 12.07$ eV), while the two other molecules (CH_2FCl and CH_2Cl_2) have the ionization energies below the ionization energy of molecular oxygen.

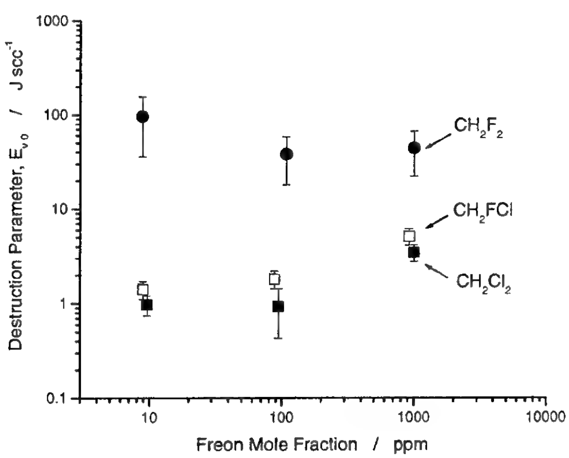

Figure 1. The destruction parameter vs. the mole fraction of freons in air.

Significant differences were observed both in the destruction efficiency and its concentration dependence for CH_2F_2 compared to the two other molecules (Fig. 1). In Fig. 1, the destruction parameter (the specific energy deposition required to reduce the concentration to the e^{-1} level) is plotted vs the mole fraction. The efficiency of the destruction of CH_2F_2 is very low and does not improve with the reduction of CH_2F_2 concentration. The characteristic specific energy deposition required for the destruction is 40 ± 17 Joule per standard cubic centimeter (J scc^{-1}) of the gas mixture. The destruction of CH_2FCl and CH_2Cl_2 is much more efficient, and the efficiencies of the destruction are concentration dependent. The efficiency is the highest at the lowest concentration (ca. 1 J scc^{-1} for 10 ppm of CH_2FCl and CH_2Cl_2). Mechanistic implications of the kinetic observations are discussed. The results are consistent with the mechanism of destruction based on the ionizations transfer ("trapping") on the impurity molecules. Partial product characterization was performed. Formic, acetic, and propionic acids were identified in the destruction products by GC-MS. Molecular chlorine was also identified in the destruction products.

Absolute rate measurements and product distribution study of the reactions of electronically excited $CF_2(^3B_1)$ with several hydrocarbons

Bart Dils, Raviraj M. Kulkarni, Shaun A. Carl and Jozef Peeters

Katholieke Universiteit Leuven, Celestijnenlaan 200F, B-3001 Leuven, Belgium

Fluorocarbon radicals have been widely studied due to their major importance in plasmas used for semiconductor etching in electronic device processing, their presence in the incineration of fluorine-containing wastes and their role in the chemistry of fluorine-containing flame suppressants. Much research has been performed on the reactivity of $CF_2(\tilde{X}\ ^1A_1)$, but hardly any on the reactivity of the electronically excited triplet state $CF_2(\tilde{a}\ ^3B_1)$. The long lifetime of $CF_2(^3B_1)$ (~1s) and the distinct possibility of substantial $CF_2(^3B_1)$ formation in halocarbon etching plasmas makes $CF_2(^3B_1)$ a likely important intermediate in plasma etching systems.

Using the photodissociation of C_2F_4 by a 193 nm excimer laser pulse to generate $CF_2(^3B_1)$ –as opposed to the chemical generation through the C_2F_4 + O reaction used by other groups– we were able to straightforwardly determine the absolute rate constants of gas phase reactions of $CF_2(^3B_1)$ with reactants such as C_3H_8, C_3H_6, iso-C_4H_8 and C_3H_4, this over a broad temperature range between 295 K and 550 K:

$CF_2(^3B_1) + C_3H_8$: $k(T) = (6.5 \pm 2.2) \times 10^{-13} \exp[-(252 \pm 130)K/T]$ cm^3 s^{-1} molecule^{-1}

$CF_2(^3B_1) + C_3H_6$: $k(T) = (7.8 \pm 2.3) \times 10^{-13} \exp[+(500 \pm 100)K/T]$ cm^3 s^{-1} molecule^{-1}

$CF_2(^3B_1)$ + iso-C_4H_8: $k(T) = (1.4 \pm 0.2) \times 10^{-12} \exp[+(762 \pm 36)K/T]$ cm^3 s^{-1} molecule^{-1}

$CF_2(^3B_1) + C_3H_4$: $k(T) = (2.1 \pm 0.5) \times 10^{-12} \exp[+(790 \pm 83)K/T]$ cm^3 s^{-1} molecule^{-1}

From the alkene data, relating the rate constants with the respective ionisation potentials, it could be concluded that the addition of $CF_2(^3B_1)$ to the double bond is an electrophilic process.

B46

Quenching Rates of Field-Ionising Rydberg States of Ar in a Fast Flow Glow Discharge Plasma

Rod S Mason, Ifor P Mortimer and Neil A Dash

Chemistry Department, University of Wales Swansea, Swansea SA2 8PP, UK
r.s.mason@swan.ac.uk

Rydberg states have been studied extensively in beam experiments under high vacuum, but hardly ever in the relatively high pressure plasma environment, although it has been frequently suggested that plasma conditions ought to favour their existence. We can detect states of Ar, Ar^R, carried by a fast flowing glow discharge plasma, in the accelerating region of a high voltage double focussing mass spectrometer, by their rapid field-ionisation and subsequent detection as Ar^+. A small positive field on the plasma side of the sampling cone prevents any existing free ions from leaving the plasma, ensuring a clean Rydberg atom spectrum.

Reactions of gases titrated into the flowing plasma, downstream of the main discharge, have been studied. Both excited state and directly ionised products were identified. The reaction follows pseudo first order kinetics and Ar^R quenching coefficients were obtained in the range from 0.1 to 3.2×10^{-10} molecules^{-1} cm^3 s^{-1} for the gases (in order of efficiency) H_2> iC_4H_{10}> SF_6> NO_2> CH_4> NO >> He.

The poster will briefly describe the apparatus, methodology and results.

Reactions of H/SO_2 adducts with Atomic Hydrogen

Xiaohua Hu and Paul Marshall*

Department of Chemistry, University of North Texas, P.O. Box 305070, Denton, Texas 76203-5070, USA
*marshall@unt.edu

Sulfur is thought to remove atomic hydrogen in flames through catalytic cycles such as

$$SO_2 + H \rightarrow \text{adduct} \qquad (1)$$

$$H + \text{adduct} \rightarrow H_2 + SO_2 \qquad (2)$$

In prior work we have investigated process (1) and noted the possibility of addition of H to either the S or O atom in SO_2 to form HSO_2 and HOSO, respectively. In the present work we consider the second step. Possible reaction paths include: (a) direct H abstraction, (b) addition to form sulfinic acid, H_2SO_2 or $S(OH)_2$, and (c) elimination of H_2 or H_2O from these three molecules.

The radical-radical interactions are investigated via ab initio approaches. We show that straightforward single electron configuration methods break down, and instead apply CASSCF and CASPT2 to investigate energies along the reaction paths for abstraction. Elimination pathways from the adducts are characterized via coupled-cluster-based methods.

We find no overall barrier either to direct formation of H_2 by abstraction, or to formation of H_2 and H_2O through addition/isomerization/elimination pathways. SO_2 to SO reduction by atomic hydrogen is faster than previously thought. The relative importance of these pathways is assessed through TST and QRRK analysis, and the implications are discussed in the context of flame chemistry and their impact on interpretation of measurements of H + SO_2 in our laboratory and elsewhere.

B47

Experimental and detailed chemical kinetic modeling study of the mutual sensitization of the oxidation of nitric oxide and methane over extended temperature and pressure ranges

Philippe Dagaut and André Nicolle
CNRS
Laboratoire de Combustion et Systèmes Réactifs
1C, Avenue de la Recherche Scientifique
45071 Orléans Cedex 2, France

New experimental results were obtained for the mutual sensitization of the oxidation of NO and CH_4 in a fused silica jet-stirred reactor (1-10 atm, 800-1150 K). Probe sampling followed by on-line FTIR analyses and off-line GC-TCD/FID analyses yielded concentration profiles for the reactants, stable intermediates and final products. A detailed chemical kinetic modeling of the present experiments was performed. An overall reasonable agreement between the present data and the modeling was obtained. The present data were simulated published kinetic reaction mechanisms for the NO to NO_2 conversion by hydrocarbons [1,2]. They failed to represent the present data at 1 and 10 atm. Furthermore, they were not able to predict the reactivity of methane without NO. According to our model, the mutual sensitization of the oxidation of CH_4 and NO proceeds viathe NO to NO_2 conversion by HO_2 and CH_3O_2. The modeling showed that at 1-10 atm, the conversion of NO to NO_2 by CH_3O_2 is more important at low temperatures (800 K) than at higher temperatures (850-900 K) where the reaction of NO with HO_2 dominates the production of NO_2. The NO to NO_2 conversion is enhanced by the production of HO_2 and CH_3O_2 radicals from the oxidation of the fuel. The production of OH resulting from the oxidation of NO promotes the fuel oxidation: NO + $HO_2 \rightarrow$ OH+ NO_2 is followed by OH + CH_4 => CH_3. At low temperature, the reaction further proceeds via $CH_3 + O_2 \rightarrow CH_3O_2$; $CH_3O_2 + NO \rightarrow CH_3O + NO_2$. At higher temperature, the production of CH_3O involves NO_2 : $CH_3 + NO_2 \rightarrow CH_3O$. The sequence is followed by $CH_3O \rightarrow CH_2O + H$; $CH_2O + OH \rightarrow HCO$; $HCO + O_2 \rightarrow HO_2$ and $H + O_2 \rightarrow HO_2$. $\rightarrow CH_2O + H$; $CH_2O + OH \rightarrow HCO$; $HCO + O_2 \rightarrow HO_2$ and $H + O_2 \rightarrow HO_2$.

1. M. Hori, N. Matsunaga, N.M. Marinov, J.W. Pitz, C.K. Westbrook, *Proc. Combust. Inst.* 27 (1998) 389-396.
2. M. Hori, Y. Koshiishi, N. Matsunaga, P. Glaude, N. Marinov, *Proc. Combust. Inst.* 29 (2002) 2219-2226.

The effect of SO_2 on SNCR: Experimental and detailed chemical kinetic modeling study

Philippe Dagaut and André Nicolle
CNRS
Laboratoire de Combustion et Systèmes Réactifs
1C, Avenue de la Recherche Scientifique
F-45071 Orléans Cedex 2, France

The effect of the addition of SO_2 on the reduction of NO by ammonia in simulated thermal de-NOx conditions was studied in a jet-stirred reactor at atmospheric pressure for various equivalence ratios (0.1-2) and initial concentrations of NO, NH_3 and SO_2 (0 to 1000 ppm). The experiments were performed at fixed residence times of 100 and 200 ms, and variable temperature, ranging from 1100 to 1450 K. It was demonstrated that the addition of SO_2 inhibits the reduction of NO by ammonia from fuel-lean to fuel-rich conditions. The effect of SO_2 on the extent of NO reduction was controversial in the literature. This study confirms that SO_2 does not reduce the efficiency of the thermal de-NOx process but shifts the optimal temperature to higher values. A kinetic reaction mechanism including a SNCR scheme [1] and a SOx sub-mechanism [2] was used to simulate these experiments. According to the model, the inhibiting effect of SO_2 is due to chain terminating processes ($H+H+M=H_2+M$) and radical pool reduction ($H+O_2+M=HO_2+M$) via the sequence of reactions $SO_2+H+M{=}{>}HOSO+M$, $HOSO+O_2{=}{>}HO_2+SO_2$, $HOSO+H{=}{>}SO_2+H_2$. The present results confirm the validity of the previously proposed kinetic reaction sub-mechanisms for the reduction of nitric oxide by ammonia and for the inhibition of the oxidation of fuels by SO_2.

1. Ø. Skreiberg, P. Kilpinen,P. Glarborg, *Combust. Flame* 136 (2003) 501.

2. P. Dagaut, F. Lecomte, J. Mieritz, P. Glarborg, *Int. J. Chem. Kinet.* 35 (2003) 564.

Cavity ring-down spectroscopy of a DC arcjet diamond depositing plasma

C.J. Rennick, J.A. Smith, M.N.R. Ashfold and A.J. Orr-Ewing

School of Chemistry, University of Bristol, Cantock's Close, Bristol BS8 1TS, UK.

Diamond deposition from plasma-activated carbon-containing gas mixtures has numerous technological applications, but from a fundamental scientific standpoint, there persists a debate over possible "growth species" - i.e., which chain of reactions leads to the most suitable carbon radical for addition to the growing diamond surface. Under low gas activation conditions (such as hot filament), this is thought to be the CH_3 radical, which has been studied previously by REMPI [1]. Experimental and theoretical studies by Gruen *et al.* [2] identified C_2 as a plausible species for diamond growth[2]. Adding C and C_2 to bare or hydrogen-terminated diamond surfaces is considered the most probable mechanism in highly activated mixtures, like those in a DC arcjet. The 10 kW DC arcjet plasma is a harsh environment with high temperatures and extreme temperature gradients, so non-invasive spectroscopy is the most preferable method for probing the chemistry of the plasma. Previous work has concentrated on spatial probing of the emission from the C_2 ($d^3\Pi_g$ – $a^3\Pi_u$) Swan band, and provides an estimate for path lengths over which C_2 absorbs for quantitative determination of radical densities by CRDS. Previously reported CRDS measurements have demonstrated line of sight concentrations of $C_2(a)$ and CH(X), and rotational line intensity analysis yielded the temperature of the plasma.

Recent work has concentrated on measurement of the ground state number densities of $C_2(X^1\Sigma_g^+)$, which lies 716 cm^{-1} below the often probed $a^3\Pi_u$ state, but exhibits a much higher reactivity to H_2, hydrocarbons and diamond surfaces, so is a more likely candidate for growth-related reactions, and was the state considered in modeling of diamond growth. CRDS measurements of $C_2(X)$ concentrations will be complemented, as before, by 2 dimensional modelling (the two dimensions being the radial direction and the central cylindrical symmetry axis of the plume) of the gas-phase chemistry and matter transfer[3].

[1] J.A. Smith, E. Cameron, M.N.R. Ashfold, Y.A. Mankelevich, and N.V. Suetin, Diam. Rel. Mater., **10**, 358 (2001).

[2] D. Horner, L. Curtiss, and D. Gruen, Chem. Phys. Lett., **233**, 243 (1995).

[3] Y. A. Mankelevich, N. V. Suetin, M. N. R. Ashfold, W. E. Boxford, A. J. Orr-Ewing, J. A. Smith and J. B. Wills, Diam. Rel. Mater., **12**, 383 (2003).

Recent Work on the $OH/CH_3OCH_3/O_2$ System Including Isotopic Studies

Tracy J. Still, Mark A. Blitz, Kenneth McKee and Paul W. Seakins

School of Chemistry, University of Leeds, Leeds, LS2 9JT
Email tracys@chem.leeds.ac.uk, p.w.seakins@chem.leeds.ac.uk

Dimethyl ether (DME) has been suggested as a possible fuel additive diesel engines. Advantages include high cetane number, reduction in combustion noise and particle emissions, lower NOx emissions. However, oxidation of DME during combustion or in the atmosphere can lead to formaldehyde, a species of significant atmospheric and environmental importance, via rearrangement of the RO_2* species.

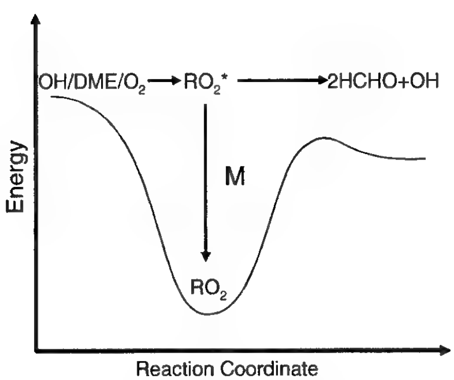

Figure 1 – PES for $OH/DME/O_2$ system

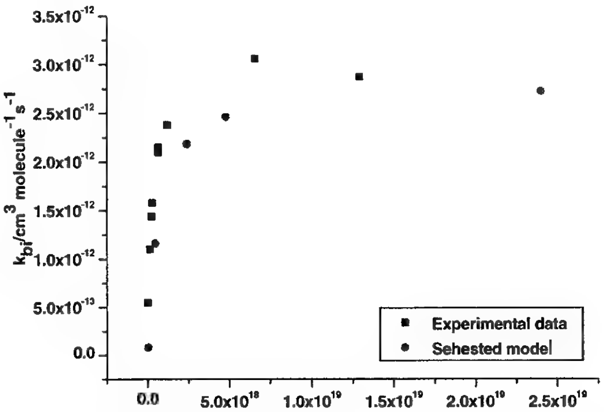

Figure 2 – Observed OH loss with pressure

At high pressures all the RO_2* is quenched to RO_2, but at lower pressures a fraction of the initially formed peroxy radical dissociates generated formaldehyde and recycling OH.
We have chosen the $OH/DME/O_2$ as a test bed for a new laser flash photolysis system with both laser induced fluorescence and gas chromatography detection, due to the practical and mechanistic interest in this system, especially the formation of formaldehyde which poses challenges for GC detection.[1]

To date we have focused on kinetic studies measuring the bimolecular rate coefficient for the OH abstraction in the absence of O_2, obtaining results in good agreement with the literature. Oxygen was then added, such at the OH abstraction is still the rate determining step, and at low pressure, the OH is recycled and the observed OH removal rate coefficient decreases in good agreement with earlier work by Sehested et al[2]. At high total pressures, the decomposition reaction is shut off and the original rate coefficient is recovered (figure 2).
Currently we are investigating the effects of deuterating the DME. The reaction of OH with d-DME will give the abstraction rate coefficient when monitoring OH, OD observation will show the effect of recycling. Finally we will be investigating HCHO production via both LIF and GC end product analysis in the near future.

[1] J.R. Hopkins, T. Still, S. Al-Haider, I.R. Fisher, A.C. Lewis, P.W. Seakins, Atmospheric Environment 37 (2003) 2557.
[2] J. Sehested, K. Sehested, J. Platz, H. Egsgaard, O.J. Nielsen, Int. J. Chem. Kinet. 29 (1997) 627.

Formation Pathway of HO_2 in the Reaction of Methoxymethyl with Molecular Oxygen

Kotaro Suzaki[1], Nozomu Kanno[2], Kenichi Tonokura[3], Mitsuo Koshi[2] and Atsumu Tezaki[1]

[1]*Department of Mechanical Engineering, The University of Tokyo*
[2]*Department of Chemical System Engineering, The University of Tokyo*
[3]*Environmental Science Centre, The University of Tokyo*

The production of hydroperoxy radical (HO_2) in the reaction of methoxymethyl radical with molecular oxygen has been monitored, where methoxymethyl radical is initially formed via H abstraction from dimethyl-ether (DME) by a Cl atom. A two-tone frequency modulation technique combined with Herriott type multi-path absorption was applied to selectively detect HO_2 at the first electronic transition in the region of 1.43 μm. At excess oxygen in which the CH_3OCH_2 + O_2 reaction completes immediately, the HO_2 yield was determined by comparison with the reference reaction of $CH_3OH/Cl_2/O_2$ system, which generate 100% of HO_2 to the initial Cl atom concentration, with the established procedure of corrections for $HO_2 + HO_2$ and $HO_2 + CH_3OCH_2O_2$ reactions.

It was found that the yield of HO_2 dramatically increases from 500 to 600 K up to the constant level of 0.6. This temperature range is 50 K lower than that of ethyl and propyl radicals, but the high temperature yield is less than the unity yields of the simplest alkyl radicals. The observed HO_2 formation profiles and the yields were well reproduced in the simulation assuming that HO_2 is formed directly as a decomposition fraction of $CH_3OCH_2O_2$ or $CH_2OCH_2O_2H$ species, or indirectly via a HCO reaction with molecular oxygen, where HCO is formed by the decomposition of $CH_2OCH_2O_2H$. This analysis indicated that the actual branching fraction to HO_2 or its precursor in the intermediate decomposition is around 0.3 at 600 K, in which the appeared yield is enhanced by the reproduction of HO_2 via OH + CH_3OCH_3. It was also suggested that contribution from secondary reactions such as HCHO + OH is not negligible at the current initial Cl concentration of 2×10^{13} atom/cm^3 and $[CH_3OCH_3]_0/[Cl]_0$ ratio of 50, though, the chlorine concentration dependence showed that this secondary contribution is only a part of the observed amount of HO_2.

In contrast with the case of the simplest alkyl + O_2 reactions, HO_2 formation from $CH_3OCH_2O_2$ or $CH_2OCH_2O_2H$ seems unfavorable since the HO_2 counterpart is not a conjugate olefin but a cyclic ethylene oxide, which may requires a higher barrier. Consequently the indirect pathway through HCO formation in the decomposition of $CH_2OCH_2O_2H$ is more likely.

Ab initio Study of Allylic Hydrogen Abstraction from Polyalkenes

M. Szori, B. Viskolcz

Department of Chemistry, Faculty of Education, University of Szeged
H-6701 Szeged, P. O. Box 396, Hungary

Allyl-type radicals are formed in many different processes, such as the hydrocarbon combustion as well as oxidation of fatty acids in cell. *Ab initio* calculations will allow accurate predictions of the potential energy surface necessary to describe the elementary steps of the reactions and to obtain reasonable branching ratio of competitive channels.

In the study of hepta-2,5-diene molecule, it is seen that an H-atom abstraction will form either a mono-allyl or di-allyl radicals. The mono-allyl radical involves 3 electrons delocalized on 3 carbons while the di-allyl involves 5 electrons delocalized on 5 carbon atoms. (see the figure).

H-atom abstractions were carried out with CH_3, i-C_3H_7, OOH and OH radicals. These reaction were studied at different levels of theories including B3LYP, BHandHLYP, G3MP2B3, QCISD(T) and CCSD(T) using a variety of basis sets.

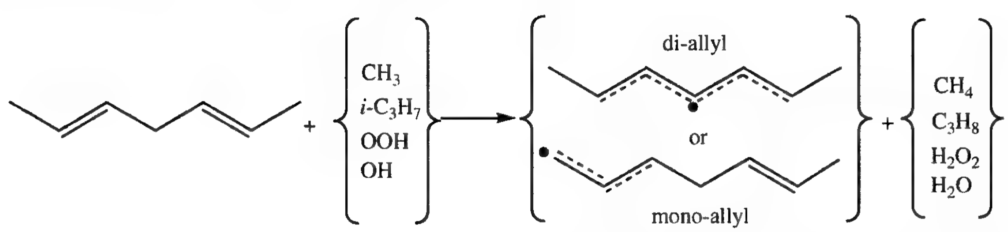

The reaction enthalpies and activation enthalpies as well as the overall kinetics will be discussed.

B50

The Oxidation of Carbon Soot in a Non-Thermal, Atmospheric Pressure Plasma: Experiment and Modelling

Anthony R. Martin and James T. Shawcross
Accentus plc, F7 Culham Science Centre, Abingdon, Oxfordshire, OX14 3ED, UK

J. Christopher Whitehead
Department of Chemistry, University of Manchester, Manchester, M13 9PL, UK

Future legislative limits mean that it is necessary to substantially reduce the levels of pollutants such as oxides of nitrogen (NOx) and particulates in the exhausts from diesel engines. One approach is to use a non-thermal plasma or a hybrid plasma-catalyst system which has the potential for the removal of both NOx and particulates.

In support of this, a programme of chemical kinetic modelling of diesel exhaust aftertreatment has been undertaken. This has the objectives of aiding the understanding of the underlying principles behind the remediation processes, the improvement of these processes, and the prediction of aftertreatment performance under conditions not investigated by experiment. This paper describes the study of the heterogeneous oxidation of carbonaceous soot representative of particulate matter in diesel exhaust.

A series of experiments were performed to determine the oxidation rates of soot in non-thermal plasma and the evolution of the gaseous end-products under a range of conditions, including temperature and gas stream composition representative of diesel exhaust. These experiments provided the input for a series of modelling studies incorporating both the homogeneous gas-phase chemistry and the heterogeneous chemistry taking place on the soot surface. The variation of experimental conditions provides the opportunity for the validation of the modelling and enables possible, different, surface reaction mechanisms to be evaluated. These comparisons are discussed in detail.

A51

Detailed chemical kinetic modelling of the gas-phase processes during straw combustion

T. Perger, I. Gy. Zsély, and T. Turányi

Department of Physical Chemistry, Eötvös University (ELTE)
H-1518 Budapest, P.O. Box 32, Hungary
Fax: +36-1209-0602, e-mail: turanyi@elte.hu

Climate change is of major concern recently and combustion of CO_2-neutral fuels is an important tool to decrease the CO_2 emission while maintaining life standards. Biofuels, including agricultural waste products like straw, are primary examples of such fuels. However, an optimization of the combustion, based on the understanding of the gas-phase chemical kinetic processes, is needed for efficient and economical applications.

As a first step of the combustion of straw, it rapidly decomposes at low temperature (below 800 °C) to a mixture of CO, CO_2, H_2, CH_4, C_2H_4 and C_2H_6 [1], therefore it is of vital importance that the combustion chemistry of these species be described accurately. Exhaust gases of straw combustion are frequently polluted with NO_x and SO_x species. Straw contains large amount of KCl, and co-combustion of straw with coal containing NaCl is a frequently applied procedure. Therefore, the gas-phase kinetics of the decomposition products of KCl and NaCl should also be taken into account.

An updated detailed combustion mechanism, based on the Leeds Methane Oxidation Mechanism [2] for the description of the fuels above, was created. Recent evaluations of Baulch et al. [3] were also taken into account. The thermodynamic parameters were updated using the latest publications. Further reaction blocks, describing the formation and decomposition of NO_x and SO_x were added. Finally, the reaction mechanism was completed with high temperature gas-phase alkali chemistry. The whole mechanism contains 523 reversible chemical reactions of 101 species.

The gas-phase chemical kinetic processes during straw combustion were modelled at conditions characteristic for industrial furnaces, but assuming idealized flow configurations. The results of plug flow reactor, perfectly stirred reactor and premixed laminar flame simulations provided semi-quantitative agreement with the measurement data determined in the furnaces.

Acknowledgement: This work was supported by the European Union project HIAL, contract No. ENK5-CT2001-00517.

[1] Werther J., Saenger M., Hartge E.-U., Ogada T., Siagi Z., Combustion of agricultural residues. *Prog. Energy and Comb. Science*, **26**, 1-27 (2000).
[2] K. J. Hughes, T. Turányi, A.R. Clague, M.J. Pilling, Development and testing of comprehensive chemical mechanism for the oxidation of methane. *Int. J. Chem. Kinet.*, **33**, 513-538 (2001)
[3] D.L. Baulch, C.T. Bowman, C.J. Cobos, R.A. Cox, T. Just, J.A. Kerr, M.J. Pilling, D. Stocker, J. Troe, W. Tsang, R.W. Walker, and J. Warnatz, *J. Phys. Chem. Ref. Data*, (2003) (in press)

Tropopause chemistry revisited: $HO_2^\bullet$-initiated oxidation as a major acetone sink

Ive Hermans[a,b], Thanh Lam Nguyen[a], Pierre A. Jacobs[b], Jozef Peeters*[a]

[a] Division of Physical and Analytical Chemistry, Department of Chemistry, KULeuven, Celestijnenlaan 200F, B-3001 Heverlee, Belgium; [b] Centre for Surface Science and Catalysis, Department of Interphase Chemistry, KULeuven, Kasteelpark Arenberg 23, B-3001 Heverlee, Belgium

* jozef.peeters@chem.kuleuven.ac.be, fax : +32 (0)16 327992

Acetone is known to be a key species in the chemistry of the Upper Troposphere and Lower Stratosphere. In this theoretical study, using amply validated methodologies, the hitherto overlooked reaction of acetone with $HO_2^\bullet$ radicals is found to lead to a fast equilibrium $(CH_3)_2C{=}O + HO_2^\bullet \rightleftharpoons (CH_3)_2C(OH)OO^\bullet$ (see figure 1). At room temperature this is shifted entirely to the left and thus of no consequence. However, near the tropopause, at $T \leq 220$ K, the equilibrium is shown to shift to the right to such an extent that the subsequent reaction of $(CH_3)_2C(OH)OO^\bullet$ with NO becomes an effective and even dominant acetone sink (figure 2). This process finally results in acetic acid, thus explaining the high observed abundance of this organic acid near the tropopause. The analogous $HO_2^\bullet + CH_2O$ reaction is likewise predicted to be an important CH_2O sink in the tropopause and to produce significant amounts of formic acid. (reference: I. Hermans, L.T. Nguyen, P.A. Jacobs, J. Peeters, submitted to JACS).

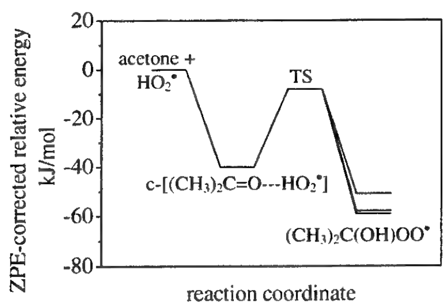

Figure 1. Potential Energy Surface of the $HO_2^\bullet$ + acetone reaction.

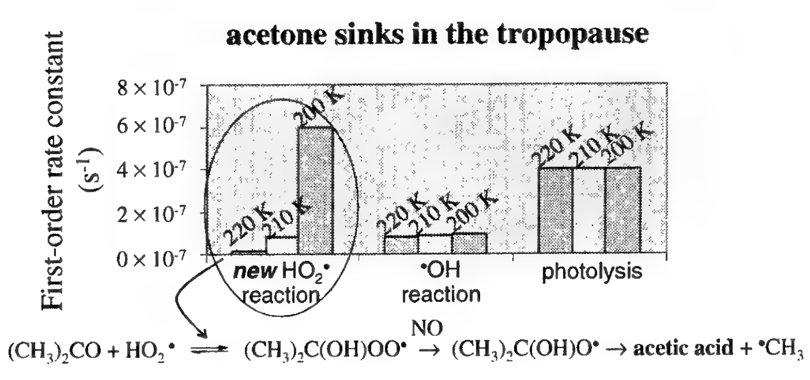

Figure 2. Importance of the newly proposed acetone sink compared with known sinks.

Rate coefficients for removal of $CN(X^2\Sigma^+, v = 2)$ from selected rotational levels between $N_i = 0$ and 57 in collisions with N_2 and C_2H_2.

Kevin M. Hickson,[1,2] Chester M. Sadowski[1,3] and Ian W. M. Smith[1]
[1] *School of Chemistry, The University of Birmingham, Edgbaston, Birmingham B15 2TT, U.K.*
[2] *Mail Stop 183-901, Jet Propulsion Laboratory, California Institute of Technology, 4800 Oak Grove Drive, Pasadena, CA 91109, U.S.A.*
[3] *Department of Chemistry, York University, Toronto, Ontario, Canada M3J 1P3*

Using an infrared-ultraviolet double resonance (IR-UV DR) method, we have determined rate coefficients ($k_{tot,i}$) for the total removal of $CN(X^2\Sigma^+, v = 2, N_i)$ radicals from selected levels between $N_i = 0$ and 57 in collisions with N_2 and C_2H_2. Additionally, state-to-state rate coefficients ($k_{i\to f}$) have been measured for rotational energy transfer in collisions of $CN(X^2\Sigma^+, v = 2, N_i = 0$ and 1) with N_2 and C_2H_2. In the case of CN + C_2H_2, by comparing the values of $k_{tot,i}$ with the sum of the state-to-state rate coefficients ($\Sigma_f\, k_{i\to f}$), we infer the rotationally state-selected rate coefficients for reaction ($k_{reac,i}$) of $CN(X^2\Sigma^+, v = 2, N_i = 0$ and 1) with C_2H_2.

B52

Kinetic Study of the Temperature Dependence of the OH Initiated Oxidation of Dimethyl Sulphide

Mihaela Albu[1,2], Ian Barnes[1] and Raluca Mocanu[2]

[1]*Physikalische Chemie/Fachbereich C, Bergische Universität Wuppertal, Gaußstraße 20, 42097 Wuppertal, Germany*

[2]*Department of Analytical Chemistry, Faculty of Chemistry, " Al.I. Cuza" University Iasi, Carol I Boulevard 11, 6000 Iasi, Romania*

Email: barnes@mailgate.uni-wuppertal.de

Dimethyl sulphide (CH_3SCH_3: DMS) is the most predominant of the naturally emitted reduced sulphur compounds released to the atmosphere. DMS is emitted in the atmosphere by oceanic and continental sources; the continental sources of DMS are minor compared with oceanic sources. Dimethyl sulphide is considered to be a potentially important climate-modulating species. The major fate of DMS in the atmosphere is reaction with OH radicals. Temperature dependent measurements of the rates of the OH initiated oxidation of DMS are necessary to understand the mechanism of this reaction and to interpret field data. For many years the recommended rate coefficients for the OH initiated oxidation of DMS were based on the work of Hynes et al. (*J. Phys. Chem.*, 1986, 90, 4148). However, recent work by Williams et al. (*Chem. Phys. Lett.*, 2001, 344, 61) suggests that the rate coefficients at temperatures below 270 K may have been considerably underestimated.

In the present work a relative kinetic technique was used to determine rate coefficients for the reaction of OH radicals with DMS under different conditions of temperature and O_2 partial pressure using the photolysis of H_2O_2 as the OH radical source. The experiments were carried out in a 336 L glass reaction chamber equipped with a system for temperature regulation to within ±1 K from 223 K to 300 K. FT-IR was used to monitor the disappearance rates of the DMS and the reference compounds (ethene, propene and iso-butene).

The results will be presented and compared with other literature data. The results at low temperature support the observation of Williams et al. for a large positive roll-off in the rate coefficient for OH + DMS below 270 K compared to the presently accepted estimated rates at these temperatures.

A53

Kinetics study of the reaction $OH + NO_2 + M$: Pressure- and temperature-dependent falloff parameters

Sivakumaran Valluvadasan, Daniel B. Milligan, William J. Bloss and Stanley P. Sander

Jet Propulsion Laboratory, California Institute of Technology, Pasadena, CA 91109 USA.

The reaction $OH + NO_2 + M$ (1) is an important sink for HO_x and NO_x radicals in the troposphere. Global, regional and urban models of O_3 production are highly sensitive to rate constants for reaction (1). There have been few studies of reaction (1) under lower tropospheric conditions, especially near 1 atm. pressure with M = air. Published rate constants differ by a factor of two. We have studied reaction (1) using improved Pulsed Laser Photolysis/Pulsed Laser Induced Fluorescence technique augmented by *in situ* optical absorption measurements of NO_2. The pressure- and temperature-dependent falloff parameters will be reported.

Index of Authors

af Ugglas, M.	43
Ahmed, M.	49
Albaladejo, J.	85, 122
Albu, M.	188
Alcaraz, C.	45, 167
Alconcel, L.S.	18
Aldegunde, J.	128
Aldener, M.	88
Al-Khalili, A.	43
Allan, M.	58
Almond, M.J.	30
Aloisio, S.	102
Althorpe, S.C.	35
Alvariño, J.M.	128
Alxneit, I.	151
Anderson, W.R.	52
Anthony, L.M.	158
Aoiz, F.J.	35, 128, 133
Aranda, A.	86
Artamonov, M.	144
Ashfold. M.N.R.	74, 125, 146, 147, 180
Ashworth, S.H.	101
Ausfelder, F.	35
Bacak, A.	19
Baeza, M.T.	90, 150
Bakowski, B.	166
Bale, C.S.E.	82
Balint-Kurti, G.G.	129, 135, 139, 144
Ball, J.C.	63
Ballesteros, B.	122
Baloitcha, E.	129
Balucani, N.	133, 134
Bañares, L.	35, 133
Bar, I.	75
Bardwell, M.	19
Barker, J.R.	78
Barnes, I.	124, 188
Bass, M.J.	130
Bauer, D.	92
Baynard, T.	89
Becerra, R.	30, 152
Bedjanian, Y.	87,
Behr, P.	60
Bentz, T.	67
Bernshtein, V.	28, 163
Blitz, M.	26, 41, 69, 96, 181
Bloss, C.	114
Bloss, W.J.	96, 97, 115, 189
Boakes, G.	22
Bobbenkamp, R.	133
Bodek, P.	151
Boganov, S.E.	152
Bowman, C.T.	53
Broekhuizen, K.	81
Brouard, M.	38, 130, 131
Brown, A.	135
Brown, S.	88
Buajarern, J.	91
Burkholder, J.B.	79, 88, 89
Bussery-Honvault, B.	133
Butkovskaya, N.I.	77
Cabañas, B.	90, 150
Campuzano-Jost, P.	76, 93
Cannady, J.P.	30
Canosa-Mas, C.E.	82, 118
Capozza, G.	34, 132, 133, 134
Carl, S.A.	44, 168, 175
Cartechini, L.	133
Casavecchia, P.	34, 132, 133, 134
Cassanelli, P.	68
Castillo, J.F.	35
Chestakov, D.A.	39
Chishima, H.	116
Choi, J.H.	33
Choi, N.	26, 41
Cireasa, R.	38, 130
Clark, A.P.	38
Clark, J.	73
Clary, D.C.	56
Cleary, P.	69
Cody, R.J.	42, 112
Collins, D.J.	171
Cool, T.A.	49
Costen, M.L.	164, 165
Cotterill, A.J.	62, 91
Couling, S.B.	83
Cox, R.A.	68
Crichton, H.J.	164
Cronin, B.	147
Crowley, J.N.	80, 99
Csizmadia, B.	160
Cuevas, C.A.	85
Dagaut, P.	178, 179
Dash, N.A.	47, 176
Daud, M.N.	135
Davey, J.	97
Dean, A.M.	50
de Miranda, M.P.	36, 128, 143
Devolder, P.	117
Deyerl, H.-J.	167
Díaz de Mera, Y.	86
Dillon, T.J.	80, 99
Dils, B.	168, 175
Dixon, R.N.	74, 146
Djurić, N.	43
Donohoue, D.	92, 93
Donovan, R.J.	136, 153
D'Ottone, L.	76
Duchovic, R.J.	137
Dyakov, I.V.	173

Dyke, J.M.	20
Egorov, M.P.	152
Ehlerding, A.	43
Elhanine, M.	167
Ellis, D.A.	63
Elsamra, R.M.I.	44, 168
Enami, S.	102
Eppink, A.T.J.B.	39
Eskola, A.	94
Estupinan, E.G.	120
Fardy, M.	76
Faustov, V.I.	152
Feigenbrugel, V.	61
Fernandes, R.X.	67
Fikri, M.	46
Fischer, I.	45, 138, 167
Fittschen, C.	117
Fleming, Z.	126
Frerichs, H.	27
Friedrichs, G.	46
Fontijn, A.	52
Ganot, Y.	75
Gao, Y.	31, 55
Georgievskii, Y.	71
Geppert, W.D.	43
Ghosh, M.V.	20
Gierczak, T.	79
Gilham, R.	62
Giri, B.R.	67, 170
Goddard, A.	95
Golan, A.	75
Goldberg, N.	30
Golden, D.M.	53
González-Lafont, A.	109
Goumri, A.	55
Gravestock, T.	96
Green, Jr, W.H.	50
Greenslade, M.E.	39
Grenda, J.M.	50
Groenenboom, G.C.	39
Guo, Y.Q.	46
Haber, L.	73
Hack, W.	54
Hancock, G.	37, 148, 166
Hansmann, B.	154
Hanson, R.K.	53
Harding, L.B.	71
Harling, A.M.	169
Harvey, J.N.	24
Hashimoto, S.	102
Hayashi, S.	108
Heard, D.E.	95, 96, 97, 98, 115, 126
Hellberg, F.	43
Henderson, D.A.	58
Herbon, J.T.	53
Hermans, I.	155, 186
Hickson, K.M.	187
Hippler, H.	51, 67, 170, 172
Ho, T.S.	144
Hollerbach, M.	27
Hölscher, D.	80, 99
Honvault, P.	133
Hopkins, R.J.	62, 100
Horn, A.B.	83
Horrocks, S.J.	37
Howle, C.R.	171
Hoyermann, K.	54
Hu, X.	177
Hurley, M.P.	63, 119
Hynes, A.J.	76, 92, 93
Ingham, T.	97
Jacobs, P.A.	155, 186
Jenkin, M.E.	114
Jeranko, T.	139
Jiménez, E.	79, 86, 122
Johnson, D.	68, 157
Johnson, G.P.	97
Jones, J.R.	74, 146
Joseph, D.M.	101
Kamińska, M.	43
Kanno, N.	156, 182
Kasper, T.	49
Kawasaki, M.	59, 102
Kelso, H.	58
Kennedy, S.A.	106
Kleissas, K.M.	21
Klippenstein, S.J.	71
Knight, R.J.	106
Koch, L.C.	103
Köhler, S.P.K.	58
Kohse-Höinghaus, K.	65
Konnov, A.A.	173
Koshi, M.	116, 156, 182
Kovacs, T.	26
Krasnoperov, L.N.	157, 174
Krasteva, N.	51
Krishtopa, L.G.	174
Krylova, I.V.	152
Kukui, A.	77
Kulkarni, R.M.	44, 175
Kusuhara, M.	121
Larsson, M.	43
Launay, J.-M.	133
Law, M.E.	49
Lawley, K.P.	136
Lazarou, Y.G.	111
LeBras, G.	77, 87, 123, 124
Le Calve, S.	61
Lee, C.	29
Lee, J.D.	126

Lelievre, S. 87
Lenzer, T. 27
Leone, S.R. 73
Leonori, F. 132, 134
Lesclaux, R. 157
Lester, M.I. 39
Leyssens, G. 61
Lindley, R.M. 104
Liu, Y. 78
Lluch, J.M. 109
Locoge, N. 117
Lohr, L.L. 78
Loock, H.-P. 140
Louis, F. 61, 141
Lovejoy, E.R. 89
Luther, K. 27, 29
Ma, Y. 105
Mabury, S.A. 63
Macdonald, R.G. 31
Manby, F.R. 144
Manzhos, S. 140
Marinakis, S. 131
Maring, H. 93
Marques, J.M.C. 142
Marshall, P. 52, 55, 177
Marston, G. 105, 106
Martin, A.R. 184
Martin, J.W. 63
Martin, M.P. 150
Martín, P. 90
Martínez, E. 85, 86, 122
Martínez-Núñez, E. 142, 145
Mason, R.S. 47, 176
Matheu, D.M. 50
Matsui, H. 110
Matsumi, Y. 23, 107, 108
Mayhew, C.A. 171
Mazurenka, M.I. 104
McCabe, D.C. 72
McIlroy, A. 49
McKee, K. 69, 181
McKee, M.L. 21
McKendrick, K.G. 25, 58, 164, 165
Meech, S.R. 17
Mellouki, A. 123, 124
Michael, J.V. 66
Milligan, D.B. 189
Mirabel, P. 61
Mitchell, D.J. 47
Mitchell, E. 55
Miyoshi, A. 121
Mocanu, R. 188
Molina, L.T. 81
Molina, M. 81
Monedero, E. 90, 150
Monks, P.S. 126
Morales, L. 86
Morel, A. 49
Morrison, M.D. 148
Mortimer, I.P. 47, 176
Müller, A. 73
Murray, B.J. 17
Murray, C. 149
Nagai, Y. 121
Nahler, N.H. 74, 146
Naidoo, J. 55
Nakajima, K. 49
Nakano, Y. 102
Nakayama, T. 23
Nasterlack, S. 172
Nebot-Gil, I. 109
Nefedov, O.M. 152
Nesbitt, F.L. 42, 112
Neumann, J. 46
Nguyen, H.M.T. 44
Nguyen, M.T. 44
Nguyen, T.L. 155, 168, 186
Nicolle, A. 178, 179
Nicovich, J.M. 21, 120
Nielsen, O.J. 119
Nishida, S. 107
Nix, M.G.D. 74, 147
Notario, A. 85
Nothdurft, J. 54
Ochando-Pardo, M. 109
O'Donnell, S.M. 123,
Ogden, J.S. 30
Oguchi, T. 110
Okumura, M. 18
Olzmann, M. 54, 67, 170, 172
Oref, I. 28, 163
Orr-Ewing, A.J. 104, 125, 149, 180
Österdahl, F. 43
Oum, K. 29
Paál, A. 43
Papadimitriou, V.C. 111
Papagiannakopoulos, P. 111
Parker, D.H. 39
Parker, M.A. 137
Parkes, A.M. 104
Parthasarathy, S. 21
Pascoe, S. 114
Paulus, M. 127
Payne, W.A. 42, 112
Pearce, J.K. 149

Pearson, P.J. 37
Peeters, J. 44, 64, 155,168,175,186
Pegus, A.T. 21
Percival, C. 19
Perger, T. 185
Peterka, D.S. 49
Pettipher, R.A. 36, 143
Peverall, R. 166
Pilling, M.J. 26, 41, 69, 97, 114, 126
Pimentel, A.S. 42, 112
Plane, J.M.C. 17, 101, 115
Plenge, J. 73
Poisson, L. 49
Pomerantz, A.E. 35
Pope, F.D. 21, 125
Pouvesle, N. 77
Preston, T.J. 38
Prince, S.E. 166
Promyslov, V.M. 152
Qadiri, R.H. 147
Rabitz, H. 144
Radenović, D.C. 39
Rajakumar, B. 72
Ramírez, V.M.R. 113
Ratajczak, E. 94
Raventos-Duran, T. 19
Ravishankara, A.R. 72, 79, 88, 89, 103
Reid, J.P. 62, 91, 100
Ren, Q. 144
Rennick, C.J. 180
Richmond, G. 164, 165
Rickard, A.R. 114
Ridley, T. 136
Riffault, V. 79
Ritchie, G.A.D. 37, 166
Robichaud, D.J. 18
Rodríguez, A. 86
Rodríguez, D. 86
Romanescu, C. 140
Roscoe, J.M. 158
Rosenwaks, S. 75
Roth, W. 45, 138, 167
Rowley, D.M. 22
Rubio, L. 131
Sadowski, C.M. 187
Salgado, S. 90, 150
Sander, S.P. 18, 189
Sato, Y. 110
Saunders, M. 148
Saunders, S.M. 114
Sawerysyn, J.P. 61
Sayer, R.M. 62, 91, 100
Scharfenort, U. 60
Schatz, G.C. 32
Schussler, T. 45, 167
Seakins, P.W. 26, 41, 69, 181
Segoloni, E. 34, 132, 133, 134
Sekiguchi, K. 29
Self, D.E. 97, 115
Semaniak, J. 43
Shallcross, D.E. 20, 125
Shamsuddin, S.M. 52
Shawcross, J.T. 184
Sheng, X. 75
Shillings, A. 104
Sidebottom, H.W. 123
Sims, I.R. 40
Sjodin, A.M. 136
Smith, C.A. 125
Smith, I.W.M. 72, 187
Smith, J.A. 180
Smith, K.M. 106
Smith, S.C. 97
Solignac, G. 124
Sommariva, R. 126
Srinivasan, N. 66
Stanton, J. 97
Stark, H. 88
Stefanopoulos, V.G. 111
Stevens, P.N. 149
Stief, L.J. 112
Still, T.J. 181
Stranges, D. 134
Striebel, F. 51, 172
Su, M.C. 66
Sulbaek Andersen, M.P. 63, 119
Sutherland, J.W. 66
Suzaki, K. 182
Suzuki, T. 108
Symes, R. 62
Szori, M. 160, 183
Taatjes, C.A. 49
Tachikawa, H. 59
Takahashi, K. 23, 107, 108
Taylor, S.E. 95
Temps, F. 46
ter Meulen, J.J. 39
Terziyski, U. 60
Tezaki, A. 156, 182
Thomas, R. 43
Thornton, L. 166
Tibbetts, D.F. 37
Timonen, R. 94
Tomas, A. 117
Tonokura, K. 116, 156, 182
Troe, J. 29, 70
Tuckett, R.P. 171
Turányi, T. 161, 162, 185
Turpin, E. 117
Uetake, M. 156

Underwood, J. 140
Vaghjiani, G.L. 159
Vallance, C. 38, 130, 131
Valluvadasan, S. 189
van der Loo, M.P.J. 39
van Roij, A.J.A. 39
Vaughan, S. 118
Vázquez, S.A. 142, 145
Vereecken, L. 64
Vieuxmaire, O.P.J. 74, 146
Villanueva, F. 90, 150
Viskolcz, B. 160, 183
Volkamer, R. 81
Volpi, G.G. 34, 132, 134
Vondrak, T. 17
Wada, R. 104
Wagner, V. 114
Wallington, T.J. 63, 119
Walsh, R. 30, 106, 152
Wang, J. 49
Wang, L. 41, 69
Warnatz, J. 48
Wayne, R.P. 82, 118
Welz, O. 170
Wenger, J.C. 123
Westmoreland, P.R. 49
Whitehead, J.C. 169, 184
Whitehouse, L. 114, 126
Williams, R.G. 106
Wine, P.H. 21, 120
Wirtz, K. 150
Wodtke, A.M. 57
Wojcik, D. 94
Xing, J.-H. 121
Zabel, F. 127
Zádor, J. 161, 162
Zare, R.N. 35
Zellner, R. 60
Zeuch, T. 54
Zhang, K. 169
Zierhut, M. 138
Zsély, I.G. 161, 162, 185